LABORATORY STUDIES OF SPONTANEOUS COMBUSTION OF A VICTORIAN BROWN COAL

by

Wiwik SUJANTI

Thesis submitted for the degree of
Doctor of Philosophy

in

The University of Adelaide
Department of Chemical Engineering
Faculty of Engineering

August 1998

DECLARATION

This work contains no material which has been accepted for the award of any other degree or diploma in any university or any other tertiary institution, and to the best of my knowledge and belief, contains no material previously published or written by another person, except where due reference has been made in the text.

I give consent to this copy of my thesis, when deposited in the University Library, being available for photocopying and loan.

SIGNED DATE : 12. 11. 1998

(Wiwik Sujanti)

To my beloved parents

ACKNOWLEDGMENTS

First of all, I would like to thank A/Prof. Dong-ke Zhang for his excellent supervision and enormous support and guidance, which have enabled me to complete this project. A/Prof. Dong-ke Zhang has given me such a good opportunity to learn a great deal about academia and different aspects of life which greatly enriched my personal and professional developments.

Financial support provided by the Cooperative Research Centre (CRC) for New Technologies for Power Generation from Low-Rank Coal and A/Prof. Dong-ke Zhang are gratefully acknowledged. I would also like to thank the Department of Chemical Engineering for a supplementary scholarship.

I sincerely thank A/Prof. Xiao Dong Chen of The University of Auckland, New Zealand, for many valuable discussions and suggestions during the study. I also wish to thank Prof. Chuguang Zheng of Huazhong University of Science and Technology, China, for measurements of the heating values of the coal samples.

I acknowledge Mr. Bruce Ide, Mr. Jason Peak, Mr. Peter Kay, Mr. Brian Mulcahy, and Mr. Andrew Wright for their excellent technical supports during commissioning the apparatus and throughout the project. Assistance of Mr. Gary Klicke and Mr. Frank Myzka for sample preparations is greatly acknowledged. Thanks also go to Ms. Marnie Telfer for the SEM analysis assistance.

My gratitude towards the staffs and colleagues at Chemical Engineering Department for many valuable discussions and advice during the study, and for providing a pleasant atmosphere during the process of my research. I also wish to thank Mrs. Lynette Kelly, Mrs. Mary Barrow, and Mrs. Elaine Minerds for the secretarial support. Thanks also to friends and staffs of Kathleen Lumley College for making life in Adelaide unforgettable.

I would also like to acknowledge my parents, sisters, and brother, for their love and support, they have given me throughout my life. Last, but not least, I am indebted to my husband, Fujio Watanabe, for his love, patience, understanding, and constant support and encouragement over the past few years.

SUMMARY

Spontaneous combustion of coal has been a serious problem for coal producers and users for many years, particularly during storage and transportation. Many experimental techniques and models have been developed and applied to study and describe the self-heating and spontaneous combustion phenomenon of coal. However, the inhomogeneity of coal, the complexity of the system, and the variability of experimental techniques used, caused various inconsistent, confusing, and sometimes conflicting results in the literature.

The primary objectives of the current study is to use different experimental techniques to study the spontaneous combustion behaviour of the same material. In such a way, the influence of system conditions involved in the different techniques can be understood with confidence, thus providing an improved understanding of the spontaneous combustion.

Three experimental techniques are used to examine the self-heating behaviour of a Victorian brown coal, which is well known to exhibit a high propensity towards spontaneous combustion. The experimental techniques used include isothermal reactors, adiabatic reactors, and wire-mesh reactors with both steady-state and unsteady-state methods. In every reactor, the critical ambient temperature of the coal, above which spontaneous combustion occurs, is measured and used to indicate its tendency towards spontaneous combustion. The higher the critical ambient temperature, the lower the risk of spontaneous combustion. Emphasis of the current study is given to not only the influence of coal properties and ambient conditions, but also the experimental techniques on the self-heating behaviour of the coal. Low-temperature oxidation kinetics of samples tested in each technique are estimated using an energy balance approach. The kinetic constants obtained are then used to estimate the coal reactivities and the critical layer thickness, above which a coal deposit is capable of undergoing spontaneous combustion.

The results obtained from the isothermal reactor experiments show that there is an optimum air flow rate with which the coal self-heating could be easily induced. The effect of air flow rate on the critical ambient temperature is also investigated in an adiabatic reactor. It is revealed that within the experimental range, the air flow rate does not affect the critical ambient temperature but the time-to-ignition. The higher the air flow rate, the shorter the time-to-ignition. It is also observed that a high ambient temperature and a humid environment help accelerate the coal spontaneous combustion. Coal particle size significantly affects the coal self-heating. The smaller the particle size, the lower the critical ambient temperature, and thus the higher the risk of spontaneous combustion. The effect of coal drying methods on the coal self-heating behaviour, and the effects of reactor size, reactor specific surface area, and coal packing density on the critical ambient temperature are also investigated in this study.

Furthermore, the results obtained from different techniques show similar trends in which the critical ambient temperature varies with coal properties, ambient conditions, packing density, and reactor size. However, substantial variations are observed in the critical ambient temperature, the time-to-ignition, and the critical layer thickness predicted from different techniques. This indicates that the experimental technique used significantly affects the coal self-heating behaviour. Accordingly, precautions must be taken when comparing the experimental results obtained from different techniques.

This thesis also aims at examining the effect of inherent inorganic matter and additives on coal spontaneous combustion. Fourteen samples are prepared, namely, the raw coal, water-washed coal, acid-washed coal, and acid-washed coal doped with eleven additives. Each of the samples is then tested in an isothermal reactor to obtain its critical ambient temperature. The relative effectiveness of the additives is determined by comparing their critical ambient temperatures with that of the acid-washed coal. Potassium chloride, Montane powder, and sodium chloride are found to be the most effective inhibitors, followed by magnesium acetate, and calcium chloride. The presence of sodium nitrate and ammonium chloride in the coal

samples does not show any significant influence on the spontaneous combustion. However, calcium carbonate, sodium acetate, potassium acetate, and pyrite promote the spontaneous combustion. The effect of additive loading is also investigated for an inhibition agent (potassium chloride) and a promotion agent (sodium acetate). It is revealed that the effectiveness of these promotion and inhibition agents is enhanced with an increase in the additive loading. Low-temperature oxidation kinetics are also estimated by an energy balance approach and compared with the self-heating potential of these samples.

The inhibition and promotion agents of coal spontaneous combustion together with the effect of anions and cations on the capability of additives to either inhibit or promote the spontaneous combustion are further studied using the wire-mesh reactor technique. Acid-washed coal, and acid-washed coal doped with fourteen additives are prepared. Each of the samples is then tested in the wire-mesh reactor to obtain its critical ambient temperature. The presence of Na^+, K^+, and Cu^{2+} in their acetic and carbonate salts, promote spontaneous combustion, while sodium chloride and hydroxide inhibit spontaneous combustion. Magnesium acetate and carbonate inhibit spontaneous combustion. Ca^{2+} in different salts behaves differently. In its chloride and acetic salts, Ca^{2+} inhibits spontaneous combustion, while in the carbonate and hydroxide forms, it promotes spontaneous combustion. From the results, it can be concluded that the capability of the additives to affect spontaneous combustion depends on both cations and anions in the additives. The effect of additive loading is also investigated for an inhibition agent (calcium acetate) and a promotion agent (sodium acetate). The effectiveness of sodium acetate to promote spontaneous combustion is enhanced with an increase in the additive loading, while that of calcium acetate remains unchanged with varying loading. Low-temperature oxidation kinetics are also estimated by an unsteady-state energy balance approach and compared with the self-heating potential of these samples.

Whether the capability of the additives to either inhibit or promote the coal spontaneous combustion is physical or chemical in nature is also examined in this study by employing the ion exchange procedure in addition to the bulk-loading

procedure. The bulk loading of additives mixes the additives and coal samples both physically and chemically, while the ion exchange mixes them only chemically. The self-heating behaviour of ion exchanged samples are compared with those of the bulk loading samples. $Cu(Ac)_2$ and KAc in the ion-exchanged samples show stronger promotion effects on spontaneous combustion than their respective bulk-loading samples, indicating that their effects on spontaneous combustion are mainly chemical in nature. On the other hand, the inhibition effect of $Ca(Ac)_2$ was mainly physical in nature, while NaAc, $Mg(Ac)_2$, $CaCl_2$, and NaCl did not show a clear evidence if their effects were chemical or physical. Therefore, whether the capability of an additive to affect the spontaneous combustion is chemical or physical, is determined by the type of the additive used. SEM analysis is also employed to examine the surface structures and cation loadings of samples, bulk-loaded and ion-exchanged with $Cu(Ac)_2$. It is observed that the pore volume of ion-exchanged sample is larger than that of bulk-loading sample. Furthermore, the amount of copper inclusion in the ion-exchanged coal particle is higher and more uniformly distributed in the coal matrix than that in the bulk-loading coal particle.

This study highlights that the coal self-heating behaviour is dependent not only on coal properties and ambient conditions, but also on the system conditions involved in the experimental techniques used. Precautions must be taken when comparing the results obtained from different techniques so that misleading information can be avoided. From the study of the effect of inherent inorganic matter and additives on coal spontaneous combustion, it is proved that the inherent inorganic matter catalyses the self-heating processes, while different additives added in the coal sample play various roles in the coal self-heating behaviour. These additives could either inhibit or promote spontaneous combustion, depending on the cations and anions in the additives, the additive loading, and the additive application procedure.

TABLE OF CONTENT

LIST OF FIGURES

LIST OF TABLES

Chapter 1

INTRODUCTION

Coal is a worldwide source of energy and will be a major part of future energy supply (Speight (1994)). As summarised by Speight (1994), there is an excess of 1000 billion tons of coal reserves throughout the world and the consumption patterns shows that coal contributes to approximately 30% of energy market share. Accordingly, with the same consumption level, there will be sufficient amount of coal for many decades or even centuries (Siegel and Temchin (1991)). Besides, the low price of coal compared to oil brings coal as a major energy source for power generation (Siegel and Temchin (1991); Speight (1994)).

Recognising the important role of coal in the current and future energy supply, an understanding of coal science and utilisation is necessary. In this particular study, we concentrate on the coal spontaneous combustion investigation which has a great impact on commercial, environmental as well as safety aspects of coal production and utilisation.

Self-heating and spontaneous combustion of stored coal or coal-like materials (such as overburden of coal deposits) have long been known to pose a serious problem for coal producers and users. This is because self-heating of coal can lead to loss of desirable coal properties, loss of product, and safety concerns especially in the transportation of coal over long distance and in underground mining (Carras (1997); Glasser and Bradshaw (1990); Kim and Chaiken (1993); Krishnawamy et al. (1996a); Krishnawamy et al. (1996b); Krishnawamy et al. (1996c); Shrivastava et al. (1992); Stott and Chen (1992); Swann and Evans (1979)).

Mine fires is a disaster for a large area operation of coal mining, and can spread further if they are not immediately attended to. Associated hazards can be imposed in coal industry. For example: gas poisoning from the liberation of carbon monoxide (Kim and Chaiken (1993)), explosion that may happen if the fires contact with adequate concentration of fire damp or methane, etc. Besides causing a huge loss to national property, these fires may create hindrance to normal production or pose a threat to surface structures, adjacent property and life, and may create pollution problems as well.

As a result of these concerns, a good understanding of spontaneous combustion mechanisms is needed so that appropriate precaution and control measures can be taken. By taking an adequate preventive measure against the outbreak of the fires, it is possible to prevent the decrease in commercial value of the coal, danger to human health and safety, and pollution problems, as well as the decrease in efficiency of energy supply and use.

It is well acknowledged that the self-heating is a very complex phenomenon (Banerjee (1985); Carras et al. (1994); Carras and Young (1994); Chen (1991); Glasser and Bradshaw (1990)). The primary cause of coal spontaneous combustion is the interaction between coal and oxygen at ambient temperatures (Banerjee (1985); Bowes (1984); Carras and Young (1994)). This interaction is exothermic, thus liberating heat. If the heat is allowed to accumulate to raise the temperature, it enhances the rate of the reaction and can lead to a spontaneous combustion. Spontaneous combustion of coal is also influenced by other factors (Banerjee (1985); Carras et al. (1994); Chen (1991); Glasser and Bradshaw (1990); Kim and Chaiken (1993)), like the presence of pyrite, and the transport of moisture between the coal and the ambient. However, two main factors to be carefully considered are the heat generation (the heat of oxidation reaction) and the heat loss to the surrounding through the external surface. The latter is usually characterised by ambient conditions and a critical size (or critical thickness), above which the stockpile becomes capable of undergoing spontaneous combustion (Bowes (1984)).

The rate of oxidation reaction significantly depends on the coal type and properties. Therefore, the physical and chemical properties of coal are important factors influencing the self-heating process. Ambient conditions, geometry of the stockpiles or dumps, and the weather fluctuation also affect the self-heating processes.

Coal is a very inhomogeneous material. Coal obtained from mine or plant may have a wide variation in its chemical and physical properties. This inhomogeneous property is exasperated by the crushing or stacking effect (Glasser and Bradshaw (1990)). As a result, it is very difficult to examine the effect of physical and chemical properties of coal on the spontaneous combustion of coal stockpiles from a laboratory (small-scale) experimental work. Furthermore, the fluctuation of ambient conditions makes the prediction of the spontaneous combustion of coal stockpiles even more difficult. Unfortunately a large scale experimental work is very tedious and expensive. The results from a large scale experimental work are also very hard to be examined thoroughly due to the complexity of the process (Chen (1996b)).

Many experimental techniques and models have been developed and applied to study and describe the self-heating and spontaneous combustion phenomenon of coal. However due to the complexity of the system, there is not a single technique that can fully describe this phenomenon (Carras and Young (1994)). Furthermore, the inhomogeneity of coal and variability of experimental conditions used produce various conflicting or inconsistent results.

Recognising all those problems, small-scale experimental studies, which are done under consistent sample and experimental conditions, are required to identify all the important parameters affecting the coal spontaneous combustion. The results obtained can then be used to verify a mathematical model for predicting the spontaneous combustion of coal stockpiles.

This research is aimed at predicting the potential of a spontaneous combustion and reducing the probability of occurrence by alternative treatment. The overall aim of the current work is to generate knowledge that may lead to the development of an

effective tool for evaluating the risk of spontaneous combustion and establishment of effective technique for controlling the spontaneous combustion.

This knowledge will have wide applications in Australian and overseas coal industries. It will assist in reducing deleterious effects on the environment, and lead to improved overall performance of one of the nation's largest industries.

The main feature of the current work is to undertake experiments using different techniques with the same coal. Three experimental techniques are used to examine the self-heating behaviour of a Victorian brown coal, which is named as Coal M throughout this thesis. These experimental techniques are isothermal reactors, adiabatic reactors, and wire-mesh reactors (with steady-state and unsteady-state methods). Emphasis is given to the influence of not only coal properties and ambient conditions, but also the experimental techniques on the self-heating behaviour of the coal. In addition, the effects of inherent inorganic matter and additives on the coal spontaneous combustion are also examined.

The work embodied in this thesis is presented in the following six chapters.

Chapter 2 presents a literature review on investigations into the spontaneous combustion. Particular emphasis is given on the review of different experimental techniques used for the spontaneous combustion studies. The investigations on the various factors affecting coal spontaneous combustion are also reviewed.

Chapter 3 describes the sample preparation and the three experimental techniques used in the current work. Data analysis methods involved in the three techniques are also discussed in this chapter.

Chapter 4 discusses the experimental results obtained from the different techniques. The influence of coal properties and experimental techniques on the self-heating behaviour of Coal M and the reactivity estimated with each technique are described

in this section. The results obtained from different techniques are also evaluated in this chapter.

Chapter 5 discusses the effect of inherent inorganic matter and additives on the self-heating behaviour of Coal M. Correlation between reactivities, obtained from the energy balance approach, and self-heating behaviour observed in the experiments is also discussed in this chapter.

Chapter 6 further examines the roles of additives in the self-heating behaviour of Coal M and the effect of cations and anions on the capability of additives to either inhibit or promote the coal spontaneous combustion. Whether the capability of an additive to either inhibit or promote the coal spontaneous combustion is physical or chemical in nature is also discussed in this chapter.

Chapter 7 evaluates the results obtained in the current work and offers an interpretation based on the low-temperature oxidation reaction mechanisms. Validity of the energy balance used for kinetics determination and the practical relevance of the current work are also discussed in this chapter.

Chapter 8 summarises the conclusions drawn from the current study and outlines recommendations for the future work.

Chapter 2

LITERATURE REVIEW

2.1 INTRODUCTION

Extensive research effort has been devoted to the study of spontaneous combustion phenomenon of various combustible materials for many years. Significant progress, in both experimental and modelling approaches, has been made in understanding the role of various factors in the spontaneous combustion phenomenon as well as the mechanisms of the low-temperature oxidation reactions. However, further detailed knowledge is still required to further clarify various conflicting information found in the literature.

This chapter reviews the previous work, both experimental and theoretical studies, on the spontaneous combustion of various combustible materials, particularly coal. This is to provide a knowledge basis for further investigation. Following the critical evaluation of the previous work, areas where more research is required are identified and form the objectives of the current thesis.

2.2 COAL

2.2.1 Introduction

Coal is heterogenous and stratified organic rock, mainly containing organic matter. It primarily consists of carbon, hydrogen, and oxygen, and lesser amount of sulfur

and nitrogen as well as other trace elements. Coal also contains ash forming inorganic components distributed as discrete particles of mineral matter throughout coal substances.

Coal originated through the accumulation of plant debris that were later covered, compacted and changed into the organic rock, namely coal. This conversion was based on biological reaction followed by a very slow pyrolysis reaction under low rate of heating (Berkowitz (1979); Juntgen and Nat (1987); Speight (1994); Van Krevelen and Schuyer (1957)). This transformation successfully leads to peat, lignite, bituminous, and anthracite, which have different properties.

Coal is classified according to their properties. The generally accepted classification is the ASTM scheme, which distinguishes among four coal classes, each subdivided into several groups as shown in Table 2.1 (Berkowitz (1979)). In the ASTM scheme, high-rank coals (medium volatile bituminous or higher rank) are classified on the basis of volatile matter and fixed carbon contents, whereas low-rank coals are defined in term of their calorific value.

The coal rank indicates the degree of coalification (Banerjee (1985); Berkowitz (1979); Juntgen and Nat (1987); Singer (1984); Speight (1994); Van Krevelen and Schuyer (1957)). The fixed carbon content and heating value increase with coal rank, whereas volatile matter and moisture contents decrease with coal rank. This implies that a higher rank coal has experienced a greater coalification compared with lower rank coals.

However, properties of coal are not only influenced by their rank but also to a certain extent depend on the kind of precursor material and the environment during coalification process (Glasser and Bradshaw (1990); Juntgen and Nat (1987); Van Krevelen and Schuyer (1957)).

Table 2.1 ASTM coal classification by rank (Berkowitz (1979))

Class and group	Fixed Carbon[a] (%)	Volatile Matter[a] (%)	Heating Value[b] (MJ/kg)
I. Anthracite			
1. Metaanthracite	> 98	< 2	
2. Anthracite	92-98	2-8	
3. Semianthracite	86-92	8-14	
II. Bituminous			
1. Low volatile	78-96	14-22	
2. Medium Volatile	69-78	22-31	
3. High Volatile A	< 69	> 31	> 32.5
4. High Volatile B			30.2 - 32.5
5. High Volatile C			24.4 -30.2 [c]
III. Subbituminous			
1. Subbituminous A			24.4 - 26.7[c]
2. Subbituminous B			22.1 - 24.4
3. Subbituminous C			19.3 - 22.1
IV. Lignite			
1. Lignite A			14.6 - 19.3
2. Lignite B			< 14.6

[a] Calculated on dry, mineral-matter-free coal; correction from ash to mineral matter made by means of Parr formula

[b] Calculated on mineral-matter-free coal with bed moisture content

[c] Coals with heating values between 24.4 and 26.7 MJ/kg are classed as high volatile C if they posses "agglutinating" properties or as subbituminous A if they do not.

2.2.2 Nature and Origin of Coal Versus Its Role in Spontaneous Combustion

Coal is an eminently inhomogeneous material (Glasser and Bradshaw (1990)). Its physical and chemical properties, and thus its propensity towards spontaneous combustion, strongly depend on both its origin and the condition under which the coalification process occurred.

Schmidt (1945) observed that coal with a higher oxygen content is more reactive towards oxidation reaction. Upon heating, the oxygen in the coal would be desorbed as carbon dioxide and carbon monoxide and thus provides more available active sites for the oxidation reaction. This supports the general information that a low-rank coal, which generally contains more oxygen than high-rank coal, is more reactive towards the spontaneous combustion.

Another work done by Van Krevelen and Schuyer (1957) showed that the ignition temperature is indeed a function of coal rank, although coals with the same rank may have very different ignition temperature as shown in Figure 2.1.

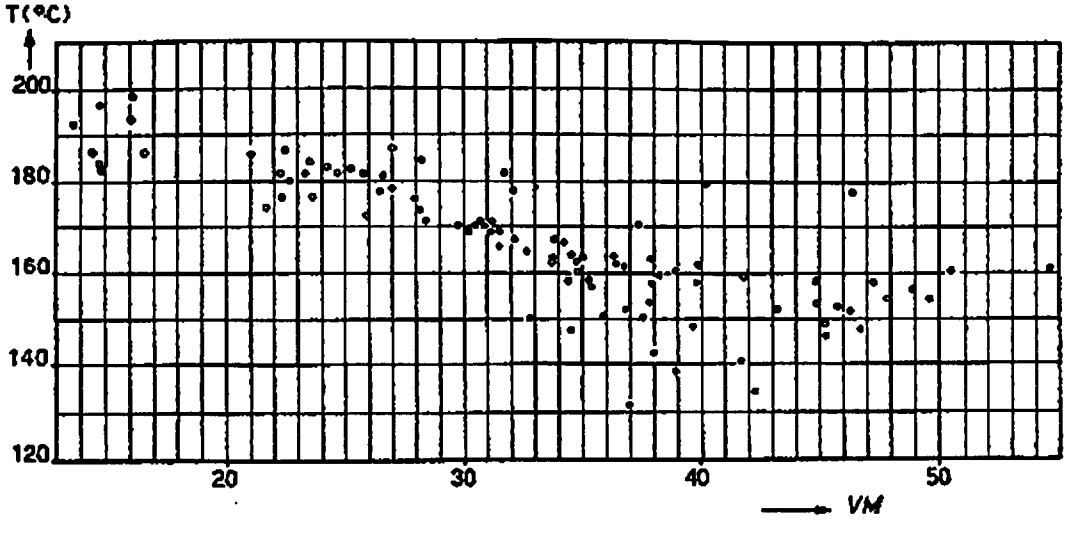

Figure 2.1 Relationship between ignition temperature and volatile matter content of coal (reproduced from Van Krevelen and Schuyer (1957))

On the other hand, Kaji et al. (1985) found that different ranks of coals could have similar active sites for the oxidation reaction and thus similar oxidation reaction rates.

From these conflicting results, it can be concluded that analyses which attempt to correlate the rate of oxidation with coal rank, is not accurate enough to predict the spontaneous combustion of coal storages or stockpiles (Glasser and Bradshaw (1990); Kim and Chaiken (1993)).

2.3 LOW-TEMPERATURE OXIDATION AND SELF-HEATING OF COAL

2.3.1 Interaction of Coal with Oxygen and Self-Heating

The primary cause of self-heating is the interaction between coal and oxygen at ambient temperatures. This interaction liberates heat. If the heat is allowed to accumulate, it enhances the rate of oxidation reaction of coal and leads to fire known as spontaneous combustion. Obviously, spontaneous combustion of coal not only depends on the interaction between oxygen and coal but also the physical conditions of the storage that satisfy the heat accumulation to initiate the spontaneous combustion. Therefore, whether the spontaneous combustion will occur or not in a given storage pile is determined by the rate of heat generated from oxidation of coal and the rate of heat loss from the pile.

Figure 2.2 illustrated the main features occurring in and around a coal stockpile, as summarised by Carras and Young (1994). Air flows into the coal stockpile by diffusion, and natural or forced convection, providing the oxygen for oxidation

reaction. Some of the heat produced is driven away from the stockpile but some stays inside the stockpile. Depending on the relative humidity of the atmosphere and the equilibrium moisture content of the coal stockpile, the water vapour transfers into or away from the stockpile. Dry coal adsorbs water vapour from the air. This process also liberates heat, thus helps accelerate the self-heating.

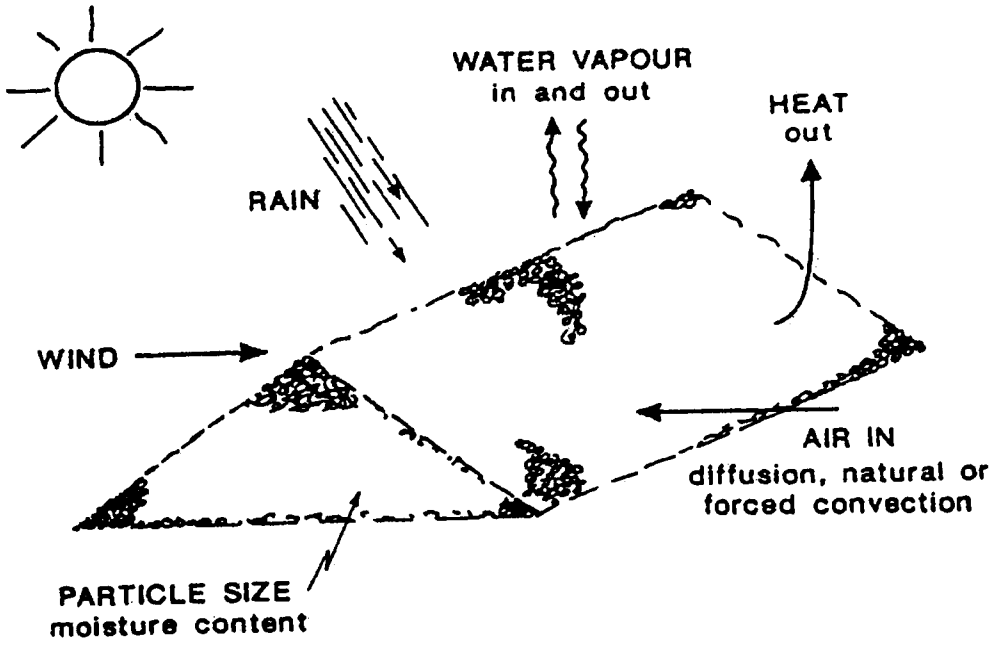

Figure 2.2 A schematic diagram of a coal stockpile undergoing self-heating under the influence of various physical and chemical processes (reproduced from Carras and Young (1994))

Outdoor stockpiles are also affected by the weather through wind, rain, and solar radiation (Carras and Young (1994); Glasser and Bradshaw (1990)). A sunny day followed by a rainy day could be a danger for coal stockpiles. The coal is dried on the sunny day. When the rain comes, however, the coal starts adsorbing the moisture, hence liberating a significant amount of latent heat which helps accelerating the self-heating process.

Physical properties of coal, such as particle size, moisture content, porosity, also significantly influence the transport processes, the overall oxidation rate and hence self-heating of coal. These are discussed in detail in Section 2.3.2.1.

There have been many studies on the self-heating phenomena of combustible materials. The main aim is to determine the critical conditions for the combustible material to undergo self-heating. Another most common aim of the previous research is to predict the safe storage time. To achieve these aims, it is necessary to precisely determine the mechanism and kinetics of the oxidation reaction at low temperatures. Obviously, these parameters should be obtained by methods which ensure realistic and representative data for full-scale storage conditions. From this point of view, the study of low-temperature oxidation mechanism of coal is important.

2.3.1.1 Low-temperature oxidation mechanism of coal

As it has been established, elementary steps involved in gas-solid reactions, when solid is consumed and there is no solid reaction product, are: (1) gas phase mass transfer (external diffusion); (2) pore diffusion; (3) chemical reaction at the solid surface (Szekely (1977)). The resistances in different steps usually varies greatly, depending on reactions that occur in the process; the step with the greatest resistance, ie. the slowest step, is the rate-controlling step. A sketch of the reaction regimes in the gas-solid reaction is illustrated in Figure 2.3 (Szekely (1977)).

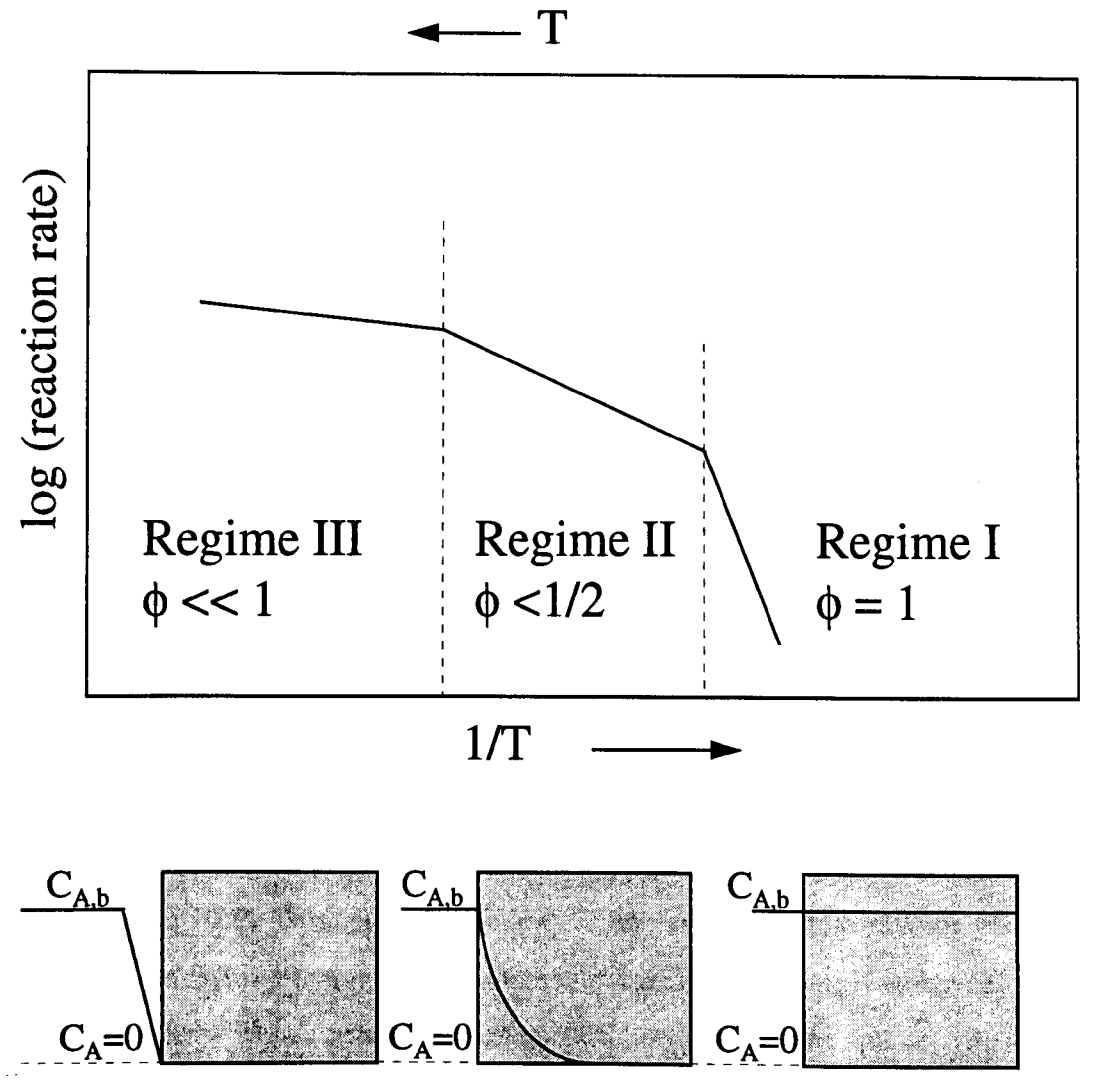

Figure 2.3 A sketch of the reaction regimes in a gas-porous solid reaction when the solid products do not form (Szekely (1977))

A reaction of a porous solid with a gas may be divided into three kinetic regimes (Fogler (1981); Harris (1997); Karsner and Perlmutter (1981); Krishnawamy et al. (1996b); Levenspiel (1972); Szekely (1977)). As shown in Figure 2.3, Regime I occurs when the temperature is so low that the chemical reaction rate is very small compared with other steps. In this regime, the concentration of the gaseous reactant is uniform throughout the porous solid and equal to that in the bulk of the gas stream. All the internal surface area of the reacting solid is available for reaction, and the whole solid reacts at a uniform rate at any given time. As the temperature

increases (Regime II), the chemical reaction rate increases and the overall reaction rate is controlled by both pore diffusion and chemical reaction. In this regime, only part of the internal area is available for the oxidation reaction and the particle reacts both internally and externally with decreasing in both diameter and density (Harris (1997)). The rate of reaction in this regime is less dependent on temperature. Further increasing temperature (Regime III) increases chemical reaction rates so greatly that the reactant is consumed on the external surface of coal, thus the overall rate is controlled by external mass transfer. This regime provides the highest overall rate and the temperature only has a slightly effect on the rate of reaction. The concentration of the gaseous reactant falls to zero at the outer surface of the solid reactant. A summary of gas reactant concentration profiles for the three regimes is presented in Figure 2.3 (Szekely (1977)).

For low-temperature oxidation reaction of coal, the process may be divided into three stages (Carras and Young (1994); Chen and Stott (1993); Clemens et al. (1991); Swann and Evans (1979)). The first stage occurs when the temperatures increase up to 70°C. This stage is primarily characterised by the formation of coal-oxygen complexes (carbonyl-containing products including aldehydes and carboxylic acids) which result from interaction between oxygen and active sites in the coal structure. As the temperature increases, these complexes will decompose into gaseous products such as carbon monoxide, carbon dioxide, and water vapour. At temperatures around 150 - 180 °C, a new set of coal-oxygen complexes (ester) forms exothermically. The oxidation process will continue until all carbon is consumed.

The sequences of low-temperature oxidation reaction of coal are described in detail by Clemens et al. (1991) as follows.

$$\text{Coal} - CH_2 - \text{Coal} \xrightarrow{\dot{R}} \text{Coal} - \dot{C}H - \text{Coal} + RH \qquad \text{(R-1)}$$

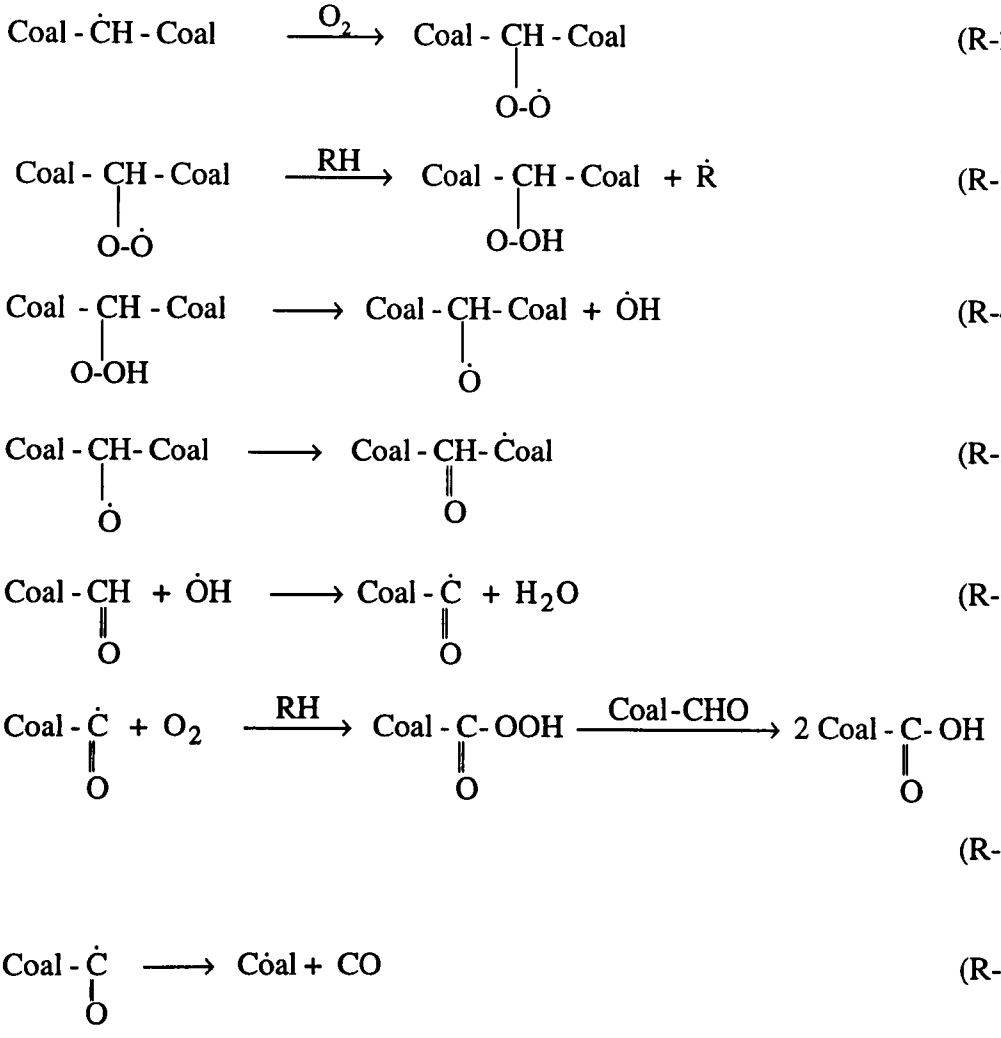

The above reactions are found to be responsible for determining the self-heating of coal at temperatures ranging from ambient to an ignition temperature (Clemens et al. (1991)).

2.3.1.2 Low-temperature oxidation kinetics of coal

To evaluate coal reactivity in the self-heating, determination of low-temperature oxidation kinetics is required. Research attempted to correlate the chemisorption rates of oxygen with the reactivity of the coal towards the self-heating using Elovich equation, has been done rather intensively (Bowes (1984); Carpenter and Giddings

(1964); Carpenter and Sergeant (1966a); Furimsky et al. (1988); Harris and Evans (1975); Kaji et al. (1987); Khan et al. (1990)). This equation is commonly used to describe the relation between the rate of oxygen adsorbed and the amount of oxygen uptake. The Elovich equation is given below.

$$\frac{dq}{dt} = a\exp(-\alpha q) \qquad (2\text{-}1)$$

Unfortunately, the laboratory results can only fit this equation in early stages of oxidation reaction and in a narrow temperature range (Bowes (1984); Harris and Evans (1975); Khan et al. (1990)). The chemisorption of oxygen decreases exponentially with the extent of sorption due to a decrease of available active sites. However, the desorption of gaseous oxidation products (carbon monoxide, carbon dioxide, and water vapour) creates fresh active sites for the chemisorption, and thus causes the deviation (Bowes (1984); Carpenter and Sergeant (1966a); Harris and Evans (1975)). Furthermore, this equation ignores the diffusion term which could cause a certain error in the reaction rate calculated.

More commonly used, however, is the Arrhenius equation (Bowes (1984); Carras and Young (1994); Schmidt (1945)):

$$\frac{dC_A}{dt} = A C_A^n \exp\left(\frac{-E}{RT}\right) \qquad (2\text{-}2)$$

The apparent order of oxidation reaction of coal at low temperatures varies from 0.5-1.0 (Bowes (1984)).

2.3.2 Factors Influencing Self-Heating

As mentioned previously, the primary cause of self-heating is the interaction between coal and oxygen in air at ambient temperature. The physical and chemical properties of coal and the ambient conditions play important roles in the self-heating processes. It has also been well acknowledged that there are other factors that also assist the self-heating of coal. They include the presence of pyrite in the coal and the action of bacteria.

Pyrite present in coal can assist oxidation reaction of coal by providing more active sites for the oxidation reaction. In moist condition, pyrite is oxidised readily according to the following reaction (Banerjee (1985); Shrivastava et al. (1992)),

$$2\,FeS_2 + 7\,O_2 + 16\,H_2O \text{ ---------> } 2\,H_2SO_4 + 2\,FeSO_4.7H_2O + 1322\ kJ \qquad \text{(R-9)}$$

As it is shown, the oxidation reaction of pyrite in the moist condition is exothermic. Thus it increases the temperature of coal and helps accelerating the oxidation reaction of coal. Furthermore, the reaction products have a greater volume than the reactant and may break down the coal structure in which they are embedded and thus provide a greater accessible surface area for oxidation reaction (Banerjee (1985); Shrivastava et al. (1992)). However, it is stated by Banerjee (1985) that pyrite is able to exert a significant effect on the coal self-heating only if it is present in considerable proportion, ie. more than 5% and with a very fine particle size.

Bacterial actions also have an effect on the self-heating of haystacks and wood but this is less significant for coal (Banerjee (1985)).

Besides these two factors, there are other factors that more significantly contribute to the self-heating of coal. These include the physical and chemical properties of coal (particle size, moisture content, porosity, and inorganic impurities), the ambient

conditions, (e.g. temperature, air humidity, air flow rate), dimension of the dump, and transport processes. These factors are explained in detail below.

2.3.2.1 Physical properties of coal

The physical properties of coal, like particle size, moisture content, voidage, and etc., influence the transport processes, the overall oxidation rate and thus self-heating of coal. This section discusses these effects.

2.3.2.1.1 *Particle Size*

The coal particle size is an important factor in self-heating processes. Theoretically, the greater the surface area per unit weight of coal, the higher the rate of oxidation. However, it was found that the rate of oxidation is independent of particle size when it is smaller than a critical diameter (Akgun and Arisoy (1994); Carpenter and Sergeant (1966a); Kaji et al. (1985); Karsner and Perlmutter (1981); Palmer et al. (1990); Smith and Lazzara (1987)). This phenomenon can be explained as follows. At ambient temperatures the rate of oxidation is very slow. For large porous particles, oxygen may not be able to penetrate inside the coal, because the mass transfer of oxygen depends on the coal particle size. Consequently, large particles do not react uniformly. Inversely, for small particles, oxygen can diffuse easily into the coal. Thus, the small particles react rather uniformly throughout the particles.

Previous investigations found that the rate of oxidation increases with a decrease in particle diameter until a critical diameter is reached (Akgun and Arisoy (1994); Carpenter and Sergeant (1966a); Kaji et al. (1985); Karsner and Perlmutter (1981); Palmer et al. (1990); Smith and Lazzara (1987)), below which the rate of oxidation reaction does not vary. Above this critical value, the oxidation rate is approximately proportional to the external surface area of the particle with the power of 0.3

(Carpenter and Sergeant (1966a)). Carpenter and Sergeant (1966a) and Palmer et al. (1990) found that the critical diameter of the coal used in their investigations are 138 and 387 μ m, respectively. Other investigators found that the critical diameter is 50 μ m (Furimsky et al. (1988)), 1 mm (Kaji et al. (1985)), and 2.31 mm (Bowes (1984)). It is believed that the critical diameter must be coal type dependent.

Karsner and Perlmutter (1982) observed that, within their experimental conditions, the rate of oxidation reaction of an Illinois bituminous coal did not change with particle sizes. They suggested that pore structure of the coal plays a more significant role in the oxidation reaction than the particle size. It has also been investigated that coal particles of different size distributions have different properties because of different H/C ratio, ash and sulphur contents, and different surface structures among those different size fractions (Palmer et al. (1990)). Therefore, to predict the reactivity of coal from changes in the surface structures may be misleading for coals that have a wide range of particle sizes. Furthermore, the temperature ranges of the process also determine whether particle size subtantially affects the coal self-heating. At high temperatures, the diffusion tends to control the reaction, thus particle size significantly affects the oxidation reaction, while at low temperatures the opposite is true.

2.3.2.1.2 *Porosity*

The pore structure of coal plays an important role in coal oxidation reactions. Coals with large pore volumes have greater oxidation rates, thus greater propensity towards self-heating process (Kaji et al. (1985); Karsner and Perlmutter (1982)).

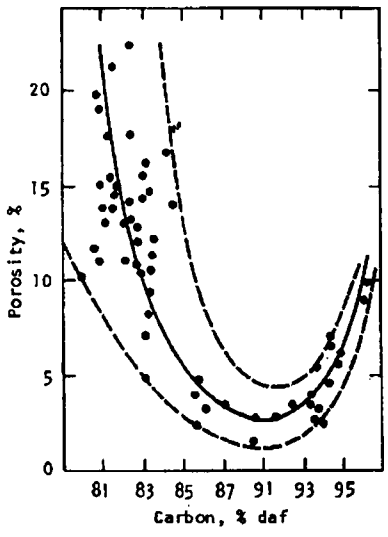

Figure 2.4 Variation of coal porosity with rank (reproduced from Berkowitz (1979))

The porosity of coal as a function of carbon content has been measured by several authors using various methods, as reviewed by Berkowitz (1979). A summary of their results is presented in Figure 2.4. It is shown that the total porosity of coal falls from about 25 ~ 30% (for lignites and subbituminous C coals) to as small as 1 or 2% (for coals containing 87-89% carbon) and then increases slightly for coals with higher carbon contents. This physical structure of coal changes as the coal combustion occurs (Singer (1984)). Kaji et al. (1985) found that pores having radii $>100\,\text{Å}$, together with oxygen-containing groups which decompose to CO_2 and/or CO, play important roles in the low-temperature oxidation reaction.

2.3.2.1.3 *Moisture Content*

The moisture content effect on the self-heating of coal has been widely reported in the literature (Banerjee (1985); Bhat and Agarwal (1996); Bhattacharya (1971); Bhattacharya (1972); Buckmaster and Kudynska (1992); Carpenter and Sergeant (1966b); Carras and Young (1994); Chen (1991); Chen (1992); Chen (1994); Chen (1996a); Chen and Stott (1993); Chen and Wake (1994); Clemens and Matheson

(1996); Dack et al. (1983); Gray and Wake (1990); Ogunsola and Mikula (1991); Ogunsola and Mikula (1992); Petit (1991); Smith and Lazzara (1987)). However, debates about how moisture content affects the oxidation reaction rate still continue.

The effect of moisture on the self-heating process is very complex. When coal moisture content is present in sufficient amount, it suppresses the self-heating process by reducing the available active sites, blocking the access of oxygen into the coal particle (the diffusion rate of oxygen in water is very low), as well as taking up the heat generated from oxidation reaction for the evaporation process (Bhat and Agarwal (1996); Bhattacharya (1971); Bhattacharya (1972); Chen (1996); Clemens and Matheson (1996)).

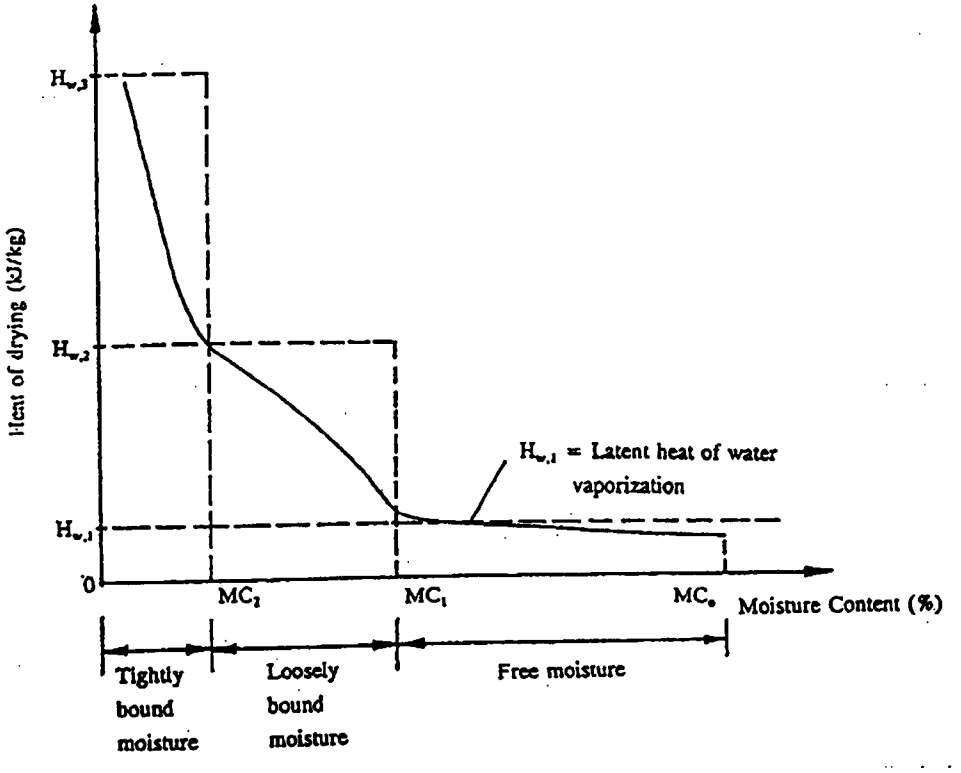

Figure 2.5 The heat of drying as a function of the moisture content (reproduced from Chen (1994)

Further work by Chen (1994) pointed out that there are more than one type of moisture existing in coal; different amounts of energy are needed to fully drive off

these moistures. The correlation between heat of drying and moisture content is shown in Figure 2.5. MC_1 and MC_2 are the 'critical moisture contents' that divide the moisture content into three ranges, ie. free moisture, loosely bound moisture, tightly bound moisture. $H_{w,1}$, $H_{w,2}$, and $H_{w,3}$ are the levels of heat required for drying in the three moisture ranges, respectively, where $H_{w,1}$ is equal to the latent heat of water vaporisation at 1 atm. It is shown that the heat of drying increases with decreasing moisture content. As there are three energy levels involved in the heat of drying, the temperature profile of coal containing different types and quantities of moisture is different.

When coal moisture content is present in a reasonably small amount, the suppressing effect will become negligible. Chen and Stott (1993) found that there is a critical moisture content, i.e. 7-17% db below which no further increase in the oxidation reaction rate occurs. This is supported by more recent work by Vance et al. (1996) and Clemens and Matheson (1996). The reason of this could be due to the catalytic effect of moisture on the processes enhancing the oxidation reaction rate (Banerjee (1985); Clemens and Matheson (1996)). As the oxidation of pyrite occurs in a moist condition, the coal moisture encourages the oxidation of pyrite. Furthermore, the moisture also acts as a catalytic agent in the formation of peroxide intermediate, which can accelerate the self-heating of coal. It has also been observed that the thermal responses of a low-rank coal, dried by heating in a nitrogen flow at 105°C, is similar to that observed when the coal dried at 30°C in nitrogen, which allows tightly bound moisture content to remain (Clemens and Matheson (1996)). This is so because the moisture affects the nature of the radical sites where the oxidation reaction occurs. The tightly bound moisture hinders the formation of stabilised radicals. This encourages a faster oxidation reaction rate that may lead to enhanced thermal response, although some of the heat may be consumed by the residual moisture for evaporation.

When the coal is dry, however, it absorbs water from the air, ie. condensation process. This process is an exothermic reaction and liberates significant heat. It has

been found that at low temperatures, the rate of heat liberated from the condensation process is more significant than that from the oxidation reaction (Bhat and Agarwal (1996); Bhattacharya (1971); Bhattacharya (1972); Smith and Lazzara (1987)). This is due to the low solubility of oxygen in water which significantly hinders the oxidation reaction to occur.

In addition, it has been pointed out that the mechanism of coal oxidation above 70°C is not the same as at lower temperatures (Berkowitz (1979); Clemens et al. (1991); Swann and Evans (1979)). Below 70°C the oxidation reaction is so slow that the restriction of the exposing active sites does not have any significant effect. However, the acidic function and peroxides are generated, which enhance the oxidation reaction (Banerjee (1985); Clemens et al. (1991); Singer (1984)). A higher moisture content promotes these reactions because oxygen dissolved in the water is responsible for the formation of peroxide. On the other hand, at temperatures above 70°C, peroxide effect is not dominant any more. Therefore, a high moisture content could prevent further increase of coal temperatures due to the evaporation of the coal moisture and restriction of the exposing active sites by the moisture.

While a pre-drying process is generally believed to accelerate the self-heating process, other work provides an opposing view (Carr et al. (1995); Chen (1994); Clemens and Matheson (1996); Deevi and Suuberg (1987); Gorbaty (1978); Inggram and Rimstidt (1984); Swan et al. (1973)). Removal of water can change the physical and chemical nature of the coal (Carr et al. (1995); Chen (1994); Clemens and Matheson (1996); Deevi and Suuberg (1987); Gorbaty (1978); Inggram and Rimstidt (1984); Swan et al. (1973)). The physical change of the coal structure from the wetting and drying processes is caused by internal stresses that arise from unequal volume changes. This takes place as water is absorbed and desorbed faster on the outer part of the particle than the inside. Changing physical nature also influences the chemical nature of the material. As a result, the extent and method of drying influence the concentration and nature of the reactive sites within a coal.

Weathering process also plays a certain role in the self-heating process. Numerous research has been devoted to examine this phenomenon (Dack et al. (1983); Inggram and Rimstidt (1984); Liotta et al. (1983); Ogunsola and Mikula (1992); Petit (1991); Shrivastava et al. (1992)). It has been reported that weathering of coal involves complex chemical and physical processes (Inggram and Rimstidt (1984); Shrivastava et al. (1992)). The absorption and desorption of water vapour occur on the surface of the coal particle are faster than inside the coal particle. Hence, the unequal volume changes would cause an internal stress. Consequently, the wetting and drying processes during weathering can lead to a physical breakdown in coal structure. This provides a greater surface area for the oxidation reaction and eases the penetration of the oxygen into the coal particle processes (Inggram and Rimstidt (1984); Shrivastava et al. (1992)). Furthermore, Inggram and Rimsdith (1984) pointed out that the major processes occurring during the weathering process may include formation of humic acids by the oxidation of organic substances in coal. These humic acids provide more sites available for hydrogen bonding of water in the monolayer which could increase the liability of coal towards the spontaneous combustion.

2.3.2.2 Ambient conditions

2.3.2.2.1 *Temperature*

The rate of oxidation reaction of coal is strongly dependent on the ambient temperature. The higher the temperature, the faster the oxidation reaction, thus the more likely the spontaneous combustion would occur. The dependence of the rate of oxidation reaction of coal on temperature follows the Arhennius law.

2.3.2.2.2 *Air Humidity*

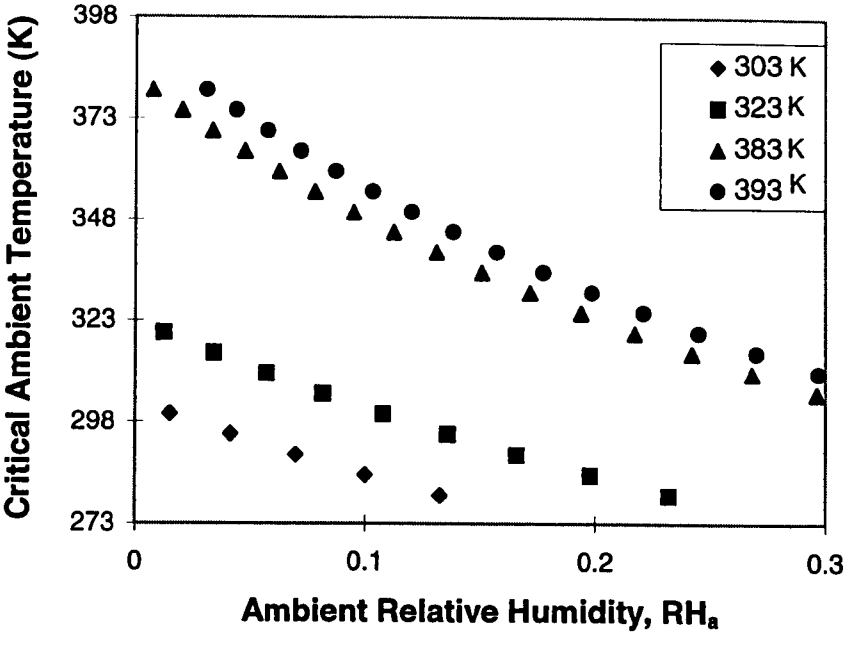

Figure 2.6 The influence of ambient relative humidity, RH_a, on the critical ambient temperature (calculated at several critical ambient temperatures under dry conditions) (Chen and Wake (1994))

The humidity of air and the equilibrium moisture content of the coal in stockpiles determine the amount of latent heat that may be added to or provided by the stockpiles. Chen and Wake (1994) developed a model, which is extended from Frank-Kamenestkii model, to examine the effect of air humidity on spontaneous combustion process. Their model provided a correlation between the critical ambient temperature, above which a thermal runaway occurs, and ambient relative humidity, as shown in Figure 2.6. It appears that the presence of moist environment significantly decreases the critical ambient temperatures, thus increases the risk of the coal to spontaneously combust. This indicates that a humid environment helps accelerate the self-heating process since it prevents a further evaporation of coal moisture (Banerjee (1985); Chen and Wake (1994); McIntosh and Tolputt (1990)).

In the case of a very dry coal, the humid environment is more prominent in providing the heat to accelerate the oxidation reaction. This is because dry coal adsorbs water vapour from the air, which liberates heat.

2.3.2.2.3 *Wind and Sun Radiation*

As mentioned previously, outdoor stockpiles are also affected by the weather through wind, rain and sun radiation. The wind provides oxygen for the oxidation reaction, and dissipates heat from the stockpiles. Because of the low thermal capacity of air, the heat dissipated into the surrounding is usually small compared with heat of oxidation or heat of drying (Clemens et al. (1991); Krishnawamy et al. (1996a)). However, a very large air flow rate can keep the coal sufficiently cool. Similarly, a very small air flow rate may not be able to supply enough oxygen for the oxidation reaction.

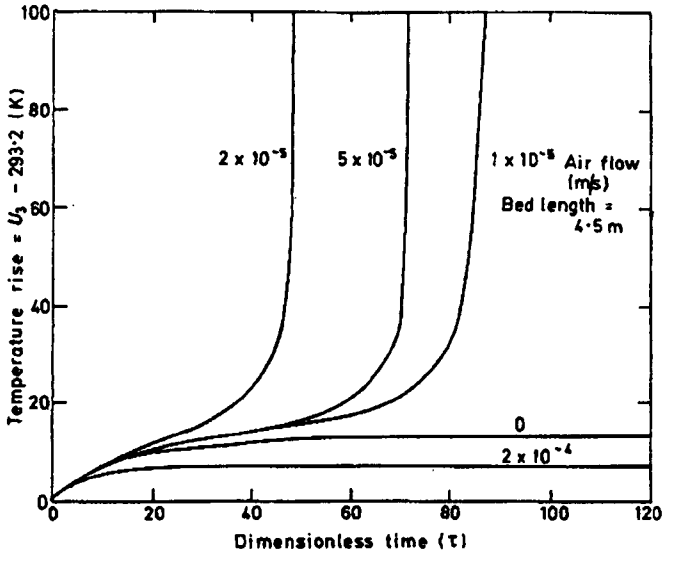

Figure 2.7 Graph showing the effect of increasing air flow on the temperature of a coal bed of length 4.5 m (reproduced from Nordon (1979))

The effect of the air flow rate on the temperature increase inside the coal bed has been simulated by Nordon (1979), and plots from his work is presented in Figure

2.7. It is shown that with no air and an air flow of 2 x 10^{-4} ms^{-1}, increases in temperature are very slow and a steady-state condition is attained. On the other hand, at intermediate air flows, i.e. 1 x 10^{-5} to 5 x 10^{-5} ms^{-1}, the temperature increases sharply. This model supports the theory described above. Later work by Schmal et al. (1985) also supports this theory. They found that the rate of temperature rise in a moist coal bed increases with the increase in air flow rate.

Further work by Glasser and Bradshaw (1990) pointed out that the effect of wind is dependent on the reaction controlling regime. In the case of chemical reaction control, the wind would take away the heat generated from oxidation reaction and make the stockpiles safer. On the other hand, if the overall reaction is controlled by diffusion, wind can provide sufficient oxygen for the oxidation reaction to occur, thus make the stockpiles less safe.

Depending on the intensity and duration of the sun radiation, it could cause the spontaneous combustion of coal stockpiles. A sunny day followed by a rainy day could be a big danger for coal stockpiles. The coal is dried on the sunny day. When the rain comes, however, the coal starts adsorbing the moisture, hence liberating a significant amount of latent heat which helps accelerating the self-heating process. Rain fall wets the coal stockpiles particularly near the surface of the stockpiles, thus suppress the self-heating there. However, this wet surface can prevent the heat loss from the interior stockpiles, thus accelerates the self-heating and spontaneous combustion of the stockpiles.

2.3.2.3 Mass and heat transport mechanisms

Transport processes occurring in the coal stockpiles significantly influence the self-heating of coal stockpiles. As has been summarised by Glasser and Bradshaw (1990) and others (Gatica et al. (1989); Young et al. (1986)), the transfer of gaseous reactants, particularly oxygen and water vapour, into the coal stockpile is caused by

natural convection. This is due to density differences between the gas inside and outside the stockpiles, arising from temperature differences; flow caused by differential pressure between inclined and flat surface of the stockpiles (e.g. wind), molecular diffusion caused by concentration gradients, and barometric and thermal breathing. The heat transfer mechanisms occurring inside the coal stockpiles are by conduction, convection, radiation, and evaporation or condensation of water vapour.

The transport processes are influenced by method of storage (compactness, pile geometry and dimensions), particle size distribution of the coal, moisture content, coal physical properties (density, specific heat capacity, thermal conductivity, etc), as well as the ambient conditions (Schmal et al. (1985)). As stated by Schmal et al. (1985), there is a correlation between the storage method, ie. the compaction of the coal inside the pile, with the transport processes. When the porosity of coal piles is small, the diffusion and conduction are responsible for the mass and heat transfer. Therefore, the temperature rise is restricted and takes a longer time to develop. When the porosity is very high, however, natural convection is the most important transport mechanism. In moderate conditions, when the coal is stored loosely with moderate pore size and air flow rate, the mass transfer is mainly by convection and the heat transfer is mainly by conduction. In this case, a high temperature can be reached in a relatively short period of time.

Krishnawamy et al. (1996a) developed a model to compare the effect of forced convection and natural convection during the self-heating process. Their model is derived by the expression developed by Brooks and Glasser (1986) :

$$G = \left\{ \frac{u_w^2}{2Lg} + \frac{\overline{T} - T_a}{\overline{T}} \right\} \qquad (2\text{-}3)$$

By using the annual average wind velocity, they found that the forced convection is more dominant compared with the natural convection before or after a thermal runaway occurs. However, the contribution of the forced convection decreases with

an increase in the length of the bed. Since the model is derived for a one-dimensional system, it may not be appropriate when it is applied to real stockpiles.

Further work of Glasser and Bradshaw (1990) has drawn a conclusion that natural convection is the only mechanism which can cause the spontaneous combustion. The other mechanisms participate as a trigger rather than the cause of the spontaneous combustion in a coal stockpile (Glasser and Bradshaw (1990)).

2.3.2.4 Dimensions of Coal Stockpiles

The maximum temperature attained by self-heating depends on stockpile size and the compaction of coal inside the stockpile. However, it has also been acknowledged that the dimensions of coal stockpile are an important factor determining the occurrence of spontaneous combustion. Since air has a small heat capacity, the heat dissipated into the surrounding is usually small compared with heat of oxidation or heat of drying (Clemens et al. (1991); Krishnawamy et al. (1996a)). Therefore, availability of oxygen in a stockpile is a more critical factor in determining the safety of the stockpile. The effect of stockpile slopes on the maximum temperature rise as a function of time was modelled by Krishnaswamy et al. (1996a) and presented in Figure 2.8. T_{max} used in Figure 2.8 was defined as maximum average temperature within the coal stockpile, while T_a was the ambient temperature. They (Krishnaswamy et al. (1996a)) pointed out that a steeper slope provides a higher driving force for convective flow and thus larger amount of oxygen available for the oxidation reaction. A stockpile with a slope within 11.3° to 18.4° is recommended for minimising the spontaneous combustion (Allan and Parry (1954); Krishnawamy et al. (1996a)).

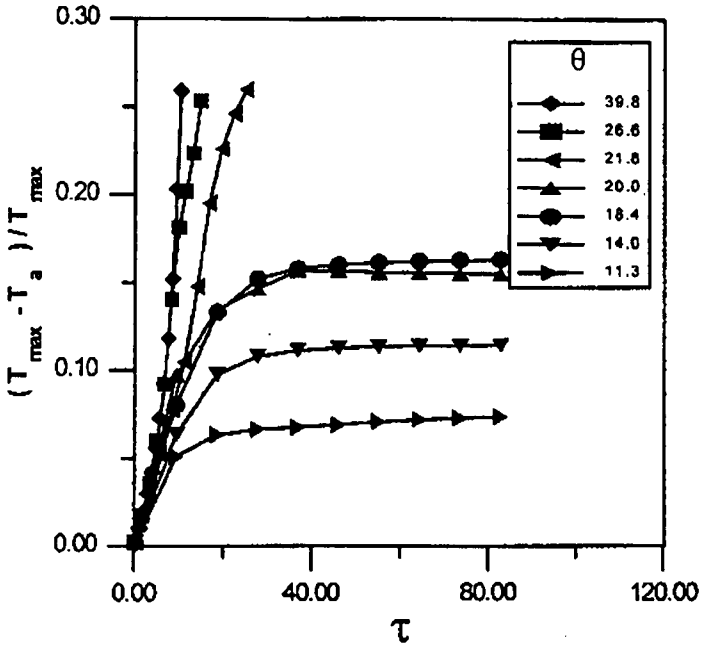

Figure 2.8 Influence of Side Slope (θ) on calculated $(T_{max}-T_a)/T_{max}$ as a function of time (τ) for u_w (wind velocity) = 4.46 ms^{-1}; ε_b (bed porosity)= 0.1 (reproduced from Krishnaswamy et al (1996a))

2.4 INHIBITION AND PROMOTION AGENTS OF SPONTANEOUS COMBUSTION OF COAL

There have been a number of studies carried out to determine the best solution of preventing the spontaneous combustion of coal (Chamberlain (1974); Evseev (1985); Smith et al. (1988)). Compaction of coal piles and inerting the atmosphere have been applied, as summarised by Smith, et al. (1988). Additives, such as carbamide, diammonium phosphate, gel solution from water glass (Evseev (1985)), aqueous solutions of inorganic salts, and salt-clay mixtures have also been examined as potential inhibition agents of spontaneous combustion of coal (Chamberlain (1974)).

Smith, et al. (1988) evaluated the effectiveness of ten additives to suppress the self-heating process in an adiabatic heating oven. A high volatile bituminous coal from Wyoming was used in the tests. They found that sodium nitrate, sodium chloride, and calcium carbonate inhibited the spontaneous combustion, whereas sodium formate and sodium phosphate stimulated the self-heating process.

In addition, it has also been found that the presence of inorganic matter in coal catalyses the oxidation reaction of coal (Durie (1991)). Therefore, the removal of inorganic matter could reduce the reactivity of coal.

2.4.1 The Effect of Inherent Inorganic Matter

The reactivity of coal towards air is strongly dependent on the rank of coal (Jenkins et al. (1973)). Low-rank coals have 200 times higher reactivity than anthracite or low volatile bituminous coal, not only because low-rank coals have more available active sites for the oxidation reaction but they also have higher contents of inorganic matter which can catalyse the oxidation reaction.

The catalytic activity of the inorganic matter inherent in the coal depends on their concentration, dispersion and chemical form in the coal matrix (Evseev (1985)). A high degree of dispersion could enhance the reactivity of the coal. Therefore, the removal of inherent inorganic matter in the coal could help change the self-heating potential of coal.

Recent work by Sujanti and Zhang (1997b; 1998a) examined the effect of inherent inorganic matter using water-washing and acid-washing. They found that removing the inherent inorganic matter increases the critical ambient temperature, and thus decrease the propensity of coal towards the spontaneous combustion.

2.4.2 The Effects of Additives

The effects of additives on the self-heating of a coal can be divided into several major aspects, ie. chemical reaction between the additives and the coal, physical effects of the additives on the coal, and additive application procedure (Smith et al. (1988)).

Chemical reactions occur between an additive and a coal may influence the self-heating tendency of the coal. This is because the reaction between the additive and the coal could reduce the active sites available for the oxidation reaction of coal, and thus the coal reactivity for the oxidation reaction. Furthermore, several additives, such as sodium acetate (NaAc), potassium acetate (KAc), and pyrite (FeS_2) have been found to have a catalytic effect on the coal spontaneous combustion (Sujanti and Zhang (1997b); Sujanti and Zhang (1998a)).

Physical changes due to the application of additives could also affect the spontaneous combustion (Smith et al. (1988)), particularly when the additives do not have any catalytic effect on the oxidation reaction. These physical changes include blockage of pore structure of coal, loss of active sites, and additional resistance for oxygen diffusion.

Moreover, the application procedure of the additives could change the coal structure, hence change the propensity of the coal toward the self-heating.

Therefore, the effect of additive on coal spontaneous combustion depends on the type of the additive which influences the chemical and physical reaction occured between the additive and coal, additive concentration, and the application procedure of additive.

2.5 REVIEW OF EXPERIMENTAL TECHNIQUES

The experimental techniques commonly used to investigate the self-heating and spontaneous combustion include (Banerjee (1985); Bowes (1984); Carras and Young (1994); Chen (1996b)):

1. examination of chemical constituents of the materials
   This technique was done either by petrological classification or rank correlation.

2. studying the effects of combustible material-oxygen interactions, which may be further divided into:
   - A. oxygen avidity studies
     - a. oxygen sorption method
     - b. humid acid formation
     - c. peroxy-complex analysis
     - d. oxidation rate studies
   - B. thermal data analysis
     - a. crossing point temperature method
     - b. TG-DTA method
     - c. calorimetry methods
       - isothermal calorimetry
       - adiabatic calorimetry
     - d. wire-mesh reactor
       - steady-state
       - unsteady-state
     - e. large-scale reactor

The most frequently used experimental techniques to study the spontaneous combustion phenomenon are discussed below.

2.5.1 Crossing Point Temperature Method

This method includes heating a sample in air in an oven and the lowest ambient temperature at which ignition occurs (when the temperature of the sample rises appreciably above the ambient temperature) is named as the critical ignition temperature or crossing point temperature of the coal (Banerjee (1985); Carras and Young (1994); Chen (1996b)). This crossing point temperature is then used as a measure of susceptibility of coal towards the self-heating. Coals with low crossing point temperatures obviously have high susceptibilities of spontaneous combustion.

Various experimental techniques and apparatus have been used to determine the crossing point temperature. Typical procedures used are given below (Carras and Young (1994)).

1. Preparation of the sample to size fractions required.
2. Placing the sample in an oven whose temperature can be steadily increased as a function of time.
3. Measuring the temperature at which the temperature of the sample exceeds that of the oven, indicating that an ignition has occurred.

Banerjee (1985) stated that the crossing point temperature normally decreases with an increase in volatile matter content, moisture content, and oxygen content of coal. However, he also stated that beyond this composition, i.e. 35% volatile matter, 9% oxygen content, or 4 to 6% moisture content, there is no significant changes in the crossing point temperature value (Banerjee (1985)).

The crossing point temperature method can be used to rank coals in terms of susceptibility towards spontaneous combustion. On the other hand, this method has following disadvantages.

1. For coals with poor reactivity, the transition to ignition point is not sharp, therefore the ignition temperature is difficult to determine.
2. Ignition temperature is not a unique coal property as it depends on many other factors, like ambient conditions, geometry and dimensions of the apparatus.
3. The experiment may not correspond to real stockpiles which involve very complex transport processes.
4. There is a possibility of misinterpretation for measuring the propensity of coals that have high moisture contents. This is because the release of the coal moisture could shift the crossing point to a higher value (Banerjee (1985)).

2.5.2 TG-DTA Methods

Thermogravimetry (TG) and differential thermal analysis (DTA) methods have also been used to estimate the combustibility of coal. The TG method involves heating a small amount of coal at a constant heating rate and recording the weight loss during the heating period in inert (pyrolysis) and oxidising environments (Chen and Mori (1995); Clemens et al. (1990)). The DTA method involves heating a small test specimen at a constant heating rate and records the instantaneous temperature difference (ΔT) between the small sample and an identically heated inert reference material. The negative or positive peaks obtained from the DTA plot describe the exothermic and endothermic reactions occurring at various temperatures (Banerjee (1985); Chen and Mori (1995); Clemens et al. (1990)). The ignition temperature of a coal is determined as the temperature at which the weight loss (TG) curve of the coal combustion is separated from the curve of the coal pyrolysis (Chen and Mori (1995)). The TG curve of coal pyrolysis is usually obtained under an atmosphere of nitrogen.

Chen and Mori (1995) have found that coal combustion process involves three stages of transitions which are classified based on the weight change and heat change of the coal samples. The three stages include the preheating (first stage),

volatile matter releasing (second stage), and coal combustion (third stage). Moreover, the TG curves showed that the combustion stage consists of two different combustion processes, ie. a high combustion rate process and a low combustion rate process. In the first combustion process, the rate of weight loss and heat released reach maxima. In the second combustion, however, the residual char is burned continuously at a lower combustion rate.

The kinetic constants are estimated using the Arhhenius model as follows,

$$\frac{dy}{dt} = \frac{dy}{dT}\left(\frac{dT}{dt}\right) = k\,(1 - y)^n \qquad (2-4)$$

$$k = A \exp\left(-\frac{E}{RT}\right) \qquad (2-5)$$

Combining Equations (2-4) and (2-5) results,

$$\ln\left((1-y)^{-n}\left(\frac{dy}{dt}\right)\right) = \ln A - \frac{E}{RT} \qquad (2-6)$$

By plotting the left hand-term versus the reciprocal of the absolute temperature, the apparent activation energy and frequency factor can be calculated.

Poor repeatability as well as the difficulty to describe complete processes occurring in the coal piles are the disadvantages of this method.

2.5.3 Calorimetry Method

This method measures various aspects of the exothermicity of oxygen-coal interaction. There are two commonly used calorimetry methods, i.e. isothermal

calorimetry and adiabatic calorimetry methods (Banerjee (1985); Carras and Young (1994); Chen (1996b)).

2.5.3.1 Isothermal calorimetry method

Coal is placed in a container which is then situated in a large heat bath held at constant temperature. Thermocouples are inserted into the coal and the heat bath to measure the heat generation and heat loss to the ambient (Banerjee (1985); Carras et al. (1994); Carras and Young (1994); Chen (1996b); Nordon et al. (1985)). Thus the heat balance during the heating process can be deduced. If analyses of the gas products are carried out, the heat of reaction of the coal with oxygen from the ambient and the rate of reaction at a constant temperature can be measured. Furthermore, it is also possible to carry out measurements at different temperatures by placing the entire isothermal calorimeter in an oven. The rates of oxidation reaction and heat generation obtained can then be used to assess the risk of the coal to spontaneously combust.

2.5.3.2 Adiabatic calorimetry method

Adiabatic calorimetry measures the temperature rise in a coal sample reacting with oxygen under adiabatic conditions. The experiment procedure typically involves a coal sample placed in a well-insulated container. Then, the system is heated under an inert environment until a preselected temperature is reached. Once the preselected temperature is reached, the inert gas is switched to air or oxygen, and the oxidation reaction of coal starts. The temperature increases as a result of the oxidation reaction. Since heat loss to the surrounding is negligible, a change of temperature of the sample can be measured and used to compare the propensity of different coals toward the spontaneous combustion (Banerjee (1985); Carras and

Young (1994); Chen (1996b)). This technique has been used rather intensively to assess the tendency of various coals toward spontaneous combustion.

2.5.4 Oxygen Sorption Method

In this technique, a coal sample is placed into a container and heated to a preselected temperature for a certain period of time. The oxygen concentration in the outlet stream is measured by an oxygen analyser (Carras and Young (1994); Chen (1996b); Young and Nordon (1978)). The data of oxygen consumed as a function of time at a certain ambient temperature is used to estimate the rate of oxidation reaction. Knowing the heat oxidation reaction of coal sample, the heat generated from the oxidation reaction can be calculated. The rates of oxidation reaction and the heat generated from the oxidation reaction can then be used to compare the self-heating potential of different coals.

Although, the oxygen sorption method is very important to determine the complete empirical oxidation reaction rate law for a given coal, this measurement is usually time consuming (Carras and Young (1994)).

2.5.5 Wire-Mesh Reactor

This method is based on the theoretical work of Frank-Kamenetskii (Bowes (1984); Carras and Young (1994); Chen (1996b); Chen and Chong (1995); Chong et al. (1997); Chong et al. (1995); Chong et al. (1996); Jones (1993); Jones (1996); Jones and Raj (1988); Jones and Wake (1990); O'Mahony and Synnott (1988)). A wire-mesh reactor of a particular size and shape, filled with coal, is placed in an air-circulated oven, the temperature of which is allowed to increase to a preselected level (Bowes (1984); Carras and Young (1994); Chen (1996b); Chen and Chong (1995); Chong et al. (1997); Chong et al. (1995); Chong et al. (1996); Jones (1993);

Jones (1996); Jones and Raj (1988); Jones and Wake (1990); O'Mahony and Synnott (1988)). This type of experiments may be operated either in steady-state or unsteady-state.

2.5.5.1 Steady-state method

For the steady-state operation, an iterative procedure is used to determine the ignition temperature (Bowes (1984); Chen (1996b); Chen and Chong (1995); Chong et al. (1997); Chong et al. (1995); Chong et al. (1996); Jones (1993); Jones (1996); Jones and Raj (1988); Jones and Wake (1990); O'Mahony and Synnott (1988)). Wire-mesh reactors are used to hold the samples. The samples are then heated in a strongly air-circulated oven. A thermocouple inside the coal indicates whether a thermal runaway takes place or not. In order to determine the critical ambient temperature for the thermal runaway, the experiment is repeated for different oven temperatures.

The following equation has been derived to determine the kinetics data of the oxidation reaction (Bowes (1984); Chen (1996b); Chen and Chong (1995); Chong et al. (1997); Chong et al. (1995); Chong et al. (1996); Jones (1993); Jones (1996); Jones and Raj (1988); Jones and Wake (1990); O'Mahony and Synnott (1988)).

$$\delta_c = \frac{E}{R T_{a,c}^2} \frac{\Delta^2 Q \rho_s A}{k_t} e^{-E/RT_{a,c}} \qquad (2\text{-}7)$$

Equation (2-7) is rearranged as follows:

$$\ln\left(\frac{\delta_c T_{a,c}^2}{\Delta^2}\right) = \ln\left(\frac{\rho_s EQA}{k_t R}\right) - \frac{E}{R T_{a,c}} \qquad (2\text{-}8)$$

The activation energy and pre-exponential factor are obtained by plotting $\ln\left(\frac{\delta_c T_{a,c}^2}{\Delta^2}\right)$ against the reciprocal of $T_{a,c}$ for various sample sizes (Δ).

The steady-state method is very time-consuming (Chen and Chong (1995)) because, not only several reactors of different sizes are needed, but iterative procedures have also to be used to determine the critical ambient temperature of each reactor. In addition, the strict boundary condition ie. a very large Biot number, is generally difficult to meet.

2.5.5.2 Unsteady-state method

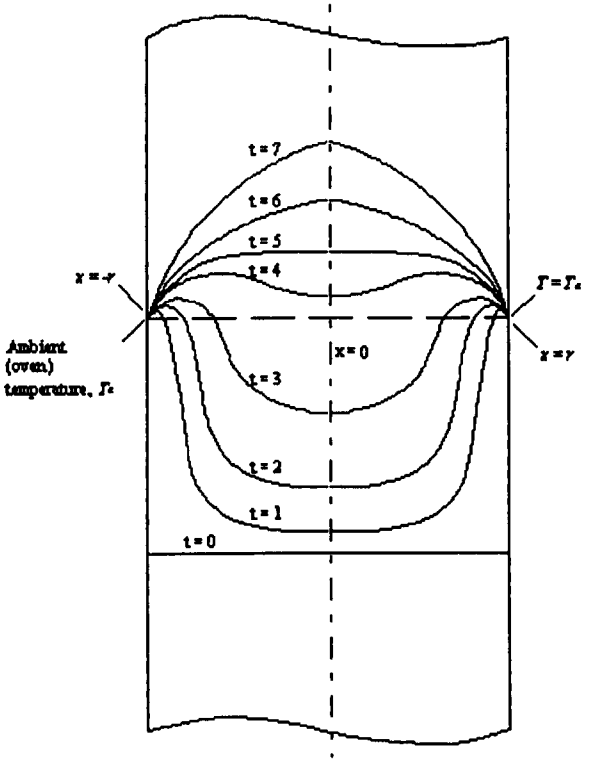

Figure 2.9 An illustration of self-ignition process within a slab starting from a temperature lower than the ambient (oven) temperature (reproduced from Chen and Chong (1995)).

Based on Gray et al. (1990; 1992) theoretical work, Chen and Chong (1995) introduced an experimental method, namely unsteady-state method. This method only requires one sample size. The principle of the unsteady-state method is based on the fact that there is a point in time during the heating of the sample, at which the conduction effect at the centre or symmetry becomes zero, as shown in Figure 2.9 (Chen and Chong (1995); Chong et al. (1997); Chong et al. (1995); Chong et al. (1996)). The zero conduction term is indicated by a flat temperature profile across the centre line of the slab as shown in Figure 2.9.

The energy conservation equation for a slab can be written as :

$$\rho_s \, Cp_s \frac{\partial T}{\partial t} = k_t \frac{\partial^2 T}{\partial x^2} + Q \rho_s \, A \exp\left(-\frac{E}{RT}\right) \qquad (2\text{-}9)$$

The left-hand side is the local enthalpy change in the solid. The first term on the right-hand side is the conductive heat transfer in the sample and the second term is the heat generation due to the oxidation reaction. This equation assumes that the reactant depletion is negligible. It is also assumed that the physical and chemical properties of coal are independent of temperature over a narrow temperature range.

When the conduction term is zero, Equation (2-9) becomes:

$$\frac{\partial T}{\partial t} = \frac{QA}{Cp_s} \exp\left(-\frac{E}{RT}\right) \qquad (2\text{-}10)$$

or

$$\ln \frac{\partial T}{\partial t} = \ln \frac{QA}{C_{p_s}} - \frac{E}{RT} \qquad (2\text{-}11)$$

Various ambient (oven) temperatures are used to obtain different crossing-point data. Plotting $\ln \frac{\partial T}{\partial t}$ against $\frac{1}{T}$ at temperatures when the conduction term is zero, E and A can be calculated.

Chen and Chong (1995; 1997) used two thermocouples to detect the crossing point temperature and cross-over time. They (Chen and Chong (1995); Chong et al. (1997); Chong et al. (1995); Chong et al. (1996)) proved that the usteady-state method requires less time and the kinetics data obtained compare reasonably well with those from the steady-state operation.

This technique seems to be simple, easy to operate and control. However, confidence yet needs to be gained when the technique is applied in situation other than those of Chen and Chong (Chen and Chong (1995); Chong et al. (1997); Chong et al. (1995); Chong et al. (1996)).

2.5.6 Large-Scale Reactor

Transport processes occurring in coal stockpiles is very important in determining the self-heating phenomena. Most small-scale experiments, using coal samples ranging from milligrams in the TG-DTA technique to a few hundreds grams in the other techniques mentioned before, cannot simulate these processes. Larger-scale testing using hundreds kilograms up to tonnes of samples may be employed to simulate these processes.

Stott et.al (1987) carried out laboratory experiments using as-mined coals (containing its "in bed" moisture content) in a 2 m long and 30 cm diameter column. They claimed that it was the first time for such experiment to successfully heat up the coal to above 100°C. Further work by Chen and Stott (Chen (1991); Chen and Stott (1997); Stott and Chen (1992)) studied the oxidation rates of several New

Zealand coals using a 2 m long and 30 cm in diameter adiabatic column. They pointed out that the complication of the practical situation. i.e. shrinkage of coal bed, oxidative aging, moisture transfer, etc caused many difficulties to correlate the experimental results obtained from laboratory experiments to the real stockpiles.

In summary, due to the complexity of various processes contributing to the spontaneous combustion, interpretation of the results obtained from large-scale experiments becomes more difficult (Stott et al. (1987); Chen (1991); Chen (1996b); Chen and Stott (1997)). Furthermore, the cost required for this experimental technique is also usually high.

2.5.7 Overall Assessment of Experimental Techniques

Of the above methods, no single method can be used to comprehensively assess self-heating and spontaneous combustion of combustible materials. The oxygen sorption method is a good indicator for predicting the property of self-heating of various coals (Carras and Young (1994)). By combining the oxygen sorption method with the isothermal calorimetry method, the empirical oxidation law can be obtained.

The basket method is the simplest and easiest technique to operate. This method could be used to obtain data suitable for kinetic analysis of the low-temperature oxidation of coal during spontaneous combustion. However, the simplicity of the theory and experiments used cause a difficulty to describe the complex process occurring during the self-heating process.

Small-scale experiments could not simulate the transport processes occurring in coal stockpiles. However, due to the complexity of the spontaneous combustion processes, the interpretation of the data obtained from a large-scale experiment is

not easy. Furthermore, a large-scale experimental technique usually involves a high operation cost.

Due to the complexity of the spontaneous combustion processes and the different system conditions involved in the different techniques, the results obtained from the same coal will vary with different experimental techniques. Unfortunately, no attempt has been made to clarify this. It is expected that the use of several experimental techniques on the same coal could help in gaining a more comprehensive understanding of the self-heating behaviour of the coal. Furthermore, the influence of the system conditions involved in the different techniques may also be examined.

A summary of the experimental techniques and conditions used by previous investigators, as well as the comments the author believes they deserve, are presented in Table 2.2.

Table 2.2 A summary of experimental techniques for spontaneous combustion studies

Reference	Coal Type	Temperature (K)	Particle Size (mm)	Type of Reactor	Comments
Karsner and Perlmutter (1981)	Coals of different ranks	423-573	0.84-2.79	fixed bed reactor	• The oxidation reaction was controlled by the rate of internal gaseous diffusion, except for the very porous coal where the rate of chemical reaction controlled the oxidation reaction. • The apparent order of the oxidation reaction for oxygen gas was about 0.7 and did not significantly change with the controlling regime.
Chen and Stott (1993)	Ohai coal (New Zealand)	323	1.70-2.10	isothermal microcalorimeter	• A critical moisture content, which a maximum oxidation rate would occur, was found to be 7-17%db.
Palmer et al. (1990)	Coals of different rank	423-573	0.07-1.00	fixed bed reactor, isothermal	• Coal fractions of different size distribution exhibited different chemical and physical properties.
Chen (1991); Chen and Stott (1997)	New Zealand coals	ambient temperature	5.00	large-scale reactor	• Various processes, which contributed to the practical situations, caused many difficulties to relate the experimental results to the real stockpiles.

Table 2.2. (Continued)

Smith and Lazzara (1987)	different US coals of various ranks	300-360	0.07-0.15	adiabatic calorimetry	• The critical ambient temperature ranged from 35°C for lignites to 135°C for bituminous coals. • The critical ambient temperature of a bituminous coal strongly depended on the oxygen content of the coal. • The critical particle size was 74-150μm. • The activation energy decreased with coal rank. The heat of wetting also depended on the coal rank.
Smith et al. (1988)	different US coals of various ranks	300-360	0.07-0.15	adiabatic calorimetry	• $NaNO_3$, NaCl, and $CaCO_3$ were found to be the most effective inhibition agents of spontaneous combustion followed by $NH_4H_2PO_4$, $CaCl_2$, NH_4Cl, NaAc, and KCl. NaCOOH and Na_3PO_4 promoted the spontaneous combustion.
Vance et al. (1996)	Renown Seam coal from Huntly East mine	313-413	0.21	adiabatic reactor	• The rate of temperature rise was the maximum at a coal moisture content of ~ 7 wt%.
Nordon et al. (1979)	Yallourn (Victoria) brown coal	323-973	3.35-9.50	packed bed reactor	• The activation energies of weathered materials was found to be independent of their moisture content.

Table 2.2. (Continued)

Chen and Mori (1995)	12 different coals	298-1173	0.037-0.074	TG-DTA	• The kinetic constants of low-reactivity combustible coals were found much smaller and less temperature dependence compared to those of the high-reactivity combustible coals.
Jones (1996)	Scottish Bituminous coal		3.00	baskets (cubic with sides of 10cm)	• A single-point estimation proved to be reliable to assess the spontaneous heating potential of various samples.
Akgun and Arisoy (1994)	Turkish coal	293-423	2.00 -5.00 5.00-10.00 15.00-20.00 20.00-50.00	large-scale reactor	• There was a critical range of particle size below which spontaneous heating under a certain condition would easily occur. • The overall rate of oxidation reaction became less sensitive to temperature as the particle size increased.
Polat and Harris (1984)	Log Yang (Victoria) brown coal	328	0.04-0.13	Beckman R11C LM 600 micro-balance (batch)	• The low-temperature oxidation of Victorian brown coal followed the continuous reaction model within a certain experimental condition.
Krishnawamy et al. (1996c)	coal from Black Thunder mine in Wright, Wyoming	350	0.30-2.00	isothermal flow reactor	• The experimental results matched well with the model derived previously (Krishnawamy et al. 1996b), which provide an explanation of the effect of particle size and temperature on the low-temperature oxidation reaction.

2.6. REVIEW OF MATHEMATICAL MODELS

The first mathematical formulation which has an application in the self-heating process was given by Semenov (1928). His formulation is based on the van't Hoff theory(1884). Semenov's model assumes that the temperature of the sample is uniform (small Biot number). Thus, the heat loss to the surrounding is mainly controlled by convection and radiation. However, if there is a temperature gradient inside the sample, resulting from an exothermically reaction of the sample, the Semenov model becomes inappropriate (Bowes (1984)).

In 1938, Frank-Kamenetskii (1969) introduced a theory to evaluate the thermal explosion with conductive heat transfer in the self-heating system with a non-uniform internal temperature distribution. Since then, there have been extensive developments in modelling the self-heating and spontaneous combustion phenomena.

Frank-Kamenetskii theory has attempted to eliminate the difficulty by modelling a system with a high Biot number. It assumes that the surface temperature of the sample is the same as the ambient temperature. Thus, the heat loss is only determined by conduction within the sample (Bowes (1984); Frank-Kamenetskii (1969)). The heat balance derived by Frank-Kamenetskii for steady-state conditions is given below.

$$k_t \nabla^2 T + Q \rho_s A \exp\left(-E/RT\right) = 0 \qquad (2\text{-}12)$$

Frank-Kamenetskii model has been used by a number of authors for different shapes of samples under different conditions (Bowes (1984); Chong et al. (1997); Chong et al. (1995); Chong et al. (1996); Duane and Synnott (1992); Jones (1996); Jones and Raj (1988); O'Mahony and Synnott (1988)). Frank-Kamenetskii model ignores reactant depletion by oxidation reaction. In addition, this model considers the

diffusion as the only transport process in the coal stockpiles. However, it has been acknowledged (Brooks and Glasser (1986); Glasser and Bradshaw (1990); Young et al. (1986)) that convection may also play an important role in the spontaneous combustion processes. Due to these reasons, the Frank-Kamenetskii model may not be accurate to describe a complex system undergoing self-heating.

Most mathematical models developed ealier are one-dimensional. In 1979, Nordon (1979) proposed a model which consists of three differential equations, i.e., conservation equations of mass (oxygen) and energy, and the rate of oxidation reaction. In this model, molecular diffusion is considered as the most important transport mechanism and natural convection is neglected. Furthermore, although the importance of the moisture effect is acknowledged, this model neglects the effect of moisture on the self-heating process. Improvement of the model was done by Schmal, et al. (1985). This model includes the effect of the moisture, but the natural convection mechanism is still neglected. More recent models (Brooks et al. (1988); Brooks and Glasser (1986); Young et al. (1986)) attempt to solve for natural convective flows in the porous coal stockpile. They prove that the flow in a stockpile is mainly caused by natural convection.

A more realistic two-dimensional model was developed by Salinger et al. (1994). This model represents reaction and transport processes within a realistically shaped stockpile, and in the surrounding air. Nonlinear interactions of chemical reaction, heat transfer, and buoyancy-driven flows within and around the stockpile are analysed in this model. The assumptions used are less restrictive since flows within the porous solid and in the surroundings are described. However, the moisture effect is neglected in this model. Further work by Chen (1996a) proposed a model which attempted to describe a full account of problems contributing to the self-heating process. The importance of ambient conditions in the self-heating process and the role of moisture in low-temperature oxidation reaction are addressed in his model.

While many valuable models have been reported, a realistic model which could be used to analyse the ignition condition of a coal stockpile accurately is still far from completion. A realistic description of chemical and physical processes, such as chemical reaction occuring in the stockpiles, moisture effects, heat transfer, pile shape and size, etc, is still required in order to obtain a more comprehensive understanding of the process. In addition, unsteady-state three-dimensional models are important to predict the behaviour of real coal stockpiles, although such models will be more difficult to solve.

The mathematical formulation should describe the rate of heat generation as well as transport processes through the stockpiles and to the surrounding (Carras and Young (1994)). In a three dimensional homogeneous porous body, the equations for energy, mass and momentum balance are described by Carras and Young (1994) as follows.

Energy balance

$$\left(1 - \varepsilon_b\right) \rho_s C_{ps} \frac{\partial T}{\partial t} + \rho_g C_{pg} \varepsilon_b \mathbf{U_g}.\nabla \mathbf{T} - \left(1 - \varepsilon_b\right) \rho_s C_{ps} k_t \nabla^2 T + G_h = 0 \qquad (2\text{-}13)$$

The first term describe the heat accumulation inside the coal matrix. The second term describes the rate at which heat is transported by gas flow. The third term is the rate of heat conduction through the coal matrix. The fourth term is the rate of heat generation, G_h, which includes heat generation due to oxidation reaction and heat absorbed or liberated from the coal through evaporation or condensation of moisture:

$$G_h = -Q(1 - \varepsilon_b)\rho_s R_o - H_w (1 - \varepsilon_b)\rho_s R_w \qquad (2\text{-}14)$$

Mass balance for oxygen

$$\varepsilon_b \frac{\partial C_A}{\partial t} + \varepsilon_b \mathbf{U_g}.\nabla C_A - D_c \nabla^2 C_A + R_o = 0 \qquad (2\text{-}15)$$

where

$$R_o = A_c C_A^n f\left(E, T, C_i, C_r\right) \qquad (2\text{-}16)$$

Mass balance for water vapour

$$\varepsilon_b \frac{\partial W}{\partial t} + \varepsilon_b \mathbf{U_g}.\nabla W - D_w \nabla^2 W + R_w = 0 \qquad (2\text{-}17)$$

where

$$R_w = A_w f\left(E_w, T, W, W_c\right) \qquad (2\text{-}18)$$

Equations (2-16) and (2-18) could not be expressed explicitly as they depend on the coal being studied.

Momentum balance

$$U_g = \frac{\kappa}{\varepsilon_b \mu}\left(-\nabla P + \rho_g g\right) \qquad (2\text{-}19)$$

Equation (2-19) is deduced from Darcy's law for fluid flow in a porous material. The first term on the right-hand-side describes the flow due to the pressure gradient, while the second term considers the buoyancy effect due to gas density change with temperature.

With appropriate boundary and initial conditions, the above set of equations can be solved numerically. However, some assumptions used in these equations cause inaccuracies in the model applications. For example, assuming that the stockpile is homogeneous porous body could cause a severe problem since the stockpiles contain a wide range of particle sizes ranging from large lumps to powders.

While substantial progress has been made to describe the self-heating behaviour of coal stockpiles, more work on model development and validation is still required. The use of data available from experimental work could minimise the assumptions made, thus increase the accuracy of the models. Furthermore, validation of the models with the data obtained from real stockpiles is essential for any model predictions to be useful.

A comparison of mathematical models of previous researchers, as well as the comments the author believes they deserve, are presented in Table 2.3.

Table 2.3 A summary of mathematical models

Ref.	Spatial dimension	Steady-state or Transient	Oxygen consumption	Convection	Coal Moisture	Solution Method	Comments
Nordon (1979)	1	Transient	Elovich Equation	Forced & Natural	-	Finite Difference	• The model took into account of the coupled transport and reaction rate in coal stockpiles • The calculation using diffusion as the only oxygen transport mechanism, resulted a maximum temperature rise of 87°C, which was much smaller than that observed in practice. Therefore, the convection, which supplied oxygen, was pointed out as a predominant mechanism to cause the spontaneous combustion.
Schmal et al. (1985)	1	Transient	Arrhenius Equation	Forced & Natural	✓	Gear program	• The model was developed for both dry and wet coals • The presence of in-situ moisture within a stockpile only delayed the onset of thermal runaway, and thus did not significantly affect the safety of a long-term storage or stockpile.

Table 2.3 (Continued)

Brooks and Glasser (1986)	1	Steady-state	Arrhenius Equation	Natural	-	analytical	• The model illustrated the coal pile as a "chimney", a vertical packed bed with a plug flow velocity field, and temperature, oxygen concentration, and pressure were considered as functions of bed distance. • The coal pile was safe when the coal particles were either small or large.
Brooks et al. (1988)	1	Steady-state	Arrhenius Equation	Natural	✓	Finite Difference	• The model studies the multiplicity of the 1-D model derived previously (Brooks and Glasser 1986) using bifurcation analysis. • There was not ignition solutions exists for sufficiently high convection which caused a high heat loss from the stockpiles.
Salinger et al. (1994)	2	Steady-state	Arrhenius Equation	Natural	✓	Galerkin Finite Element	• The model represented reaction and transport within a stockpile and transport and flow to the surrounding. • A better understanding of the roles of various transport mechanisms on ignition behaviour and nonlinear coupling between the transport mechanisms were provided in the model solutions.

Table 2.3 (Continued)

Krishnawamy et al. (1996a)	2	Transient	Arrhenius Equation	Forced & Natural	-	Finite Difference	• Slope of the side of a stockpile, wind velocity, and bed porosity, exerted the strongest influence on the safety aspect of an open coal stockpile. • A steep slope of the stockpile side enhanced the propensity of spontaneous combustion

2.7 CONSLUSION FROM LITERATURE REVIEW AND OBJECTIVES OF CURRENT STUDIES

2.7.1 Conclusions from Literature Review

1. Self-heating and spontaneous combustion of coal involve complex physical and chemical processes. There have been numerous studies in the literature, aiming at improving understanding of the spontaneous combustion. A range of laboratory experimental techniques, including the isothermal reactor test, adiabatic reactor test, wire-mesh reactor test with both steady-state and unsteady-state operation, large-scale reactor, etc., have been developed and used by various researchers in their respective studies. Reports on pilot-scale to full-scale coal stockpile tests are also available, though relatively fewer. The critical temperature, above which an ignition (thermal runaway) would occur, is usually measured and used to compare the tendency of coal samples toward spontaneous combustion.

2. It is generally accepted in the literature that coal reactivity towards low-temperature oxidation plays a key role in the self-heating process of the coal. Therefore, a significant effort has been made to determine the oxidation kinetics and reactivity of coal under ambient conditions. Most of the above-mentioned laboratory techniques allow the low-temperature oxidation kinetics to be estimated using either energy or mass balance analyses. It is evident that the low-temperature oxidation reactivity increases with a decrease in coal rank. Thus low-rank coals generally have a high propensity towards spontaneous combustion.

3. Physical properties of coal significantly influence the spontaneous combustion behaviour of coal stockpiles. It has been generally accepted that rate of the low-

temperature oxidation increases with decreasing particle size until a critical size is reached, below which the oxidation rate becomes invariant with particle size for a given coal. This is because for small particles, intra-particle diffusion does not affect the overall oxidation reaction rates while for larger particles, it does. While the critical diameter is believed to be coal-type dependent, surface structure of coal and process condition, which determine the reaction regime of the process, also affect the role of particle size in the spontaneous combustion.

Similarly, the oxidation rate is also believed to increase with increasing porosity of the coal. However, only pores having radii >100 Å play important roles in the low-temperature oxidation reaction while smaller pores are difficult for oxygen to penetrate through. This is because smaller pores were blocked by the adsorption of oxygen and/or the gas products and thus prevent the oxidation reaction.

Coal moisture plays complex roles in the self-heating process. Various conflicting information has been reported in the literature. The presence of water in coal obviously consumes a certain amount of heat generated from the low-temperature oxidation due to evaporation of the moisture as well as limiting the access of oxygen into the coal particle, thus delaying the self-heating of coal. This effect dominates at relatively high temperatures (> 70°C). While at lower temperatures (< 70°C), the oxidation of coal is enhanced by the coal moisture as atmospheric oxygen can be dissolved in the water to form peroxides and acidic functional groups which promote the ability of coal towards the low-temperature oxidation reaction. Obviously, the quantity of coal moisture together with the ambient conditions strongly determines the role of moisture content in the self-heating.

4. Ambient conditions, including ambient temperature, air humidity, wind, solar radiation as well as rain fall also affect the spontaneous combustion to various degrees. The higher the ambient temperature, the faster the initial oxidation reaction rate. A humid environment tends to accelerate the self-heating. This is because, for a wet coal, the high ambient humidity prevents further evaporation of coal moisture,

while a very dry coal can absorb moisture from the air which liberates heat. The roles of wind around a coal stockpile are two folds. While the wind controls the heat loss from the pile external surface into the ambient, it is also responsible for oxygen supply into the pile for the oxidation reactions. Which of these two effects dominates is a complex issue, depending on a number of factors such as geometry of coal stockpile, wind speed, air humidity and coal moisture content, etc. Solar energy incident on coal stockpiles enhances the self-heating process, particularly within a layer of the surface. However, whether this will develop into spontaneous combustion depends on the intensity and duration of the solar radiation. Rain fall in most cases only wets the layer near the surface of a stockpile, thus self-heating near the surface is suppressed. However, this wet shell can stop heat loss from interior stockpile to the surface. Thus the rain fall would encourage the self-heating and spontaneous combustion inside the stockpile.

5. Spontaneous combustion in coal stockpiles is also influenced by the pile geometry and dimensions, because of the dependence of transport process (heat transfer and oxygen diffusion) on these parameters. It has been acknowledged that an angle of 11.3-18.4° of the pile slope minimises the possibility of spontaneous combustion. It appears, however, this would be dependent on the direction of wind and solar radiation. Given everything else being equal, large piles have greater tendency towards spontaneous combustion than smaller piles due to, again, different transport processes occurring in piles of different dimensions.

6. There have been very few studies in the literature on the effect of inherent inorganic matter on the self-heating and spontaneous combustion of coals. Limited number of studies indicate that inherent and added inorganic matters do affect the spontaneous combustion properties of coals. It has been observed that, particularly for low-rank coal in which inherent inorganic matter is usually rich, water-washing and acid-washing of a coal can change the critical temperature to different extents because different amounts of inherent catalysts are removed by the water-washing and acid-washing. Similarly, addition of different inorganic matter into the coal also

alters the critical temperature, thus the spontaneous combustion propensity of the coal. The additives reducing the critical temperature are called promotion agents, while those increasing the critical temperature are referred to as inhibition agents.

7. Mathematical modelling studies of spontaneous combustion, ranging from single particle analysis to full scale dump modelling, have also been vastly reported in the literature. These models generally use either heat transfer analysis or mass balance approach, or a combination of both. Model predictions conforming to specific conditions have been achieved, but generalisation of the modelling approach is still rather limited owing to the complexity of the spontaneous combustion problem.

2.7.2 Gaps in Present State of Knowledge

1. Although various experimental techniques have been developed for spontaneous combustion studies, the use of these different techniques on the same coals has not been reported. Because of the complexity of the spontaneous combustion problem and the different system conditions involved in the different techniques, the results obtained from the same coal will most likely to vary when the different techniques are used. However, no attempt has appeared in the literature to explain these possibilities.

2. There has been very little work examining the effect of inherent inorganic matter on the spontaneous combustion of coal. Different inorganic matter in the coal matrix can play different roles during the low-temperature oxidation. While some inorganic matter may catalyse the oxidation reaction, the others may inhibit the combustion. Though there has been such information on coal combustion at high-temperatures, studies at low-temperatures, prevailing conditions of spontaneous combustion, are very few.

3. The primary property of a coal that determines the spontaneous combustion tendency is the low-temperature oxidation reactivity. The kinetic study of the low-temperature oxidation of coal continues to be an important step in understanding coal self-heating and spontaneous combustion, particularly for any new coals concerned. However, experimentally determined kinetics and coal reactivity often strongly depend on the experimental techniques used. It appears that how these different techniques contribute to the difference in the observed kinetics have not been very well established in the literature.

4. Although a general trend of the effect of the ambient humidity on spontaneous combustion process has been well established in the literature, a quantitative, or even a casual correlation of practical relevance has not been developed. Also, the effect of coal particle size should be dependent on coal type. For new coals concerned, the effect of particle size should be assessed experimentally and in particular, the critical size determined.

5. In almost all previous experimental studies, the air flow rate used in the experiments (e.g. isothermal or adiabatic methods) was usually fixed. However, the air flow rate, which may simulate the wind effect, not only determines the amount of oxygen available for the oxidation reaction and thus the rate of heat generation, but also influences the rate of heat removal from the reaction system. Therefore, for a given coal, there should be an optimum air flow rate for each type of reactor (size, dimension, etc.) at which the spontaneous combustion becomes the most easily possible.

6. Mathematical models heavily rely on necessary assumptions which usually over-simplify the complex conditions involved in a spontaneous combustion process. For example, coal stockpiles are often assumed to be homogeneous. This is necessary in order to solve the transport equations. However, coal stockpiles are rarely uniform in particle size distribution and other chemical and physical properties vary as well, which are too complicated to be precisely modelled mathematically. Therefore, to a

large extent mathematical modelling of spontaneous combustion requires experimental data to fine-tune the models.

2.7.3 Objectives of Current Studies

Based on the literature review, conclusions and gaps in present knowledge identified, several key areas are isolated as requiring further investigation in the present project with the following objectives:

1. Due to the complexity of the spontaneous combustion processes, different experimental techniques, thus different system conditions, will result in different observations when they are applied to the same material. Therefore, the primary objectives of the current project will be to use different experimental techniques, namely, isothermal reactor, adiabatic reactor, and wire-mesh reactor (steady-state and unsteady-state methods) to study the spontaneous combustion behaviour of the same material. In such a way, the influence of system conditions involved in the different techniques can be understood with confidence. It is expected that the results from such different systems will help provide an improved understanding of the spontaneous combustion.

2. Inherent inorganic matter present in coal can influence the spontaneous combustion processes. The present project is also aimed to investigate these effects. The amount of the inherent inorganic matter will be varied by water-wash and acid-wash, and spontaneous combustion tests of the resulting samples will be carried out on an isothermal reactor. The effect of the inorganic matter can be further understood by addition of various inorganic additives with different amounts to the acid-washed sample. This will provide better understanding of the role of the inorganic matter in the low-temperature oxidation processes. It is also possible to identify additive agents that may suppress or inhibit the spontaneous combustion.

3. Determination of low-temperature kinetics using different experimental techniques is also an important objective of the present project. The energy balance analysis technique will be applied with consideration of different system conditions. More reliable low-temperature oxidation kinetics and coal reactivity can then be deduced for further development of mathematical modelling of spontaneous combustion.

4. Air flow rate used in the experiments influences the self-heating process of a coal. This simulates the effect of wind on self-heating in a coal stockpile. In the present project, the air flow rate will be varied in the isothermal and adiabatic reactors to determine the optimum flow rate at which the spontaneous combustion can be most easily induced. This will help understand the influence of transport processes on coal spontaneous combustion.

The present study focuses on experimental studies of spontaneous combustion. A Victorian brown coal (Coal M), known to have very high spontaneous combustion tendency has been chosen for this project to achieve the objectives. The particle size will be varied to determine the effect of particle size on the coal self-heating behaviour. Air dried in silica gel column and humidified by bubbling through a water column will also be used to study the spontaneous combustion behaviour of the Coal M under these conditions. While mathematical modelling will not be attempted in the present project, the information and knowledge gained from this study will be of great help to further development of a comprehensive model for spontaneous combustion.

A flow chart indicating technical approach and strategies to achieve the objectives is presented in Figure 2.10.

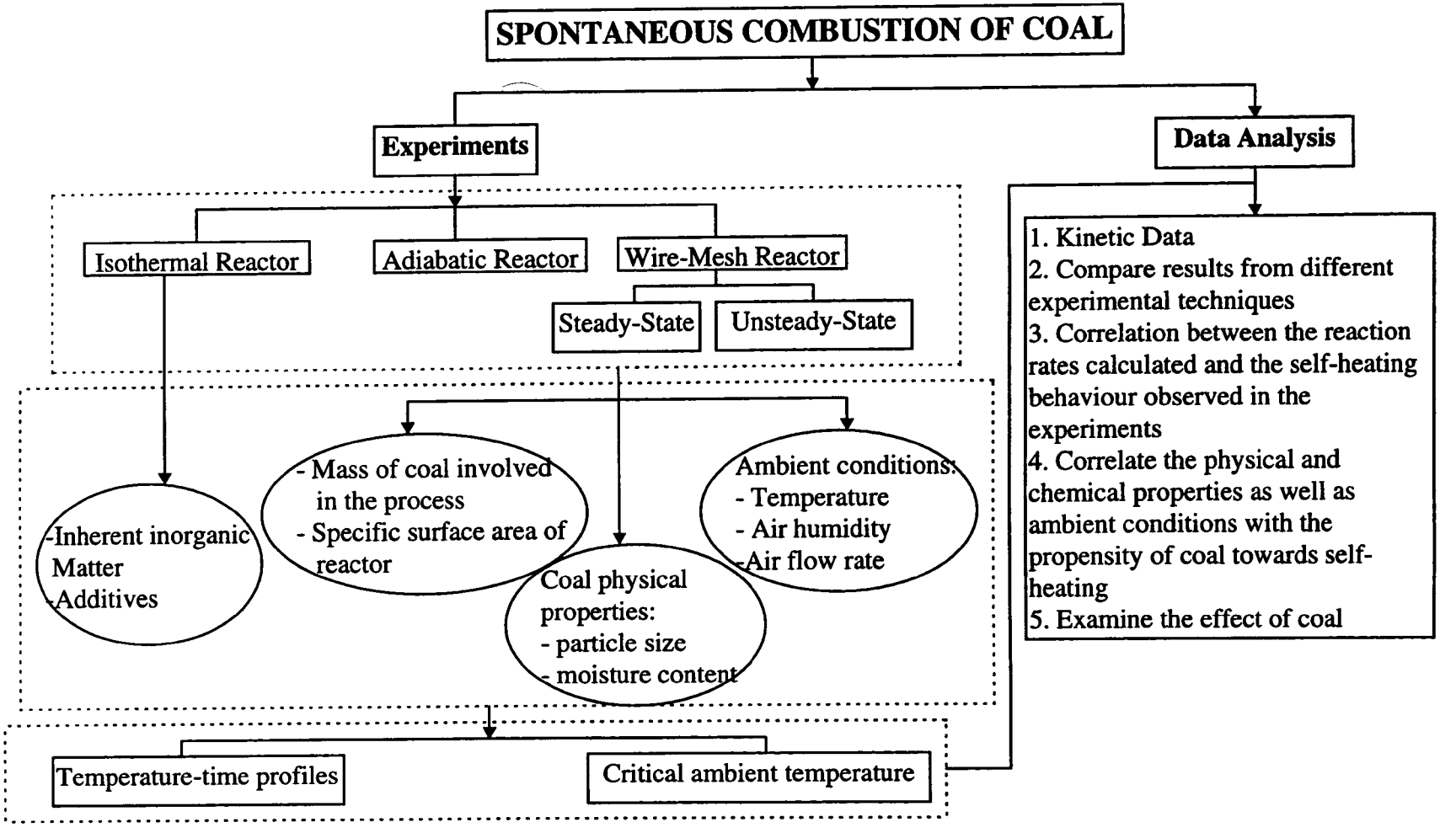

Figure 2.10 Flow chart of technical approaches and strategies to achieve the objectives

Chapter 3

EXPERIMENTAL TECHNIQUES AND DATA ANALYSIS

There have been various laboratory techniques used for assessing the spontaneous combustion behaviour of various combustible materials. The effects of coal type and properties on the self-heating behaviour of coal have been examined extensively for many years. However, the influence of experimental techniques has not been addressed. Accordingly, in the present study, three different experimental techniques, namely isothermal reactors, adiabatic reactors, and wire-mesh reactors (both steady-state and unsteady-state methods), are used to study the spontaneous behaviour of a Victorian brown coal. This chapter contains detailed descriptions of these three techniques and their procedures as well as the data analysis involved.

3.1 SAMPLES PREPARATION

A Victorian brown coal (Coal M) which is well known to have a high susceptibility towards spontaneous combustion, was chosen for this study. Table 3.1 shows the proximate, ultimate, and inorganic analyses of the coal (Durie (1991)).

The coal samples used in this study, were obtained at three different times and from different locations. Therefore, some varieties in chemical and physical properties of these samples are expected. Accordingly, these coals are named as Coal M1, Coal M2, and Coal M3.

Table 3.1 Proximate, ultimate, and inorganic analysis of Coal M (Durie (1991))

Proximate Analysis			
Moisture %	Volatile Matter %db	Fixed Carbon %db	Ash %db
61.30	48.30	48.70	3.00

Ultimate Analysis, %db					
C	H	N	O	Organic Sulfur	S_{Total}
67.40	4.70	0.70	26.94	0.26	0.26

Inorganic Analysis, %db						
Na	Mg	Fe	Si	Al	K	Ca
0.09	0.31	0.21	0.14	0.08	0.07	0.30

Coal M1 was used in the preliminary study, to examine the role of physical properties of coal (moisture content and particle size) and ambient conditions (temperatures, air humidity, and air flow rate) using isothermal reactors. Coal M2 was used in the study of the effect of inherent inorganic matter and additives on spontaneous combustion. Coal M3 was used in experiments using adiabatic and wire-mesh reactors as well as in experiments to study the effect of additive loading (both bulk loading and ion exchange) and reactor size on coal spontaneous combustion using isothermal reactors.

Preparation of coal samples in the current study includes drying, sieving of coal sample to suitable particle size ranges, washing to remove the inherent inorganic matter, and bulk additives loading and ion-exchange to add a require amount of inorganic matter to the acid-washed coal.

3.1.1 Drying

The coal sample used for the experiments was freshly picked up from the mine. It has a high moisture content, ie. higher than 60%. Since a high coal moisture content significantly delays the experimental time, the coal samples used in most experiments were dried in nitrogen environment at 105 °C.

To investigate the effect of coal moisture content on its self-heating, fresh coal, air-dried coal (ie. the coal was brought to contact with the air until it was saturated), and nitrogen-dried coals were used. The last samples were prepared by heating the coal sample at 105 °C and 65 °C in nitrogen.

3.1.2 Sizing

The coal samples were sieved into several particle size ranges. To investigate the effect of particle size on the critical ambient temperature, four particle size ranges were chosen. They were 2.36 ~ 4.00 mm, 1.00 ~ 2.36 mm, 0.25 ~ 1.00 mm, and 0.15 ~ 0.25 mm. The size fractions of 1.00 ~ 2.36 mm were also used in the preliminary experiments and adiabatic experiments, while the size fractions of 0.25 ~ 1.00 mm were used in the isothermal and wire-mesh experiments.

3.1.3 Water-Washing and Acid-Washing

Double-deionised water-washed and acid-washed samples were prepared to investigate the effect of inherent inorganic matter on the spontaneous combustion. Double-deionised water-washing can remove the water-soluble inorganic matter and acid-washing can remove most of the inorganic matter (Durie (1991)).

3.1.3.1 Water-washing

A 600 gram coal sample was placed in a 5 litre beaker. Three litre distilled water was added to the beaker. The slurry was stirred and heated at 85-90 °C for 4 hours, and then cooled down to room temperature and filtered. The coal sample was washed with distilled water until the chloride ion was not shown in the filtrate. The sample was then dried in nitrogen at 105 °C for overnight, which allowed the water to be evaporated. Finally the sample was sieved. The 0.25 ~ 1.00 mm size fraction was retained and stored for use in the experiments

3.1.3.2 Acid-washing

Acid-washing can remove most of the inherent inorganic matter in coal. Therefore, the effect of inherent inorganic matter on the self-heating behaviour of coal can be eliminated by treating the coal with acids. Hydrochloric (HCl) acid was used in the present study for the acid-washing.

1.5 litres of 12M HCl acid solution was added into 1.5 litre distilled water in a 5 litre beaker. The diluted solution was stirred as approximately 600 grams of the raw coal was added to the beaker. The slurry was stirred and heated to 85-90 °C for 4 hours, and then cooled down to room temperature and filtered off. The coal sample was then washed with double-deionised water until all chloride ion was not shown in the washing water. The sample was dried in nitrogen at 105 °C for overnight, which allowed the water to be evaporated. Finally, the samples were sieved. The 0.25 ~ 1.00 mm size fraction was retained and stored for use in the experiments.

3.1.4 Bulk-Loading of Additives

To investigate the effect of individual inorganic components on spontaneous combustion, eleven additives were added into the acid-washed coal (Sujanti and

Zhang (1997b; 1998a)). They were pyrite (FeS_2), potassium acetate (KAc), sodium acetate (NaAc), calcium carbonate ($CaCO_3$), sodium nitrate ($NaNO_3$), ammonium chloride (NH_4Cl), calcium chloride ($CaCl_2$), magnesium acetate ($Mg(Ac)_2$), sodium chloride (NaCl), potassium chloride (KCl), and Montan powder ($CaCl_2$ powder + 3% sodium dodecyl sulphate (SDS)). Water soluble additives (KAc, NaAc, $NaNO_3$, NH_4Cl, $CaCl_2$, $Mg(Ac)_2$, NaCl, and KCl) were dissolved in double-deionised water to form solutions with a concentration of 4.76%(wt.). 2.5 litres of a solution and 600 gram of acid-washed coal were mixed to form slurry. The mass ratio of the additives in a solution to the acid-washed coal is 25%. The slurry was continuously stirred for 24 hours. The liquid in the slurry was then allowed to drain through a filter, and the resulting paste was dried in a nitrogen oven at 105 °C for overnight, which allowed the water to be evaporated. Chemical analysis confirmed that the samples prepared in such a way contain about 6%(wt.) additive. Water insoluble additives (FeS_2, $CaCO_3$, and Montan Powder) were added to the coal as solid powders and the mixtures were well mixed. The concentration of water insoluble additives in the coal samples is 5%(wt.) All samples were sieved and the 0.25 ~ 1.00 mm size fraction was retained and stored for use in the experiments.

To investigate the effect of additive loading 1, 5, and 15%(wt.) of KCl and NaAc were applied to the acid-washed coal (Sujanti and Zhang (1997a; 1998a)). The additives were mixed with water to form a solution and were then added to acid-washed coal and mixed. The concentration of the additives in the coal samples were 1, 5, and 10%(wt.), respectively. All samples were dried in a nitrogen oven at 105 °C for overnight, which allowed the water to be evaporated. The samples were then sieved, and the 0.25 ~ 1.00 mm fraction was retained and stored for use in the experiments.

3.1.5 Ion-Exchange

Ion-exchange was employed in the present study to examine the effect of application procedure on the effectiveness of the additives applied. The bulk loading of additive

mixed the additives and coal sample both physically and chemically, while the ion exchange mixed them only chemically. It is believed that with the ion exchange procedure, the additive can be well distributed into the coal matrix (Ye (1994)).

An appropriate mass of selected chemicals was dissolved in distilled water to form the solution of a required concentration. The solution concentration used for each additive was 0.5M, except for $Cu(Ac)_2$ which was 0.25M. To examine the effect of additive solution concentrations on the capability of the additives to affect spontaneous combustion, samples with 0.1M and 1.0M of NaAc and $Ca(Ac)_2$ solutions were also prepared. Approximately 1 kg of the acid-washed coal sample and 5 litres of the additive solution were mixed in a flask and shaken for 24 hours. The slurry was then filtered. Double-deionised water was added into the flask to wash the coal remaining in the flask until most of the remaining coal was washed out. The filtered coal samples were dried in nitrogen at 105 °C for overnight, which allowed the water to be evaporated. The samples were then sieved. The size fraction of 0.25 ~ 1.00 mm of the sample was retained for the use of experiments.

3.2 EXPERIMENTAL TECHNIQUES AND DATA ANALYSIS

Three experimental techniques, namely, isothermal reactors, adiabatic reactors, and wire-mesh reactors with both steady-state and unsteady-state methods were selected in this project to gain a more comprehensive understanding of the self-heating and spontaneous combustion processes.

The isothermal reactors were used rather intensively throughout this study, to investigate the effect of coal properties, ambient conditions as well as inorganic matter, on the self-heating behaviour of Coal M. The adiabatic reactors were also used to investigate the self-heating behaviour of Coal M. However, since the heat loss to the surrounding could be neglected in the adiabatic reactors, a change of the

sample temperature directly indicates the heat generated from the oxidation reaction and can be used to compare the propensity of the sample towards self-heating. The wire-mesh reactors were also applied in order to obtain data suitable for kinetic analysis of the low-temperature oxidation of coal during spontaneous combustion.

The detail of experimental techniques, the operation procedures and data analyses involved in the three experimental techniques are presented in the following sections.

3.2.1 Isothermal Reactors

3.2.1.1. Apparatus

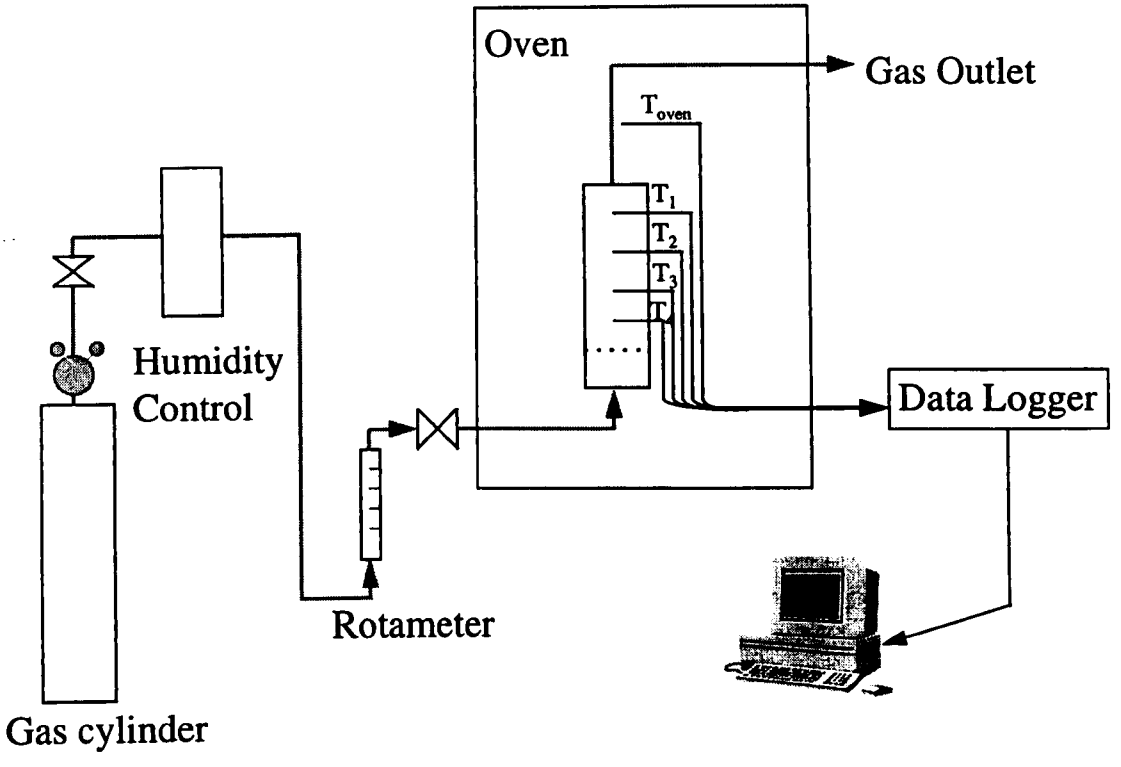

Figure 3.1 Schematic diagram of the apparatus for isothermal experiments

A schematic diagram of an isothermal reactor used in this work is shown in Figure 3.1. The experimental system consists of the following components:

(i) a nitrogen gas cylinder and an air line from compressor;
(ii) humidity controls;
(iii) rotameters to monitor and control the gas flow rate;
(iv) an eighteen meter copper tube to preheat the gas entering the reactors to an oven temperature;
(v) an oven;
(vi) isothermal reactors;
(vii) a data logger to record the temperature data; and
(viii) a computer

The oven is a micro-processor controlled oven with a volume capacity of 150 litres. The temperature range of the oven is 50 - 200 °C with an accuracy of ± 0.5 °C.

Table 3.2 Specifications of isothermal reactors

Reactor I.D.	Reactor Dimensions		Mass of sample used (g)
	Diameter (cm)	Height (cm)	
R-1	9.8	27.0	1000
R-2	8.0	15.0	350
R-3	6.0	12.0	140
R-4	4.0	8.0	30

Four stainless-steel cylindrical isothermal reactors were used in this study. The dimensions of these reactors are given in Table 3.2. These four isothermal reactors can be filled with 1000, 350, 140, and 30 g of coal, respectively. The smallest reactor was used to investigate various factors affecting the spontaneous combustion, while the other reactors were employed to examine the effect of reactor size on the self-heating behaviour of coal M. The isothermal reactors consist of a

perforated plate to distribute the gas uniformly to the coal sample. Four K-type thermocouples were inserted inside each reactor to monitor temperatures along the reactor axis. A gas (N_2 or air) was preheated in an 18 m long copper tube to the oven temperature before passed through the coal sample from the bottom of the reactor. The data acquisition system used in this study is a data logger (Datataker 500).

In order to vary the humidity of air, the air stream could be dehumidified by passing the air through the silica gel column or humidified by bubbling the air through a water column.

3.2.1.2 Experimental Procedures

The received coal was sieved into desired particle size fractions using a sieve-shaker. A certain amount of coal, filling around 80% of the reactor volume, was oxidised in an isothermal reactor with a once-through air stream.

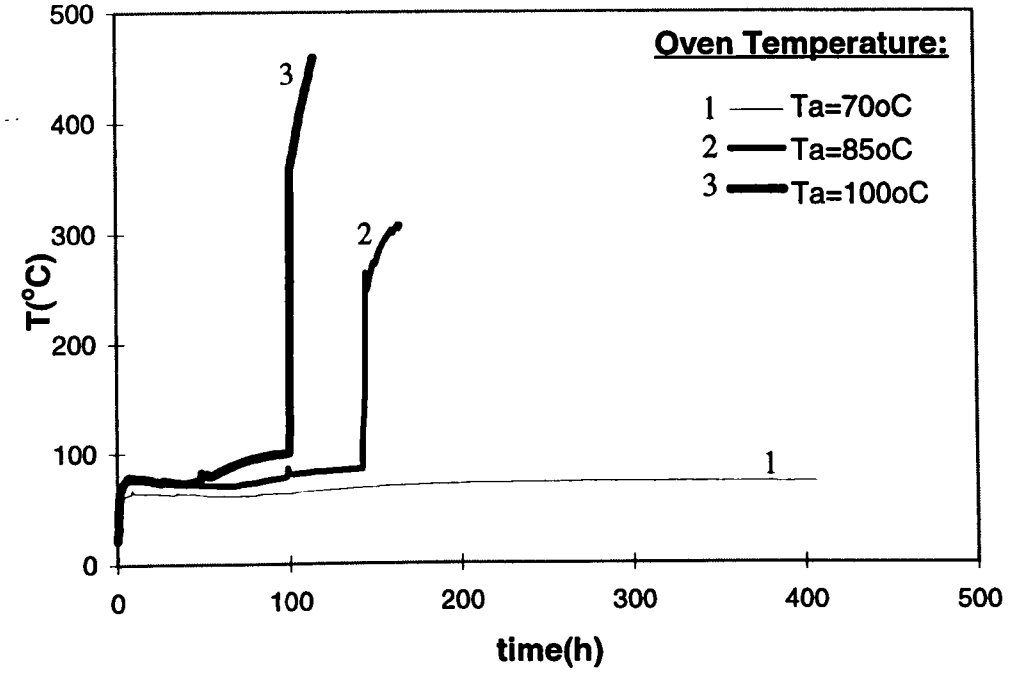

Figure 3.2 Temperature histories of fresh Coal M3 in an isothermal reactor (R-1) at several oven temperatures

The oven was first preheated to a preselected temperature. During this stage, nitrogen gas passed through the reactor at 100 ml min^{-1} (N.T.P.) to minimise any pre-oxidation. Once the desired temperature was reached, air then replaced the nitrogen at the same flow rate and was maintained throughout the experiment. A data acquisition system was activated to record the temperature.

In preliminary experiments, attempts were also made to follow the gas products in the exiting gas from the reactor using a Gas Chromatography (GC). However, no detectable CO or CO_2 was noticed, nor was oxygen depletion at temperatures of interest. This was apparently due to the low reaction temperatures (thus slow reaction rates) and the small quantity of coal samples used. Therefore, temperature measurement was chosen as the sole technique to monitor development of spontaneous combustion in these experiment.

The experiment was terminated either when a thermal runaway occurred or when the temperature of the sample continued to level off towards the oven temperature. Typical temperature profiles of the fresh Coal M3 in an isothermal reactor (R-1) are shown in Figure 3.2. The four thermocouples read essentially the same temperature values while in the coal bed. However, the depletion of the reactant during the oxidation reaction may cause the other thermocouples being left in the empty spaces in the upper portion of the reactor. Therefore, temperature readings obtained from the bottom thermocouple are used to represent the coal temperature in the bed. It can be seen that at temperatures below 85 °C, the thermal runaway did not occur, so that the experiments were terminated when the average temperature along the reactor showed a trend to level off. However, at 85 °C, thermal runaway occurred. Experiments were repeated for different oven temperatures until the critical ambient temperature of a sample was determined. Repeatability of the critical ambient temperature values determined was confirmed by carrying out the experiments for each sample at the same temperatures and essentially the same critical ambient temperature value was obtained. Thus, for each sample, the critical ambient temperature was taken as the average of the lowest temperature at which the thermal runaway occurred and the highest temperature at which the thermal runaway did not

occur. Typical temperature profiles of the fresh Coal M3 in different sizes of isothermal reactors, R-2, R-3, and R-4, are shown in Figures 3.3, 3.4, and 3.5, respectively.

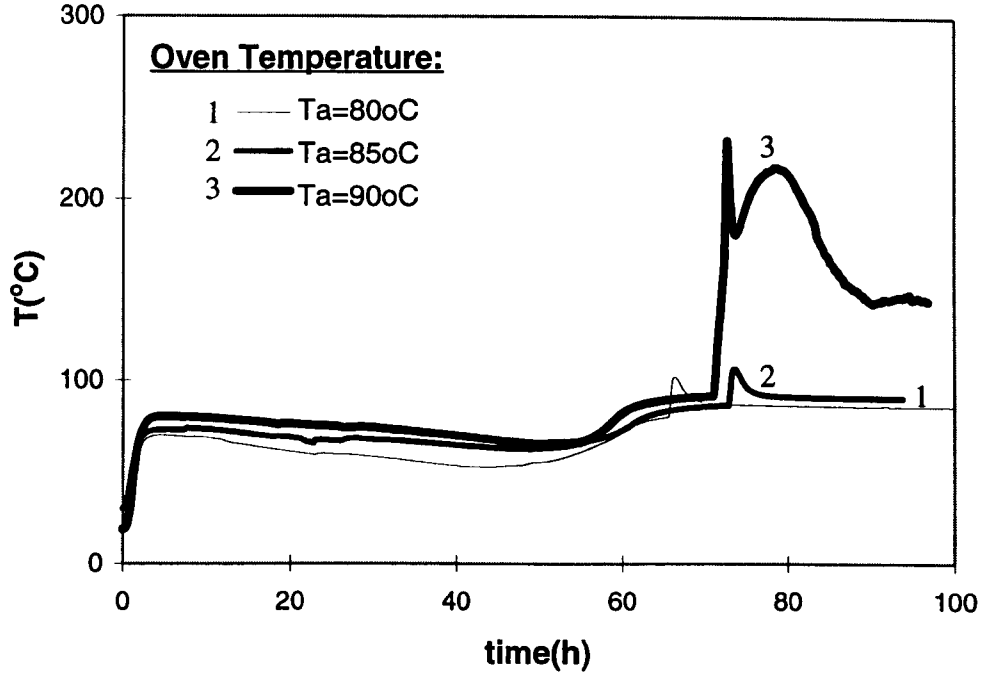

Figure 3.3 Temperature histories of fresh Coal M3 in an isothermal reactor (R-2) at several oven temperatures

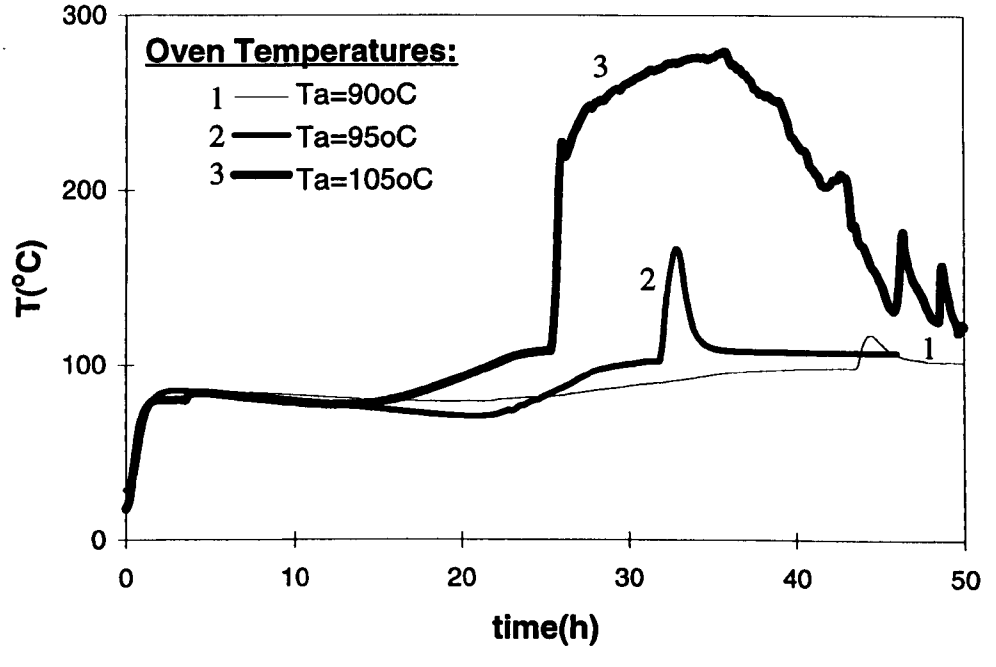

Figure 3.4 Temperature histories of fresh Coal M3 in an isothermal reactor (R-3) at several oven temperatures

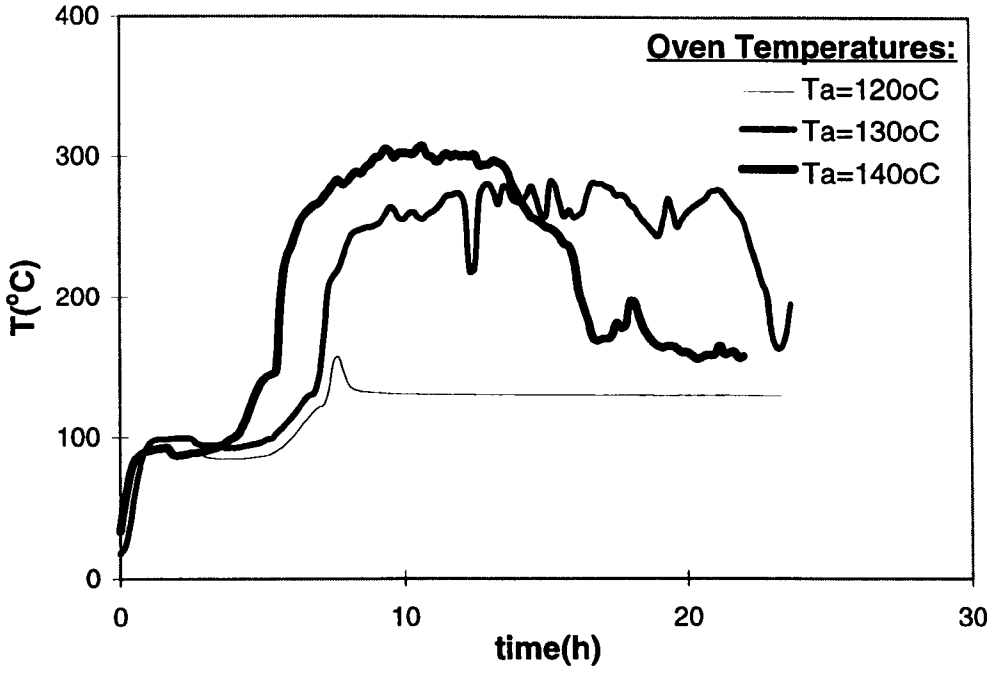

Figure 3.5 Temperature histories of fresh Coal M3 in an isothermal reactor (R-4) at several oven temperatures

The critical ambient temperatures obtained were then used to compare the tendency of various coal samples towards spontaneous combustion. The higher the critical ambient temperature, the lower the propensity of coal towards the spontaneous combustion.

Figures 3.2 to 3.5 present the temperature profiles of the coal from the beginning of the experiments. It is shown that the larger the reactor, the longer the time required for the sample to reach oven temperature.

3.2.1.3 Data Analysis

In order to compare the reactivities of the samples and correlate the reactivities with their self-heating behaviour observed in the experiments, low-temperature oxidation kinetics were estimated by an energy balance approach. The energy balance for a sample in an isothermal reactor can be written as:

$$Cp_s \rho_s \left[\frac{dT}{dt}\right]_o = QA\, e^{-\frac{E}{RT_o}} P_{O_2}^n - h\,S\,(T-T_g) - h_c\,S_r\,(T-T_o) \qquad (3\text{-}1)$$

where the left hand side (LHS) is the heat accumulation in the coal sample. The first term of right-hand-side (RHS) is the heat generated from the oxidation reaction, the second term is the heat transfer between the coal and the flowing gas, and the last term of RHS is the heat transfer between coal and the ambient through the reactor wall.

At a point when the coal temperature is equal to the oven temperature, (T_o), there is no heat loss from the coal sample to the ambient. Therefore, the last term of the RHS is cancelled. Likewise, since the gas flow into the reactor is is also at the oven temperature, there is no heat being added in or carried away from the coal by the flowing gas. Accordingly, the second term of the RHS is also cancelled, and Equation (3-1) reduces to:

$$Cp_s \rho_s \left[\frac{dT}{dt}\right]_o = QA\, e^{-\frac{E}{RT_o}} P_{O_2}^n \qquad (3\text{-}2)$$

The value of physical and chemical properties of the coal used for calculation can be found in Table 3.3. P_{O_2} is the partial pressure of oxygen, which is 21 kPa in the present case. The apparent reaction order, n, is assumed to be 1.

Table 3.3 Property data of the coal

Physical and Chemical Properties	
Specific Heat Capacity (J $kg^{-1}K^{-1}$)	1550.00
Thermal Conductivity (W $m^{-1}K^{-1}$)	0.23
Density (kg m^{-3})	1350.00
Heat of Oxidation Reaction (MJ kg^{-1})	22.90

According to Equation (3-2), from a linear plot of $\ln\left[\frac{dT}{dt}\right]_o$ versus $\frac{1}{T_o}$, the apparent kinetic constants, A and E, can be determined. Figures 3.6 and 3.7 show typical plots of $\ln\left[\frac{dT}{dt}\right]_o$ versus $\frac{1000}{T_o}$ for the raw and acid-washed Coal M3. Since it is evident that a linear relation between $\ln\left[\frac{dT}{dt}\right]_o$ and $\frac{1}{T_o}$ does exist, and that the temperature inside the reactor is noticed to be uniform, Equation (3-2) can be used as a technique for estimation of apparent kinetics of coal in such spontaneous combustion tests.

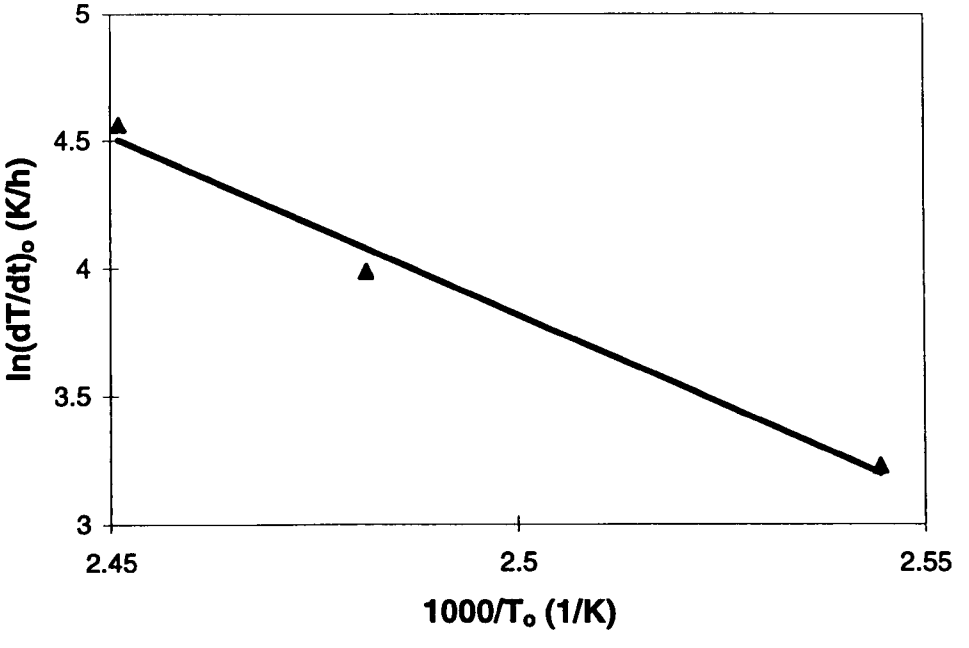

Figure 3.6 A typical linear plot of $\ln\left[\frac{dT}{dt}\right]_o$ versus $\frac{1000}{T_o}$ for the nitrogen-dried Coal M3 for estimation of apparent oxidation kinetics of coal

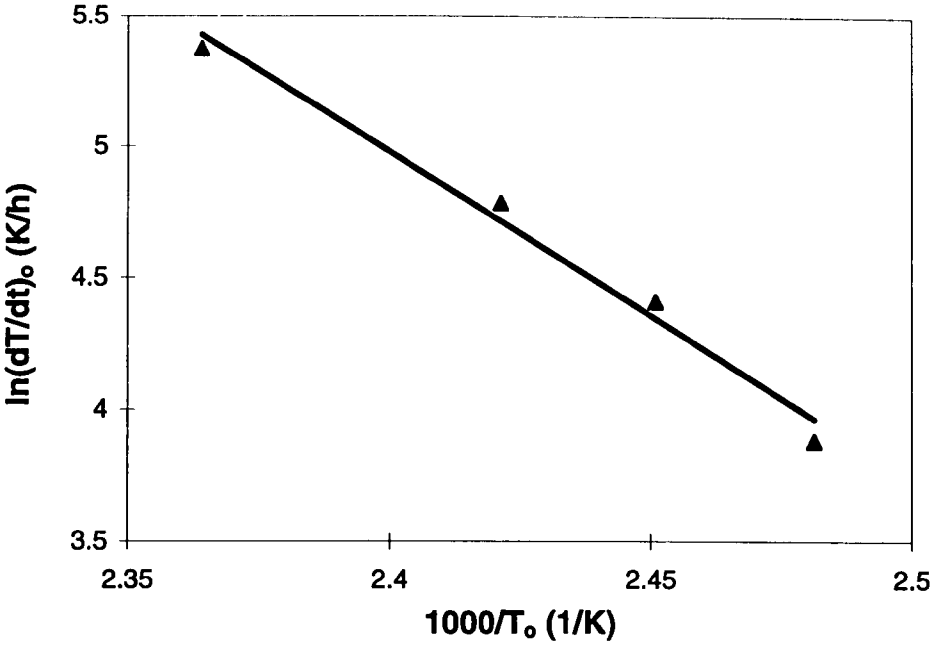

Figure 3.7 A typical linear plot of $\ln\left[\frac{dT}{dt}\right]_o$ versus $\frac{1000}{T_o}$ for the acid-washed Coal M3 for estimation of apparent oxidation kinetics of coal

Estimation of The Critical Layer Thickness

Two main factors affecting the spontaneous combustion are the heat generation (the heat of oxidation reaction) and the heat loss to the surrounding through the external surface. The latter is determined by the ambient conditions and the size or dimensions of the stockpile. The size or dimensions of the stockpile is more possible to be controlled than the ambient conditions. Therefore, it is necessary to predict the critical layer thickness of a coal deposit, above which it becomes capable of spontaneous combustion.

The kinetic constants estimated from Equation (3-2) can be used to predict the critical thickness of a coal deposit (Δ) according to the Frank-Kamenetskii approach (Bowes 1984).

$$\Delta = \sqrt{\frac{\delta_c R T_a^2 k_t}{EQA\rho_s e^{-E/RT_a}}} \qquad (3\text{-}3)$$

where δ_c is the Frank-Kamenetskii parameter (dimensionless) which strongly depends on the shape of the solid and the boundary conditions involved in the process. Early work by Frank-Kamenetskii (Bowes 1984) assumed that the rate of external heat transfer to the surroundings is significantly greater than heat conduction within the solid, ie. an infinite Biot number (Bi) case. With this assumption, the values of δ_c have been found to be 0.88 for infinite slabs and 2.89 for equicylinders (Bowes 1984).

3.2.1.4 Experimental Errors

There are many factors which could contribute to the experimental errors. The potential errors in the isothermal reactor experiments were identified during the preliminary experiments. Precautions have been taken to minimise them, as described below.

- To minimise any preoxidation reaction, all samples were kept in air-tight containers before use in the experiments and the sample preparations were done under nitrogen environment.
- The oven and thermocouples were calibrated at the early stages of this work to eliminate any errors in temperature readings. The temperature fluctuation inside the oven is $\pm 0.5^{\circ}C$, while the thermocouples had a precision of $\pm 0.1^{\circ}C$.
- Repeatability of the critical ambient temperatures determined was confirmed by carrying out the experiments for each sample at the same temperatures and essentially the same critical ambient temperature value was obtained. Thus, for each sample, the critical ambient temperature was taken as the average of the lowest temperature at which the thermal runaway occurred and the highest temperature at which the thermal runaway did not occur, with an accuracy of $\pm 2.5^{\circ}C$.

- The humidity of air was maintained constant in a dry condition by passing the air through a silica gel column.
- The compactness of the coal sample could affect the self-heating behaviour of coal. Therefore, a similar packing was maintained throughout the experiments. To ensure a constant packing density, the reactors were loosely filled, without pressing, with a desired amount of coal sample for each experiment.
- The temperature of gas entering the reactor was maintained at the same value as the oven temperature to minimise heat loss. An eighteen meter copper tube was used for this purpose. A thermocouple was installed on the gas line near the reactor entrance to measure the gas temperature before entering the reactor.
- It was ensured there was not any leakage in the gas line by using water soap to check for leaks.
- The energy balance in Equation (3-2) was applied only when the coal temperature equals to the oven temperature. Therefore, before switching from nitrogen to air, the coal temperatures at different locations of the reactor were ensured to be uniform. The coal temperatures along the reactor axis were recorded in the datataker every 10 minutes.
- All experiments were repeated to ensure the consistent results.

3.2.2 Adiabatic Reactors

3.2.2.1 Apparatus

Adiabatic reactors (thermal flasks) of 0.3 and 1 litre in capacity, namely A-1 and A-2, were also used in this study. Experimental procedures in this technique were similar to those for isothermal reactors. However, since the heat loss to the oven can be neglected, an increase of temperature of the sample due to the oxidation reaction can be easily detected and used to compare the propensity of the samples toward the self-heating. Three K-type thermocouples were inserted inside each reactor to monitor temperatures along the reactor axis. A gas (N_2 or air) was preheated in an

18 m long copper tube to the oven temperature, and then passed through the coal sample from the bottom of the reactor. The data acquisition system used in this study is a data logger (Datataker 500). A schematic diagram of an adiabatic reactor used in this work is shown in Figure 3.8.

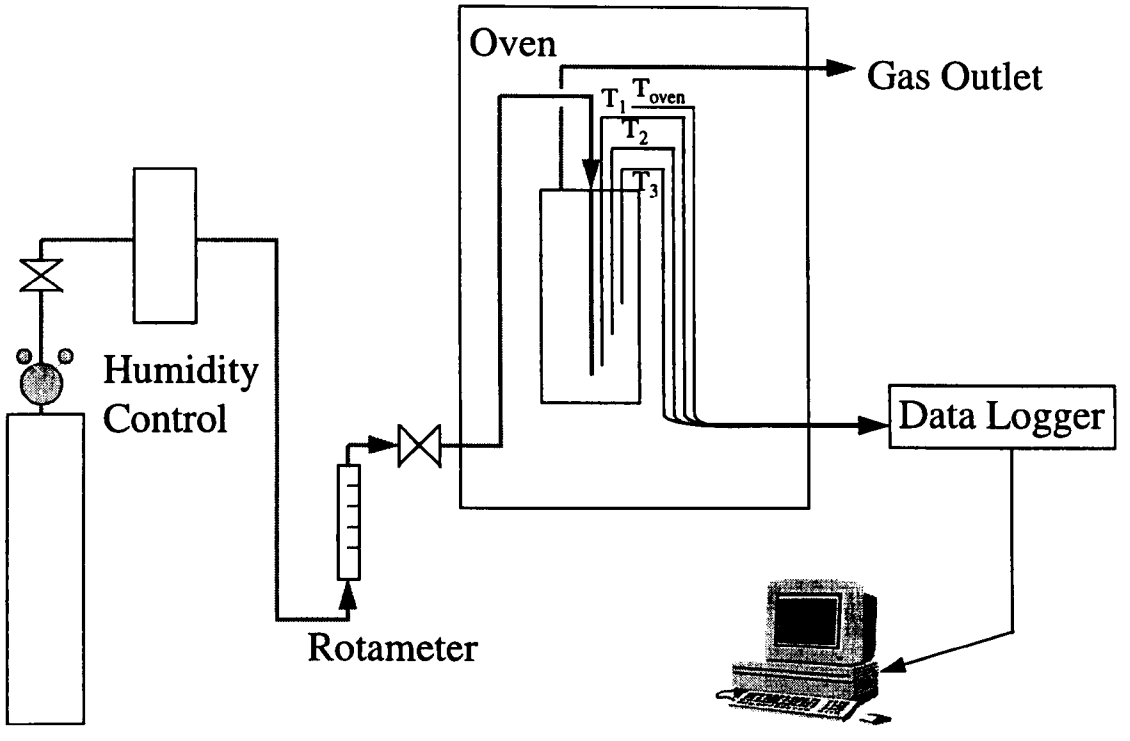

Figure 3.8 Schematic diagram of the apparatus for adiabatic reactor experiments

3.2.2.2 Experimental Procedures

The received coal was sieved into desired particle size fractions using a sieve-shaker. A certain amount of coal, was oxidised in an adiabatic reactor with a once-through air stream.

The same procedure as used in the isothermal reactor, firstly, the oven was preheated to a preselected temperature. During this stage, nitrogen gas passed through the reactor at 100 ml min^{-1} (N.T.P.) to minimise any pre-oxidation. Once the desired temperature was reached, air then replaced the nitrogen at the same flow

rate and was maintained throughout the experiment. A data acquisition system was activated to record the temperature.

The experiment was terminated either when a thermal runaway occurred or when the temperature of the sample continued to level off towards the oven temperature. The nitrogen-dried coal was used in the experiments to minimise the preheating time. Typical temperature profiles of the nitrogen-dried Coal M3 in an adiabatic reactor (A-2) with air flow rate of 100 ml min^{-1} are shown in Figure 3.9. It can be seen that at temperatures below 90 °C, the thermal runaway did not occur, so that the experiments were terminated when the average temperature along the reactor showed a trend to level off. However, at 90 °C, thermal runaway occurred. Thus, the critical ambient temperature was taken as 85±5 °C. A sudden drop in the coal temperature observed at oven temperature of 90 °C, was caused by an electricity shut down which stopped the compress air and thus the air flow into the system. Experiments were repeated for different oven temperature, at a 10 °C interval, until the critical ambient temperature of a sample was determined.

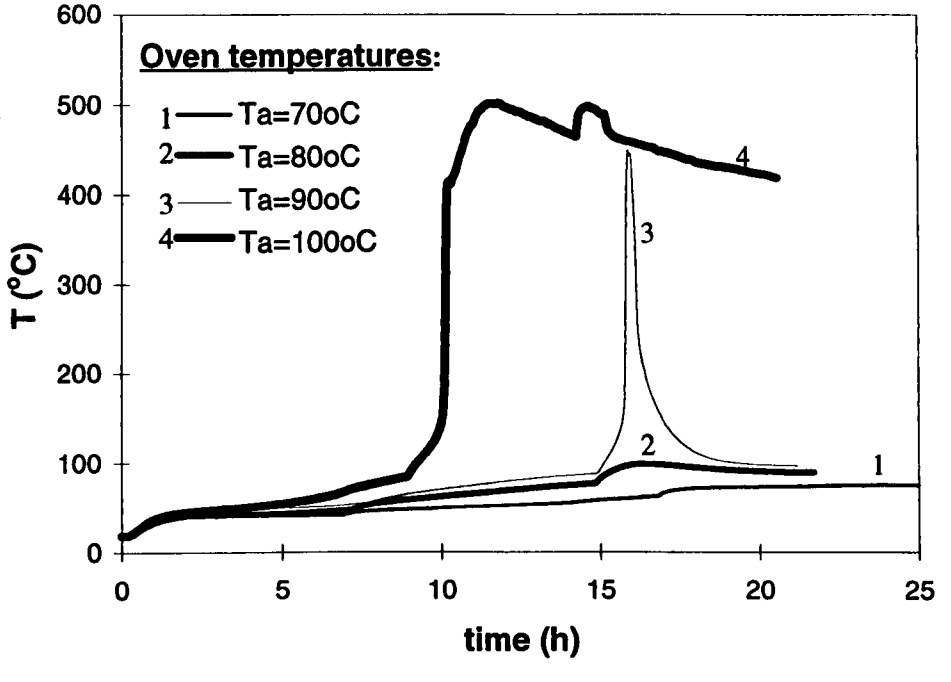

Figure 3.9 Temperature histories of a nitrogen-dried Coal M3 in an adiabatic reactor (A-2) at several oven temperatures at air flow rate of 100 ml min^{-1}

The critical ambient temperature obtained were then used to compare the tendency of various coal samples towards spontaneous combustion. The higher the critical ambient temperature, the lower the propensity of coal towards the spontaneous combustion.

3.2.2.3 Data Analysis

The data analysis involved in this technique was the same as that of in the isothermal reactor. Equation (3-2) which derived from the heat balance when the coal temperature equals to the oven temperature are used to determine the E and A. These kinetic constants can then be used to calculate the critical layer thickness of the coal according to Equation (3-3).

3.2.2.4 Experimental Errors

The experimental errors involved in this technique were also similar to those in the isothermal reactors. They are described in detail below.

- To minimise any preoxidation reaction, all samples were kept in air-tight containers before use in the experiments and the sample preparations were done under nitrogen environment.
- The oven and thermocouples were calibrated at the early stages of this work to eliminate any errors in temperature readings. The temperature fluctuation inside the oven is $\pm 0.5^{o}C$, while the thermocouples had a precision of $\pm 0.1^{o}C$.
- Repeatability of the critical ambient temperatures determined was confirmed by carrying out the experiments for each sample at the same temperatures and essentially the same critical ambient temperature value was obtained. Thus, for each sample, the critical ambient temperature was taken as the average of the lowest temperature at which the thermal runaway occurred and the highest temperature at which the thermal runaway did not occur, with an accuracy of $\pm 5\ ^{o}C$.

- The humidity of air was maintained constant in a dry condition by passing the air through a silica gel column.
- The compactness of the coal sample could affect the self-heating behaviour of coal. Therefore, a similar packing was maintained throughout the experiments. To ensure a constant packing density, the reactors were loosely filled, without pressing, with a desired amount of coal sample for each experiment.
- The temperature of gas entering the reactor was maintained at the same value as the oven temperature to minimise heat loss. An eighteen meter copper tube was used for this purpose. A thermocouple was installed on the gas line near the reactor entrance to measure the gas temperature before entering the reactor.
- It was ensured there was not any leakage in the gas line checked with water soap.
- The energy balance in Equation (3-2) was used only when the coal temperature equals to the oven temperature. Therefore, before switching from nitrogen to air, the coal temperatures at different locations of the reactor were ensured to be uniform. The coal temperatures along the reactor axis were recorded in the data logger every 10 minutes.
- All experiments were repeated to ensure the consistent results.

3.2.3 Wire-Mesh Reactors

The wire-mesh reactor was also used in the present work. Cylindrical wire-mesh containers were used to confine coal samples for the experiments. Both steady-state and unsteady-state methods were employed in this experimental technique. For the steady-state method, the critical ambient temperature, above which a thermal runaway in a sample occurred, were determined on four equicylinder reactors to enable calculations of the oxidation kinetics. For the unsteady-state tests, a transient energy balance analysis was applied at the crossing point, where the thermal conduction around the centre of the cylinder became zero, to calculate the oxidation kinetics. The kinetic constants estimated, from both the steady-state and unsteady-state methods were then used to predict the critical thickness of a coal deposit.

3.2.3.1 Apparatus

The experimental setup used in this study is shown schematically in Figure 3.10. The oven was supplied with a PID controller which ensures the fluctuation temperature to be within the oven of 0.5 °C. To fulfil the conditions for the steady-state method, a rigorous air agitation was provided by a built-in fan to ensure that the Biot number was significantly large. The datataker used in this setup was the same as that used in the isothermal and adiabatic reactor experimental setup.

A Coal M3 was used in this study. Freshly picked coal sample was dried in nitrogen at 105 °C for overnight and then sieved. A size of 0.25 ~ 1.00 mm was retained and stored in tightly sealed baskets for use in all experiments.

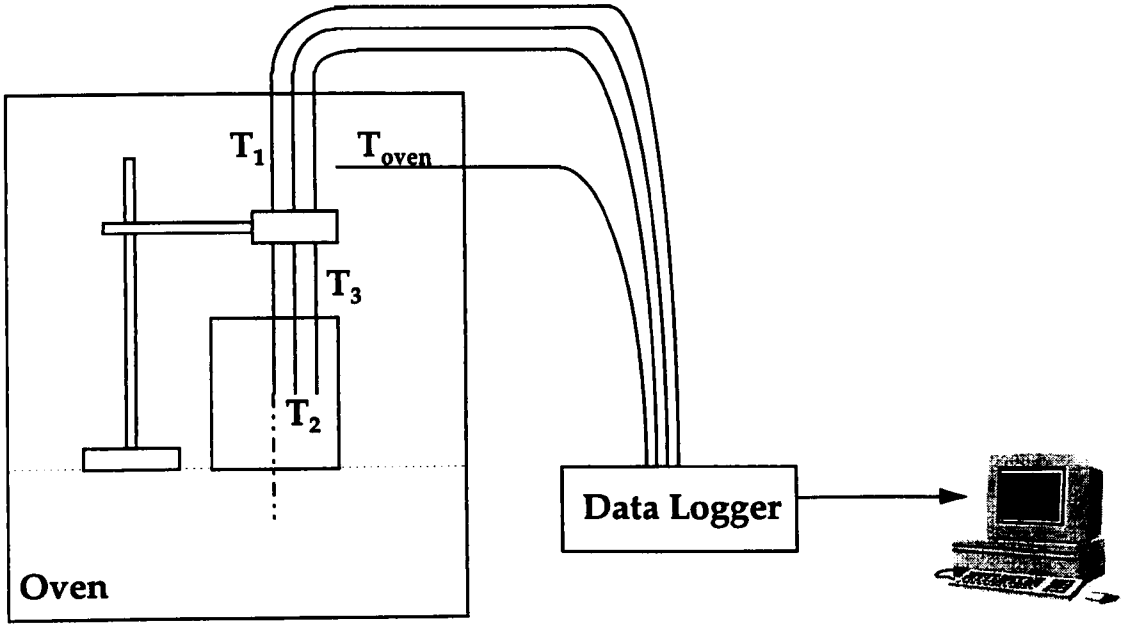

Figure 3.10 Schematic diagram of the apparatus for wire-mesh reactor experiments

Seven cylindrical wire-mesh reactors, made of No. 30 mesh (32 SWG), were used to confine coal samples in the experiments. The dimensions of these reactors were given in Table 3.4. Note that the first four reactors (B-1 to B-4) were equicylinders (diameter equals to height), while the last four (B-4 to B-7) were of the same volumetric capacity. Three 1 mm K-type thermocouples were inserted inside each

reactor, separated by a distance (Δr) along the cylinder radius, to monitor the sample temperatures. The first thermocouple (T_1) was placed at the geometric centre of the sample. The distances between thermocouples, also presented in Table 3.4 for different reactors, have been optimised to achieve the best sensitivity of the radial temperature derivatives. The thermocouples were connected to the data acquisition system to record the sample temperatures during each experiment. To ensure that the thermocouples stay in their right positions, a stand mounted thermocouples was made and shown in Figure 3.11. The shaded section in Figure 3.10 was enlarged in Figure 3.11 (section X-X). These thermocouples were then connected to the data acquisition system to record the temperatures during each experiment.

Table 3.4 Specifications of cylindrical wire-mesh reactors

Reactor I.D.	**Frank-Kamenetskii Parameter** δ_c	**Reactor Dimensions**		**Distance Between Thermocouple Centres (Δr)** (mm)
		Diameter (mm)	**Height** (mm)	
B-1	2.89	25.0	25.0	3.0
B-2	2.89	40.0	40.0	6.0
B-3	2.89	60.0	60.0	7.0
B-4	2.89	75.0	75.0	10.0
B-5	2.11	40.0	260.0	6.0
B-6	2.33	60.0	120.0	7.0
B-7	5.49	95.0	47.5	12.0

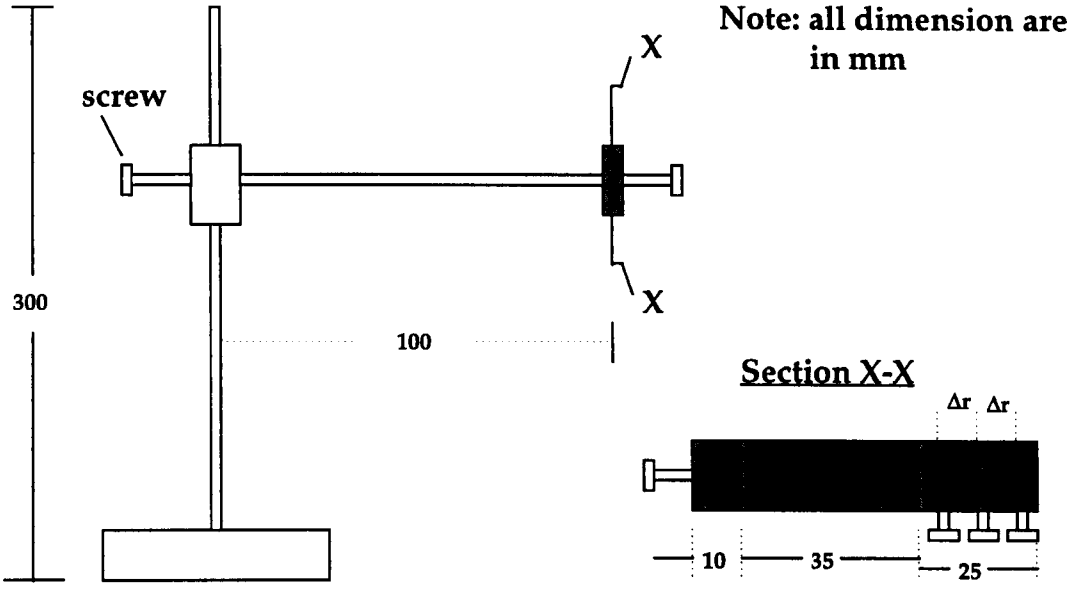

Figure 3.11 A drawing of a stand mounted thermocouples

3.2.3.2 Experimental Procedures

The reactors were loosely filled with a coal sample, without pressing to ensure the packing density is constant, and placed in an electrically heated oven. To fulfil the conditions for the steady-state method, a rigorous air agitation was provided by a built-in fan to ensure that the Biot number is significantly large. An iterative procedure was used to determine the critical ambient temperature for each reactor, by varying the oven temperature with an interval of 1 °C. The critical ambient temperatures obtained from the center thermocouple's reading (T_1) were then used to estimate the kinetics. Typical temperature-time plots of Reactor B-1 for various ambient (oven) temperatures are shown in Figure 3.12. As can be seen, at oven temperatures below 153 °C, spontaneous combustion did not occur. However, at 153 °C the self-ignition occurred. Thus, the critical ambient temperature for Reactor B-1 was taken as 152.5 ± 0.5 °C. Repeatability of the critical ambient temperature measurement was confirmed by repeating experiments; essentially the same critical ambient temperature value was obtained for the same sample. Typical temperature-time plots of other reactors, ie. B-2 to B-7, are shown in Figure 3.13 to Figure 3.18,

respectively. These Figures also show how the experimental time varies with the reactor sizes. This will be discussed in detail in the Chapter 4 of this thesis.

In the unsteady-state method, to find the crossing point when the thermal conduction term near the centre of the cylinder becomes zero, ie.

$$\frac{1}{r}\frac{\partial}{\partial r}\left(r\frac{\partial T}{\partial r}\right)\cong 0 \qquad (3\text{-}4)$$

or in the finite-difference form

$$\frac{T_3-2T_2+T_1}{(\Delta r)^2}+\frac{1}{r_2}\frac{T_3-T_1}{2(\Delta r)}\cong 0 \qquad (3\text{-}5)$$

The radial derivative of temperature readings for the three thermocouples were computed until Equation (3-5) was satisfied. Typical temperature histories and $\frac{1}{r}\frac{\partial}{\partial r}\left(r\frac{\partial T}{\partial r}\right)$ versus time for Reactor B-1 to B-7 at a certain oven temperature are presented in Figures 3.19 to 3.25, respectively. The crossing point temperature, Tp, and the rate of temperature rise at the centre can then be determined when $\frac{1}{r}\frac{\partial}{\partial r}\left(r\frac{\partial T}{\partial r}\right)$ equals to zero, as indicated on Figures 3.19 to 3.25.

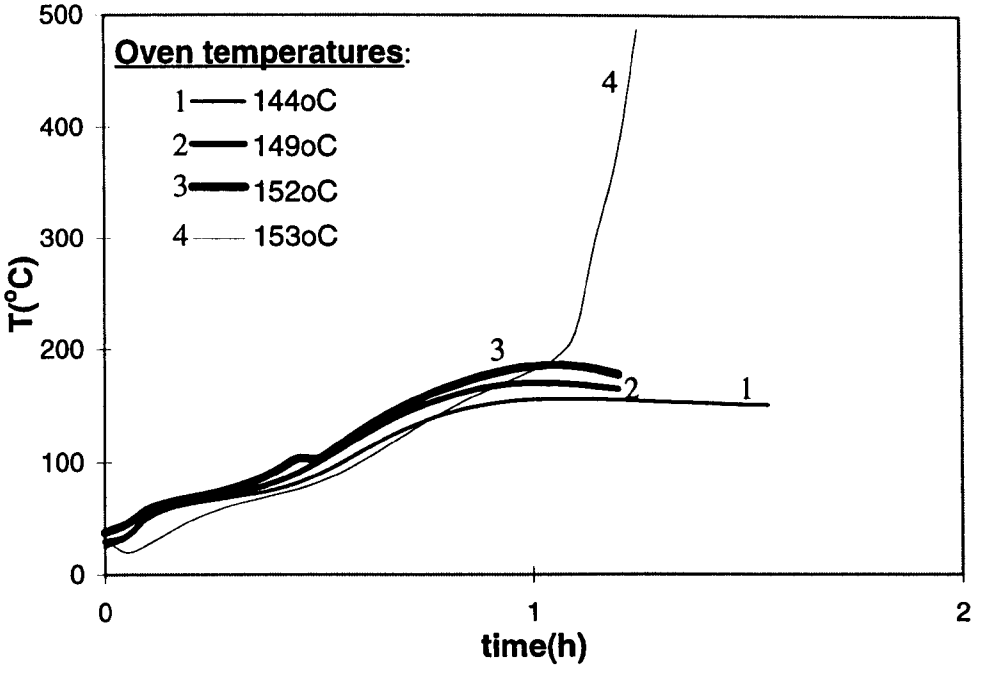

Figure 3.12 Steady-state method for determination of the critical ambient temperatures: temperature histories of coal tested in Reactor B-1 at several oven temperatures

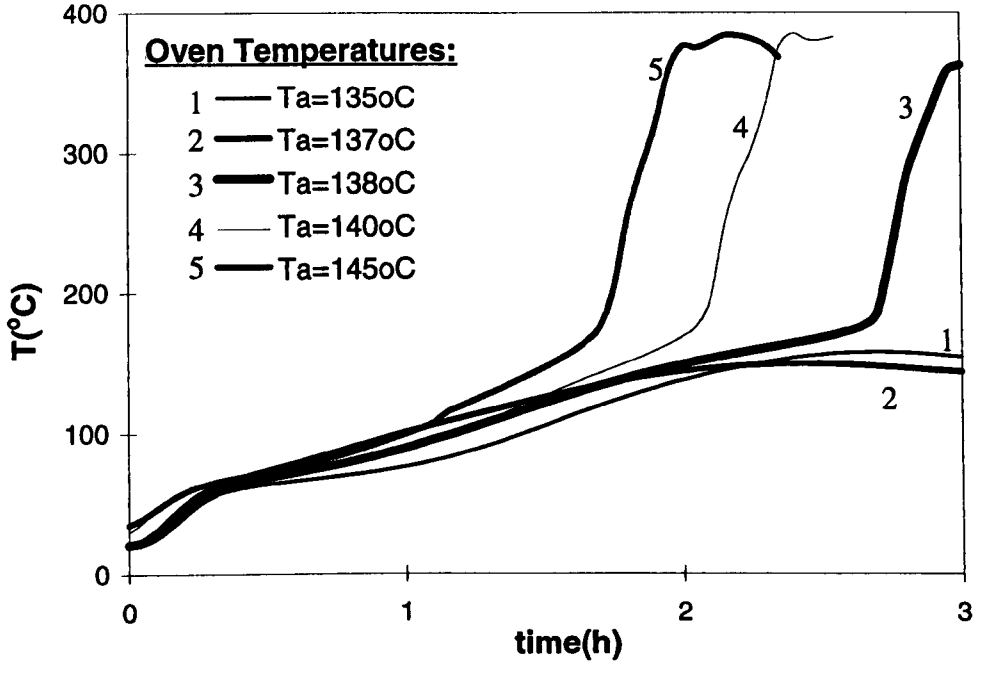

Figure 3.13 Steady-state method for determination of the critical ambient temperatures: temperature histories of coal tested in Reactor B-2 at several oven temperatures

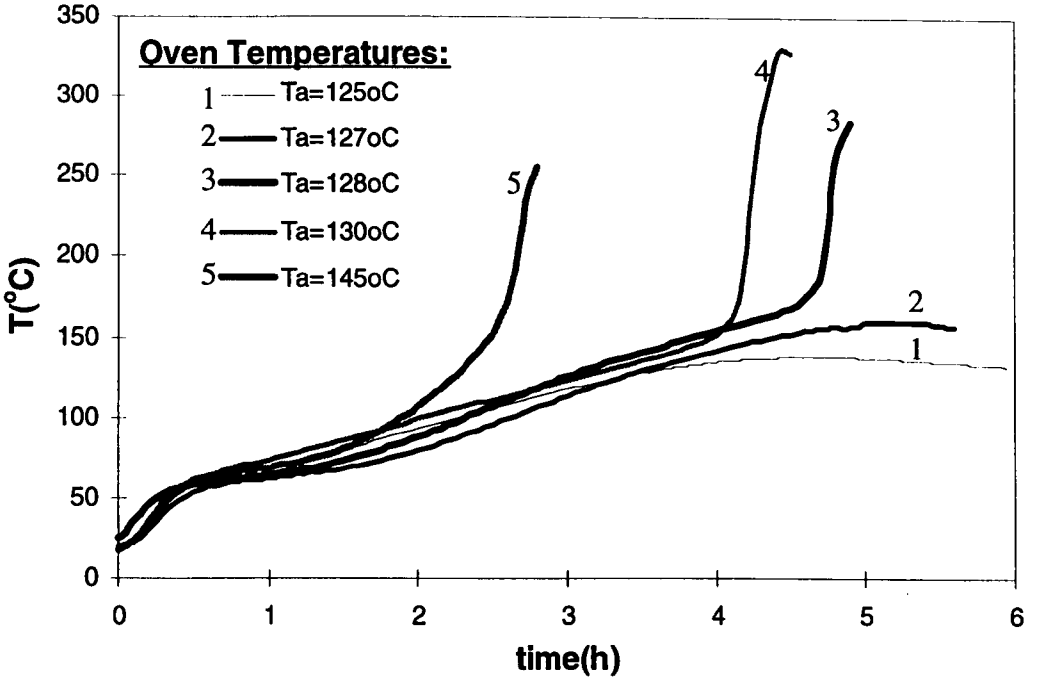

Figure 3.14 Steady-state method for determination of the critical ambient temperatures: temperature histories of coal tested in Reactor B-3 at several oven temperatures

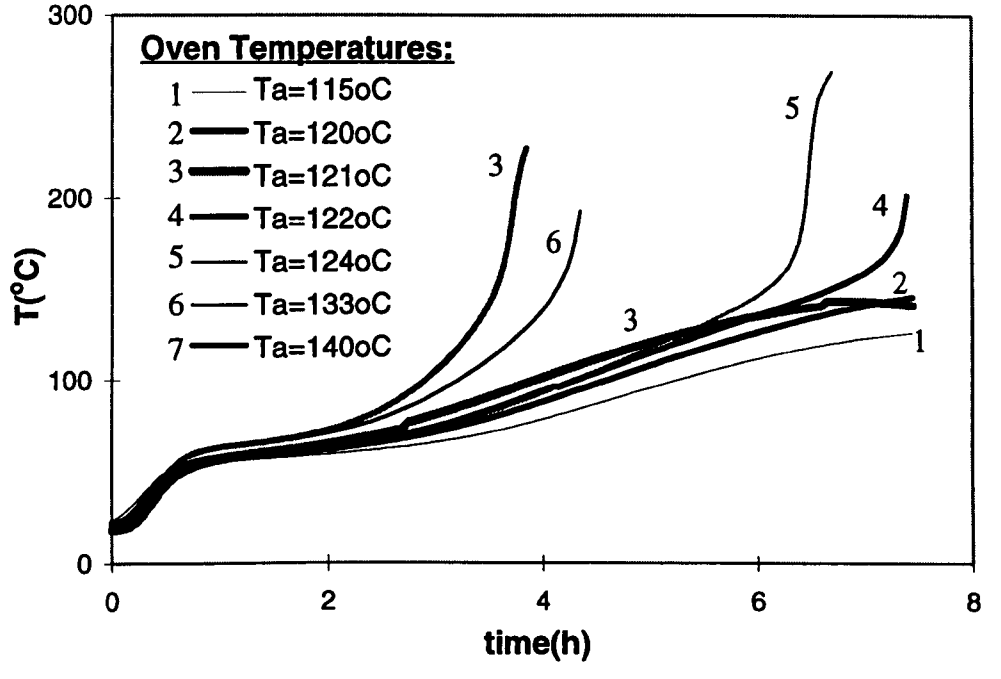

Figure 3.15 Steady-state method for determination of the critical ambient temperatures: temperature histories of coal tested in Reactor B-4 at several oven temperatures

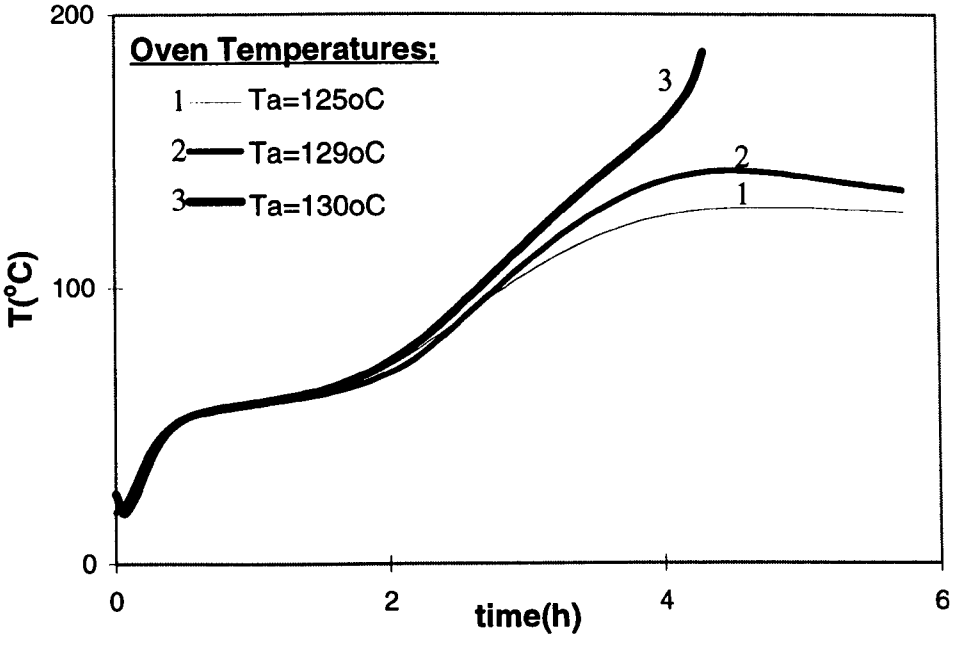

Figure 3.16 Steady-state method for determination of the critical ambient temperatures: temperature histories of coal tested in Reactor B-5 at several oven temperatures

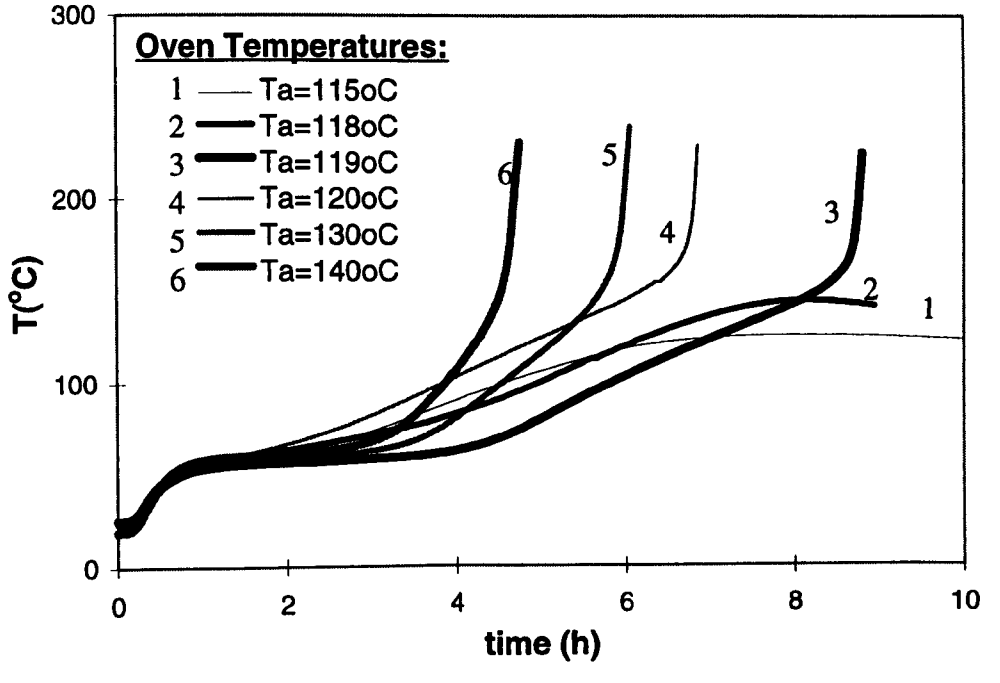

Figure 3.17 Steady-state method for determination of the critical ambient temperatures: temperature histories of coal tested in Reactor B-6 at several oven temperatures

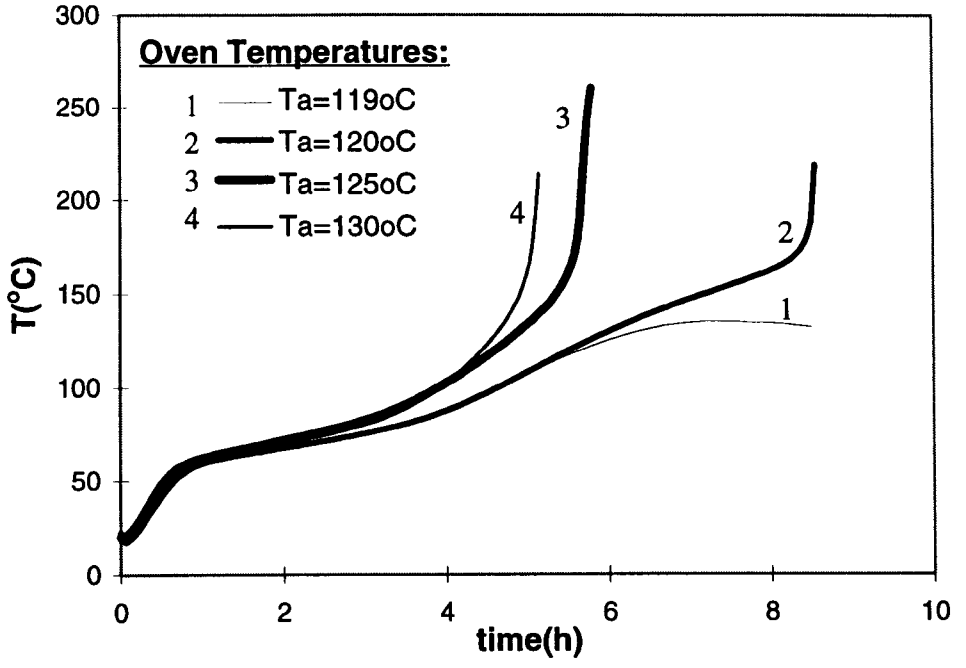

Figure 3.18 Steady-state method for determination of the critical ambient temperatures: temperature histories of coal tested in Reactor B-7 at several oven temperatures

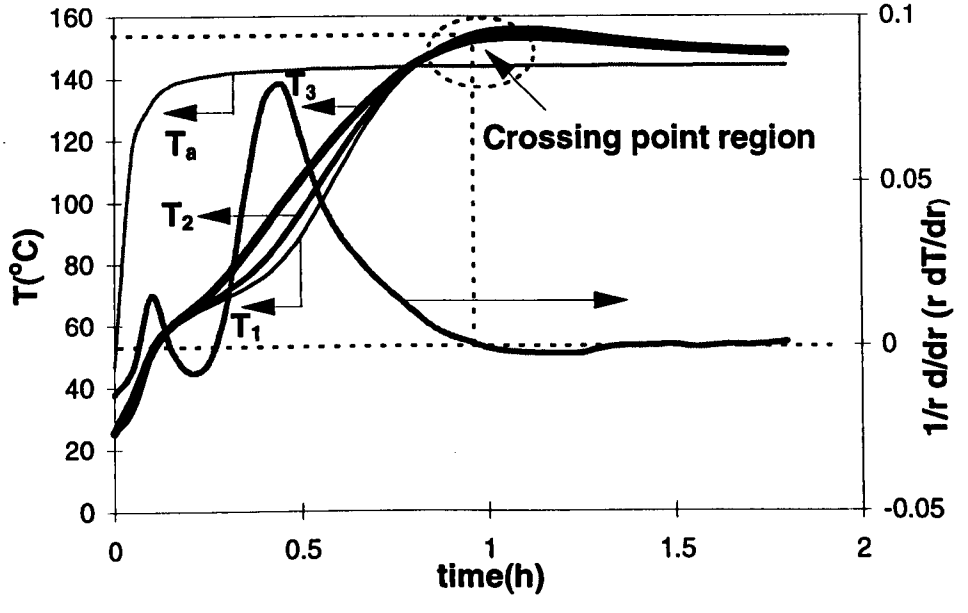

Figure 3.19 Unsteady-state method for determination of the crossing point: temperature readings (left Y-axis) and computed radial temperature derivative (right Y-axis) as a function of time in Reactor B-1 at oven temperature (Ta) of 144 °C

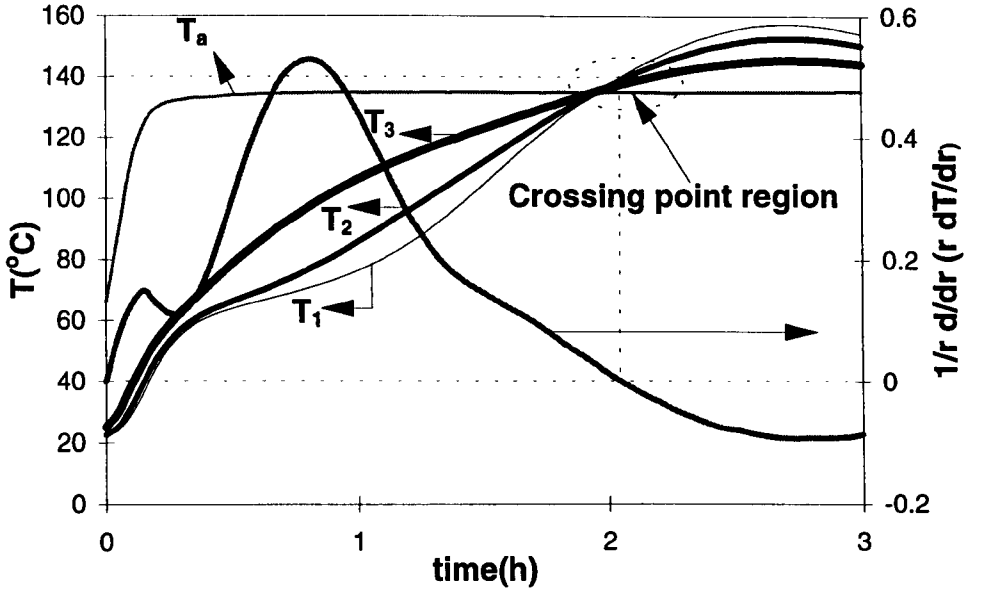

Figure 3.20 Unsteady-state method for determination of the crossing point: temperature readings (left Y-axis) and computed radial temperature derivative (right Y-axis) as a function of time in Reactor B-2 at oven temperature (Ta) of 135 °C

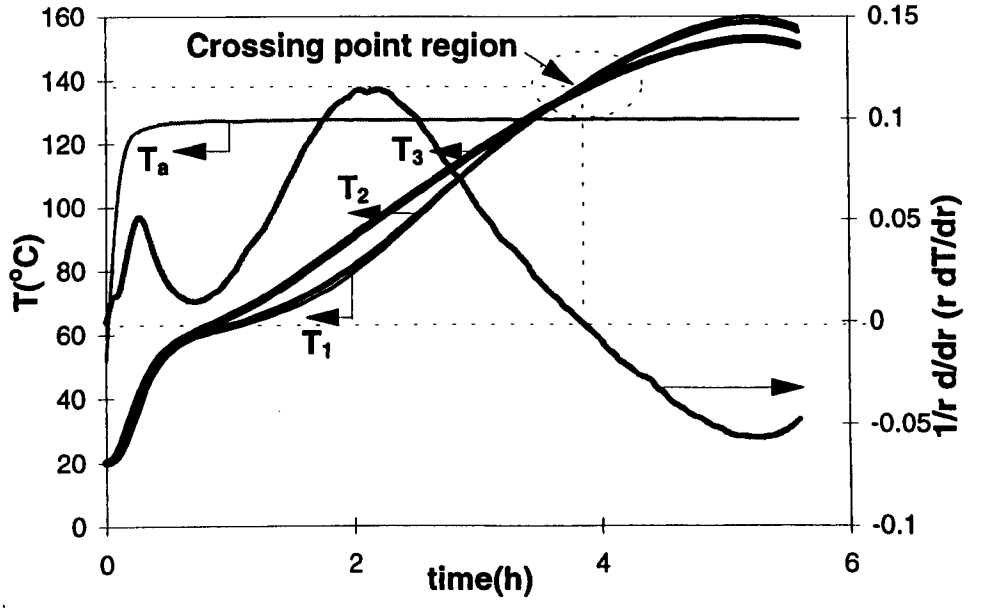

Figure 3.21 Unsteady-state method for determination of the crossing point: temperature readings (left Y-axis) and computed radial temperature derivative (right Y-axis) as a function of time in Reactor B-3 at oven temperature (Ta) of 127 °C

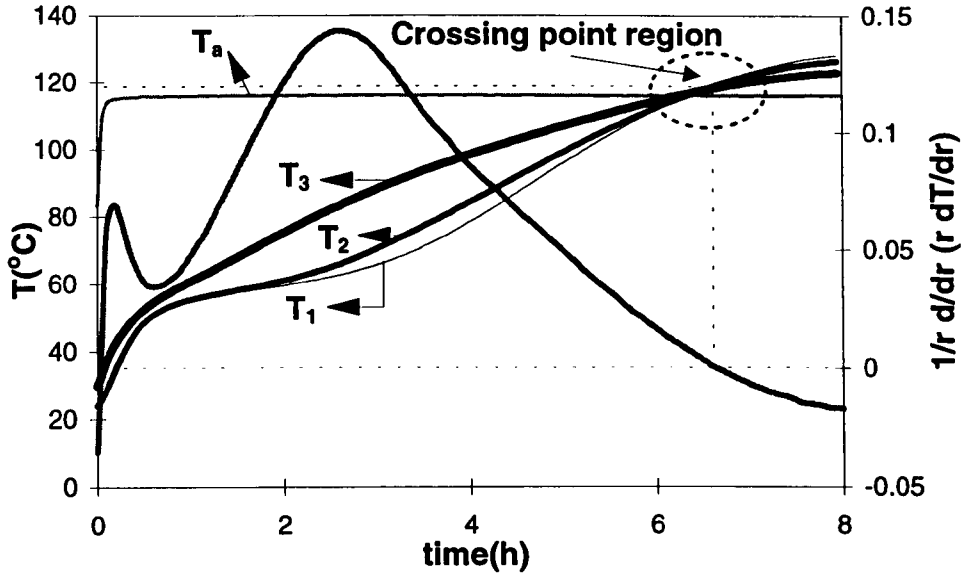

Figure 3.22 Unsteady-state method for determination of the crossing point: temperature readings (left Y-axis) and computed radial temperature derivative (right Y-axis) as a function of time in Reactor B-4 at oven temperature (Ta) of 115 °C

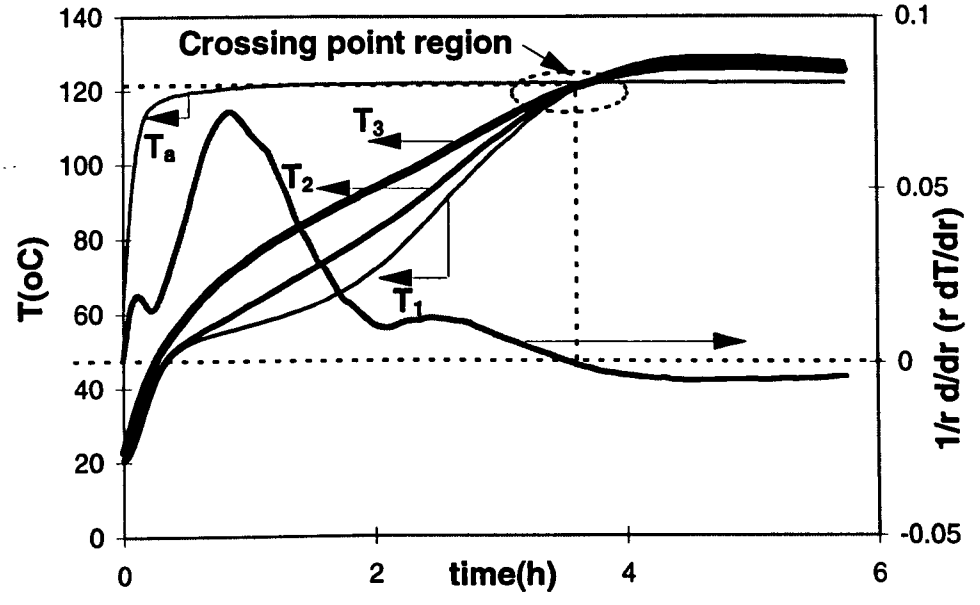

Figure 3.23 Unsteady-state method for determination of the crossing point: temperature readings (left Y-axis) and computed radial temperature derivative (right Y-axis) as a function of time in Reactor B-5 at oven temperature (Ta) of 120 °C

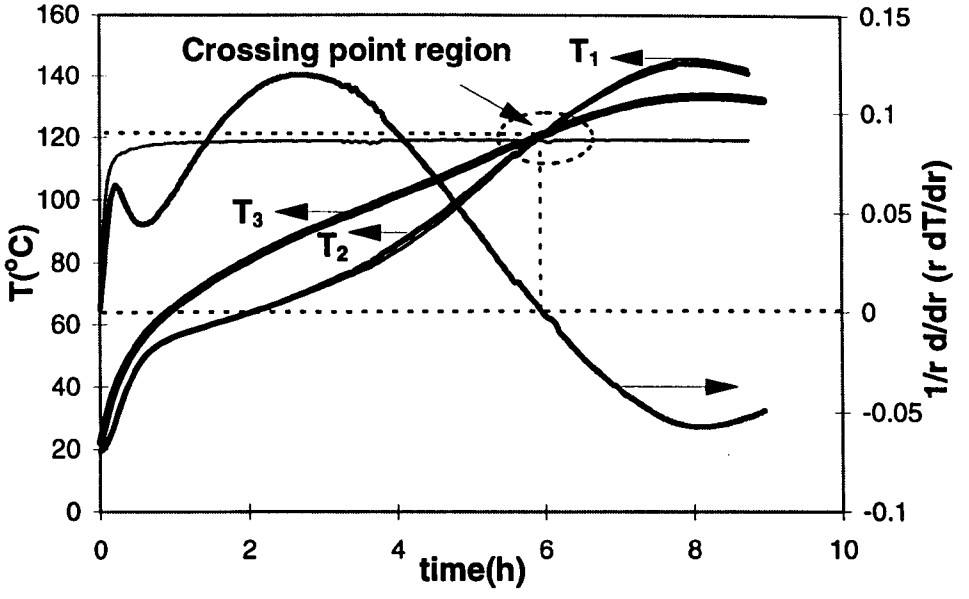

Figure 3.24 Unsteady-state method for determination of the crossing point: temperature readings (left Y-axis) and computed radial temperature derivative (right Y-axis) as a function of time in Reactor B-6 at oven temperature (Ta) of 118 °C

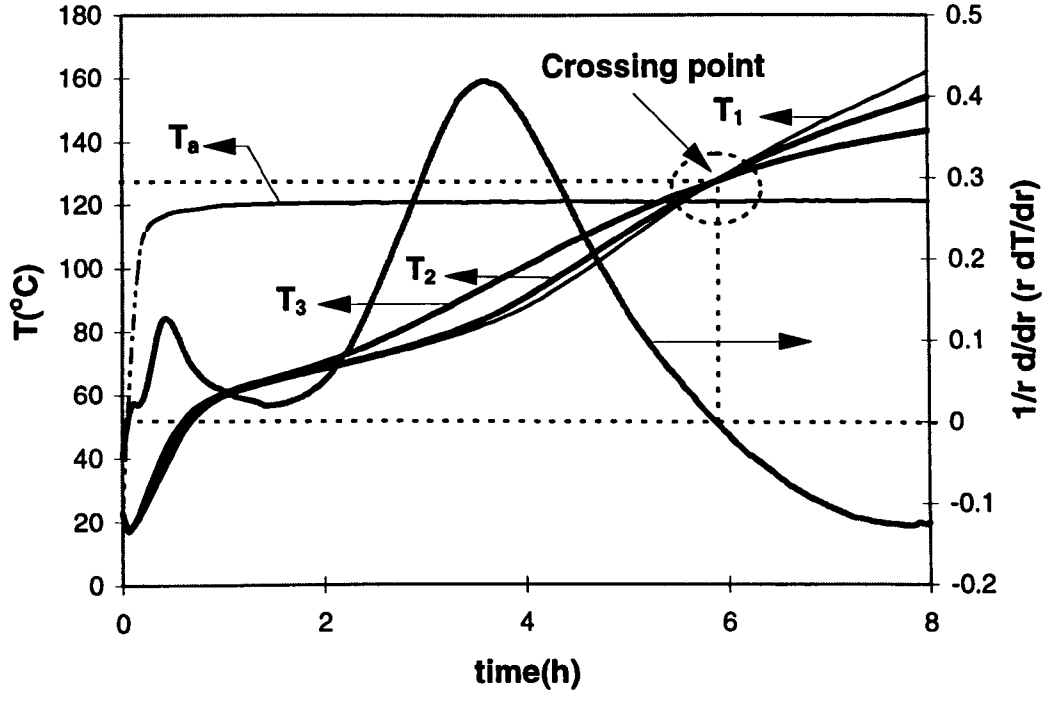

Figure 3.25 Unsteady-state method for determination of the crossing point: temperature readings (left Y-axis) and computed radial temperature derivative (right Y-axis) as a function of time in Reactor B-7 at oven temperature (Ta) of 120 °C

3.2.3.3 Data Analysis

The low-temperature oxidation kinetics were estimated by an energy balance approach. The unsteady-state energy balance for a porous reactive solid, when the reactant depletion is neglected, can be written as:

$$\rho_s \, Cp_s \frac{\partial T}{\partial t} = k_t \nabla^2 T + Q \rho_s \, A \exp\left(-\frac{E}{RT}\right) \qquad (3\text{-}6)$$

where the left-hand-side is the local enthalpy change in the solid, and on the right-hand-side are the local heat conduction in the sample and heat generation due to the oxidation reaction, respectively. The physical and chemical properties of coal may be assumed to be independent of temperature (Bowes (1984)).

Steady-State Analysis

As has been stated in Chapter 2, for the steady-state method, solutions to Equation (3-6), when the left-hand-side becomes zero, have been found for several standard geometrises (Bowes (1984)):

$$\delta_c = \frac{E}{R T_{a,c}^2} \frac{\Delta^2 Q \rho_S A}{k_t} e^{-E/RT_{a.c}} \qquad (3\text{-}7)$$

where δ_c is the Frank-Kamenetskii parameter (dimensionless) which strongly depends on the shape of the solid. Furthermore, a strict boundary condition (Bi >>1) is ensured to be satisfied. Values of δ_c for various cylindrical reactors used are calculated according to Bowes (1984) and listed in Table 3.4.

Rearranging Equation (3-7), the following equation arrives:

$$\ln\left(\frac{\delta_c T_{a,c}^2}{\Delta^2}\right) = \ln\left(\frac{\rho_s EQA}{k_t R}\right) - \frac{E}{R T_{a,c}} \qquad (3\text{-}8)$$

Equation (3-8) is the basis of the steady-state method for estimation of oxidation kinetics. By measuring the critical ambient temperature, $T_{a,c}$, as a function of reactor size, A and E can be determined from the linear plot of $\ln(\delta_c T_{a,c}^2/r^2)$ and $1/T_{a,c}$. The critical thickness (Δ) of a coal deposit, say an infinite slab, can then be predicted from the kinetics constants according to Equation (3-3).

Unsteady-State Analysis

As has also been described in Chapter 2, the unsteady-state method is based on the fact that during unsteady-state heating of a solid, there is a point in time (or temperature) at which the thermal conduction term near the geometric symmetry of the sample becomes zero (Gray et al. (1992; 1990)), then, Equation (3-6) reduces to

$$\left(\frac{\partial T}{\partial t}\right)_{T=T_p} = \frac{QA}{Cp_s}\exp\left(-\frac{E}{RT_p}\right) \qquad (3\text{-}9)$$

or

$$\ln\left(\frac{\partial T}{\partial t}\right)_{T=T_p} = \ln\frac{QA}{C_{p_s}} - \frac{E}{RT_p} \qquad (3\text{-}10)$$

where T_p is the temperature at the symmetry when the conduction term is zero (Chen and Chong (1995); Chong et al. (1997); Chong et al. (1995); Chong et al. (1996)). Equation (3-10) is the basis of the unsteady-state method (Chen and Chong (1995)) for estimation of oxidation kinetics. Ideally, only one reactor size is required, and experiments can be repeated at several different ambient temperatures to determine the crossing point temperatures and the rates of temperature rise at the

crossing points. The linear plot between $\ln\left(\frac{\partial T}{\partial t}\right)_{T=T_p}$ and $\frac{1}{T_p}$ then yields the kinetic constants, A and E. The kinetic constants thus estimated can again be used to predict the critical thickness according to Equation (3-3).

3.2.3.4 Experimental Errors

There are many factors which could contribute to the experimental errors in the wire-mesh reactor experiments. Precautions have been taken to minimise them. These precautions include:

- The sample was treated carefully to prevent any pre-oxidation reaction. The sample was dried in a nitrogen environment at 105 °C to shorten the experimental time and eliminate the effect of coal moisture on the coal self-heating. All samples were kept in air-tight containers before used in the experiments.
- The oven and thermocouples were calibrated at the early stages of this work to eliminate any errors in temperature readings. The temperature fluctuation inside the oven was ± 0.5 °C, while the thermocouples have a precision of ± 0.1 °C.
- A stand mounted thermocouples was used to ensure the thermocouples stay in their right positions.
- Repeatability of the critical ambient temperatures determined was confirmed by carrying out the experiments for each sample at the same temperatures and essentially the same critical ambient temperature value was obtained. Thus, for each sample, the critical ambient temperature was taken as the average of the lowest temperature at which the thermal runaway occurred and the highest temperature at which the thermal runaway did not occur, with an accuracy of $\pm$ 0.5 °C.
- The compactness of the coal sample could affect the self-heating behaviour of coal. Therefore, a similar packing was maintained throughout the experiments. To ensure a constant packing density, the reactors were loosely filled, without pressing, with a constant amount of coal sample for each experiment.

- For the unsteady-state experiments, the periphery ignition (ie. when the ignition starts from the coal layer near the surface and not from the center of the sample) is not expected. Therefore, the initial temperature of coal and the oven temperature were ensured to be lower than the critical ambient temperature.
- All experiments were repeated to obtain consistent results.

3.3 SUMMARY

Based on the fact that there are many conflicting results reported in the literature, three most frequently used experimental techniques, have been chosen for this research. These techniques are employed to study the self-heating behaviour of a Victorian brown coal. The use of different techniques on the same coal enables examination of the influence of various experimental conditions on the understanding of spontaneous combustion phenomenon. The next chapter presents and compares the experimental results obtained from different techniques.

Chapter 4

RESULTS AND DISCUSSION

In Chapter 3, the three different experimental techniques for the spontaneous combustion study along with the experimental procedures have been reported. This chapter summarises the results obtained from these techniques. A comparison of the results obtained by different techniques is made in the last section of this chapter.

4.1 RESULTS FROM ISOTHERMAL REACTOR EXPERIMENTS

Isothermal reactors have been used intensively to examine the effects of coal properties and ambient conditions on the spontaneous combustion. The effect of packing density and reactor size were also investigated using this technique. The following sections discuss these in detail.

4.1.1 Factors Influencing Self-Heating

4.1.1.1 The effect of air flow rate

The air flow rate not only determines the amount of oxygen available for the oxidation reaction and thus the rate of heat generation, but also influences the rate of heat removal from the reaction system. Because of the low thermal capacity of air, the heat dissipated into the surroundings is usually small compared with the heat of

oxidation or heat of drying (Krishnawamy et al. (1996)). However, a very large air flow rate can keep the coal sufficiently cool. Similarly, a very small air flow rate may not be able to supply enough oxygen for the oxidation reaction (Nordon (1979)). It is believed that, for a given coal, there should be an optimum air flow rate at which spontaneous combustion is most favoured.

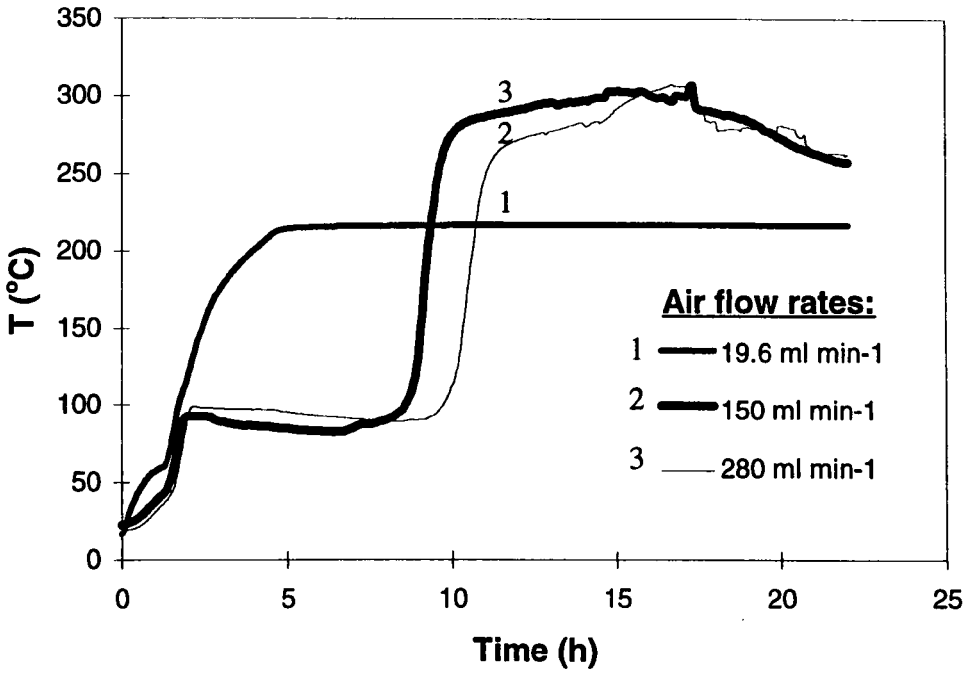

Figure 4.1 Temperature histories of fresh Coal M1 at several air flow rates in an isothermal reactor (R-4) at an ambient temperature of 200 °C

Figure 4.1, which was obtained from experiments using fresh Coal M1 with a particle size fraction of 1.00 ~ 2.36 mm tested in an isothermal reactor (R-4) at 200 °C, shows the effect of air flow rate on the self-heating process. It can be seen that at an air flow rate of 19.6 ml min^{-1}, the thermal runaway did not occur, while at higher air flow rates (100 and 280 ml min^{-1}) the thermal runaway occurred. The delay in temperature increase at around 100 °C was apparently caused by evaporation of coal moisture. The temperature profiles of the coal with air flow rates of 150 and 280 ml min^{-1} were similar, and indicated that there was no oxygen limitation within that range of air flow rate.

To further clarify this phenomenon, a narrower range of air flow rates were used, as shown in Figure 4.2. The fresh Coal M1 with a particle size fraction of 1.00 ~ 2.36 mm was tested in an isothermal reactor (R-4) at an oven temperature of 153 °C. Similar to Figure 4.1, Figure 4.2 shows that at an air flow rate of 50 ml min^{-1}, the thermal runaway did not occur, which indicated that the air flow rate of 50 ml min^{-1} was too low. On the other hand, at higher air flow rates (100 to 180 ml min^{-1}), there was sufficient oxygen for the oxidation reaction, thus the thermal runaway occurred. The temperature profiles of Coal M1 with air flow rates between 100 and 180 ml min^{-1} were similar, and again indicated that there was not any oxygen limitation in that range of air flow rate. Therefore, for the rest of the experiments using isothermal reactor (R-4), an air flow rate of 100 ml min^{-1} was used.

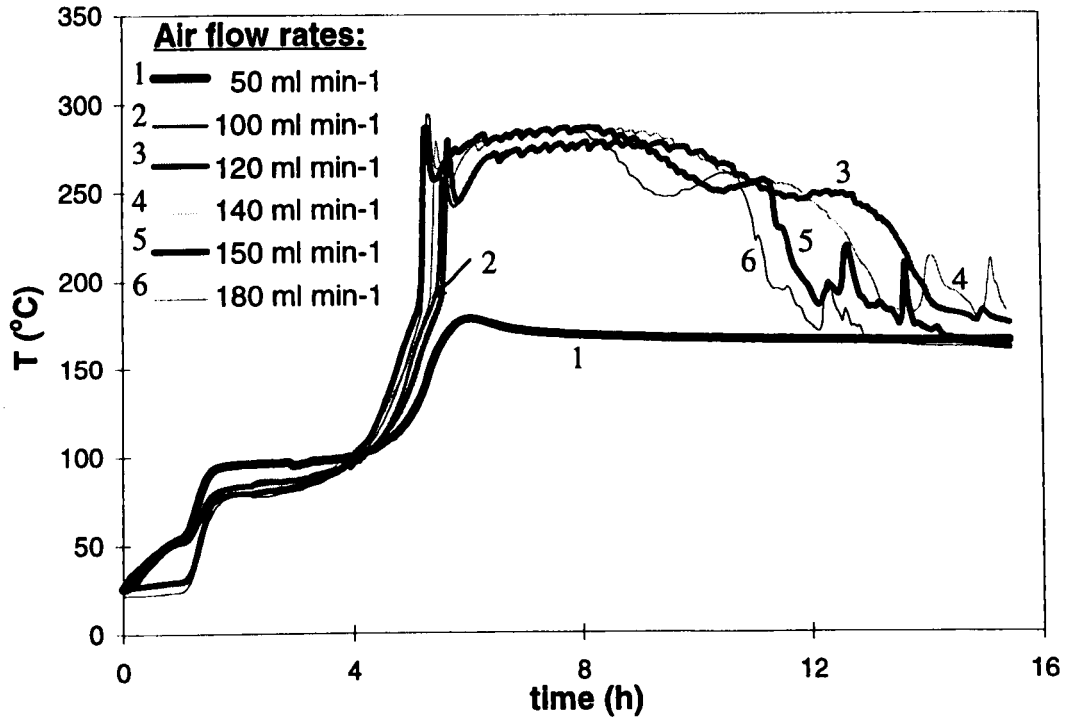

Figure 4.2 Temperature histories of fresh Coal M1 at several air flow rates in an isothermal reactor (R-4) at an ambient temperature of 153 °C

4.1.1.2 The effect of ambient temperature

Temperature profiles of the $Mg(Ac)_2$-added-Coal M2 with a particle size of 0.25 ~ 1.00 mm in an isothermal reactor (R-4) are shown in Figure 4.3(a). It can be seen that at temperatures below 155 °C, the thermal runaway did not occur, while at 155 °C thermal runaway occurred. Accordingly, the higher the ambient temperatures, the higher the probability of spontaneous combustion. Similar trends for KAc-added-Coal M2, NaAc-added-Coal M2, $CaCl_2$-added-Coal M2, NaCl-added-Coal M2, and KCl-added-Coal M2 are shown in Figure 4.3.

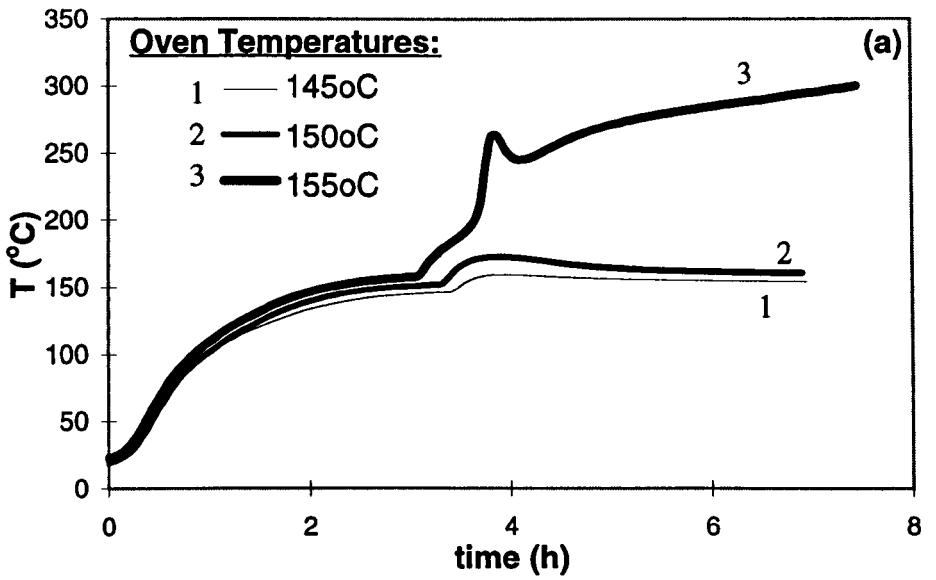

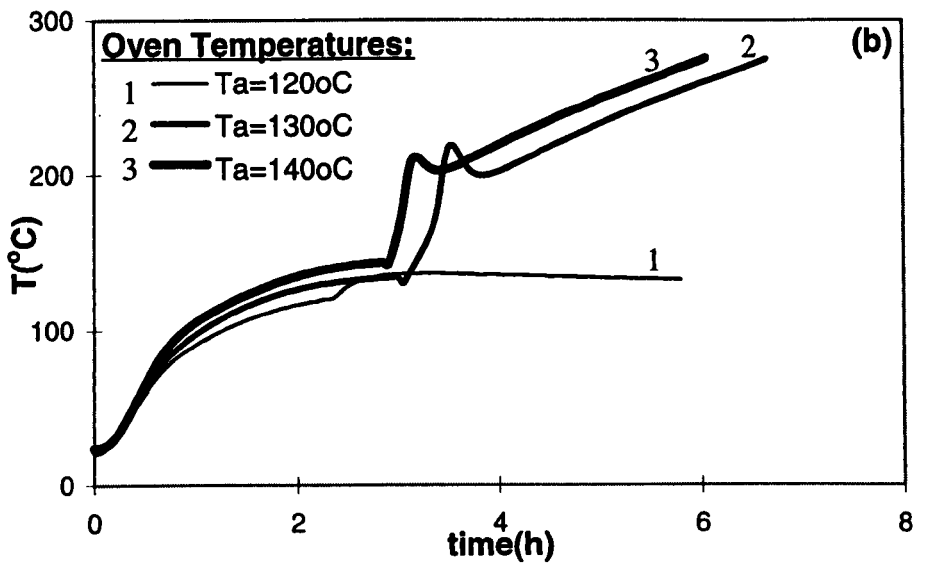

Figure 4.3 (Continued on the next page)

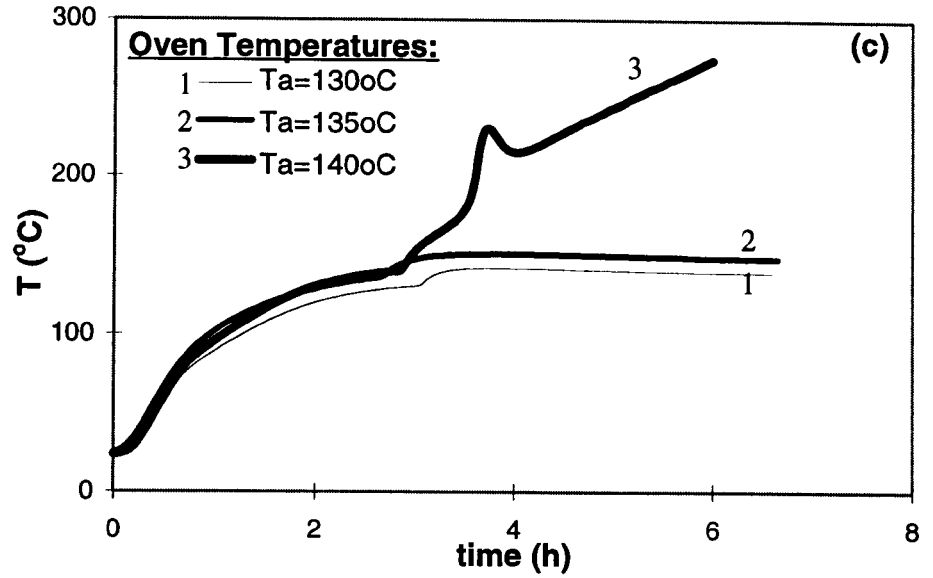

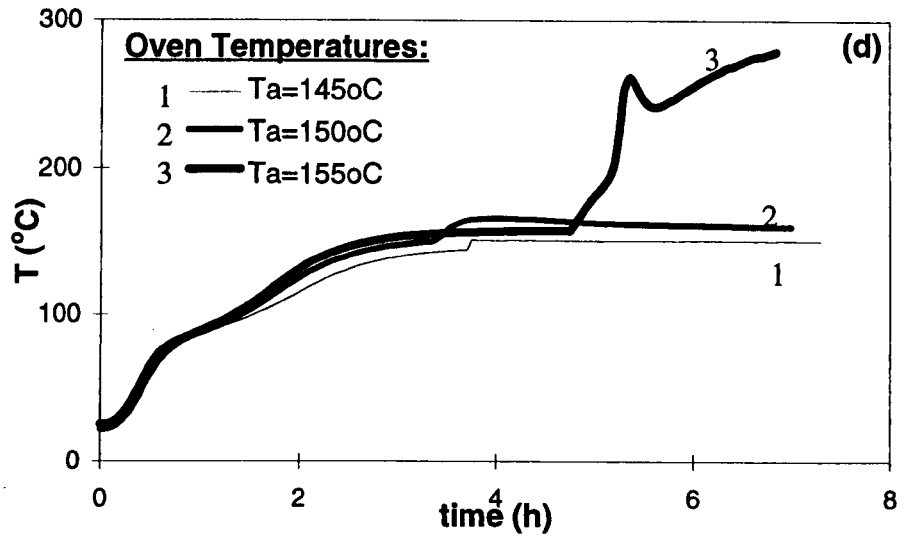

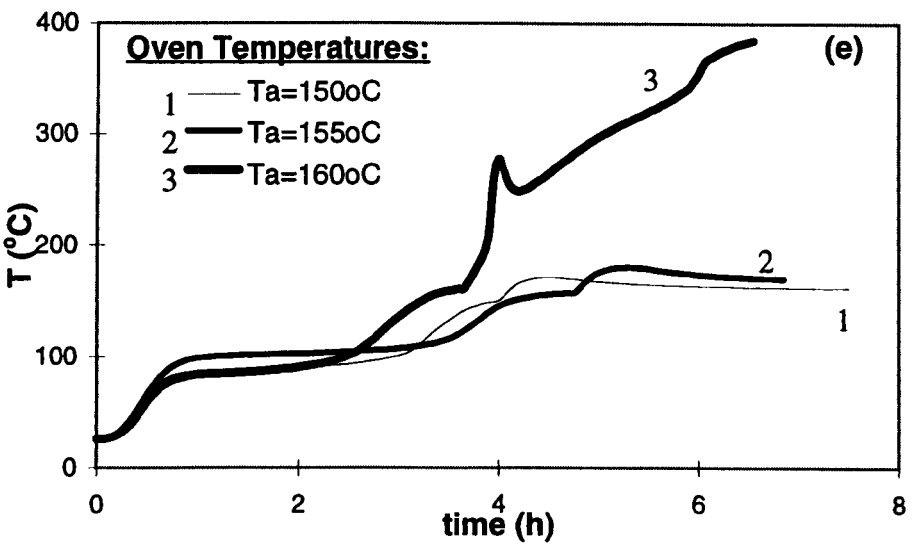

Figure 4.3 (Continued on the next page)

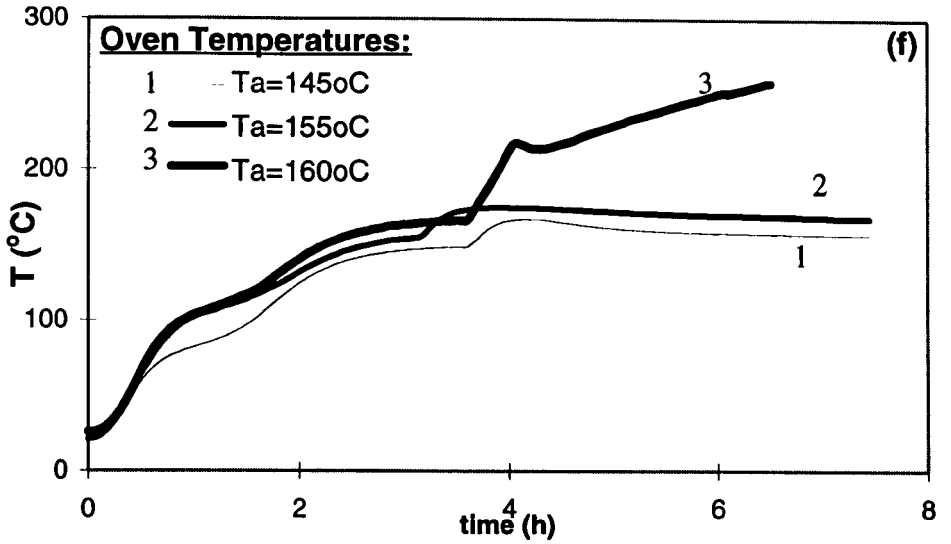

Figure 4.3 Temperature histories of (a) $Mg(Ac)_2$-added-coal; (b) KAc-added-coal; (c) NaAc-added-coal; (d) $CaCl_2$-added-coal; (e) NaCl-added-coal; and (f) KCl-added-coal, in an isothermal reactor (R-4) at several oven temperatures

An interesting feature is observed in Figure 4.3 that a hump existed in the temperature histories for all samples. At beginning, the temperatures of coal samples increased slowly due to relatively low oxidation rates at low-temperatures and evaporation of tightly bound moisture in the samples. As they became completely dried, the temperatures of the samples increased sharply. Then, at a reasonably high temperature, e.g. 250 °C for most of the samples, the temperatures decreased before increasing again. This may be due to endothermic decomposition of carboxyl groups (partial devolatilisation) which absorbed heat (Durie (1991)). As the endothermic devolatilisation processes weakened over a period of 20 ~ 30 minutes, the oxidation reaction dominated again and the temperatures increased, leading to a thermal runaway.

4.1.1.3 The effect of ambient humidity

The effect of air humidity was examined using dried air and humidified air. Dried air was obtained by passing the air through the silica gel column, while humidified air was obtained by passing the air through the water column. Figure 4.4 shows the results obtained from the experiments using fresh Coal M1, which contained ~ 64% moisture, in an isothermal reactor (R-4). The oven temperature used in the experiments was 200 °C, while the air flow rate and particle size range were 100 ml min^{-1} and 1.00 ~ 2.36 mm, respectively. It is observed that a humid environment enhanced the self-heating process. This is because a humid environment prevented a further evaporation of coal moisture, and thus increased the risk for the coal to spontaneously combust.

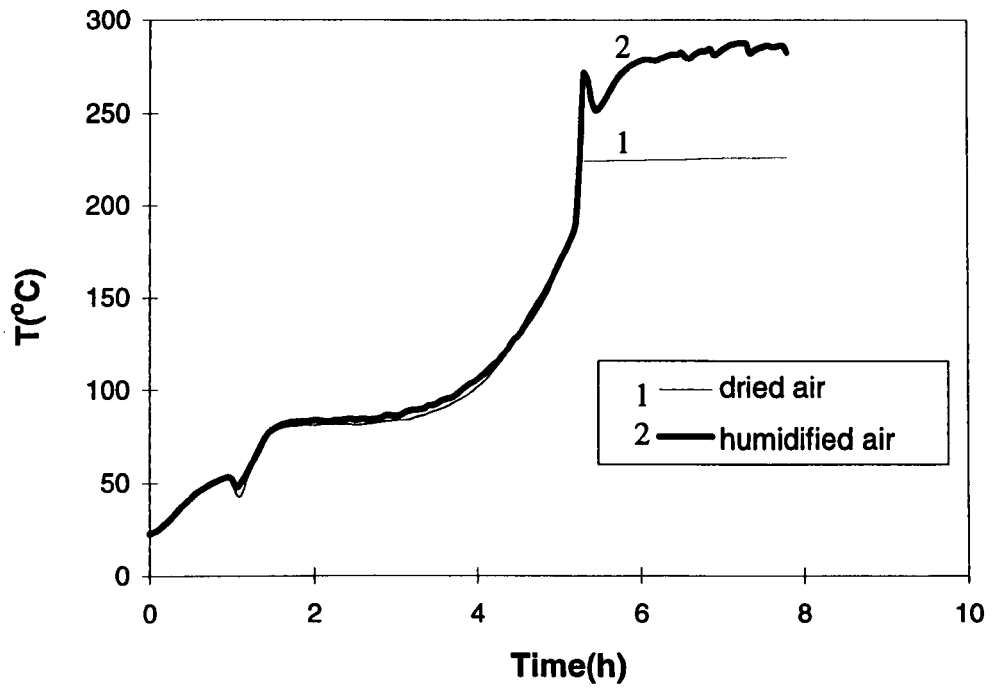

Figure 4.4 Temperature histories of fresh Coal M1 at two different air humidities in an isothermal reactor (R-4)

4.1.1.4 The effect of coal particle size

Figure 4.5 shows the effect of particle size on the temperature profiles of the fresh Coal M1 tested in an isothermal reactor (R-4). The oven temperature and air flow rate used in the experiments were 153 °C and 100 ml min^{-1}, respectively. It is shown that the sample of a size fraction 0.25 ~ 1.00 mm experienced a sharp temperature increase immediately after the nitrogen gas was replaced by air, whereas temperature profiles of the other two samples remained at the oven temperature. Accordingly, a smaller particle size reached a higher temperature. This is because its larger surface area per unit weight of coal resulted in a high overall oxidation reaction rate.

Further work was carried out to examine the effect of particle size on the critical ambient temperature, above which a thermal runaway occurs, using Coal M2. As shown in Figure 4.6, the larger the particle size, the higher the critical ambient temperature, thus the lower the propensity of coal towards the spontaneous combustion.

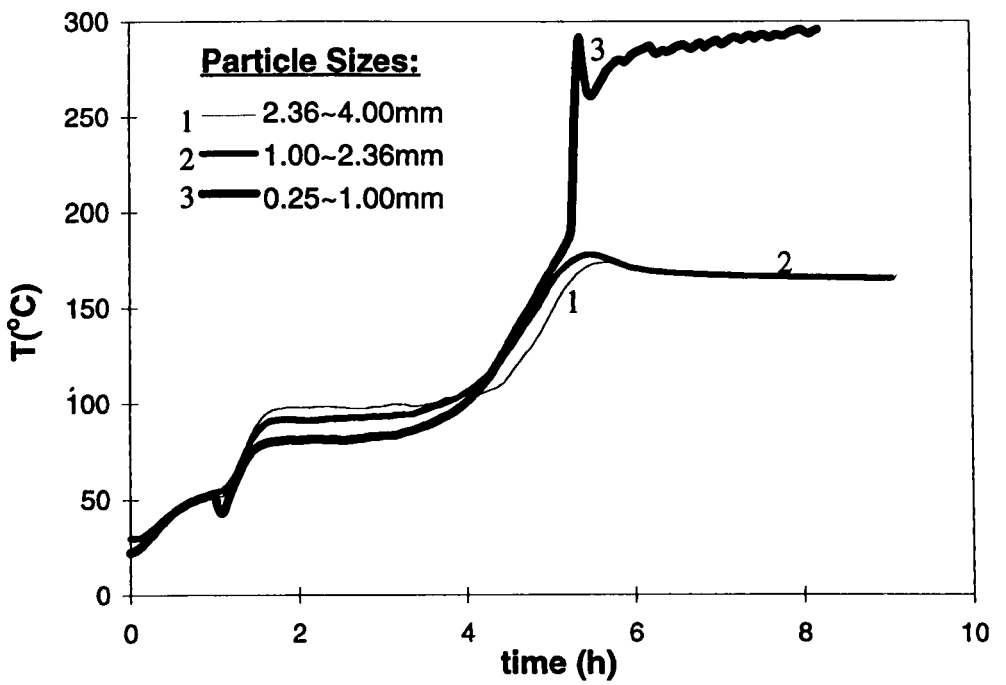

Figure 4.5 Temperature histories of fresh Coal M1 of several particle sizes in an isothermal reactor (R-4) at 153 °C

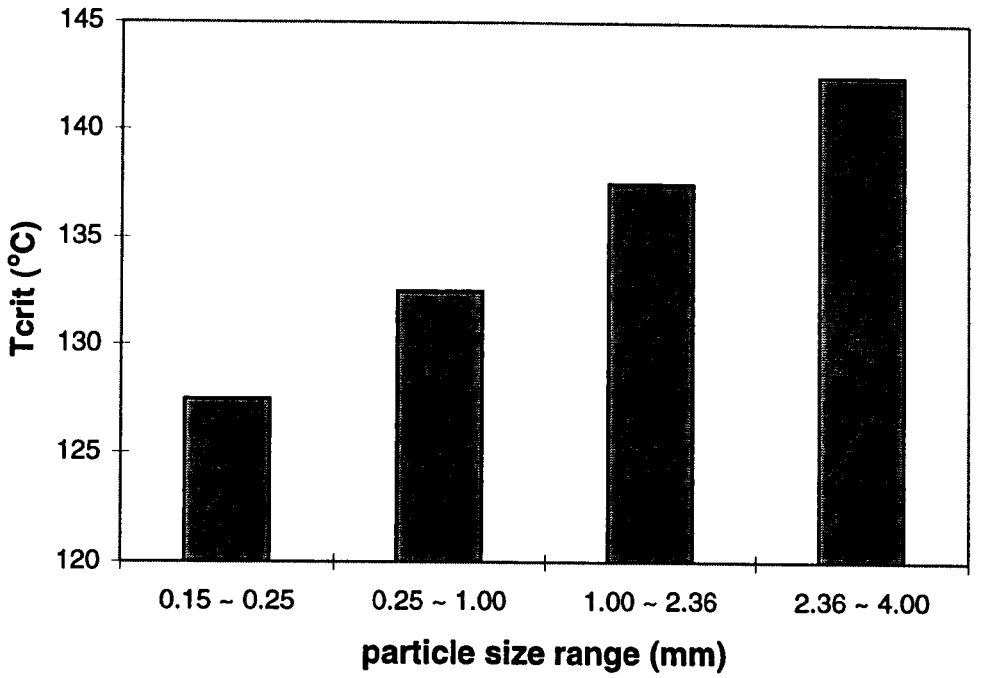

Figure 4.6 A plot of critical ambient temperature versus particle size

4.1.1.5 The effect of drying methods

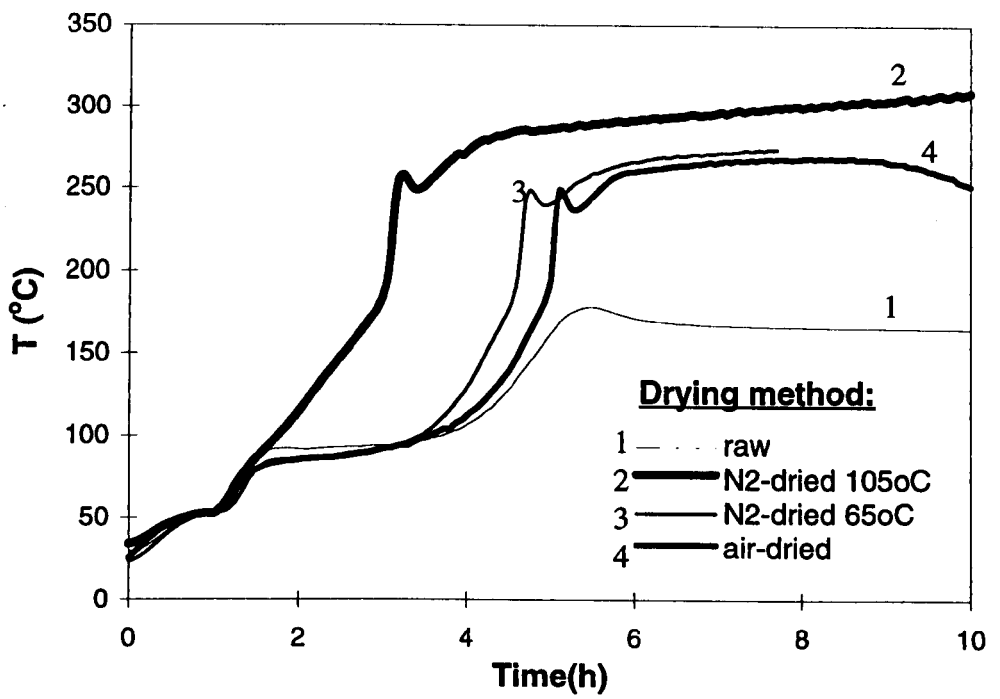

Figure 4.7 Temperature histories of Coal M1 with different drying methods in an isothermal reactor (R-4)

Figure 4.7 shows the effect of coal drying methods on spontaneous combustion of Coal M1. The experiments were run in an isothermal reactor (R-4) at 153 °C, and air flow rate of 100 ml min^{-1}. The particle size fraction was 1.00 ~ 2.36 mm. It is shown that the temperature increase of the raw coal was very slow due to the evaporation of the coal moisture, which consumed a large fraction of the heat generated from the oxidation reaction. Furthermore, oxygen diffusion inside the wet coal may have been delayed since the moisture presented an additional resistance to oxygen diffusion in the coal. On the other hand, the temperature of the sample dried at 105 °C in nitrogen increased sharply within an hour of the experiment, which reveals that a dry coal has a high propensity towards self-heating. Furthermore, although the sample dried at 65 °C in nitrogen contained less moisture than the sample dried in air at ambient temperature, the difference in their temperature profiles was very little. This could be due to the wetting and drying processes during the air-drying process that lead to a physical breakdown in coal structure. This process increased the active sites available for the oxidation reaction and eased the oxygen penetration into coal particle, thus accelerating the oxidation reaction (Inggram and Rimstidt (1984); Shrivastava et al. (1992)).

4.1.2 The Effect of Isothermal Reactor Sizes

To examine the effect of reactor size on the self-heating process, three larger isothermal reactors were constructed, with 27, 15, and 12 cm in height and 9.8, 8 and 6 cm in diameter, respectively. The four isothermal reactors, named as R-1, R-2, R-3, and R-4, respectively, were filled with 1000, 350, 140, and 30 g of raw Coal M3, and the critical ambient temperature of each reactor was determined. As shown in Figure 4.8, in general, it is observed that the critical ambient temperature decreased with increasing coal mass. However, the correlation between the critical ambient temperatures and the coal mass was not rectilinear. Since whether a spontaneous combustion occurs or not is determined mainly by two competing processes: the rate of heat generation due to oxidation, and the rate of heat loss to the surroundings which depends on the external surface area. Thus, the critical

ambient temperature was plotted against the reactor specific external surface area in Figure 4.9. It is seen that the critical ambient temperature increased linearly with reactor specific external surface area. This suggests that for a given coal, the spontaneous combustion in the isothermal reactors is controlled by the external heat transfer environment.

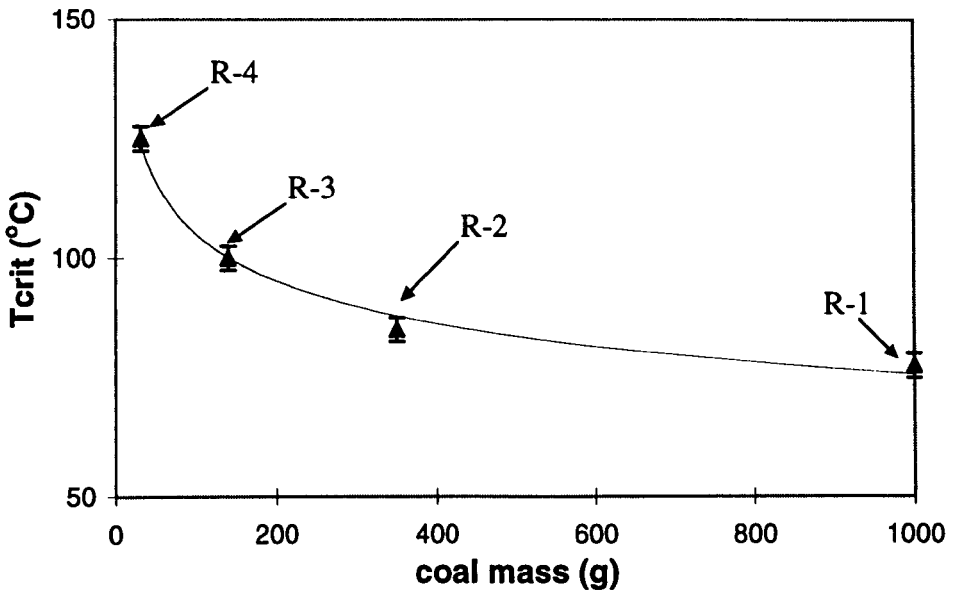

Figure 4.8 A plot of critical ambient temperature versus mass of raw Coal M3

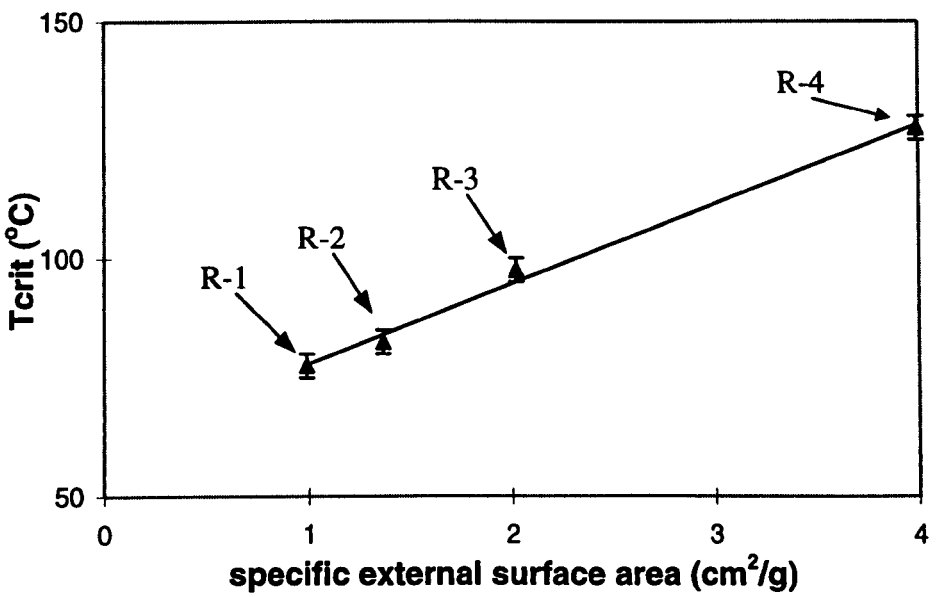

Figure 4.9 A plot of critical ambient temperature versus reactor specific external surface area

4.1.3 Estimation of Oxidation Kinetics

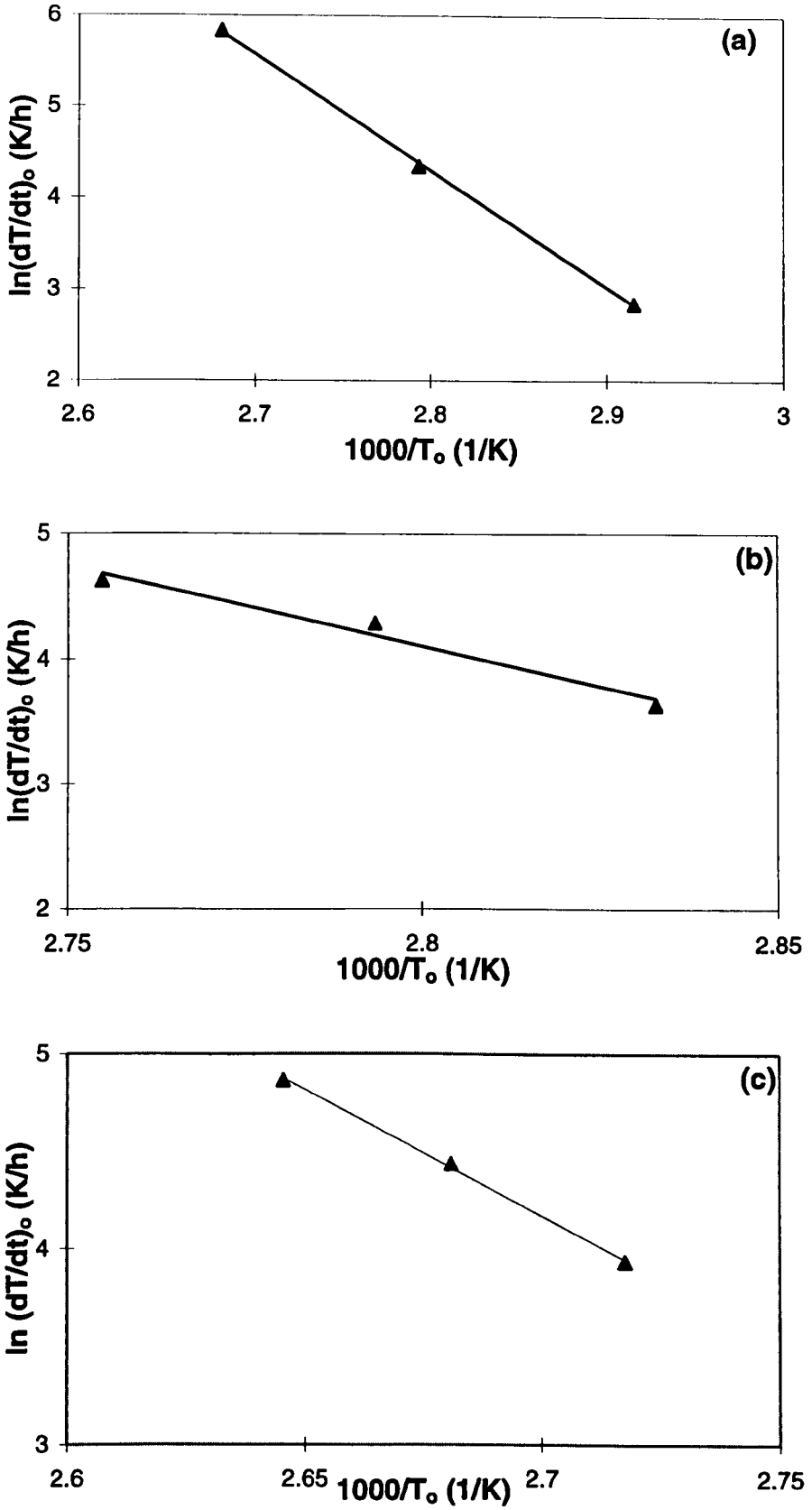

Figure 4.10 (Continued on the next page)

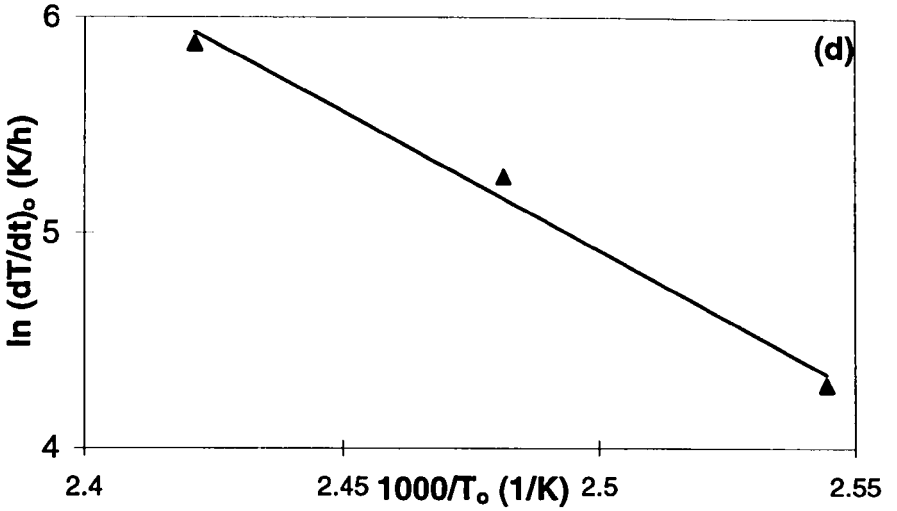

Figure 4.10 A linear plot of $\ln\left[\frac{dT}{dt}\right]_o$ versus $\frac{1000}{T_o}$ for fresh Coal M3 in reactor (a) R-1; (b) R-2; (c) R-3; and (d) R-4

The apparent kinetic parameters, E and A, of these four reactors (R-1, R-2, R-3, and R-4) were determined using Equation (3-2). Figure 4.10 shows linear plots of $\ln\left[\frac{dT}{dt}\right]_o$ versus $\frac{1}{T_o}$ for the coal sample in isothermal reactor R-1, R-2, R-3, and R-4. The ranges of T_o over which the kinetic experiments were carried out in isothermal reactors R-1, R-2, R-3, and R-4 were 70-100 °C, 80-90 °C, 90-110 °C, and 120-140 °C, respectively. It is found that the values of E obtained from these reactors were similar, while those of A were significantly different, as summarised in Table 4.1. Figure 4.11 shows the plot of estimated apparent reactivity (ρ_a) of Coal M3 in different isothermal reactor sizes. It is shown that the smaller the reactor size, thus the larger the specific external surface area, the lower the reactivities. As summarised by Chen (1996) the value of A varies with temperature, and extent of reaction. It was observed during the experiments that the larger the reactor, the lower the critical ambient temperature required for the thermal runaway to occur, and the longer the time required to reach the thermal runaway. These together with the experimental errors were responsible for the deviations observed.

Table 4.1 Summary of apparent kinetic constants estimated of Coal M3 in isothermal reactors with different sizes

Reactor I.D.	E (kJ mole^{-1})	A (kg m^{-3} Pa^{-1} s^{-1})
R-1	106.2	2.99×10^{8}
R-2	105.5	1.97×10^{8}
R-3	107.4	1.09×10^{8}
R-4	107.1	1.60×10^{7}

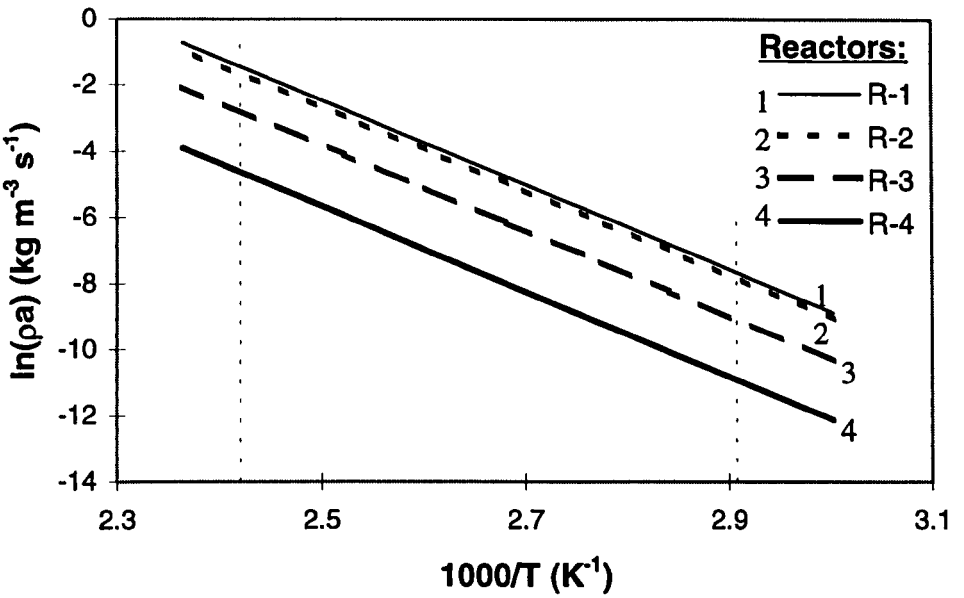

Figure 4.11 The effect of reactor size on the estimated reactivity of coal oxidation in air between 70 and 140 °C

4.1.4 Estimation of the Critical Layer Thickness

The kinetic constants were used to predict, according to Equation (3-3), the critical thickness of an infinite coal deposit slab which has been chosen as a common basis for comparison. The results are shown in Figure 4.12. It is seen that the critical thickness of a coal deposit decreased with increasing ambient temperature, as expected. There were some variations in the predictions from the four different

isothermal reactors. The maximum variance decreased with temperature, and was about 79% at 70 °C and 5% at 140 °C. It is also shown in Figure 4.12 that the smaller the reactor size, the larger the critical thickness predicted. According to Equation (3-3), only E and A are the responsible variables for critical thickness prediction, while the other variables were assumed to be constant. The E values for different reactors have been found to be similar while A values were significantly different. The difference in A values resulted in a significant deviation in the critical thickness calculated, particularly at low temperatures. Furthermore, the smallest isothermal reactor has the largest specific external surface area for the heat transfer.

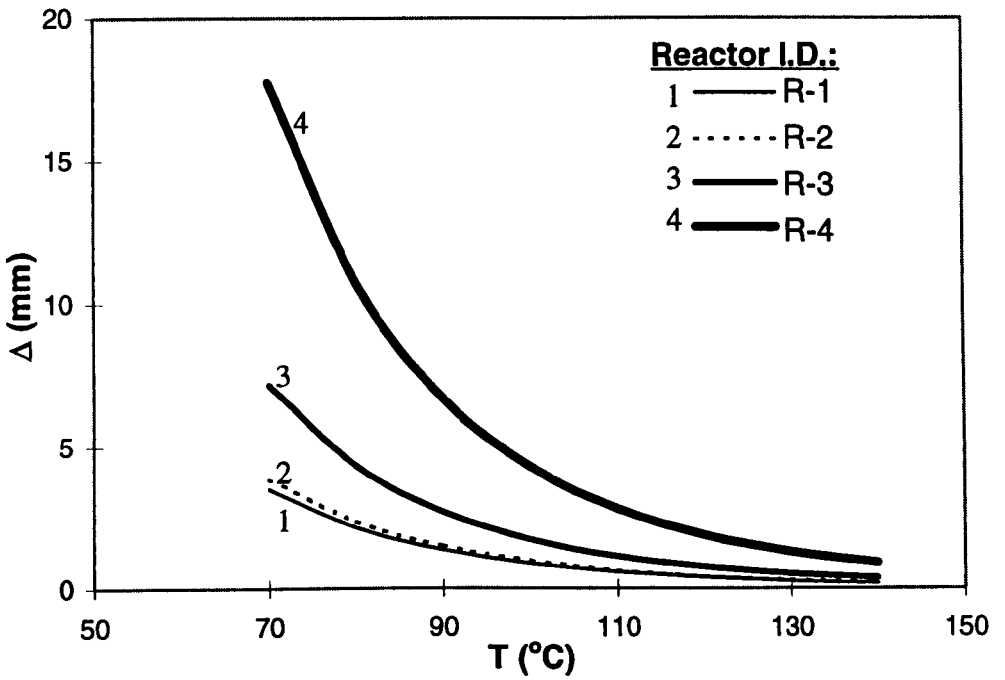

Figure 4.12 A comparison of critical thicknesses of coal deposits (slabs) capable of spontaneous combustion estimated from isothermal reactors of different sizes

4.1.5 The Effect of Packing Density

Experiments were also carried out to examine the effect of packing density on the coal critical ambient temperature. An isothermal reactor (R-4) was used to determine the critical ambient temperature of raw Coal M2 in various packing densities. As shown in Table 4.2, three different levels of packing densities, namely PI-1, PI-2, and PI-3, were used for this purpose. The packing density was varied by pressing different amount of coal into the reactor.

Table 4.2 Summary of critical ambient temperatures and kinetic constants estimated of raw Coal M2 tested in an isothermal reactor (R-4) with different packing densities

Packing I.D.	Packing Density ($kg\ m^{-3}$)	Tcrit (°C)	E ($kJ\ mol^{-1}$)	A ($kg\ m^{-3} s^{-1} Pa^{-1}$)
PI-1	298.4	132.5 ± 2.5	108.4	3.03×10^{6}
PI-2	447.6	127.5 ± 2.5	133.3	2.25×10^{10}
PI-3	557.0	127.5 ± 2.5	130.4	4.74×10^{9}

The critical ambient temperatures of Coal M2 tested in an isothermal reactor (R-4) with various packing densities were summarised in Table 4.2 . It is shown that coal with packing density PI-1 owned the highest critical ambient temperature (132.5 ± 2.5 °C), while the critical ambient temperature of coal with packing PI-2 and PI-3 were the same (127.5 ± 2.5 °C). The packing density affects the heat and mass transfer in the system. The higher the packing density, the lower the heat loss. On the other hand, a very high packing density could hinder the oxygen diffusion into the system, and thus reduces the oxidation reaction rate. As shown in Table 4.2, the critical ambient temperature of coal with packing density PI-2 was lower than that with PI-1. This indicated that in both system there was sufficient oxygen for the oxidation reaction, and therefore a lower heat loss in coal with higher packing density, i.e. PI-2, offered a higher risk of spontaneous combustion. Increasing the

packing density to PI-3, however, could not further lower the critical ambient temperature. This could imply that packing PI-3 was so high that significantly restricted the oxygen diffusion, and thus slower the oxidation reaction. Typical temperature profiles of fresh Coal M2 tested in an isothermal reactor (R-4) with three different packing densities, PI-1, PI-2, and PI-3, are shown in Figure 4.13.

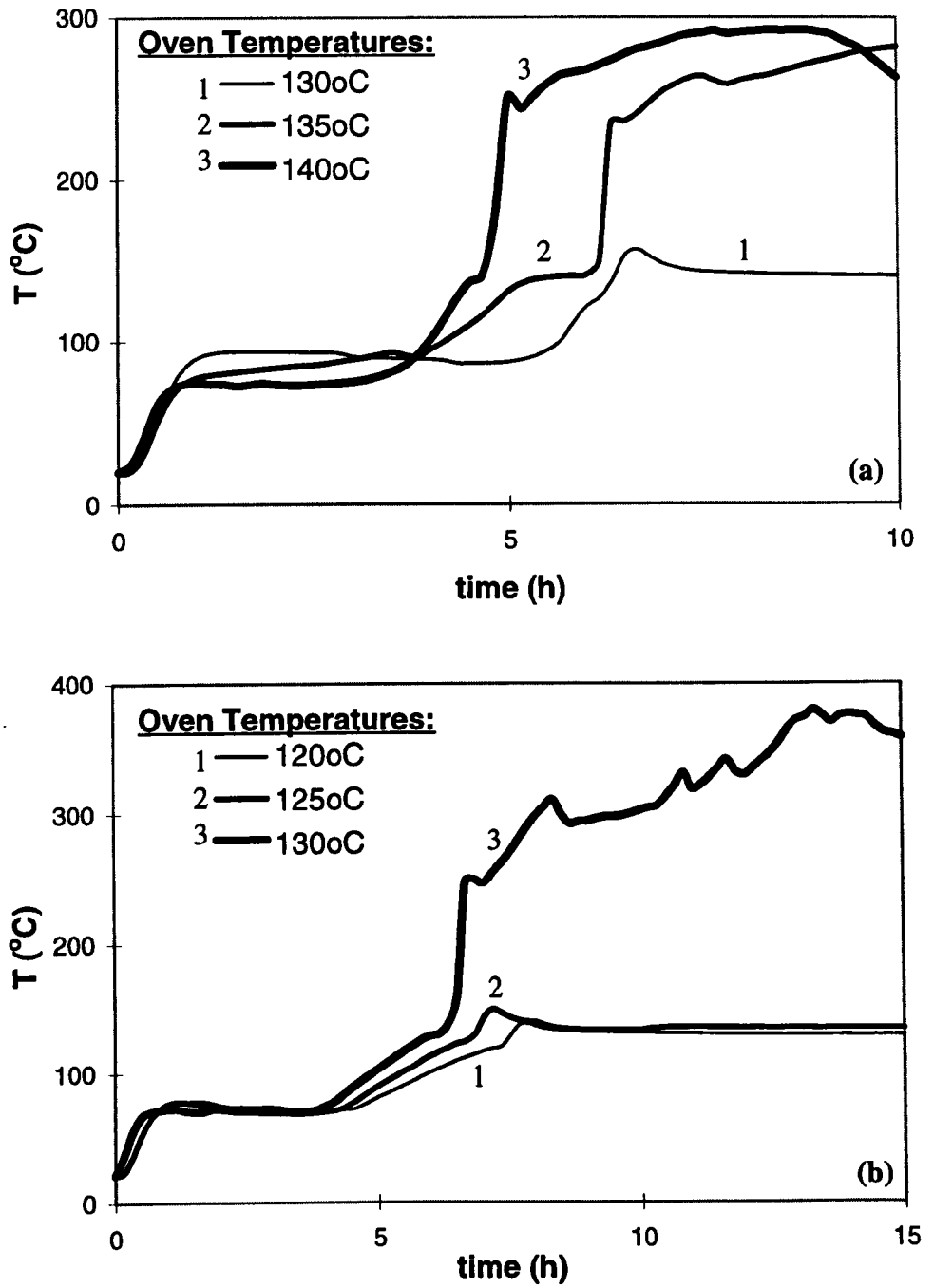

Figure 4.13 (Continued on the next page)

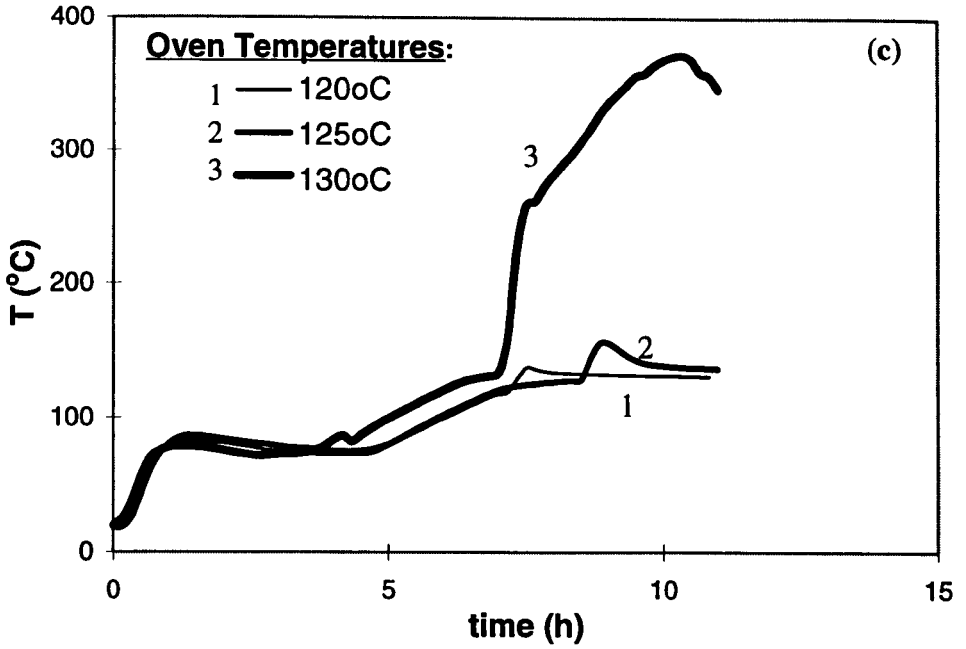

Figure 4.13 Temperature histories of raw Coal M2 in an isothermal reactor (R-4) with packing density of (a) 298.4 kg m^{-3}; (b) 447.6 kg m^{-3}; and (c) 557.0 kg m^{-3}

To further examine the effect of packing density on coal spontaneous combustion, the apparent kinetic parameters, A and E, of the raw Coal M2 in various packing densities were estimated according to Equation (3-2). Figure 4.14 shows typical linear plots of $\ln\left[\frac{dT}{dt}\right]_o$ versus $\frac{1}{T_o}$ for Coal M2 in an isothermal reactor (R-4) with packing densities of 298.4, 447.6, and 557.0 kg m^{-3}. The range of T_o over which the kinetic experiments were carried out was 120-140 °C.

The values of A and E estimated from different packing densities were also summarised in Table 4.2. These kinetic constants, A and E, were then used to estimate the coal reactivities. Figure 4.15 plots the reactivities of the coal with different packing densities. It is shown that coal with packing density PI-1 had the lowest reactivities which corresponded to the highest critical ambient temperature observed. Figure 4.15 also shows that although, within the experimental accuracy, coal with packing densities PI-2 and PI-3 had the same critical ambient temperature, coal with packing density PI-2 was more reactive towards the oxidation reaction.

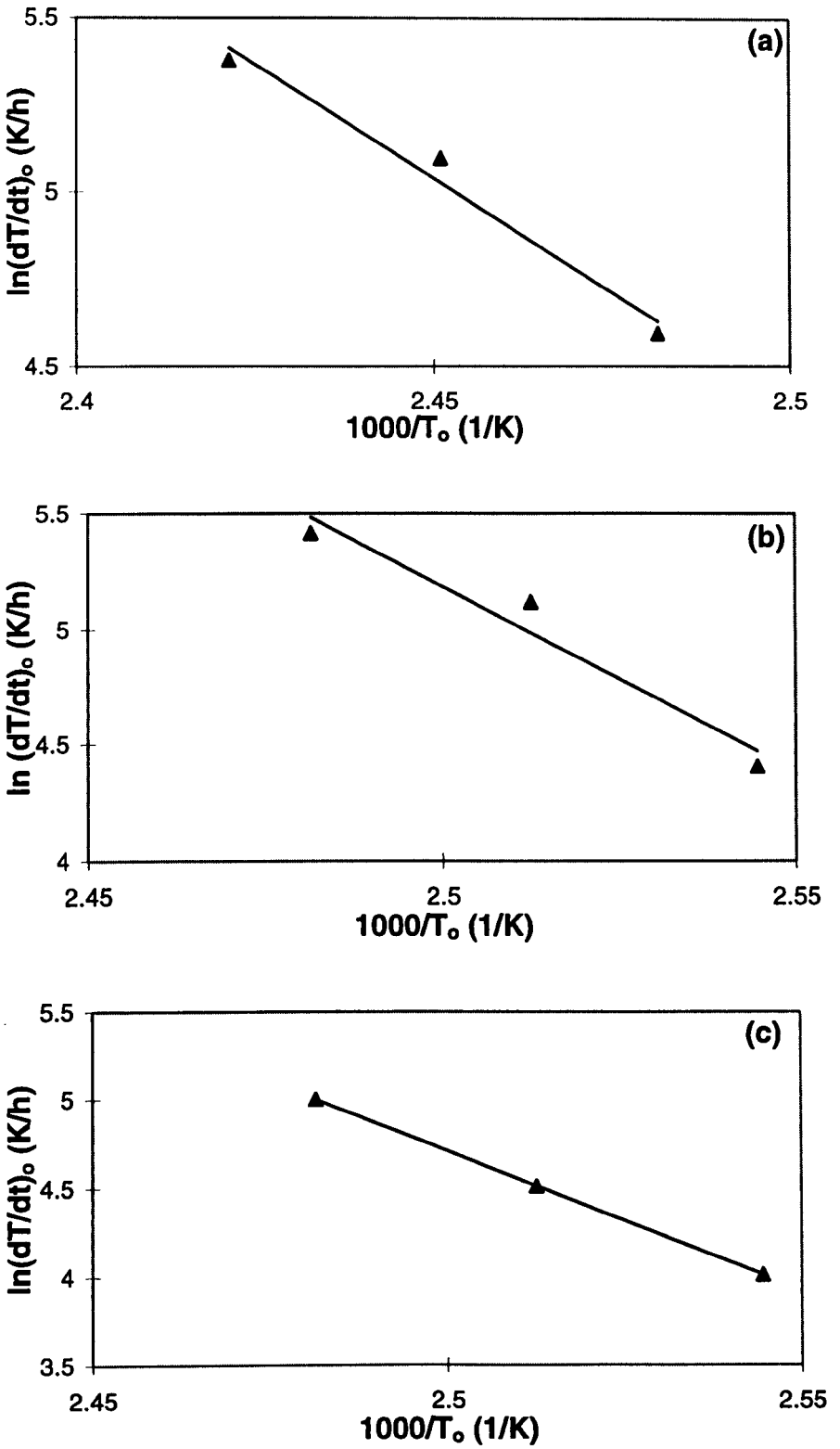

Figure 4.14 A linear plot of $\ln\left[\frac{dT}{dt}\right]_o$ versus $\frac{1000}{T_o}$ for fresh Coal M2 in an isothermal reactor (R-4) with packing density of (a) 298.4 kg m^{-3}; (b) 447.6 kg m^{-3}; and (c) 557.0 kg m^{-3}

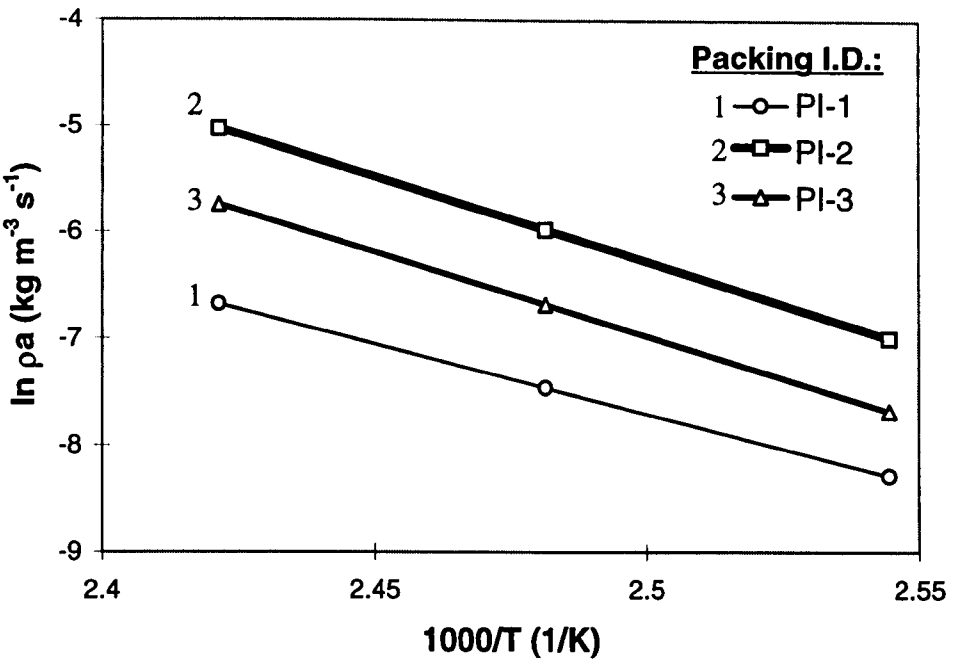

Figure 4.15 The effect of packing density on the estimated reactivity of coal oxidation in air between 120-140 °C

4.1.6 Time-To-Ignition

4.1.6.1 The effect of ambient temperature and air flow rate

The time-to-ignition is defined as the time required for the coal to experience thermal runaway. Figure 3.2 shows the temperature histories of fresh Coal M3 in an isothermal reactor (R-1) at several oven temperatures. It is shown that at an oven temperature of 85 °C, the thermal runaway occurred after about 145 hours of experiment, while at 100 °C the thermal runaway occurred after about 100 hours of experiment. Accordingly, the higher the ambient temperature, and thus the faster the oxidation reaction rate, the shorter the time-to-ignition. A similar trend can also be seen in Figures 3.5 and 4.13.

To obtain a more accurate measurement of the time-to-ignition, the first-order and second-order time derivatives of coal temperature were calculated. Figure 4.16

presents plots of the coal temperature, first-order time derivative of temperature (dT/dt) and second-order time derivative of temperature (d^2T/dt^2) against time for Coal M3 tested in an isothermal reactor (R-1) at 85 and 100 °C. It is revealed that the time-to-ignition is the time when the temperature acceleration (d^2T/dt^2) reached maxima, which were 144 and 100.47 hours for coal tested in reactor R-1 at 85 and 100 °C, respectively. Similar trends can also be found in Figure 4.17 for the coal tested in isothermal reactor (R-4) at 130 and 140 °C. It is noticed that the time-to-ignition of the coal tested at 130 and 140 °C were 7.36 and 5.28 hours, respectively.

Furthermore, it is also observed that the time-to-ignition varied with the air flow rate. Figure 4.18 shows plots of the coal temperature, first-order time derivative of temperature (dT/dt) and second-order time derivative of temperature (d^2T/dt^2) against time for Coal M1 tested in an isothermal reactor (R-4) at 153 °C at air flow rates of 120, 140, and 150 ml min^{-1}. The time-to-ignitions obtained were 5.52, 5.30, 5.14 hours, for their respective air flow rates. This implies that, if the availability of oxygen is not a limiting factor, a high air flow rate accelerates the self-heating process.

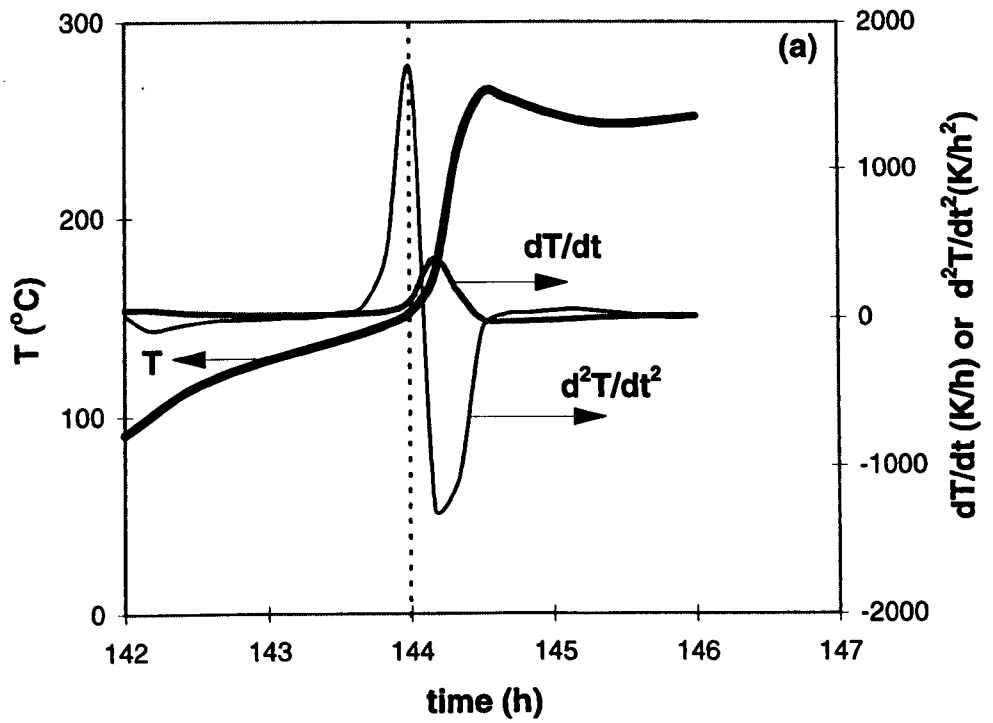

Figure 4.16 (Continued on the next page)

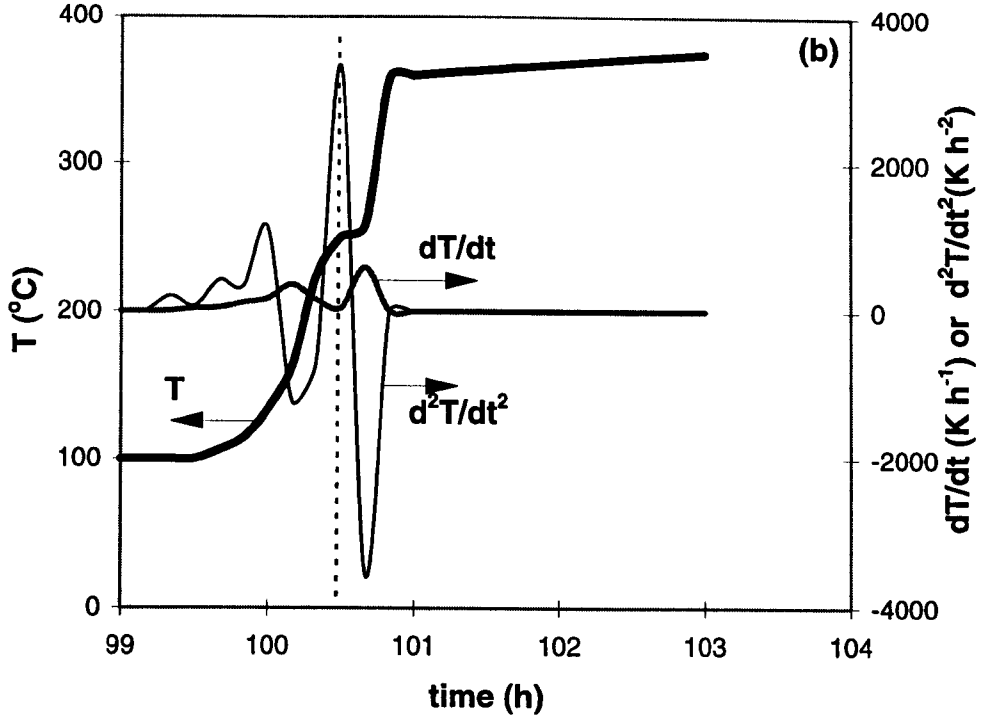

Figure 4.16 Determination of time-to-ignition for Coal M3 tested in an isothermal reactor (R-1) at oven temperature of (a) 85 °C; and (b)100 °C

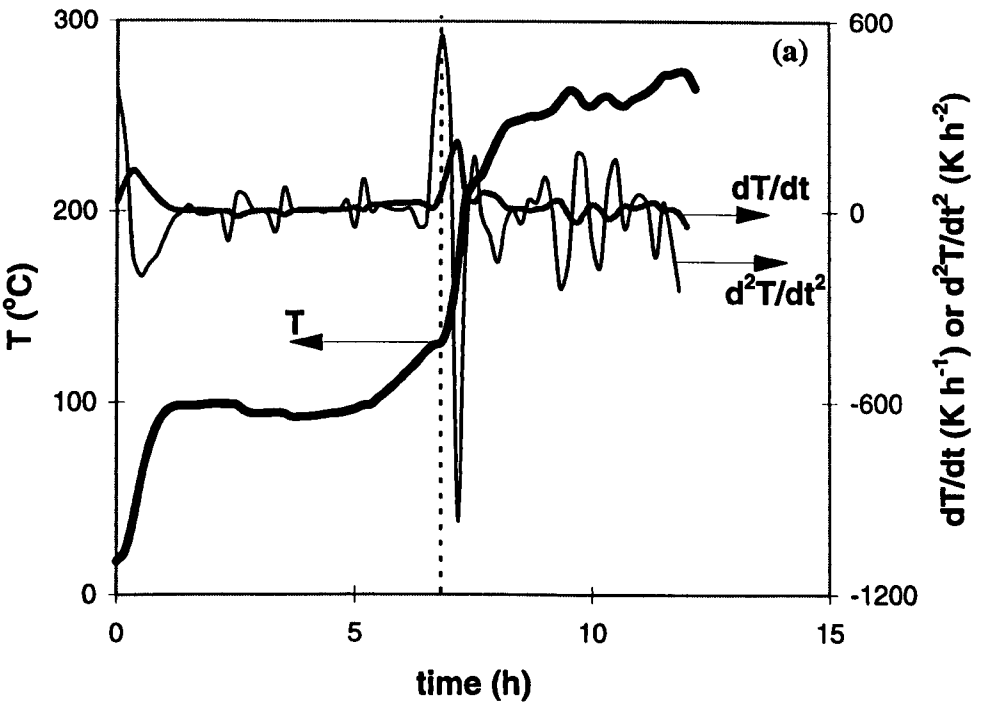

Figure 4.17 (Continued on the next page)

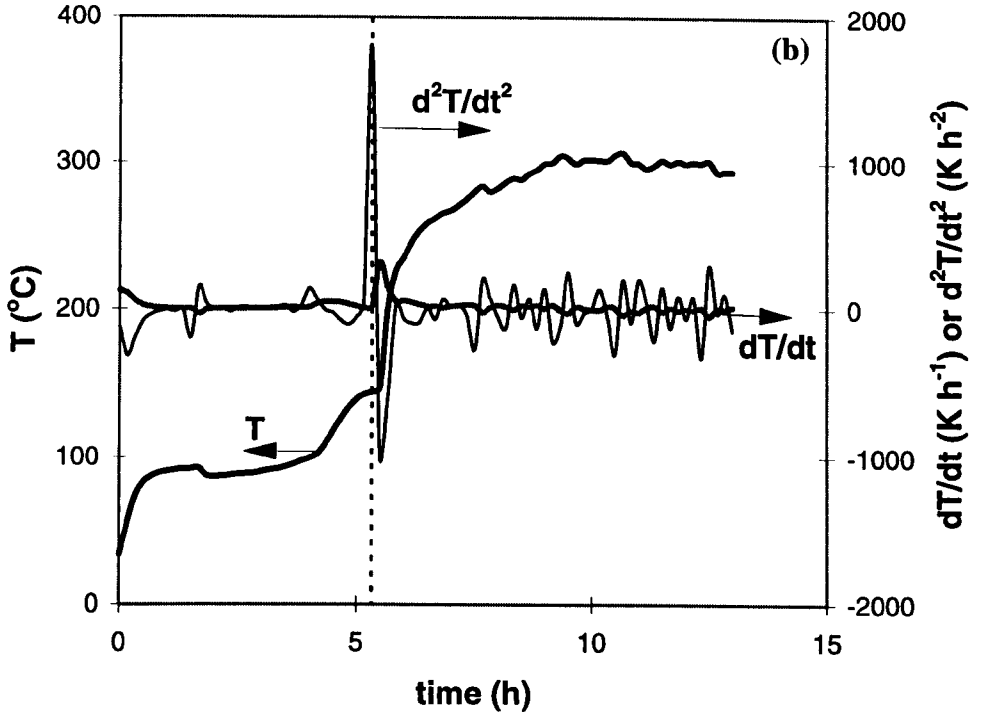

Figure 4.17 Determination of time-to-ignition for Coal M3 tested in an isothermal reactor (R-4) at oven temperature of (a) 130 °C; and (b)140 °C

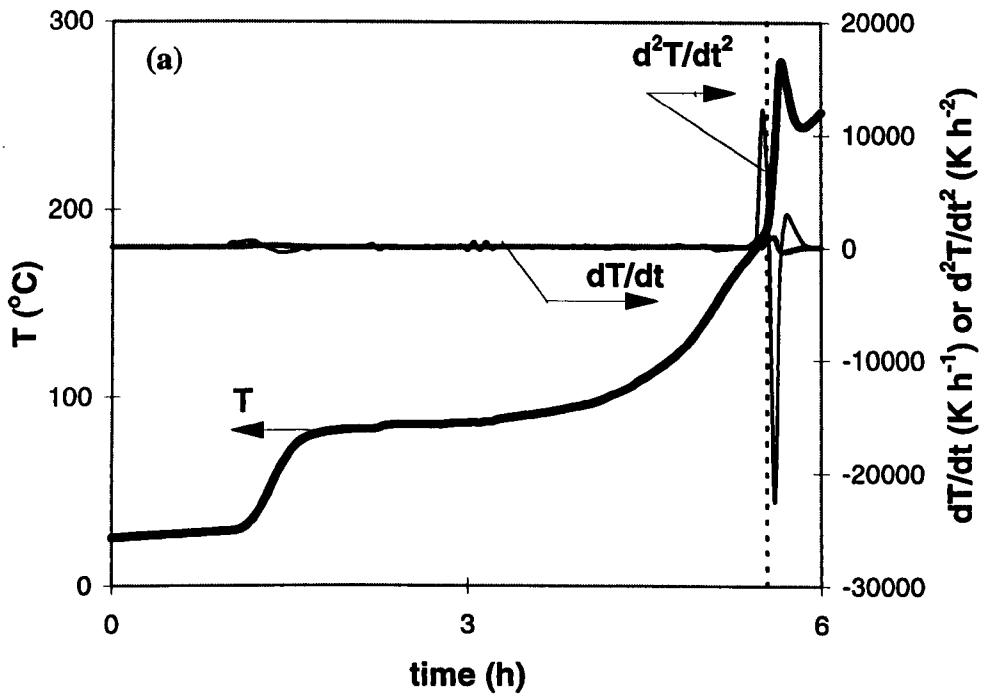

Figure 4.18 (Continued on the next page)

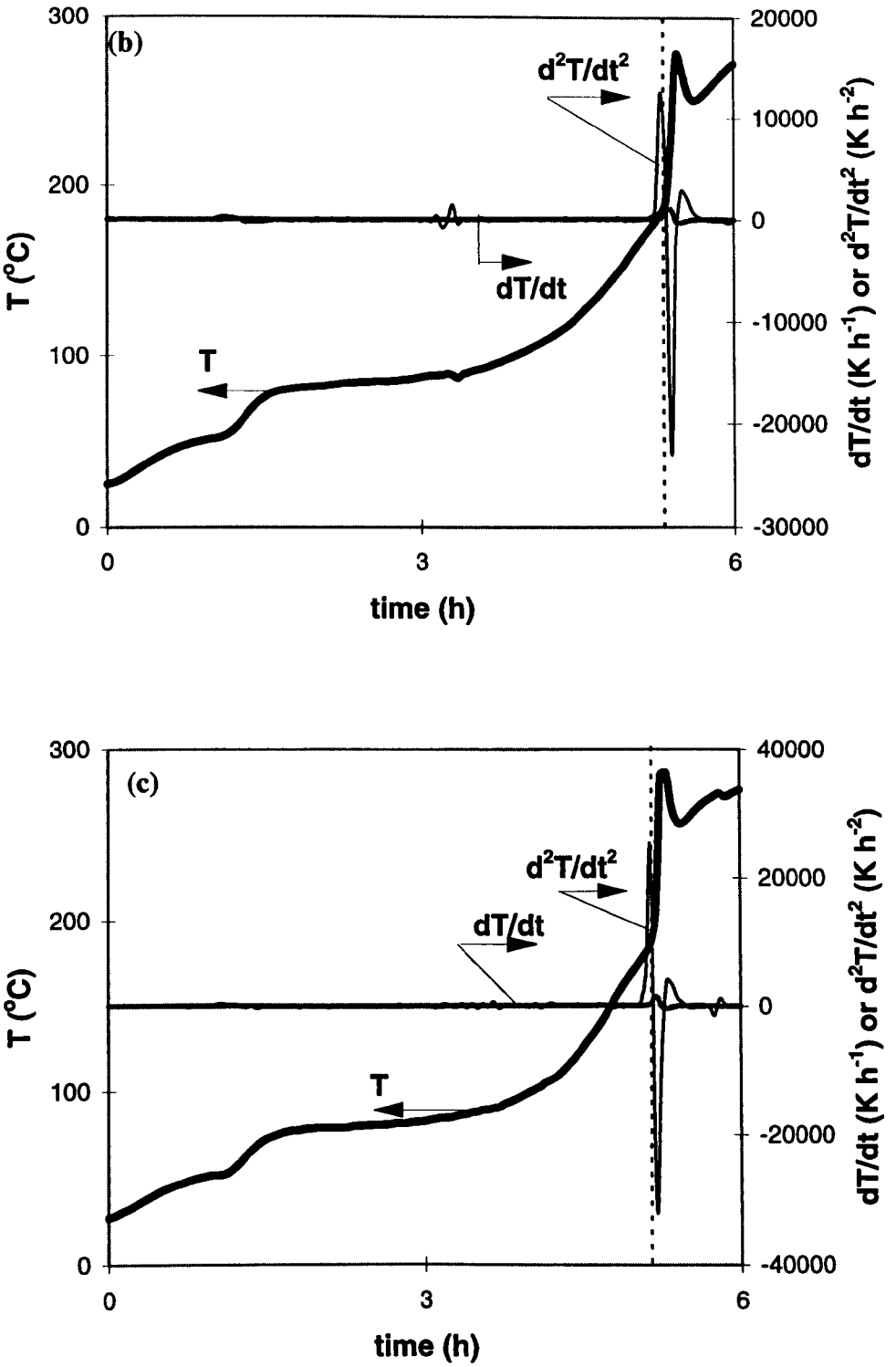

Figure 4.18 Determination of time-to-ignition for Coal M1 tested in an isothermal reactor (R-4) at 153 °C at air flow rate of (a) 120 ml min^{-1}; (b) 140 ml min^{-1}; and (c) 150 ml min^{-1}

4.1.6.2 The effect of particle size and coal drying methods

The time-to-ignition was also found to vary with coal particle size. Figure 4.19 plots the time-to-ignition determination for Coal M1 with particle size ranges 2.36~4.00, 1.00~2.36, 0.25~1.00, and 0.15~0.25 mm, respectively. The experiments were run in an isothermal reactor (R-4) at the lowest ambient temperature at which the thermal runaway occurred. The time-to-ignition obtained for the coal with these particle size fractions were 2.52, 3.04, 3.05, and 3.48 hours, respectively. It is noted that the larger the particle size, the shorter the time-to-ignition. This is because the larger the particle size, the higher the critical temperature for the thermal runaway to occur. A high temperature significantly shortened the time-to-ignition.

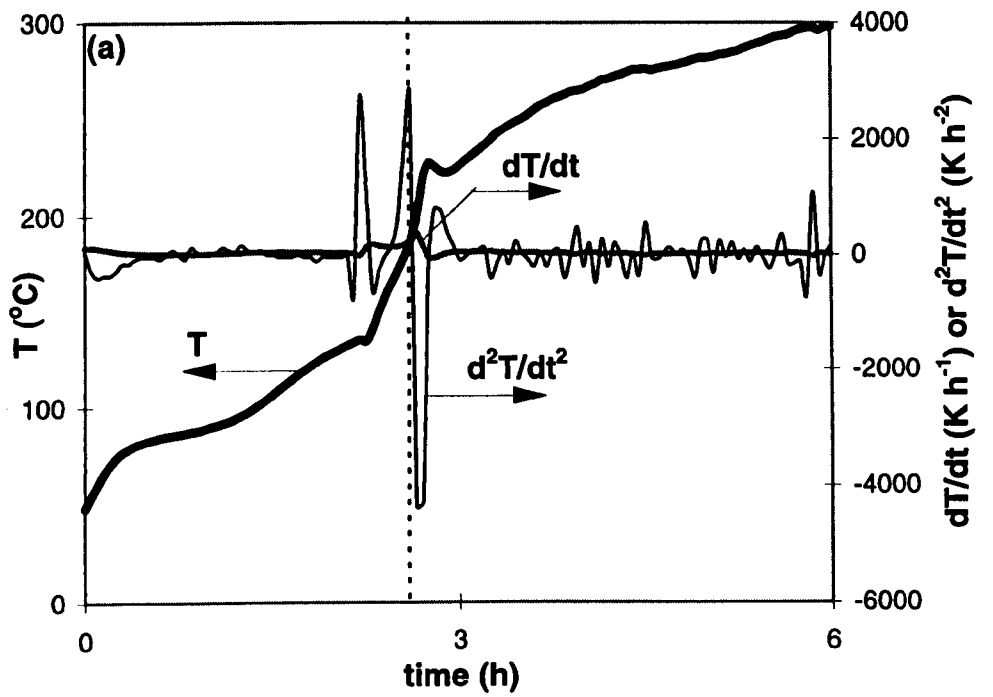

Figure 4.19 (Continued on the next page)

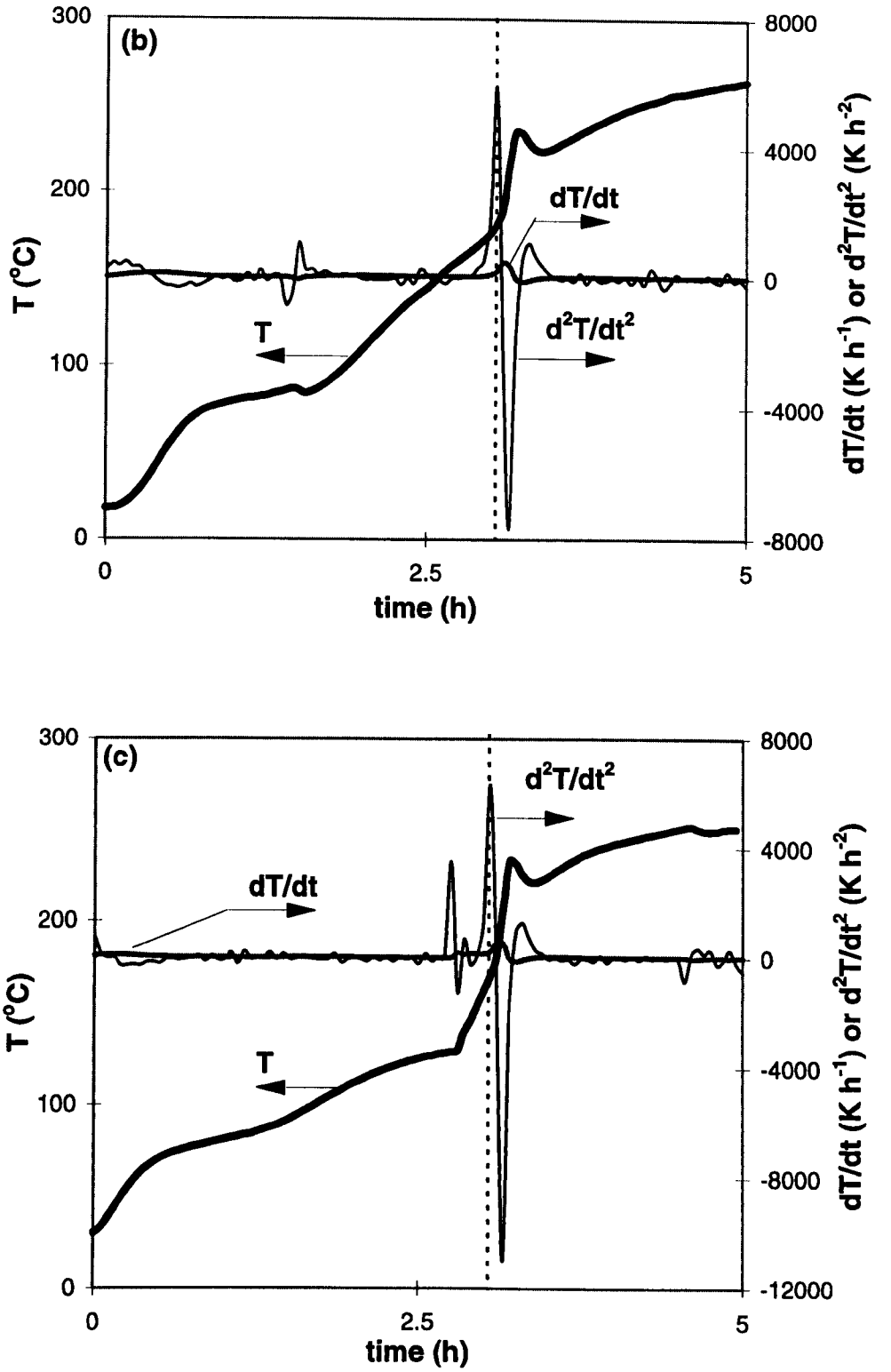

Figure 4.19 (Continued on the next page)

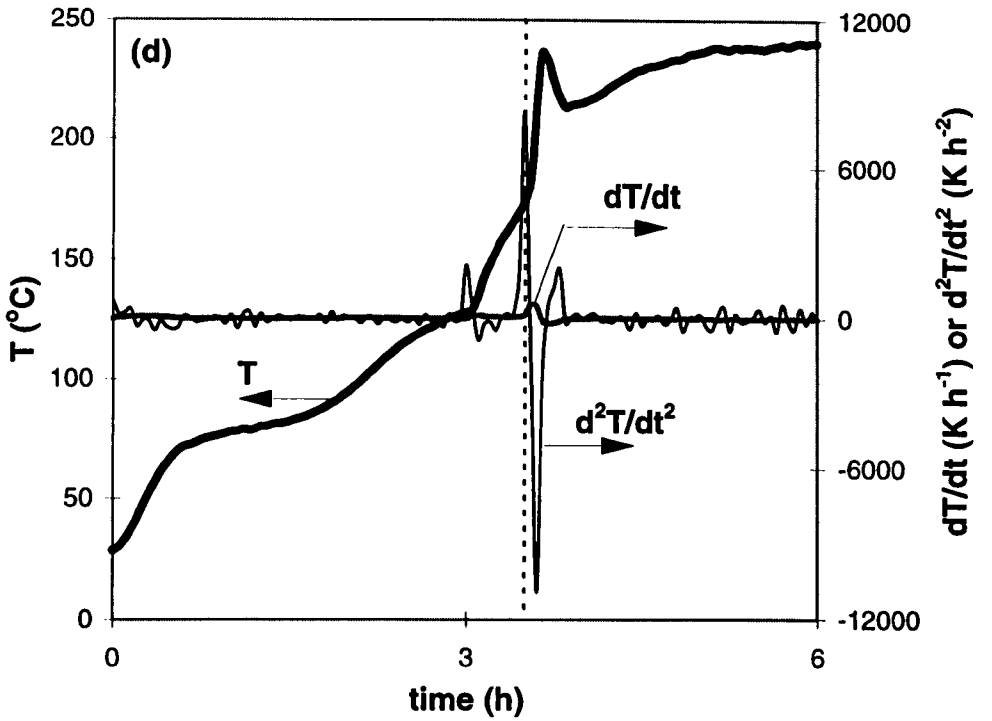

Figure 4.19 Determination of time-to-ignition for Coal M1 tested in an isothermal reactor (R-4) at 153 °C with a particle size fraction of (a) 2.36 ~ 4.00 mm; (b) 1.00 ~ 2.36 mm; (c) 0.25 ~ 1.00 mm; and (d) 0.15 ~ 0.25 mm

Different drying methods were also found to affect the time-to-ignition. Figure 4.20 shows plots of coal temperature, first-order time derivative of temperature (dT/dt) and second-order time derivative of temperature (d^2T/dt^2) against time for Coal M1 dried in different methods, and tested in isothermal reactor (R-4) at 153 °C. The time-to-ignition obtained from the coal dried in nitrogen at 105 and 65 °C and from the air-dried coal sample were 3.04, 4.59, and 4.96 hours, respectively. It is shown that time-to-ignition of the coal sample dried in nitrogen at 105 °C was the shortest, followed by the coal dried in nitrogen at 65 °C and coal dried in air at ambient temperature. This implied that the less the coal moisture content, the quicker the thermal runaway occurred.

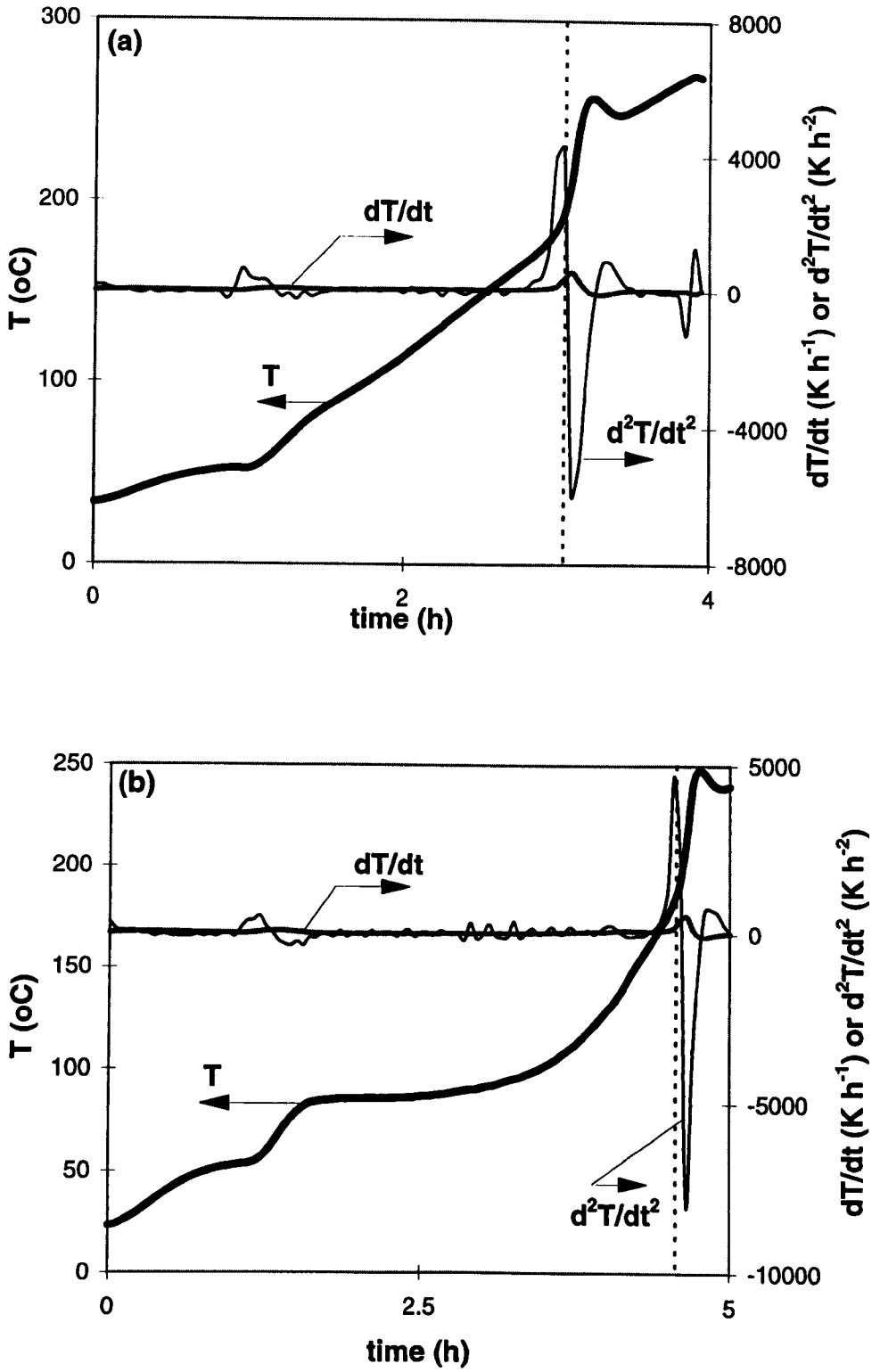

Figure 4.20 (Continued on the next page)

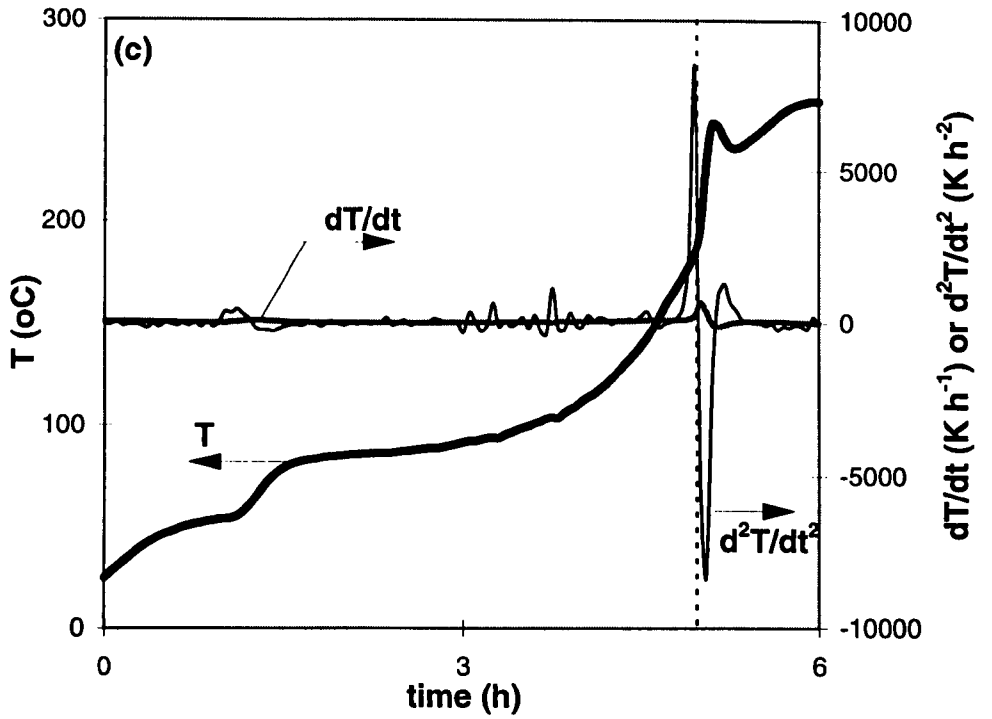

Figure 4.20 Determination of time-to-ignition for Coal M1 tested in an isothermal reactor (R-4) at 153 °C for (a) coal dried in nitrogen at 105 °C; (b) coal dried in nitrogen at 65 °C; and (c) air-dried coal

4.1.6.3 The effect of reactor size

Figure 4.21 plots the temperature histories of fresh Coal M2 in different isothermal reactor sizes. Each temperature history was plotted at the lowest ambient temperature at which the thermal runaway occurred. It is shown that the smaller the reactor size, the shorter the time-to-ignition.

To compare the time-to-ignition of the coal tested in different isothermal reactor sizes, Figures 4.16(a), 4.22 (a) and (b), and 4.17(a) for the coal tested in isothermal reactors R-1 to R-4, respectively, may be noted. The time-to-ignition of different reactor sizes obtained were summarised in Table 4.3.

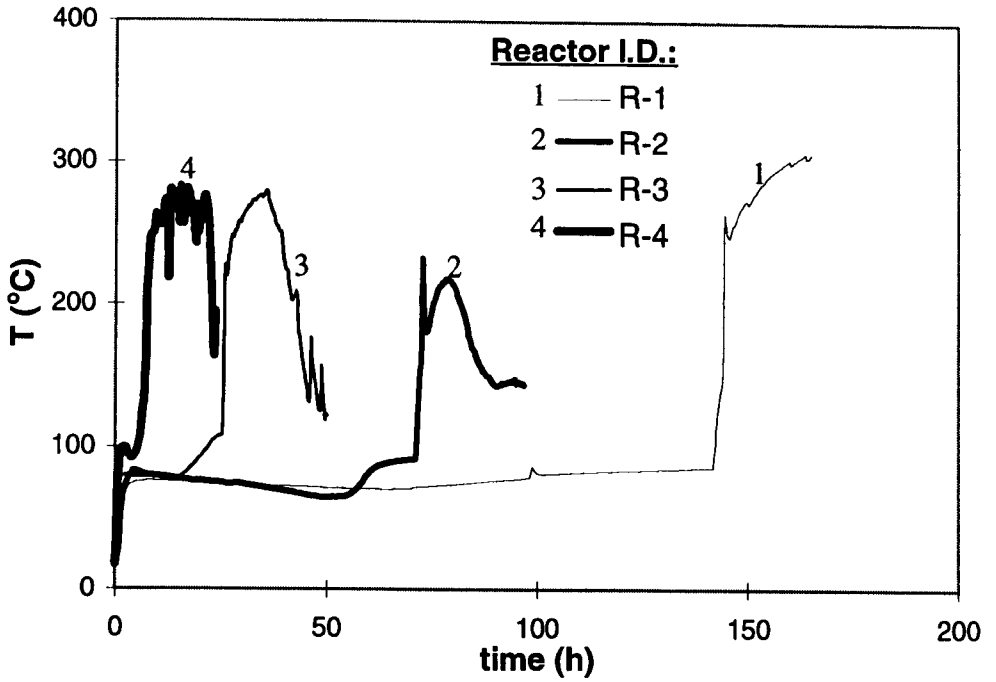

Figure 4.21 Temperature histories of fresh Coal M3 in different isothermal reactor sizes at their critical ambient temperature

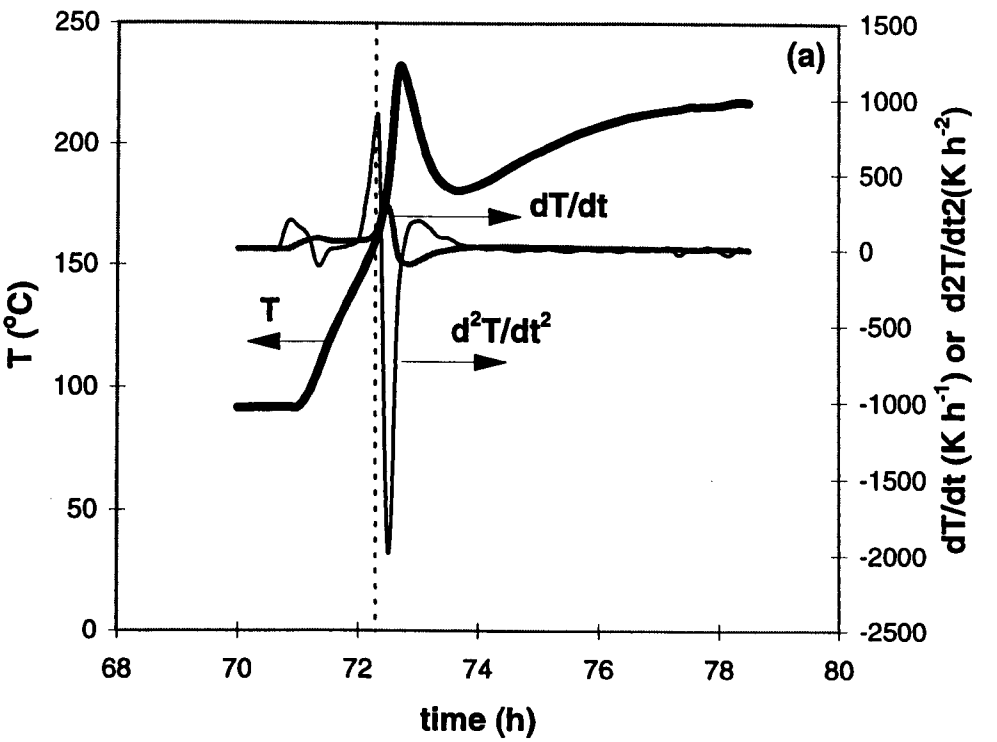

Figure 4.22 (Continued on the next page)

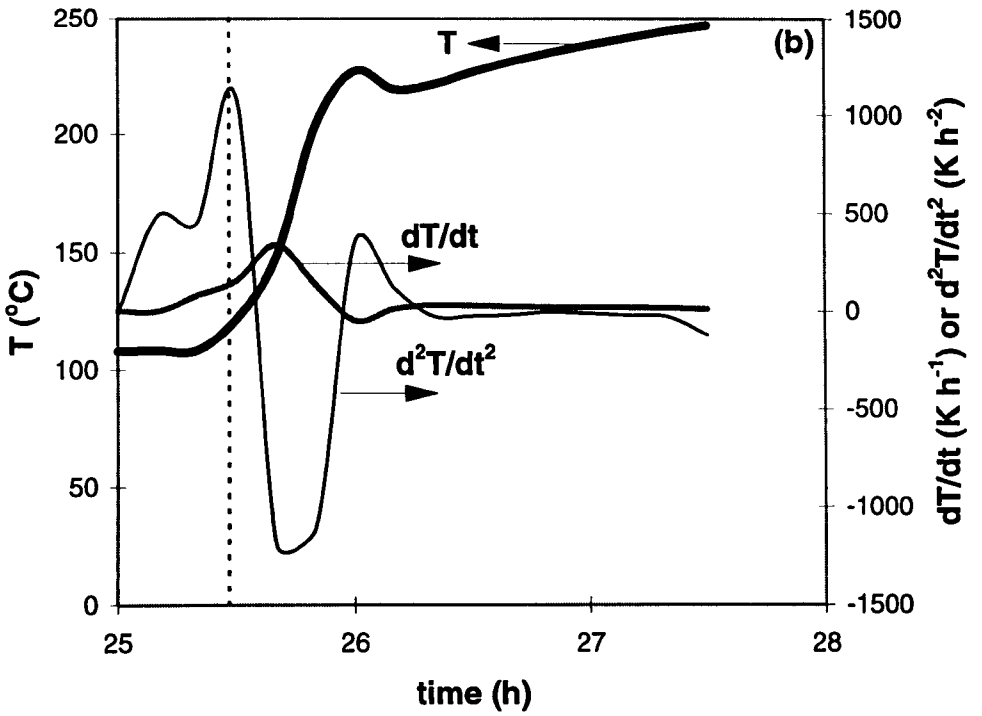

Figure 4.22 Determination of time-to-ignition for Coal M3 tested in an isothermal reactor (a) R-2 at 95 °C; and (b) R-3 at 105 °C

Table 4.3 Summary of the time-to-ignition of Coal M3 tested in different isothermal reactor sizes at their respective critical ambient temperature

Reactor I.D.	T_{crit} (°C)	Time-to-ignition (h)
R-1	85	144.0
R-2	90	72.3
R-3	105	25.5
R-4	130	7.4

4.1.6.4 The effect of packing density

The time-to-ignition was also found to vary with the coal packing densities. Figure 4.23 plots the temperature histories of fresh Coal M2 with three different packing densities tested in an isothermal reactor (R-4). Each temperature history was plotted

at the lowest ambient temperature at which the thermal runaway occurred. It is shown that the lower the packing density, the shorter the time-to-ignition. Figure 4.24 presents the plots of time-to-ignition determination for Coal M3 with coal packing density of PI-1, PI-2, and PI-3, respectively, at the lowest ambient temperature at which the thermal runaway occurred, in an isothermal reactor (R-4). The time-to-ignition obtained from the coal PI-1, PI-2, and PI-3, were 6.06, 6.45, and 7.00 hours, respectively.

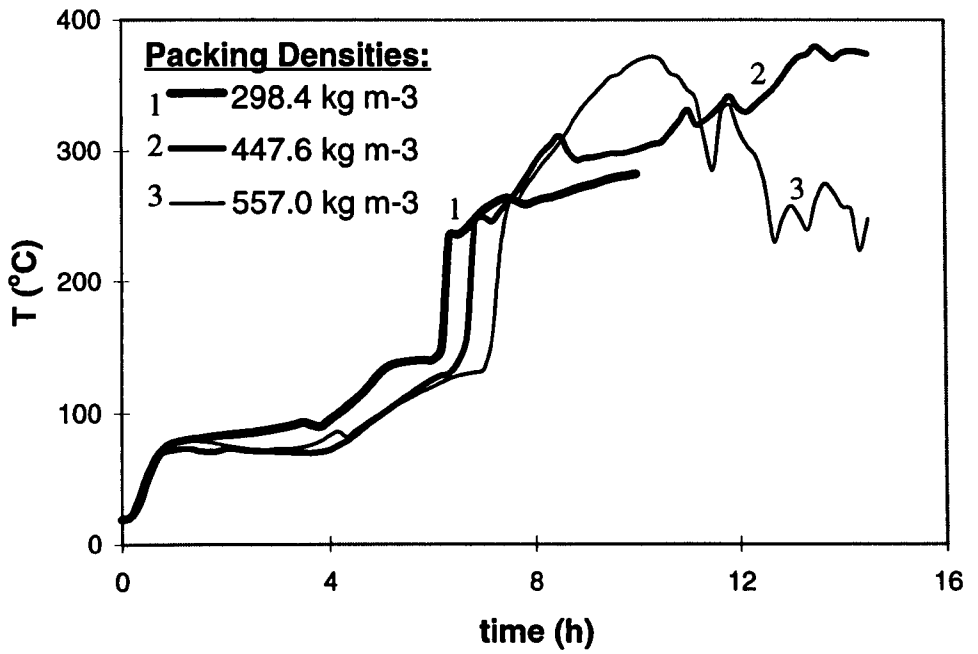

Figure 4.23 Temperature histories of fresh Coal M2 in an isothermal reactor (R-4) with different packing densities at the lowest ambient temperature at which thermal runaway occurred

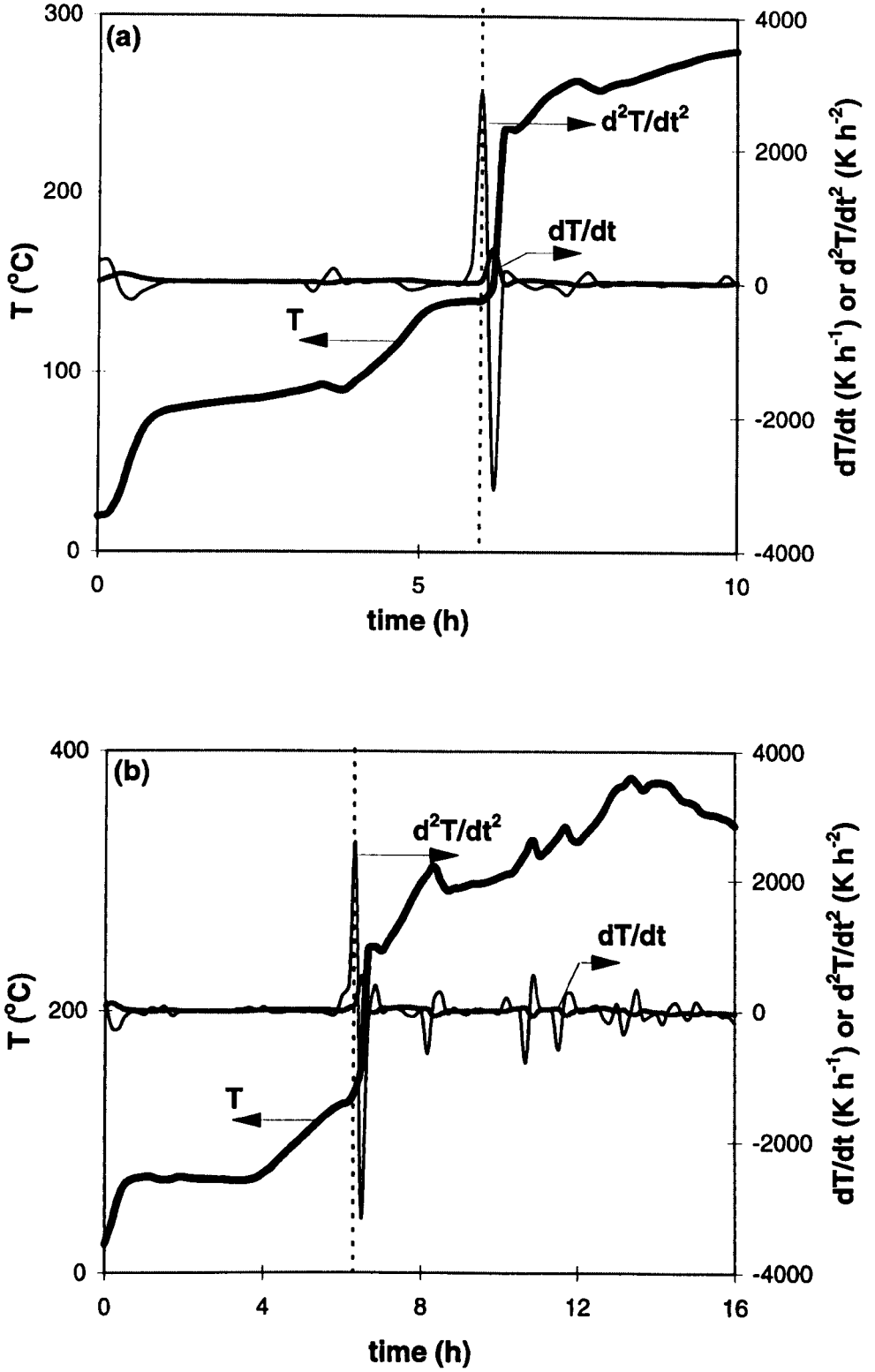

Figure 4.24 (Continued on the next page)

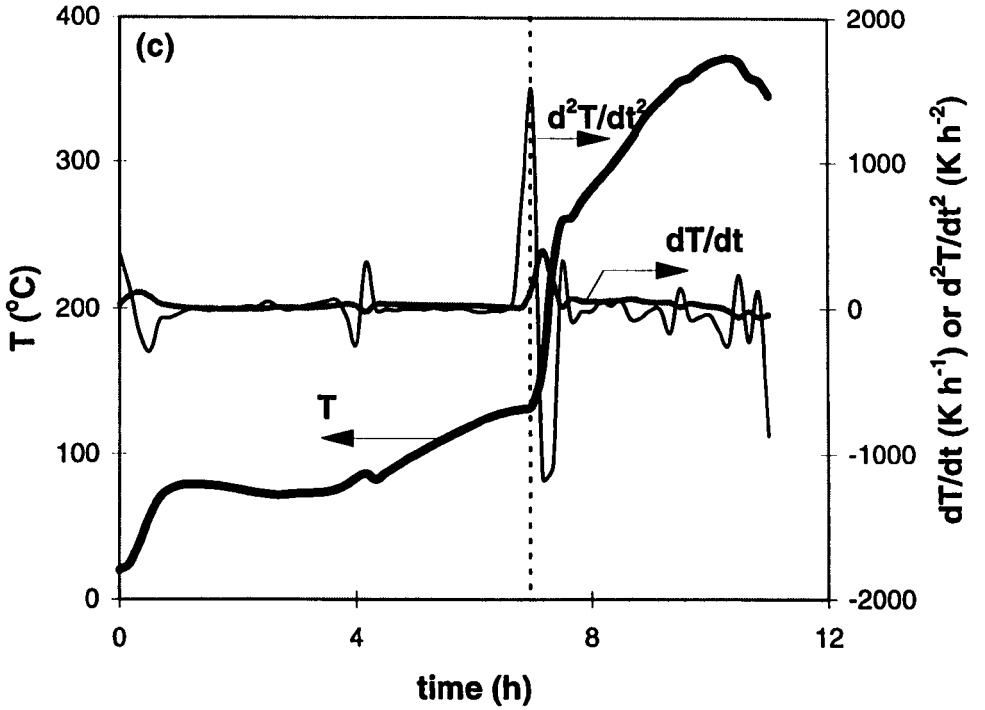

Figure 4.24 Determination of time-to-ignition for Coal M3 tested in an isothermal reactor (R-4) with packing density of (a) 298.4 kg m^{-3} at 135 °C; (b) 447.6 kg m^{-3} at 130 °C; and (c) 557.0 kg m^{-3} at 130 °C

4.2 RESULTS FROM ADIABATIC REACTOR EXPERIMENTS

To further investigate the spontaneous combustion phenomenon of Coal M, an adiabatic reactor technique was also used in this study. The experiments using this technique took a much longer time than those of isothermal reactors. This is because in the adiabatic reactor, the heat can only be transferred to the coal sample from the inlet gas. Furthermore, since the heat loss to the surroundings in an adiabatic reactor could be neglected, an increase of sample temperature due to the oxidation reaction, and thus the final temperature reached, was much higher than that of in an isothermal reactor. The increase of coal temperature in the adiabatic reactor can then be used to compare the propensity of the samples toward the self-heating more accurately.

4.2.1 The Effect of Air Flow Rate

The effect of air flow rate was also investigated in this method. A nitrogen-dried Coal M2 with a particle size of 1.00 ~ 2.36 mm was used in the experiments. As shown in Figure 4.25, the higher the air flow rate, the faster the rate of temperature rise. It is also observed that after about 2.5 hours of the experiments, the rate of temperature rise of coal with the highest air flow rate (280 ml min^{-1}), was slightly lower than that with 100 ml min^{-1}. This is because a higher air flow rate provided more oxygen available for the oxidation reaction, and thus the reactant was consumed faster. The oxidation reaction was slower as the reactant available for the oxidation reaction diminished. Furthermore, the high air flow rate could have driven the heat away to the ambient, and thus cooled down the sample temperature.

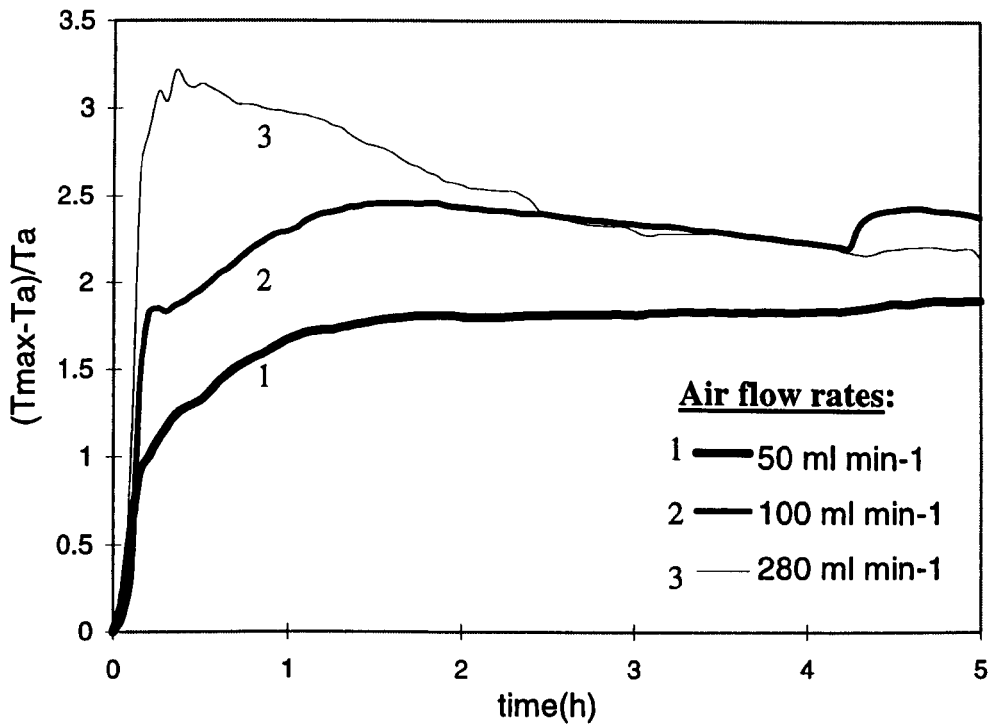

Figure 4.25 Rates of temperature rise of nitrogen-dried Coal M2 at several air flow rates in an adiabatic reactor (A-2) at 145 °C

To further examine the effect of air flow rate in the adiabatic reactor, the critical ambient temperatures of the samples with two different air flow rates, ie. 100 and 280 ml min^{-1} were determined. Typical temperature histories of nitrogen-dried Coal M2 at air flow rate of 100 and 280 ml min^{-1} are shown in Figures 3.9 and 4.26, respectively. A sudden drop in the coal temperature observed for experiments at an oven temperature of 90°C, was caused by an electricity shut down which stopped the compress air and thus the air flowed into the system. From the experimental results, it is found that within the range of air flow rates chosen, the critical ambient temperatures of the samples were the same (85 ± 5 °C). Therefore, it can be concluded that within the experimental range, the air flow rate did not significantly affect the critical temperature reached but the time-to-ignition. The higher the air flow rate, the faster the ignition occurred.

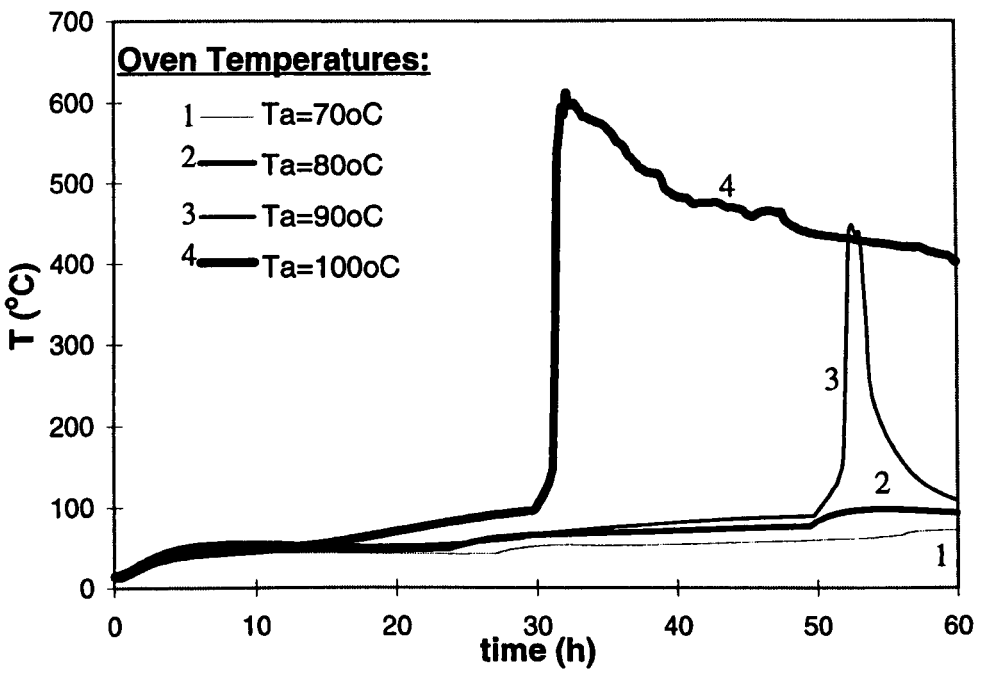

Figure 4.26 Temperature histories of a nitrogen-dried Coal M2 sample at several oven temperatures at air flow rate of 280 ml min^{-1} in an adiabatic reactor (A-2)

4.2.2 The Effect of Adiabatic Reactor Sizes

To examine the effect of adiabatic reactor size on the self-heating process, 1 and 0.3 litre-capacity adiabatic reactors were used. These adiabatic reactors, named as A-1, A-2, were filled with 450 and 100 g of coal, respectively. The critical ambient temperature of each reactor was then determined. Figure 4.27 shows temperature histories of nitrogen-dried Coal M3 tested in adiabatic reactors A-1 and A-2. The particle size range used was 1.00 ~ 2.36 mm. It is observed that the critical ambient temperatures of coal tested in the reactors A-1 and A-2 were the same (95 ± 5 °C). In the adiabatic reactors, the heat loss to the ambient is negligible. Since the rate of heat generation per unit volume is independent of reactor volume or sample mass (but depends on temperature), the adiabatic reactor size did not affect the critical ambient temperature of the coal sample.

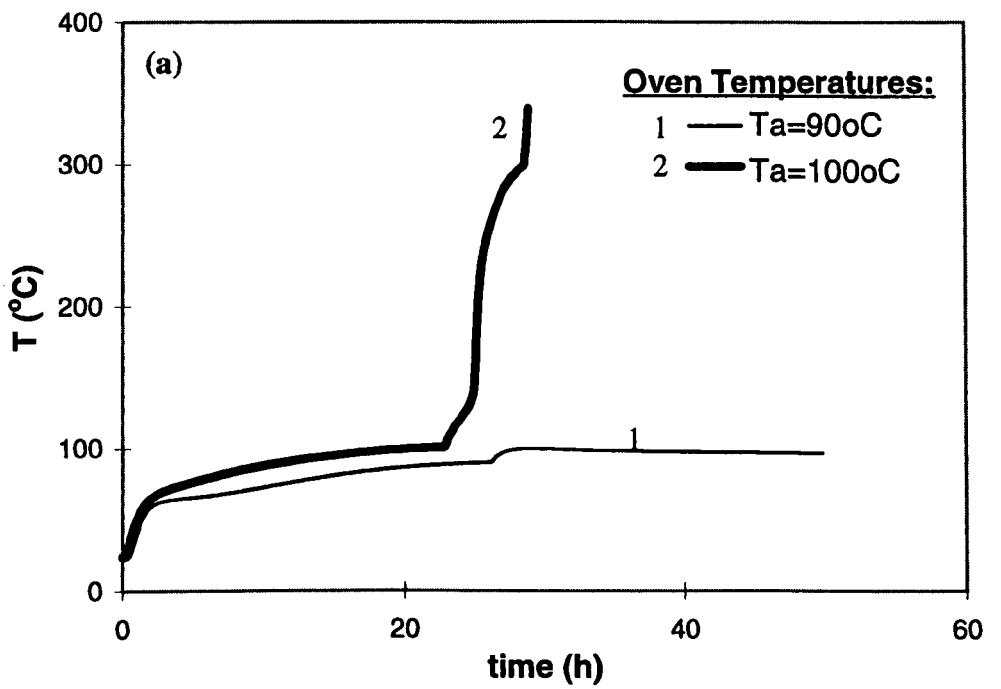

Figure 4.27 (Continued on the next page)

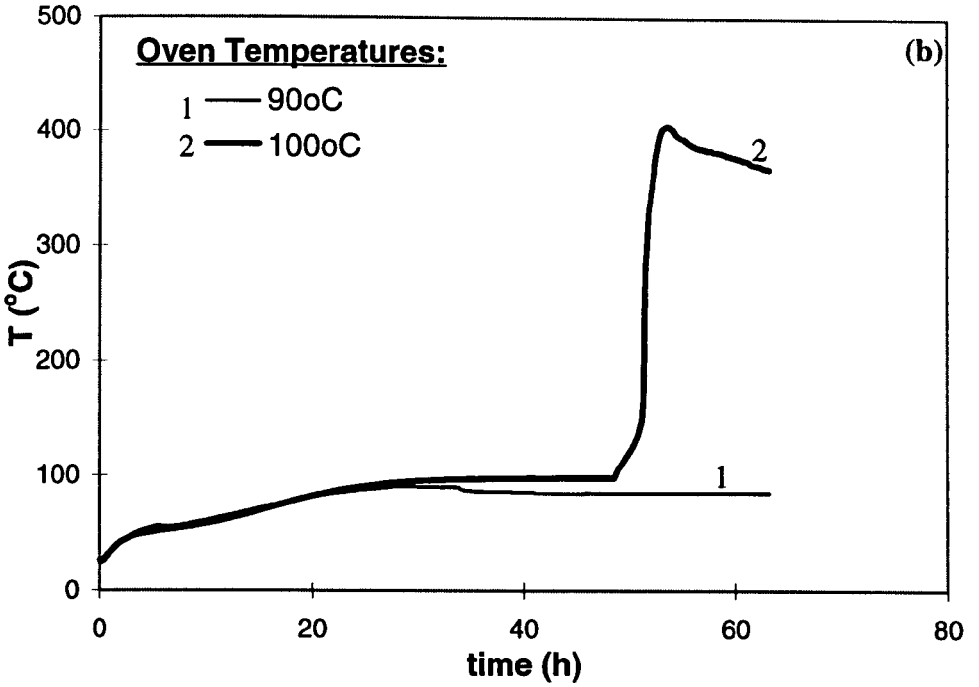

Figure 4.27 Temperature histories of a nitrogen-dried-Coal M3 sample at several oven temperatures in reactor (a) A-1; and (b) A-2

4.2.3 Oxidation Kinetics Estimation

The apparent kinetic parameters, A and E, of Coal M3 were also determined according to Equation (3-2). Figure 4.28 shows linear plots of $\ln\left[\frac{dT}{dt}\right]_o$ versus $\frac{1}{T_o}$ for raw Coal M3 in adiabatic reactors, A-1 and A-2. The range of T_o over which the kinetic experiments were carried out was 90-100 °C. It is found that the E values obtained from adiabatic reactor A-1 and A-2 were the same, ie. 78.1 kJ mol^{-1}, respectively. However, the A values were slightly different, ie. 2.21 × 10^3, and 3.32 × 10^3 kg m^{-3} s^{-1} Pa^{-1} for A-1 and A-2, respectively. This could be due to the experimental errors as has been addressed before. Furthermore, it was also observed during the experiments that the rate of temperature increases in A-1 when the sample temperature equals to oven temperature was lower compared to that in A-2. As a result, the reactivity of A-1 was slightly lower than A-2 , as shown in Figure 4.29.

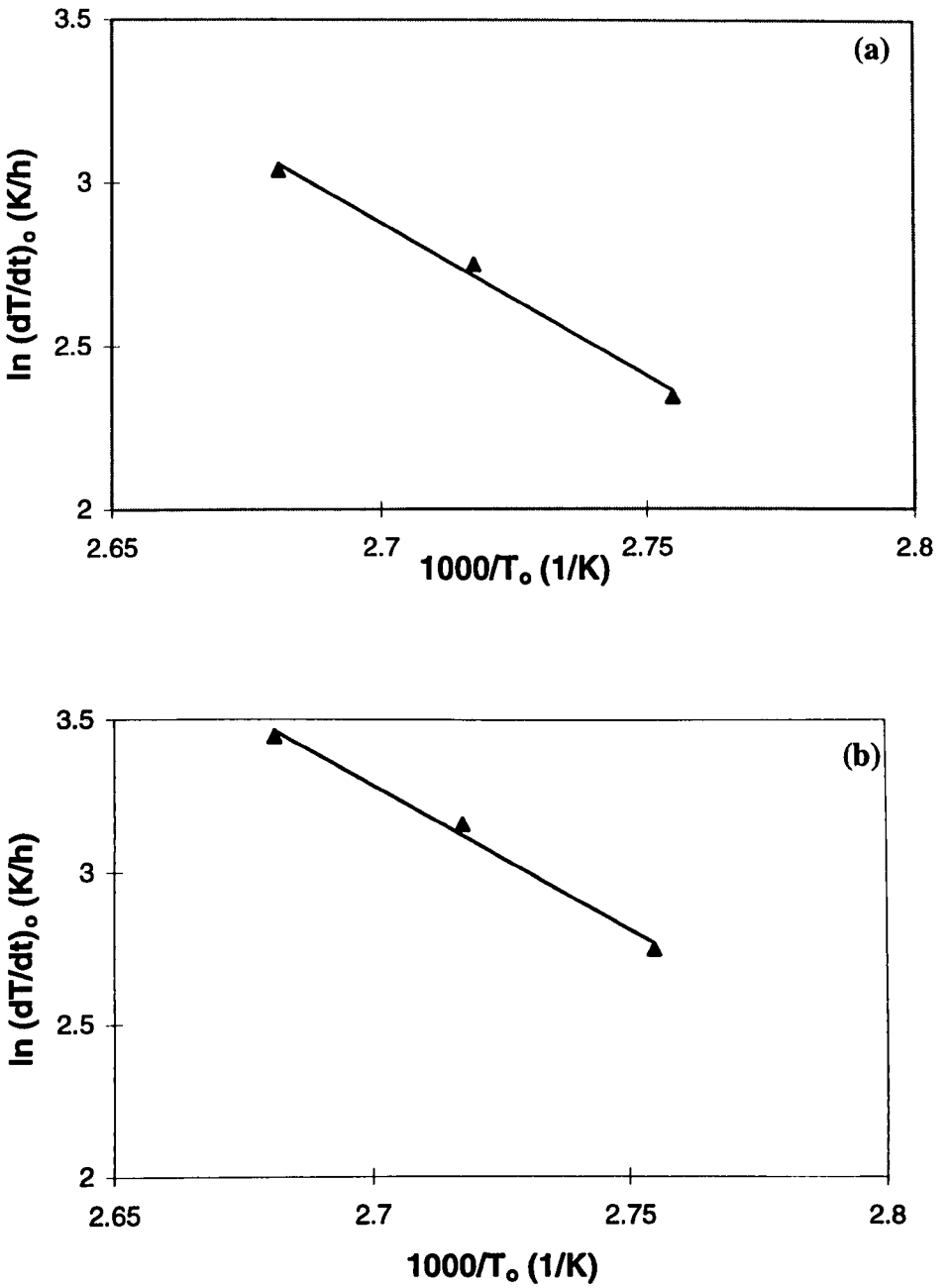

Figure 4.28 A linear plot of $\ln\left[\frac{dT}{dt}\right]_o$ versus $\frac{1000}{T_o}$ for raw Coal M3 in a reactor

(a) A-1; and (b) A-2

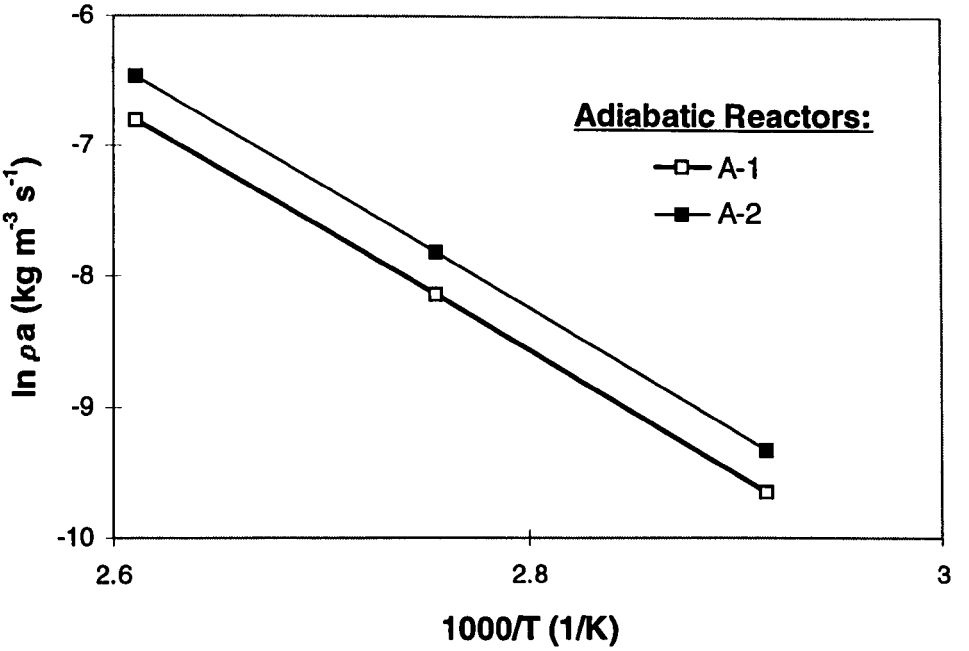

Figure 4.29 The effect of reactor size on the estimated reactivity of coal oxidation in air between 80 and 100 °C in the adiabatic reactors

4.2.4 Estimation of the Critical Layer Thickness

The kinetic constants, E and A, were used to predict, according to Equation (3-3), the critical thickness of a coal deposit which has been chosen as a common basis for comparison. The plots of the critical thicknesses as a function of temperature for both adiabatic reactors A-1 and A-2 are shown in Figure 4.30. Similar to the trends observed in the isothermal reactors, the critical thickness of the coal deposit predicted from adiabatic reactor decreased with increasing ambient temperature. There were small variations in the critical thickness predictions from the two different adiabatic reactor sizes. The maximum variance decreased with temperature, and was about 20% at 80 °C and 9% at 100 °C. As can be seen in Equation (3-3), the E and A values were the only responsible variables for critical thickness prediction, while other variables were assumed to be constant. The E values for two different reactors were the same while the A values showed a slight

difference. This together with experimental errors caused a small deviation in the critical thickness calculated, particularly at low temperatures.

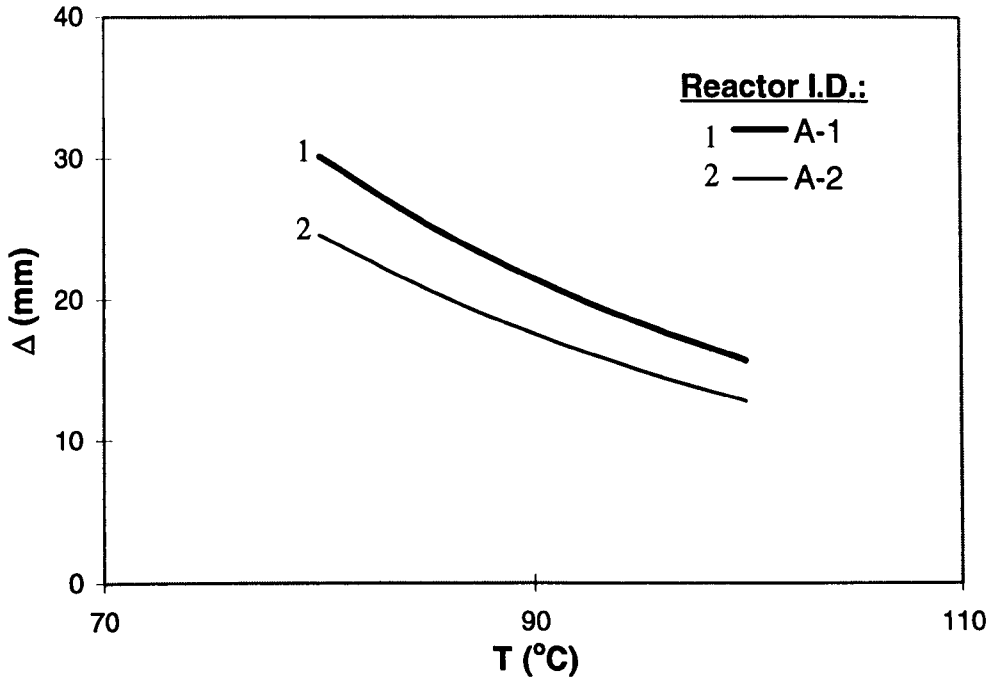

Figure 4.30 A comparison of critical thicknesses of coal deposits (slabs) capable of spontaneous combustion estimated from adiabatic reactors A-1 and A-2

4.2.5 Time-To-Ignition

Figure 3.9 shows the temperature histories of a nitrogen-dried Coal M2 tested in an adiabatic reactor (A-2) at several oven temperatures, and at air flow rate of 100 ml min^{-1}. It is shown the higher the ambient temperature, the shorter the time-to-ignition. A similar trend can also be seen in Figure 4.26 for Coal M2 tested in an adiabatic reactor (A-2) at several oven temperatures, and at air flow rate of 280 ml min^{-1}.

To determine the time-to-ignition of Coal M2 tested in an adiabatic reactor (A-2) at several oven temperatures, the second-order time derivative of temperature (d^2T/dt^2) was calculated and plotted against time. Figure 4.31 shows the plots of Coal M3

tested in a reactor A-2 at 90 and 100 °C, and the time-to-ignition obtained were 52.79 and 33.49, respectively.

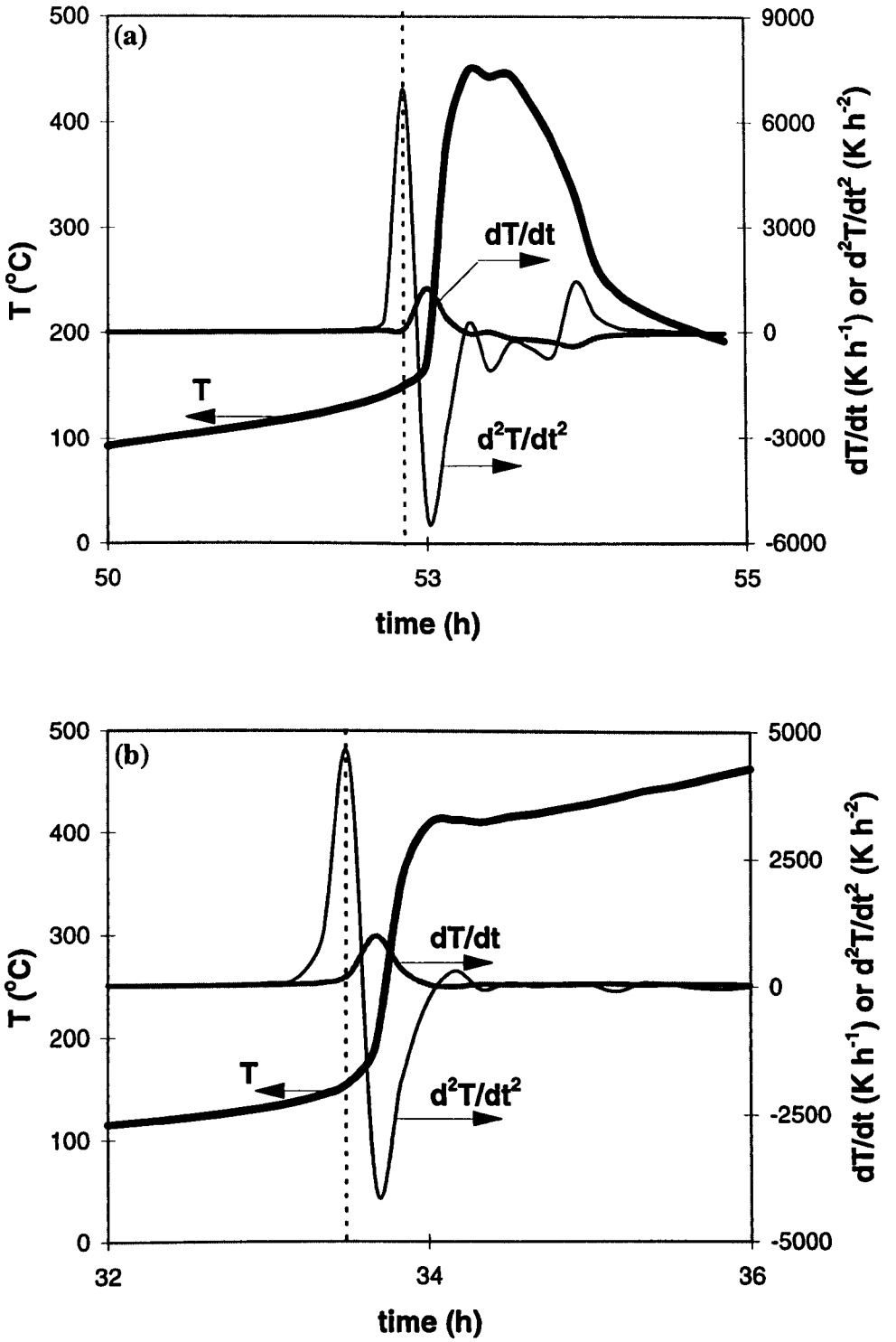

Figure 4.31 Determination of time-to-ignition for Coal M2 tested in an adiabatic reactor (A-2) at air flow rate of 100 ml min^{-1} at oven temperature of (a) 90 °C; and (b) 100 °C

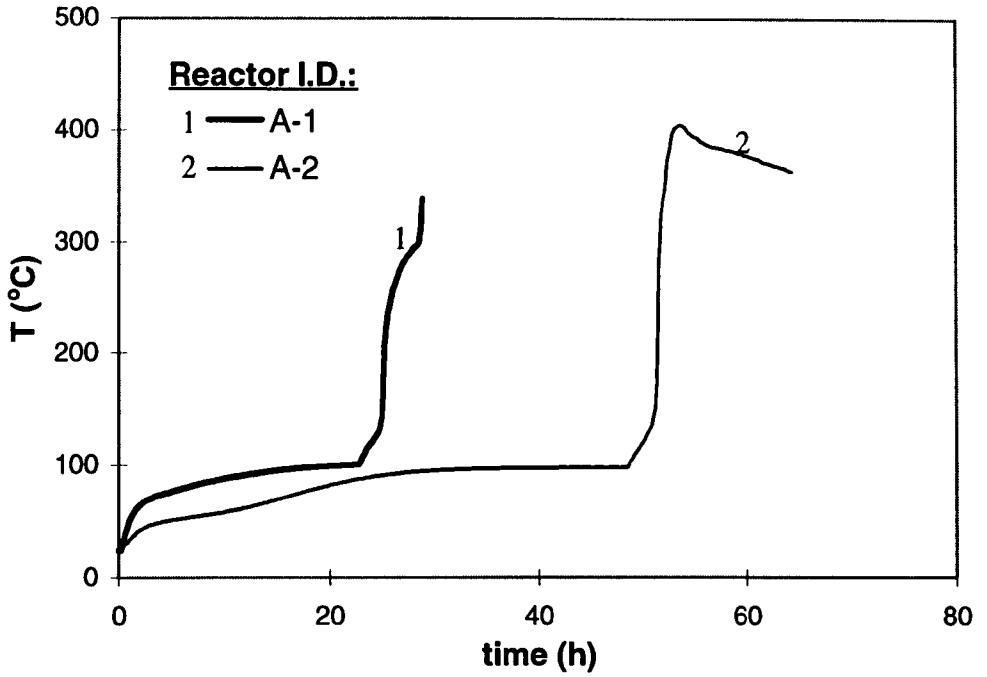

Figure 4.32 Temperature histories of a nitrogen-dried Coal M3 sample in different adiabatic reactor sizes at 100 °C

Furthermore, it is also observed that the time-to-ignition varied with the adiabatic reactor sizes. Figure 4.32 plots the temperature histories of a nitrogen-dried-Coal M3 tested in two different adiabatic reactor sizes at 100 °C. It is noticed that the coal sample tested in reactor A-1 experienced the thermal runaway quicker than that tested in reactor A-2.

To determine the time-to-ignition of Coal M3 tested in the two adiabatic reactors, plots of the coal temperature, first-order time derivative of temperature (dT/dt) and second-order time derivative of temperature (d^2T/dt^2) against time were drawn in Figure 4.33. It is observed that the coal sample tested in reactor A-1 experienced the thermal runaway after 24.82 hours, while in reactor A-2, the thermal runaway occurred after 51.13 hours. Accordingly, the larger the reactor size, the shorter the time-to-ignition which is opposite to the trend observed in the isothermal reactors. Since the heat loss in the adiabatic reactor can be neglected, the larger amount of coal in the reactor A-1 provided a higher heat generation dues to the oxidation

reaction. The high heat generation significantly accelerated the oxidation reaction, and thus shortened the time-to-ignition.

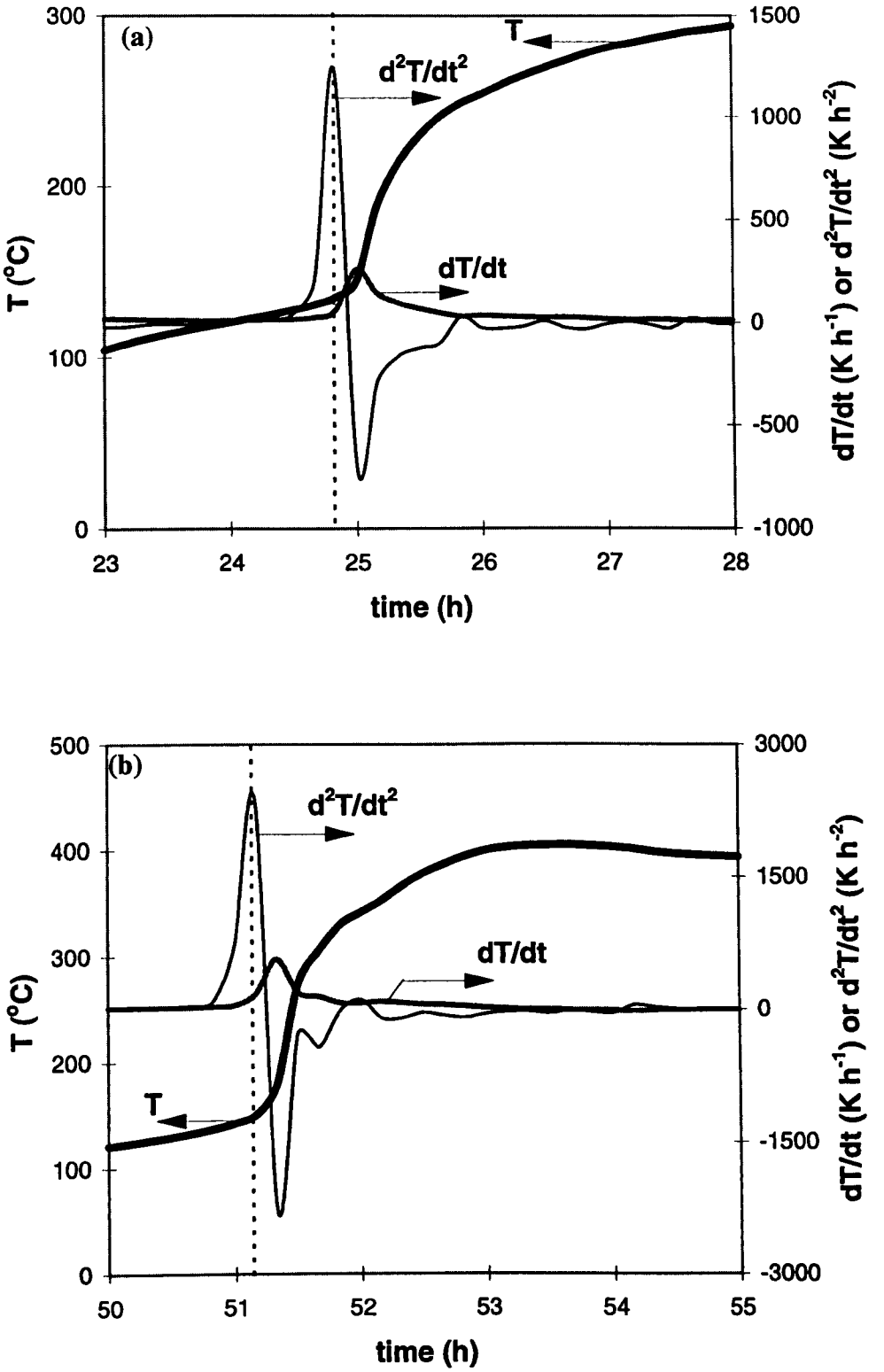

Figure 4.33 Determination of time-to-ignition for Coal M3 tested at 100 °C in reactor (a) A-1; and (b) A-2

4.3 RESULTS FROM WIRE-MESH REACTOR EXPERIMENTS

Extensive research efforts, in both mathematical modelling (Chen and Chong (1995); Gray et al. (1984); Gray et al. (1992); Gray et al. (1990); Griffiths (1992)) and experimentation (Chen and Chong (1995); Chong et al. (1997); Chong et al. (1995); Chong et al. (1996); Jones and Raj (1988); Jones and Wake (1990); O'Mahony and Synnott (1988)), have been devoted to predicting the critical sizes of various materials. Steady-state wire-mesh reactor tests coupled with the Frank-Kamenetskii analysis had been a very popular approach until recently, when Chen and Chong (1995) started to use an unsteady-state method. In this method, thermal equilibrium within the test sample is no longer required. The heating rate ($\partial T/\partial t$) at the sample centre, when the thermal conduction around the geometric centre of the sample becomes zero is measured, and the unsteady-state energy balance analysis enables estimation of oxidation kinetics of the sample (Chen and Chong (1995); Chong et al. (1997); Chong et al. (1995); Chong et al. (1996)). However, a critical comparison between those two methods has not yet been discussed in the literature.

The present work employed seven cylindrical wire-mesh reactors to study the low-temperature oxidation behaviour of a Victorian brown coal using both the steady-state and unsteady-state methods. For the steady-state method, the critical ambient temperatures, above which a thermal runaway in a sample occurred, were determined for seven cylindrical reactors to enable calculations of the oxidation kinetics. The plots of temperature histories of coal tested in reactors B-1 to B-7 at several oven temperatures for the steady-state method are shown in Figures 3.12 to 3.18, respectively. For the unsteady-state method, the unsteady-state energy balance analysis was applied at the crossing point, where the thermal conduction around the centre of the cylinder became zero, to calculate the oxidation kinetics. The plots of temperature readings and computed radial temperature derivative as a function of time in wire-mesh reactors B-1 to B-7 are shown in Figures 3.19 and 3.25. The

kinetic constants estimated, from both the steady-state and unsteady-state methods were then used to predict the critical thickness of a coal deposit (an infinite slab). A critical comparison between these two methods is offered, and the influence of reactor size on the critical ambient temperature and critical thickness is also discussed in the following sections.

4.3.1 The Effect of Reactor Size and Shape

The critical ambient temperature measured with the steady-state method is an indication of the tendency of a coal towards self-heating and spontaneous combustion. The critical ambient temperature, however, is dependent on the size and shape of the sample being tested. Figure 4.34 shows the variation of measured critical ambient temperatures with reactor volume. While a general trend that the larger the reactor, the lower the critical ambient temperature measured, was observable, the data was somewhat scattered for reactors of the same volume but different diameter-to-height ratios (Reactors B-4 to B-7).

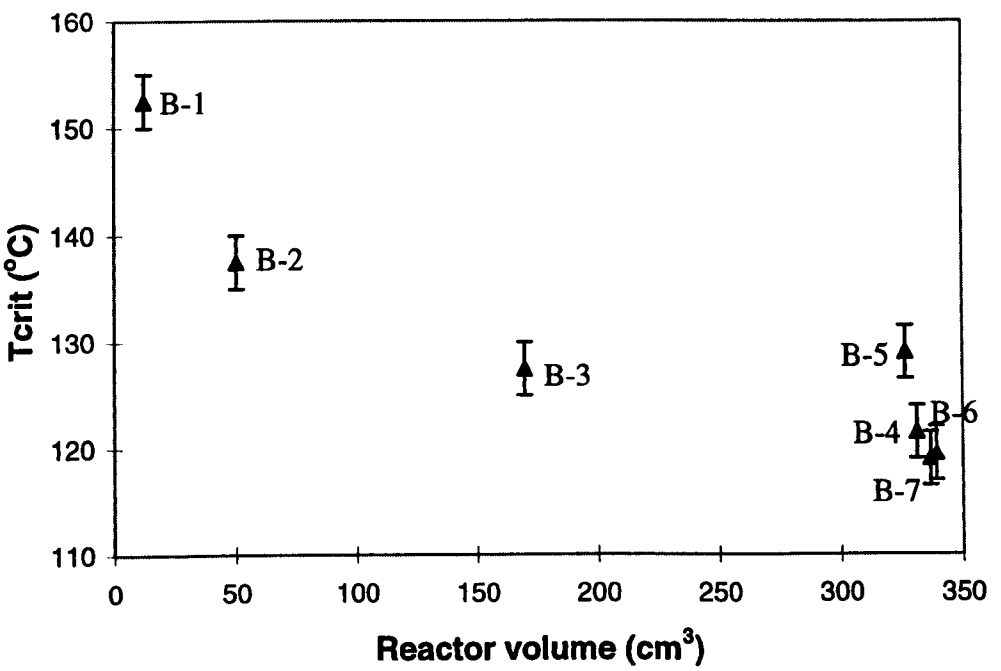

Figure 4.34 A plot of critical ambient temperature versus reactor volume

On the other hand, a very good linear correlation existed between the critical ambient temperature and specific external areas of the reactors, regardless of their shape (diameter-to-height ratios), as evident in Figure 4.35. In the steady-state measurement, the dominant heat transfer was due to convection on the external surface of the reactor (ie. a large Bi number), while the rate of heat generation per unit volume was independent of reactor volume or sample mass (but depends on temperature). Therefore, an increase in the specific external area of the reactor resulted in a higher critical ambient temperature.

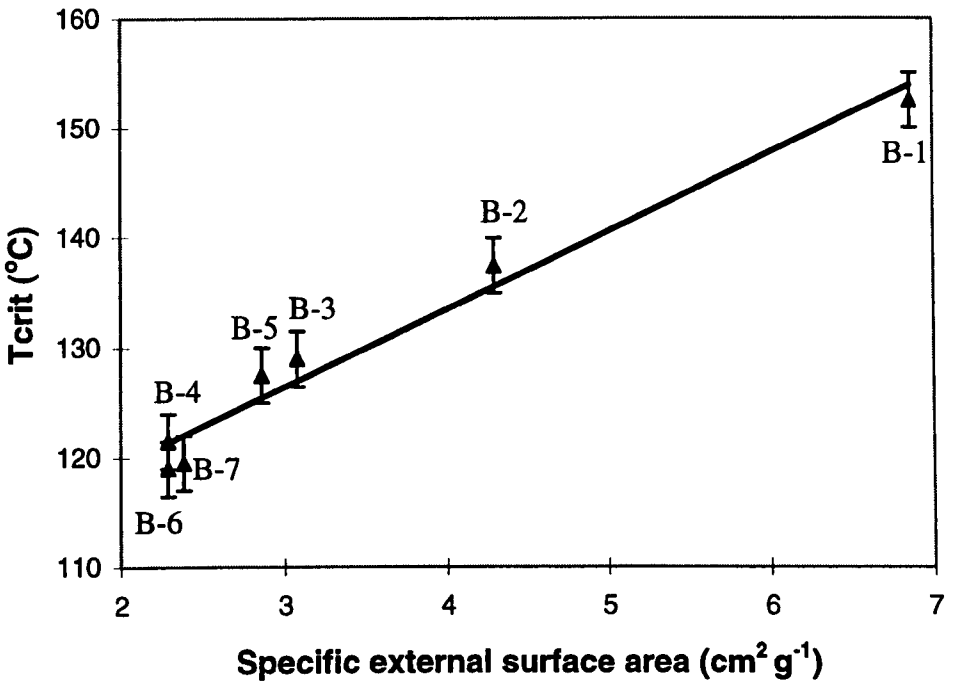

Figure 4.35 A plot of critical ambient temperature versus specific external surface area of reactors

4.3.2 Oxidation Kinetics Estimated from Steady-State and Unsteady-State Method

The critical ambient temperatures determined from the seven cylindrical reactors of different sizes were used to estimate the oxidation kinetics according to Equation (3-

7), as shown in Figure 4.36. An excellent linear plot between $\ln(\delta_c \bullet T_{a,c}^2 / r^2)$ and $1000/T_{a,c}$ was evident, which gave kinetic constants: A = 4.36×10^5 s^{-1} and E = 92.1 kJ mol^{-1}.

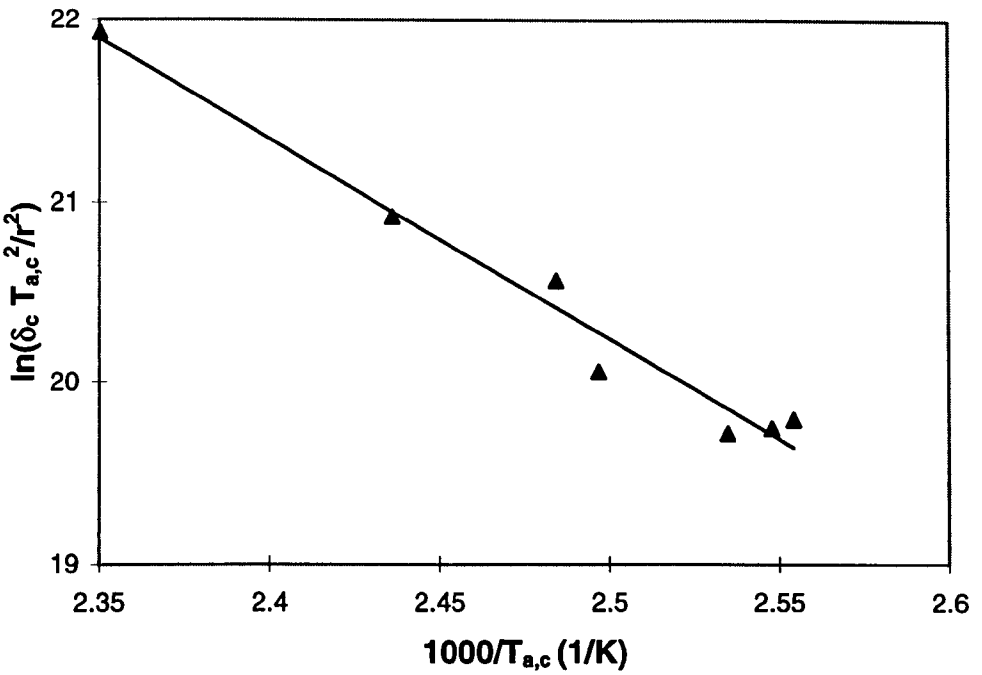

Figure 4.36 Determination of kinetic constants A and E from steady-state method: a linear plot of $\ln(\delta_c T_{a,c}^2/r^2)$ versus $1000/T_{a,c}$

To calculate the kinetic constants from the unsteady-state method, $\ln(\partial T / \partial t)_{T=T_p}$ at the crossing point was plotted against the reciprocal of the crossing point temperature, $1000/T_p$, for each of the seven reactors in Figure 4.37. Again, a good linear correlation for each of the reactor was evident. There were, however, some differences among the plots for different reactors. This is most likely due to experimental errors, such as variation in packing densities of samples in the reactors and slight dislocation of thermocouples. These differences are believed to be random, as no correlations with the reactor size or shape could be identified.

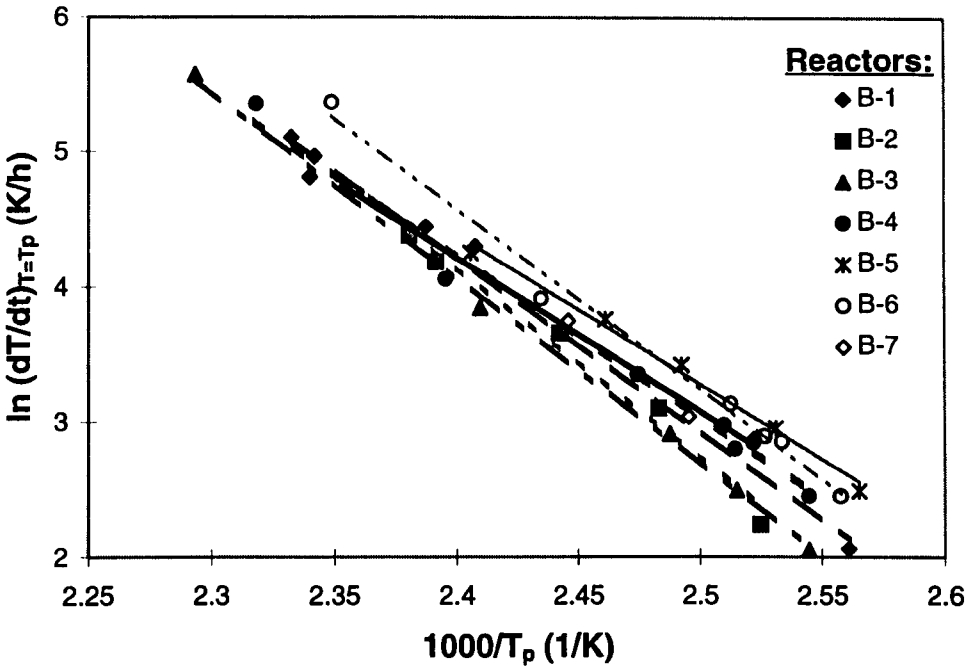

Figure 4.37 Determination of kinetic constants A and E from unsteady-state method: linear plots of $\ln(dT/dt)_{T=Tp}$ versus $1000/T_p$ for various reactor sizes

Table 4.4 Summary of kinetic constants calculated from the unsteady-state method for different reactors

Reactor I.D.	E (kJ mol^{-1})	A (s^{-1})
B-1	108.0	3.22×10^{7}
B-2	117.5	4.61×10^{8}
B-3	114.8	1.96×10^{8}
B-4	100.6	3.91×10^{6}
B-5	101.2	6.08×10^{6}
B-6	111.3	1.21×10^{8}
B-7	94.7	6.93×10^{5}

The oxidation kinetics have then been estimated according to Equation (3-10) for each of the reactors. The values of A and E from the unsteady-state method were summarised in Table 4.4. Variation in both A and E values can again be seen, and

generally a higher E value corresponded to a higher A value. This means that these apparent kinetics would indicate a similar reactivity of the coal. Again, the above mentioned random experimental errors might hold the responsibility.

4.3.4 Estimation of The Critical Layer Thickness with Both Steady-State and Unsteady-State Methods

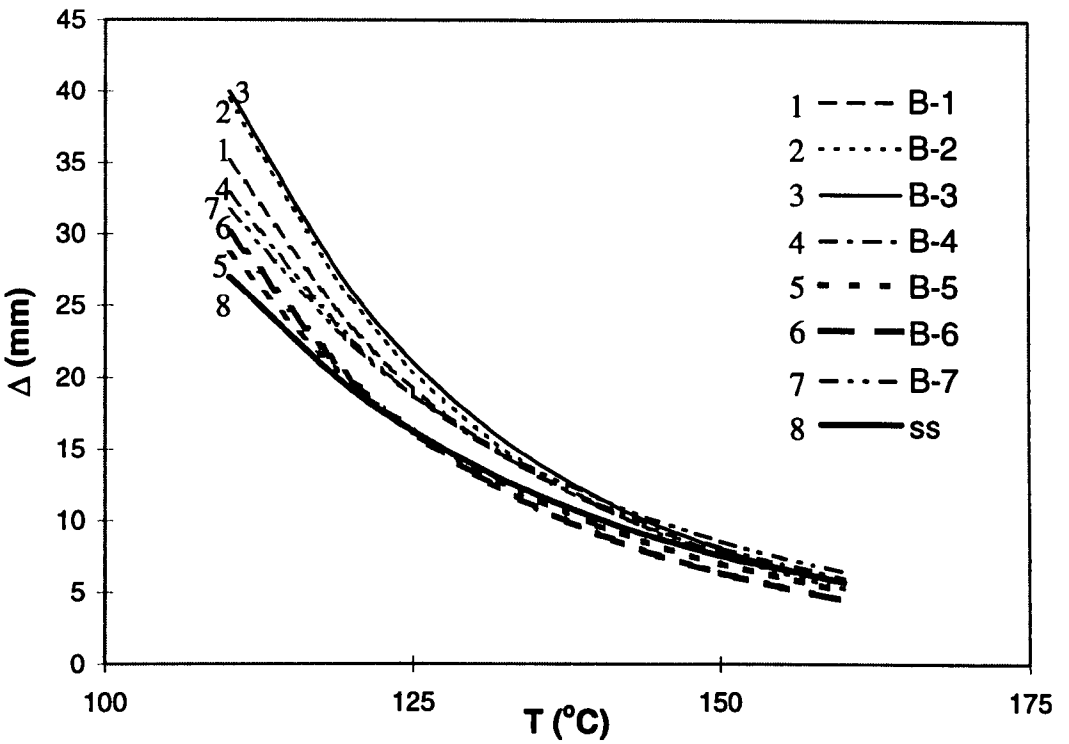

Figure 4.38 A comparison of critical thicknesses of coal deposits (slabs) capable of spontaneous combustion estimated using both steady-state (line 8) and unsteady-state (lines 1-7 for different reactors) methods

The kinetic constants were then used to predict, according to Equation (3-3), the critical thickness of an infinite coal deposit slab which has been chosen as a common basis for comparison. The results are shown in Figure 4.38. Clearly, the critical thickness of the coal deposit decreased with increasing ambient temperature, as the trend shown in both isothermal and adiabatic reactors. It must be noted that the critical thickness predicted from the steady-state method compared very well

with those from the unsteady-state method. There were some variations in the predictions from the unsteady-state method using seven different reactors. The maximum variance decreased with temperature, and was about 33% at 110 °C and 5% at 160 °C. These variations are reasonable, given the nature of the experimental work and for reasons discussed before. Nevertheless, the results obtained from this work implies that the unsteady-state method can be used to replace, with confidence, the steady-state method for a more efficient analysis of spontaneous combustion of coal (Sujanti et al. (1998b))

4.3.5 The Effect of Packing Density

Table 4.5 Summary of critical ambient temperatures and kinetic constants estimated of Coal M2 in a wire-mesh reactor (B-1) with different packing densities

Packing I.D.	Packing Density ($kg\ m^{-3}$)	Tcrit (°C)	E ($kJ\ mol^{-1}$)	A ($kg\ m^{-3} s^{-1} Pa^{-1}$)
PW-1	407.4	165.5 ± 0.5	113.9	5.55×10^{7}
PW-2	611.2	157.5 ± 0.5	109.2	3.17×10^{7}
PW-3	814.9	153.5 ± 0.5	104.7	1.13×10^{7}
PW-4	978.0	149.5 ± 0.5	103.3	7.05×10^{6}

Experiments were also carried out to examine the effect of packing density on the critical ambient temperature using wire-mesh reactor technique. A wire-mesh reactor (B-1) was employed to determine the critical ambient temperature of raw Coal M2 in various packing densities. As shown in Table 4.5, four different levels of packing densities, namely PW-1, PW-2, PW-3, and PW-4, were used for this purpose.

The critical ambient temperature of the coal in each packing density was determined and summarised in Table 4.5. It is shown that the higher the packing density, the lower the critical ambient temperature. This indicates that a high coal packing density significantly hinders the heat loss to the surroundings, and thus increases the risk of coal to spontaneously combust. Typical temperature profiles of raw Coal M2 with four different packing densities, PW-1, PW-2, PW-3, and PW-4, tested in a wire-mesh reactor (B-1) are shown in Figure 4.39.

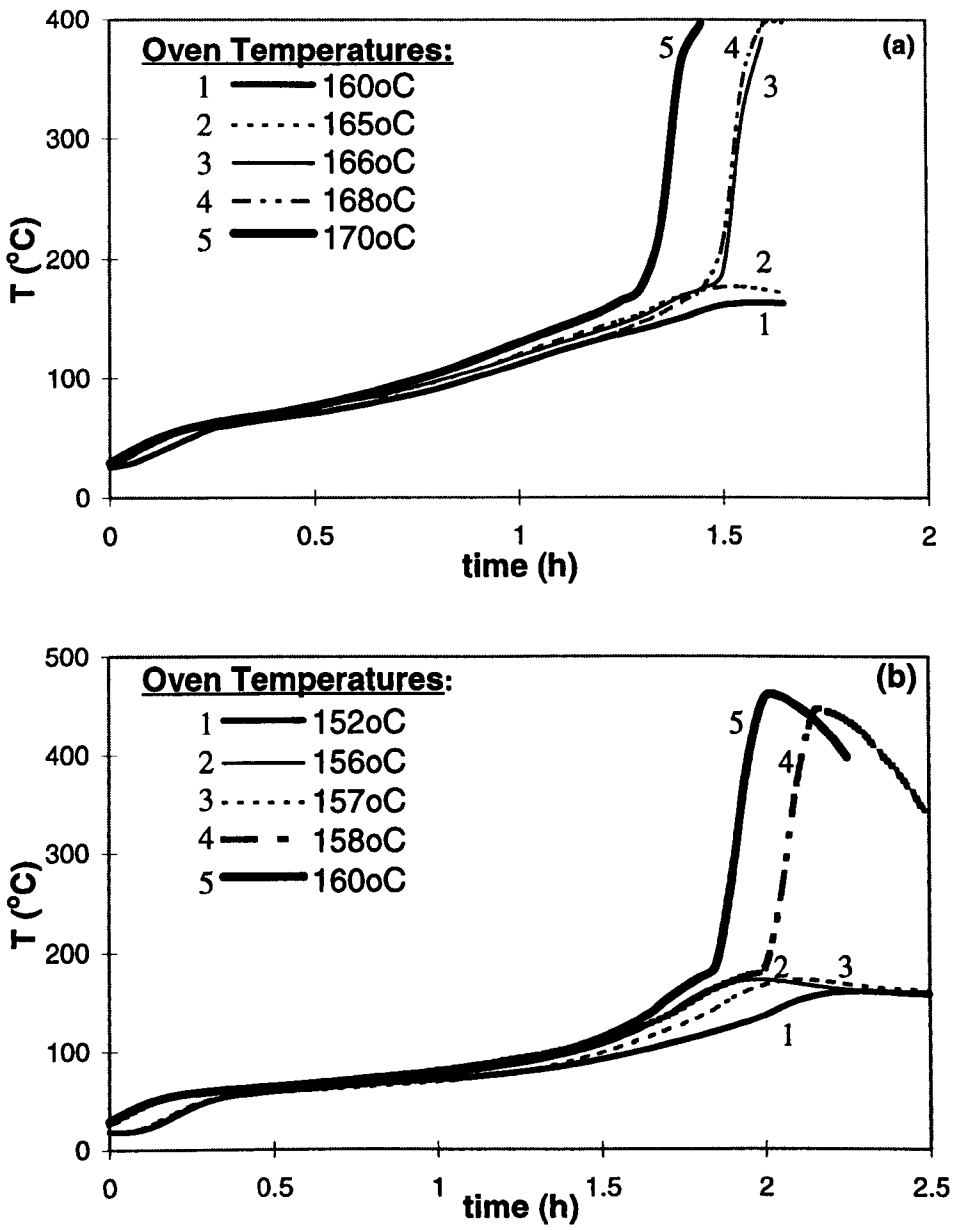

Figure 4.39 (Continued on the next page)

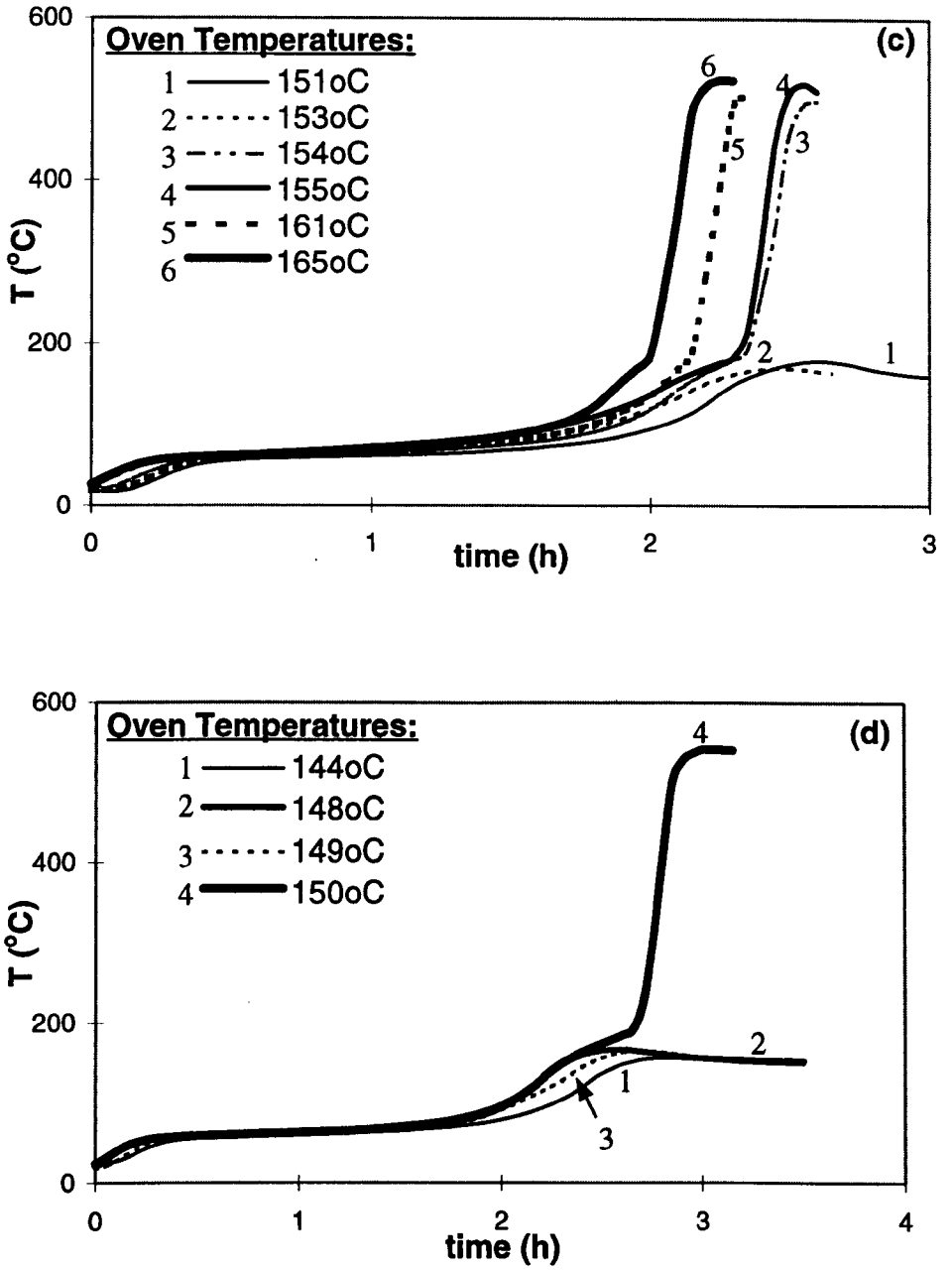

Figure 4.39 Temperature histories of raw Coal M2 in a wire-mesh reactor (B-1) with a packing density of (a) 407.4 kg m^{-3}; (b) 611.2 kg m^{-3}; (c) 814.9 kg m^{-3}; and (d) 977.9 kg m^{-3}

To further examine the effect of packing density on coal spontaneous combustion, the apparent kinetic parameters, A and E, of Coal M2 in different packing densities were determined according to Equation (3-10). Figure 4.40 shows typical linear plots of $\ln\left[\frac{dT}{dt}\right]_{T=Tp}$ versus $\frac{1}{T_p}$ for Coal M2 tested in a wire-mesh reactor (B-1)

with packing densities of PW-1, PW-2, PW-3, and PW-4. The range of T_o over which the kinetic experiments were carried out was 140-170 °C.

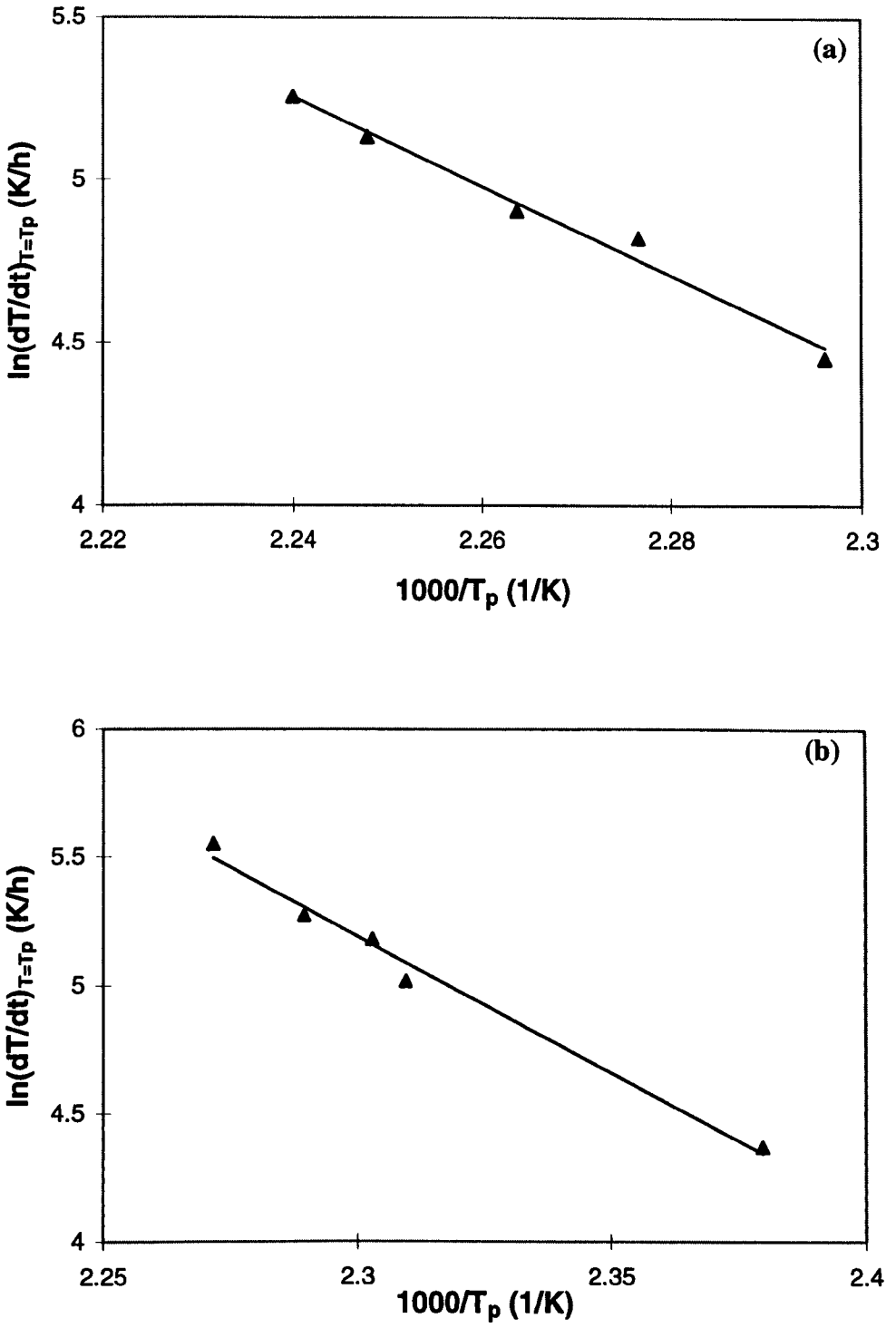

Figure 4.40 (Continued on the next page)

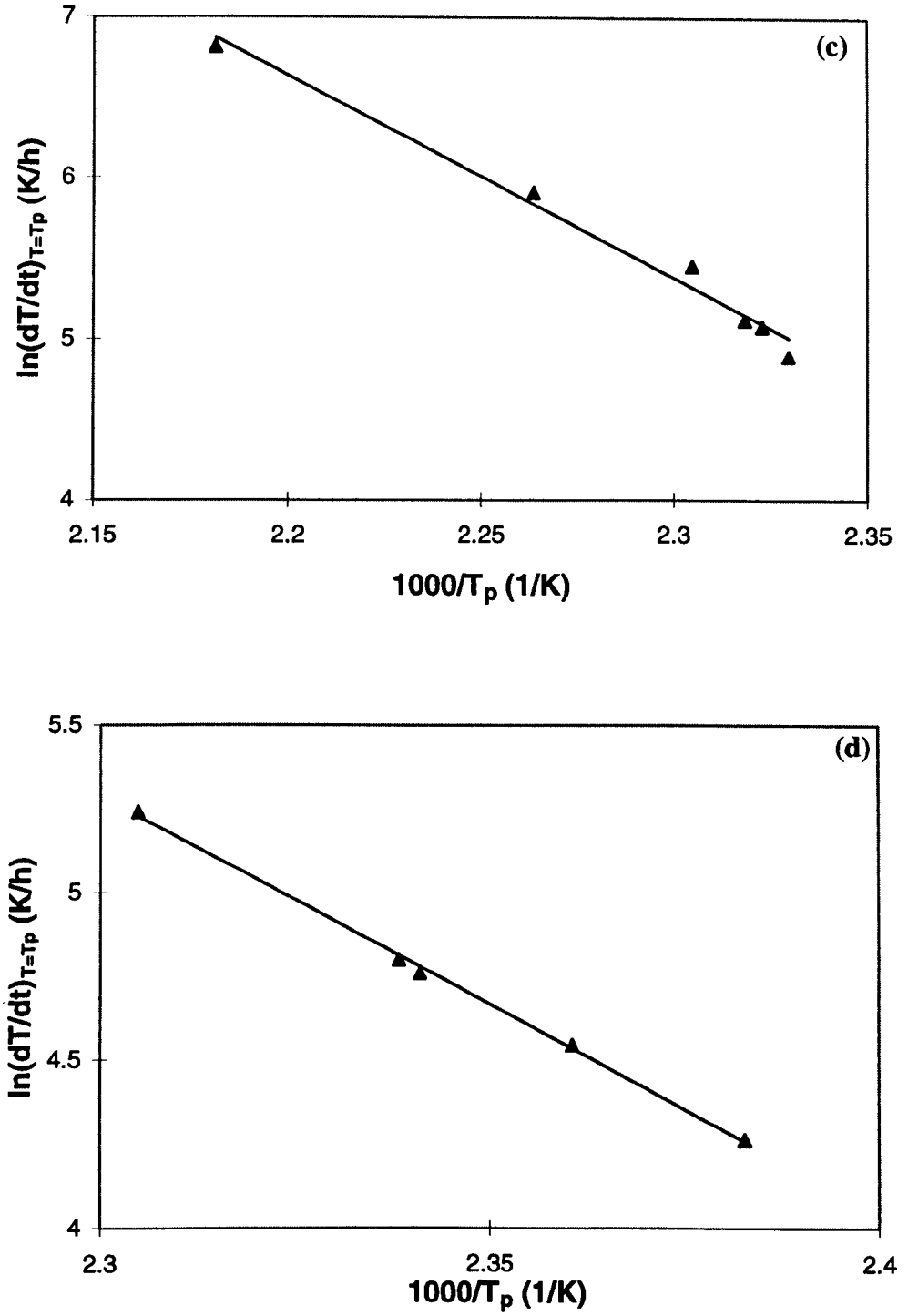

Figure 4.40 A linear plot of $\ln\left[\frac{dT}{dt}\right]_{T=Tp}$ versus $\frac{1000}{T_p}$ for raw Coal M2 in a wire-mesh reactor (B-1) with a packing density of (a) 407.4 kg m^{-3}; (b) 611.2 kg m^{-3}; (c) 814.9 kg m^{-3}; and (d) 977.9 kg m^{-3}

The values of A and E estimated from different packing densities were also summarised in Table 4.5. The kinetic constants obtained were then used to estimate the coal reactivities. Figure 4.41 plots the reactivities of the coal in different packing densities. It is shown that coal with the lowest packing density, i.e. PW-1, had the lowest reactivities which corresponded to the highest critical ambient temperature observed. Similarly, the reactivity of coal with packing density of PW-2 was lower than that with PW-3 and PW-4.

The kinetic constants, A and E, were also used to predict, according to Equation (3-3), the critical thickness of an infinite coal deposit slab. The results are shown in Figure 4.42. It is noticed that the critical thickness of the coal deposit decreased with increasing ambient temperature, as expected. There were some variations in the predictions from three different packing densities. The maximum variance decreased with temperature, and was about 47% at 140 °C and 10% at 170 °C. It is also shown in Figure 4.42 that in general, the lower the packing density the larger the critical layer thickness predicted, which is well related to the coal reactivities estimated.

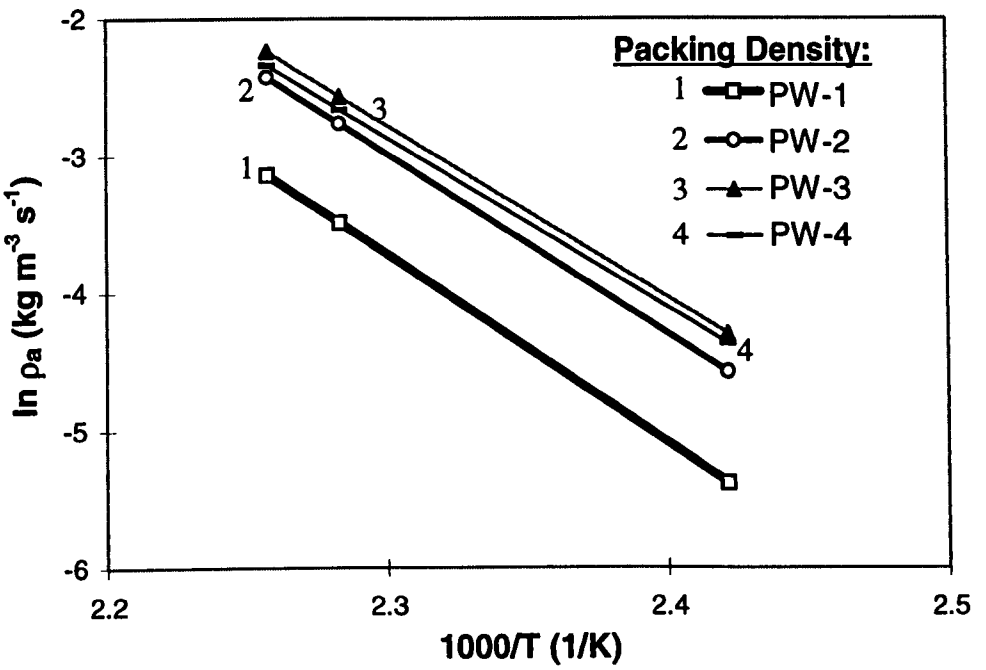

Figure 4.41 The effect of packing density on the estimated reactivity of coal oxidation in air between 140-170 °C

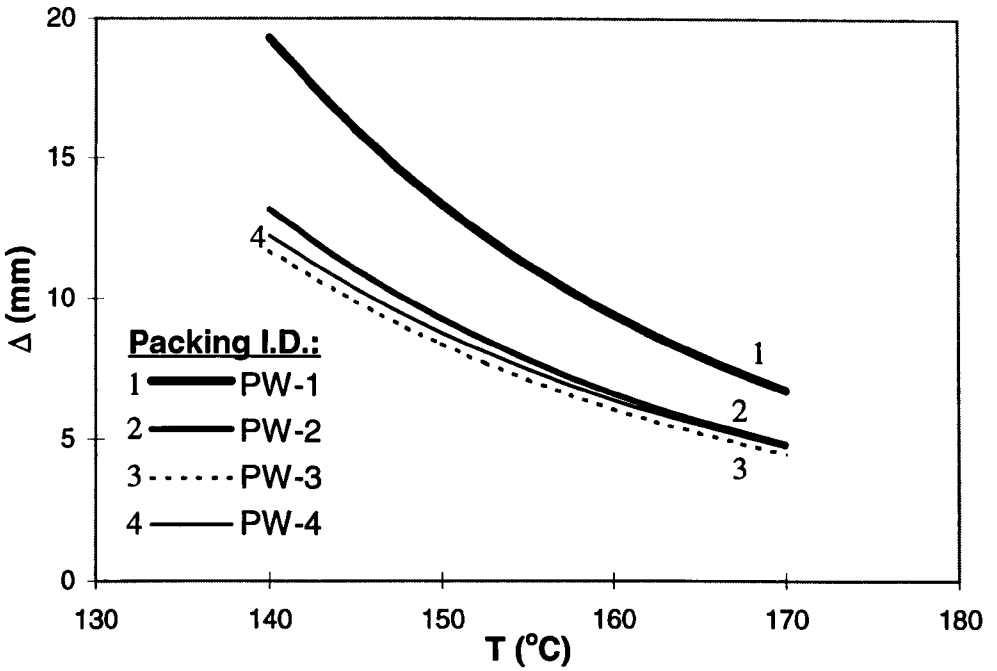

Figure 4.42 A comparison of critical thicknesses of coal deposits (slabs) capable of spontaneous combustion estimated from a wire-mesh reactor (B-1) of different packing densities

4.3.6 Time-To-Ignition

4.3.6.1 The effect of ambient temperature

Figure 3.13 shows the temperature histories of nitrogen-dried Coal M3 tested in a wire-mesh reactor (B-2) at several oven temperatures. It is shown that the higher the ambient temperature, the quicker the thermal runaway occurred. A closer examination using the second-order time derivative of temperature shown that at an oven temperature of 138 °C, the thermal runaway occurred after about 2.67 hours of experiment, while at 140 and 145 °C the thermal runaway occurred after 2.06 and 1.73 hours of experiment, respectively. The plots of time-to-ignition determination are shown in Figure 4.43 for ambient temperatures of 138, 140, and 145 °C.

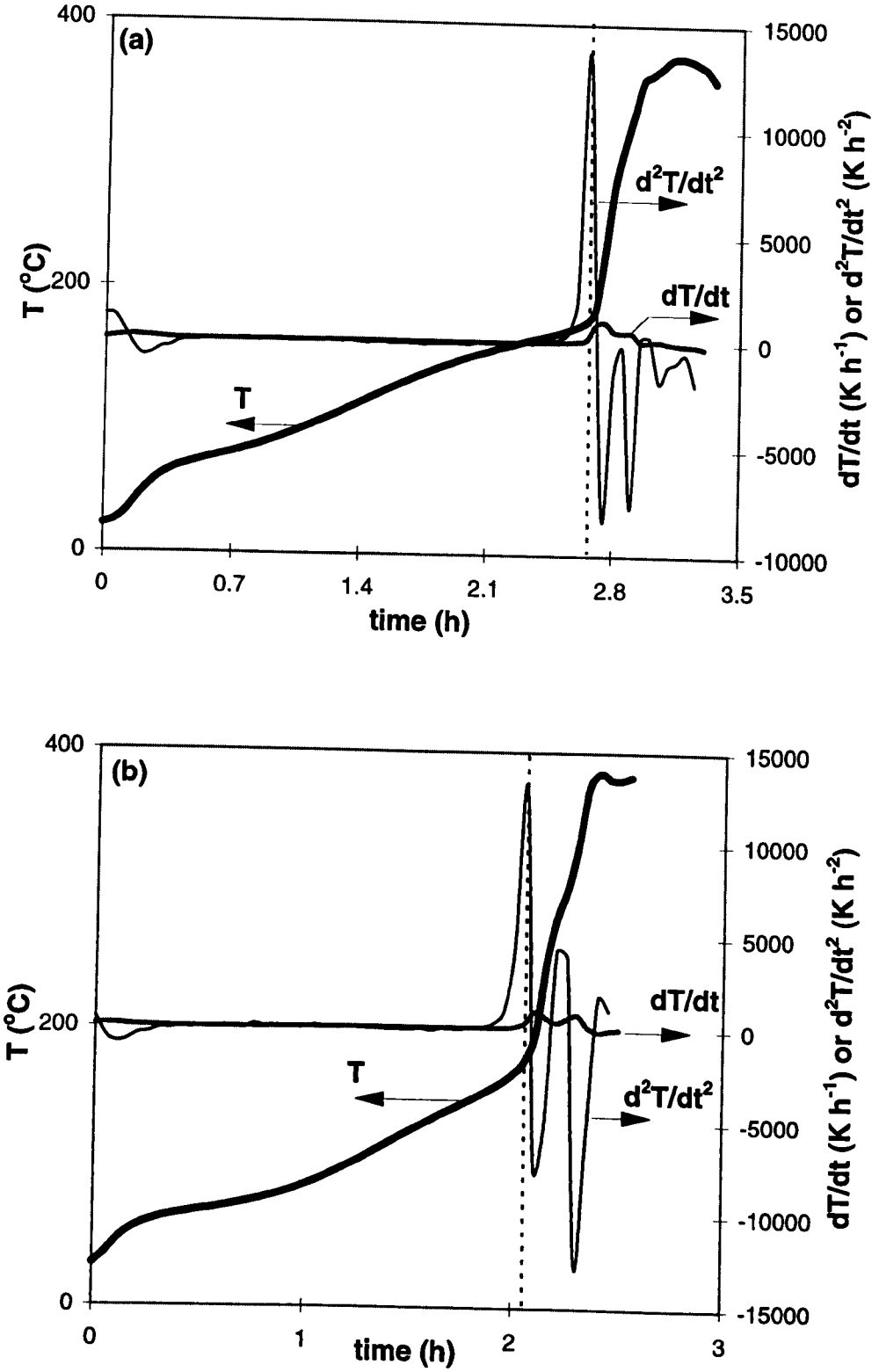

Figure 4.43 (Continued on the next page)

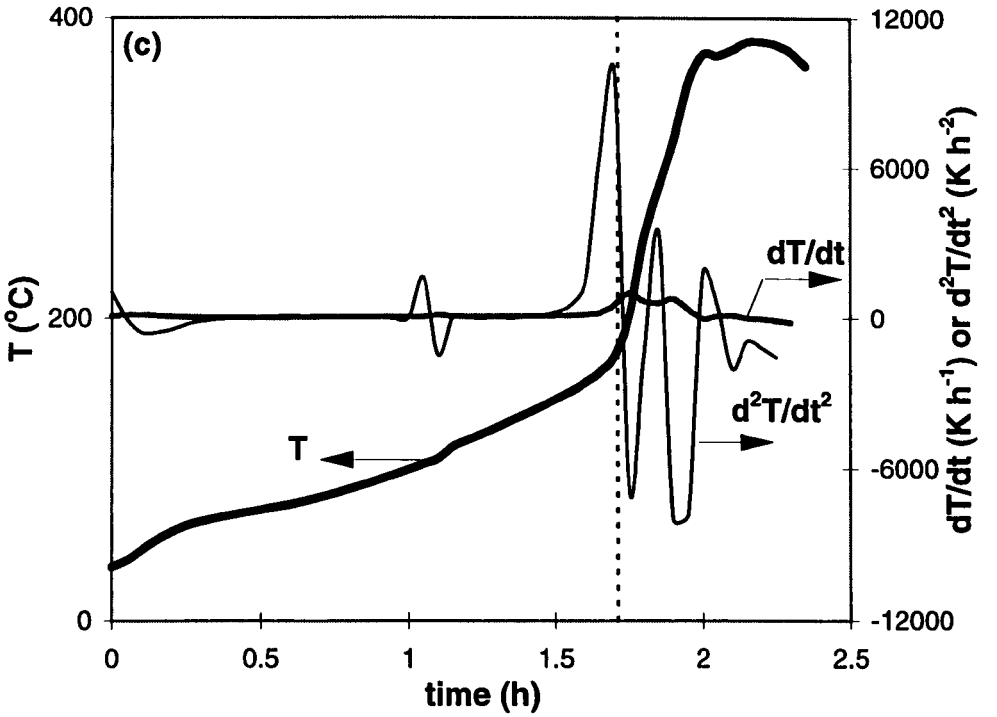

Figure 4.43 Determination of time-to-ignition for Coal M3 tested in a wire-mesh reactor (B-2) at an oven temperature of (a) 138 °C; (b) 140 °C; and (c) 145 °C

4.3.6.2 The effect of reactor sizes

Time-to-ignition also varied with the wire-mesh reactor sizes. Figure 4.44 plots the temperature histories of nitrogen-dried Coal M3 tested in different wire-mesh reactor sizes. Each temperature history was plotted at the lowest temperature at which thermal runaway occurred. In general, it can be seen that the larger the reactor specific external surface area, the shorter the time-to-ignition. This was because the larger the reactor specific external surface area, the higher the critical ambient temperature for the thermal runaway to occur. A high temperature significantly shortened the time-to-ignition. The plots of the time-to-ignition determination for Coal M3 tested in reactor B-1 to B-7 at their respective critical ambient temperatures were drawn in Figures 4.45(a), 4.42(a), and 4.45((b)-(f)), respectively. The time-to-ignition obtained from different wire-mesh reactor sizes were then summarised in Table 4.6.

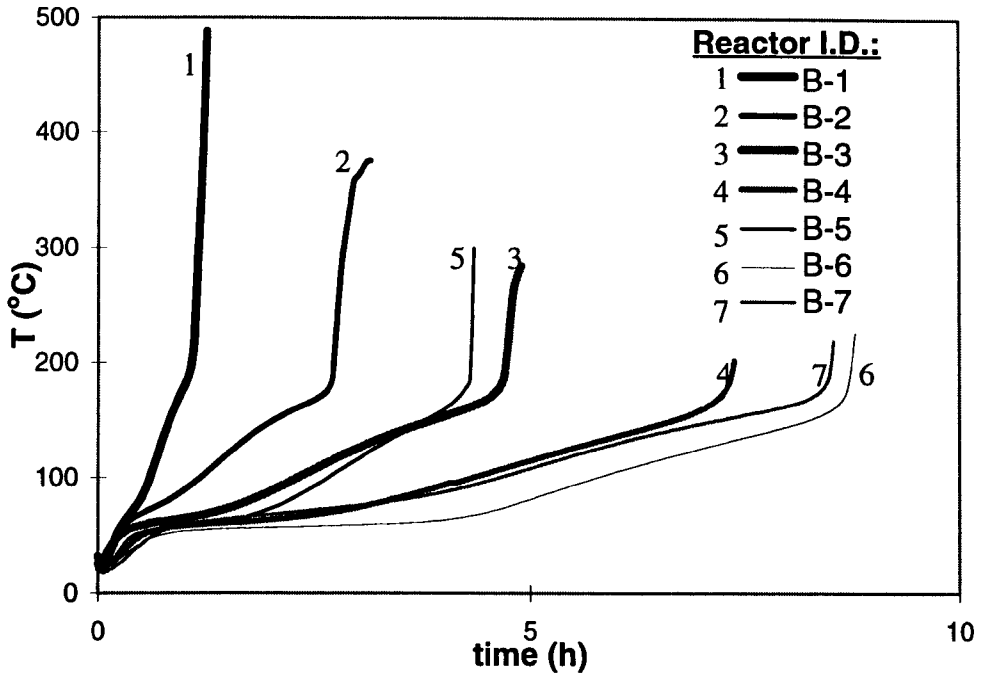

Figure 4.44 Temperature histories of nitrogen-dried Coal M3 tested in different wire-mesh reactor sizes at their critical ambient temperatures

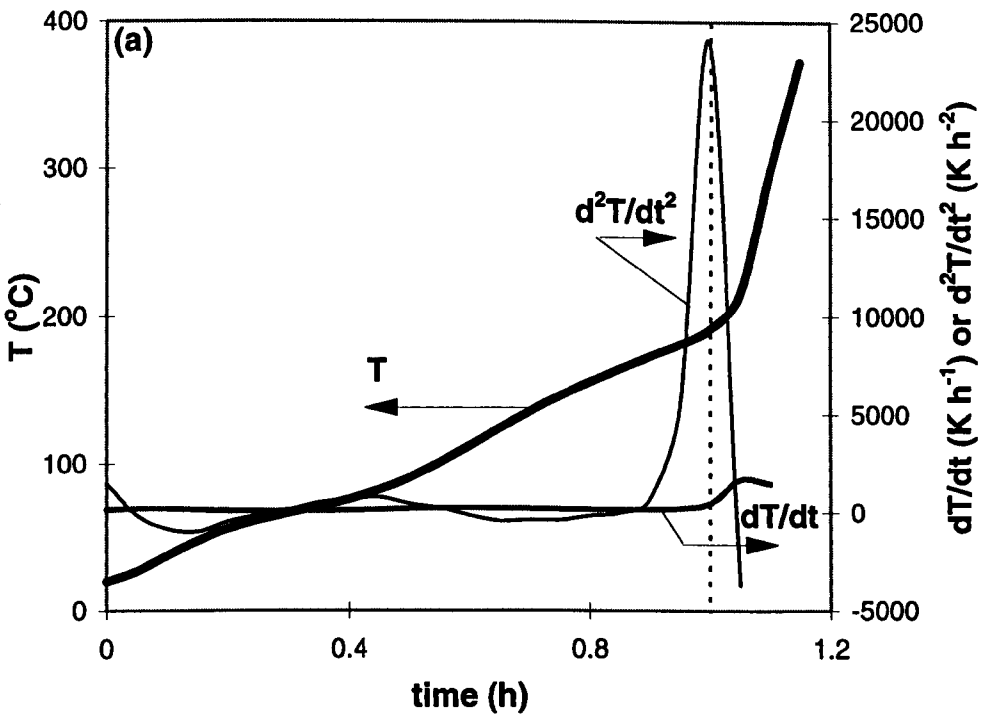

Figure 4.45 (Continued on the next page)

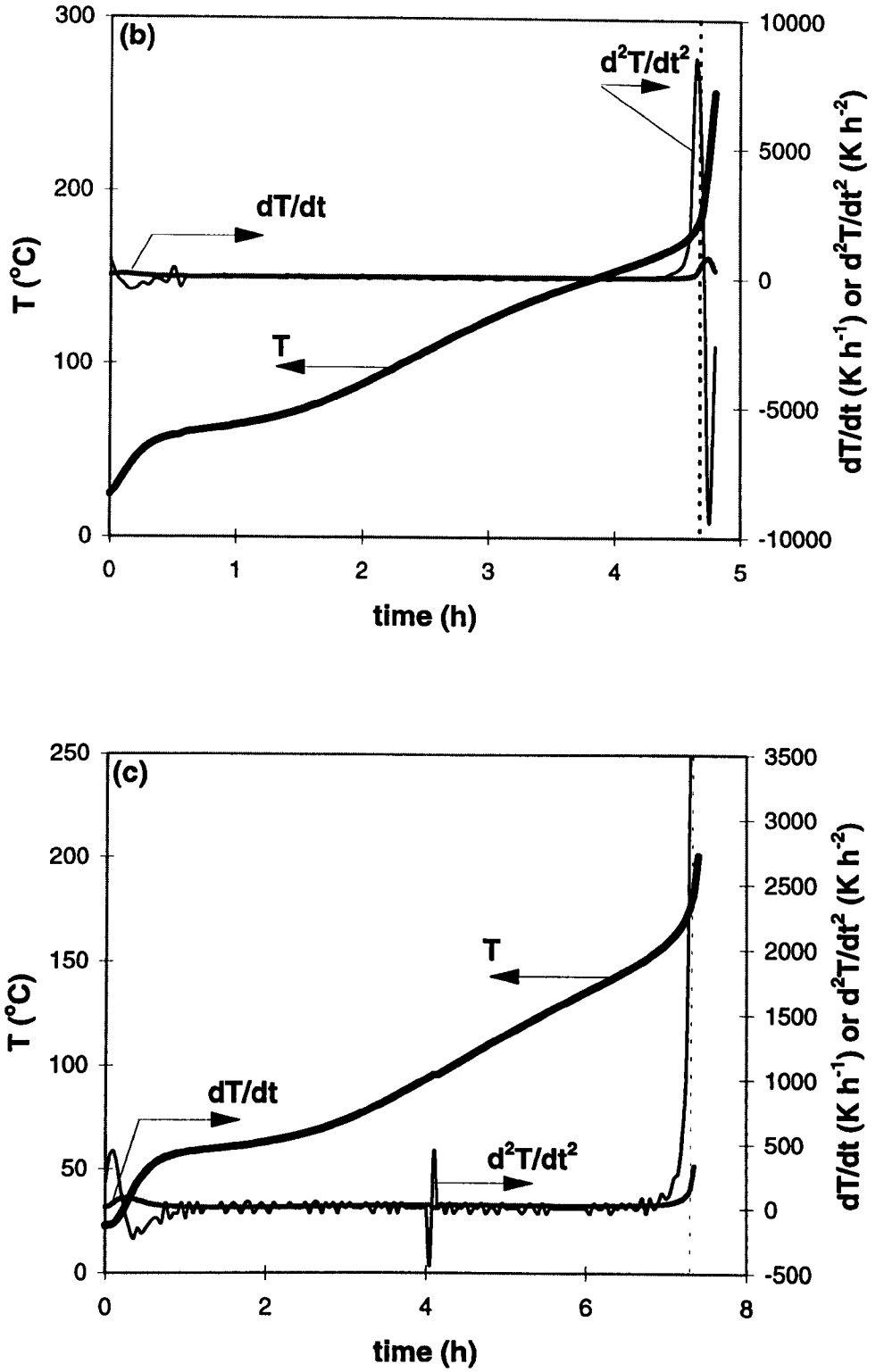

Figure 4.45 (Continued on the next page)

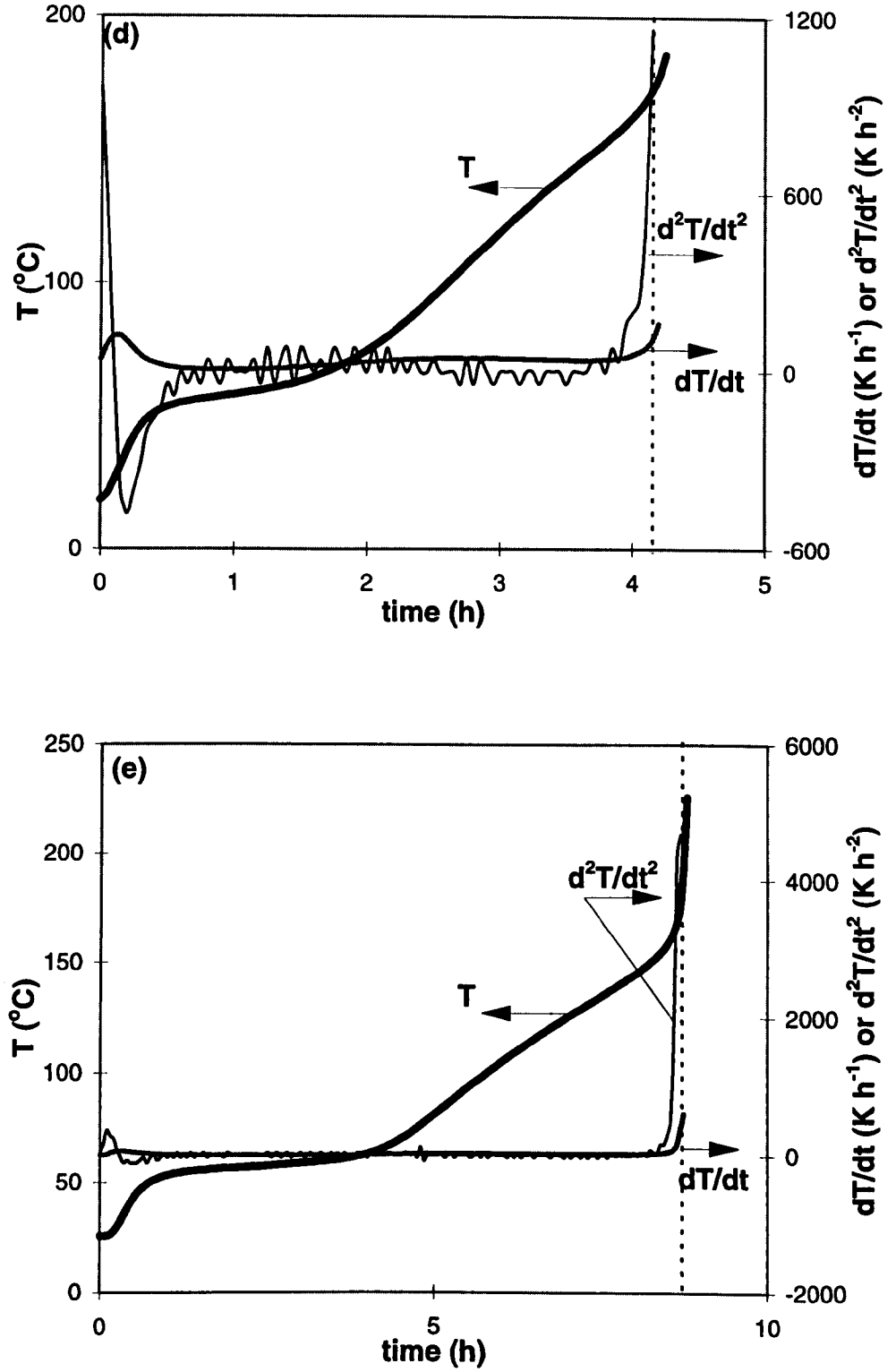

Figure 4.45 (Continued on the next page)

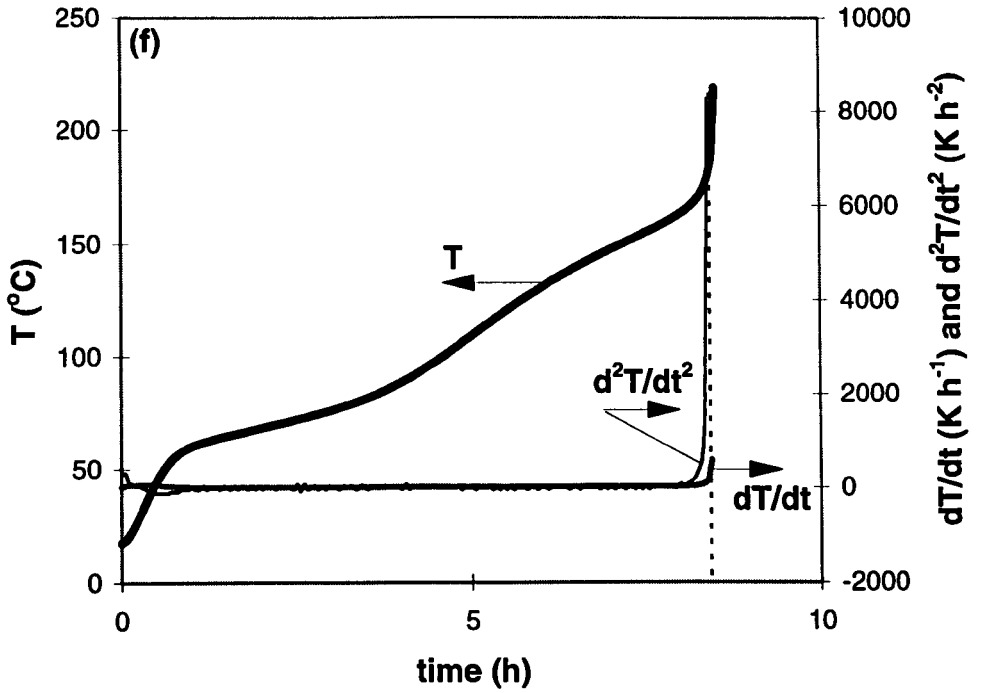

Figure 4.45 Determination of time-to-ignition for Coal M3 tested in a wire-mesh reactor (a) B-1 at 153 °C; (b) B-3 at 128 °C; (c) B-4 at 122 °C; (d) B-5 at 130 °C; (e) B-6 at 119 °C; and (f) B-7 at 120 °C

Table 4.6 Summary of time-to-ignition of Coal M3 tested in different wire-mesh reactor sizes at their critical ambient temperatures

Reactor I.D.	T_{crit} (°C)	Time-to-ignition (h)
B-1	153	1.01
B-2	138	2.67
B-3	128	4.71
B-4	122	7.37
B-5	130	4.17
B-6	119	8.63
B-7	120	8.36

4.3.6.3 The effect of packing density

Similar to the results obtained from the isothermal experiments, the time-to-ignition obtained from wire-mesh experiments also varied with the coal packing densities. Figure 4.46 plots the temperature histories of raw Coal M2 with four different packing densities, tested in a wire-mesh reactor (B-1). Each temperature history was plotted at their critical ambient temperatures. It is shown that the lower the packing density, the shorter the time-to-ignition. The time-to-ignition calculation for different coal packing densities was carried out using the second time derivatives of temperature. The plots for coal with various packing densities were presented in Figure 4.47, and the time-to-ignition obtained were summarised in Table 4.7. It is noted that a high coal packing density accelerates coal self-heating.

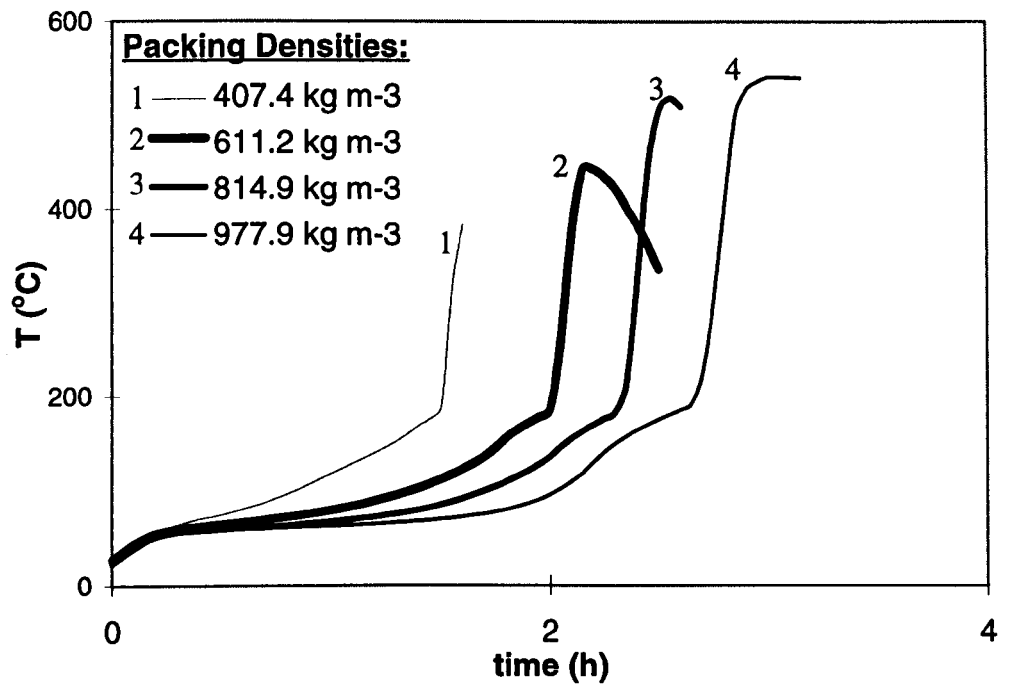

Figure 4.46 Temperature histories of raw Coal M2 in a wire-mesh reactor (B-1) with different packing densities at their critical ambient temperature

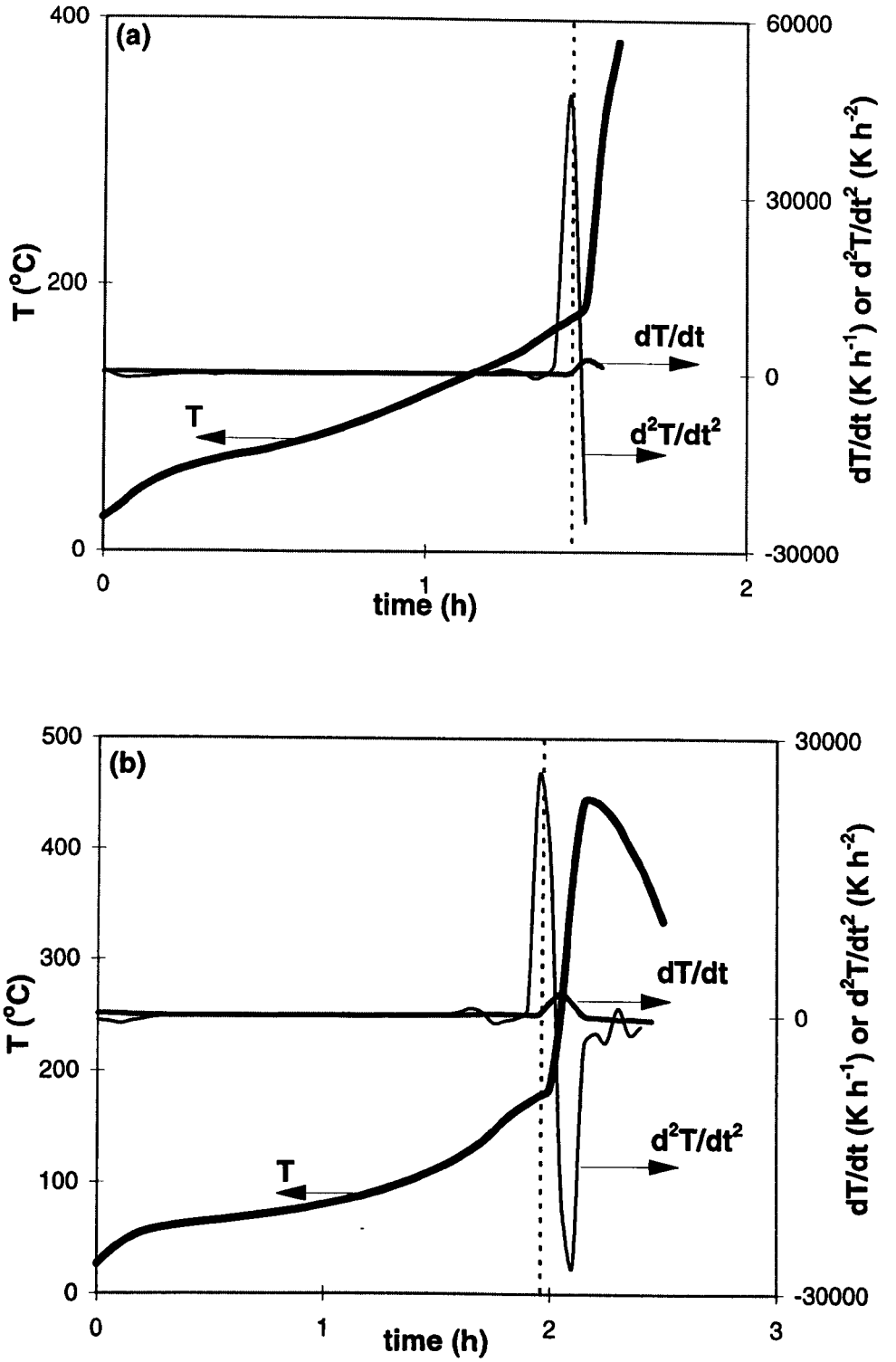

Figure 4.47 (Continued on the next page)

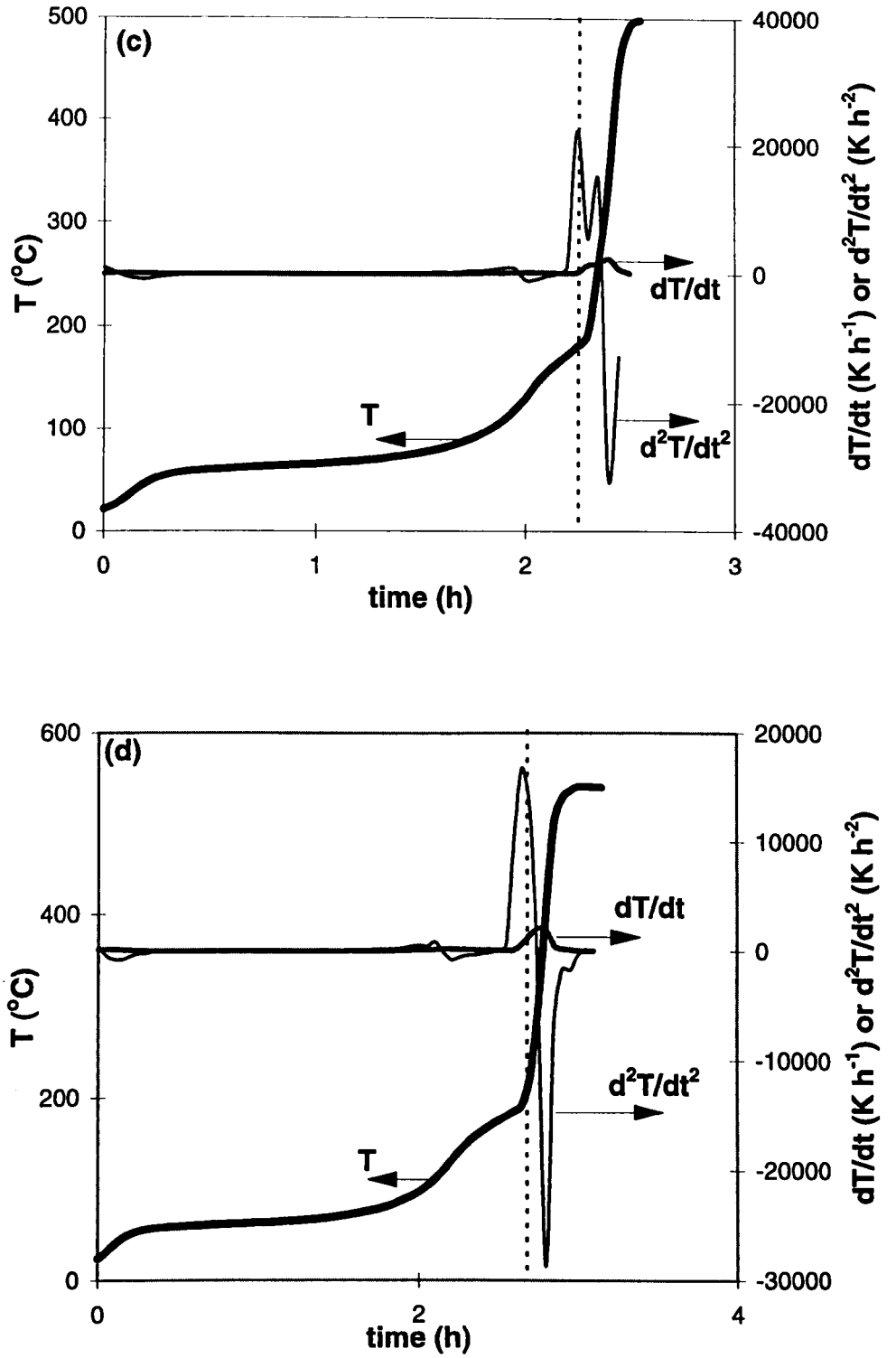

Figure 4.47 Determination of time-to-ignition for Coal M2 tested in a wire-mesh reactor (B-1) with coal packing densities of (a) 407.4 kg m^{-3} at 166 °C; (b) 611.2 kg m^{-3} at 158 °C ; (c) 814.9 kg m^{-3} at 154 °C; and (d) 977.9 kg m^{-3} at 150 °C

Table 4.7 Summary of the time-to-ignition of Coal M3 tested in wire-mesh reactor (B-1) in different packing densities at their respective ambient temperature.

Packing I.D.	T_{crit} (°C)	Time-to-ignition (h)
PW-1	166	1.37
PW-2	158	1.96
PW-3	154	2.26
PW-4	150	2.48

4.4 COMPARISON OF RESULTS OBTAINED FROM DIFFERENT TECHNIQUES

The three different laboratory techniques for spontaneous combustion study along with their experimental results have been described in the previous section of this thesis. It has been noted that there were similar trends in which the critical ambient temperature varied with the coal properties, ambient conditions, and the reactor sizes. However, a substantial variation in the critical ambient temperature, maximum temperature reached, time-to-ignition, and critical layer thickness predicted from different techniques were observed. This provides an opportunity to relate the experimental results with the experimental conditions used in the different techniques. Comparison of several parameters observed from different techniques is presented in Table 4.8.

Table 4.8 Comparison of several parameters observed from different techniques

Experimental Technique	Reactor I.D.	m (g)	A_s (cm^2/g)	T_{crit} (°C)	T_{max} (°C)	t_i (h)
Isothermal (fresh coal)	R-1	1000.0	0.99	77.5 ± 7.5	500.0	144.0
	R-2	350.0	1.36	82.5 ± 2.5	300.0	72.3
	R-3	140.0	2.02	97.5 ± 2.5	300.0	25.5
	R-4	31.5	3.94	127.5 ± 2.5	300.0	7.4
Adiabatic (N_2-dried coal)	A-1	450.0		95.0 ± 5.0	-	24.8
	A-2	100.0		95.0 ± 5.0	650.0	51.1
Wire-Mesh (N_2-dried coal)	B-1	5.0	6.86	152.5 ± 0.5	500.0	1.4
	B-2	17.5	4.29	137.5 ± 0.5	400.0	2.7
	B-3	60.0	2.86	127.5 ± 0.5	350.0	4.7
	B-4	115.0	2.29	121.5 ± 0.5	300.0	7.4
	B-5	115.0	3.08	129.5 ± 0.5	250.0	4.2
	B-6	115.0	2.38	118.5 ± 0.5	300.0	8.6
	B-7	115.0	2.41	119.5 ± 0.5	300.0	8.4

Note m : mass of coal

A_s : reactor specific external surface area

T_{crit} : critical ambient temperature

T_{max} : maximum temperature can be reached

t_i : time-to-ignition

The summary of the isothermal results was obtained from the experiments using fresh coal, while for the other techniques, they were obtained from nitrogen-dried coal. In the isothermal and adiabatic reactor techniques, the use of fresh coal extended the times required for the coal temperature to reach ambient temperature (t_{N2}) at least twice longer, compared with those of nitrogen-dried coal. It has been attempted to use the fresh coal for the adiabatic experiments (Reactor A-2).

However, it was found that the times required for the coal temperature to reach ambient temperature was too long (1~3 weeks depending on the coal mass involved in the process). Therefore the nitrogen-dried sample was then used for this technique. In the wire-mesh reactor experiments, the nitrogen-dried coal sample was used to eliminate the effect of coal moisture content. The differences in the sample types (fresh or nitrogen-dried sample) and particle size range used in each technique must be noted, since it could cause some deviations in the results obtained.

4.4.1 Critical Ambient Temperature

It is shown in Table 4.8 that the critical ambient temperatures obtained from different techniques differed significantly. The critical ambient temperatures of both isothermal and wire-mesh reactors varied with the coal mass and reactor specific external surface area of the reactors, while those of adiabatic reactors did not. As stated previously, spontaneous combustion depends on two competing processes: the rate of heat generation due to oxidation reaction, and the rate of heat loss to the surroundings. If available oxygen is not a limiting factor, then, the rate of heat generation per unit mass of coal is independent from the reactor size or shape, while the rate of heat loss to the surroundings is strongly dependent on the external surface area. In the adiabatic reactor, the heat loss through the external surface area of the reactor was negligible. Therefore, the critical ambient temperature of the adiabatic reactor (95 ± 5 °C) did not change significantly with reactor sizes. On the other hand, in the isothermal and wire-mesh reactors, the heat generated from the oxidation reaction can be dissipated to the ambient through the external surface area of the reactors. Therefore, the critical ambient temperature of the coal samples changed according to the reactor size, or more precisely, with specific external surface area of the reactor.

Since heat in the isothermal and wire-mesh reactors were easier to dissipate than in the adiabatic reactors, the critical ambient temperatures of the samples in the isothermal and wire-mesh reactors were higher than those in the adiabatic reactors.

The negligible heat loss in the adiabatic reactor caused a sharp temperature increase of coal sample due to the oxidation reaction to a relatively high temperature (~ 650°C for most adiabatic experiments).

It is also observed that the critical ambient temperatures of the coal samples tested in the wire-mesh reactors were higher than those in isothermal reactors. This is because the nature of wire-mesh reactor surface allowed the heat dissipated to the ambient easily. In addition, the forced convection provided by the oven in the wire-mesh experiments, made the heat dissipation even quicker. These two factors significantly slower the oxidation reaction rate of the coal in the wire-mesh reactor, and thus increased the coal critical ambient temperature.

4.4.2 Time-To-Ignition

The time-to-ignition of the coal tested in different techniques was defined as the time required for the coal to experience thermal runaway, and was determined when the temperature acceleration (d^2T/dt^2) reached maxima. It is observed during the experiments that the time-to-ignition varied with ambient conditions, coal particle size, coal drying method, coal packing density, and reactor size. In general, it is observed that, regardless the experimental techniques used, the higher the ambient temperature, the shorter the time-to-ignition. Air flow rate was also found to affect the time-to-ignition. The higher the air flow rate, the shorter the time to ignition. This indicates that the heat dissipated to the surroundings by air was small compared to the heat of oxidation reaction. Therefore, a high air flow rate provided a larger amount of oxygen for the oxidation reaction, and thus accelerating the coal self-heating.

Furthermore, it is also observed that the larger the particle size, the shorter the time-to-ignition. This is because the larger the particle size, the higher the critical ambient temperature for thermal runaway to occur, and thus the shorter the time-to-ignition.

Low coal moisture content and packing density were also found to accelerate the thermal runaway.

Regardless the experimental technique used, it is found that the time-to-ignition varied with reactor sizes. For the coal tested in the isothermal and wire-mesh reactors, it is observed that the larger the reactor size, or more precisely the smaller the reactor specific external surface area, the longer the time-to-ignition. This is due to the lower critical ambient temperature required for the thermal runaway to occur in the larger reactor, which decelerated the oxidation reaction, and thus the self-heating process. In the adiabatic tests, however, it is observed that the larger the reactor size, the shorter the time-to-ignition. As stated previously, the heat loss in the adiabatic reactor was negligible. Therefore, providing there was sufficient amount of oxygen for the oxidation reaction, a large amount of coal presented in reactor A-1, generated more heat of oxidation reaction.

To summarise, in a system in which there is sufficient oxygen for the oxidation reaction, the higher the ambient temperature, the shorter the time-to-ignition.

4.4.3 The Effect of Reactor Size

The effects of reactor size and reactor specific external surface area on the critical ambient temperature were examined in isothermal, adiabatic and wire-mesh reactor techniques. The experimental results from these techniques indicate that unless the adiabatic condition is fulfilled, the spontaneous combustion behaviour of a given coal depends on the external heat transfer environment. The larger the reactor specific external surface area, the higher the rate of heat loss to the surroundings, and thus the propensity of the coal spontaneous combustion is reduced. For both isothermal and wire-mesh reactors, the critical ambient temperature increased linearly with specific external surface area as shown in Figures 4.9 and 4.34, respectively. This indicates the important role of external heat transfer area in spontaneous combustion process.

Furthermore, it is also observed that within a similar reactor specific external surface area, the critical temperatures of coal in the wire-mesh reactors were higher than those of in the isothermal reactors. This could be due to the nature of the wire-mesh experiments which allowed the heat to dissipate to the ambient easily.

4.4.4 The Effect of Packing Density

Experiments using isothermal and wire-mesh reactors were carried out to examine the effect of packing density on the critical ambient temperature of raw Coal M2. The packing density was varied by changing the amount of coal packed in the same reactor volume. Three different levels of packing densities, i.e. 298.42, 447.62, and 557.04 kg m^{-3} were used in the isothermal experiments, and four levels, i.e. 407.44, 611.16, 814.87, and 977.85 kg m^{-3} were used in the wire-mesh experiments. In general, it is observed that the higher the packing density, the lower the critical temperature.

Furthermore, it is also noticed that the effect of packing density on the coal critical ambient temperature tested in the wire-mesh reactor was more prominent than that in the isothermal reactor. The nature of the experimental techniques may hold the responsibilities. In the isothermal reactor, the heat was dissipated to the ambient through the reactor surface mainly due to temperature difference between the surface and the ambient. The heat was also carried away from the system by the air which was flowed from the bottom of the reactor. Since the air flow rate was reasonably small, the heat dissipated by the air was not a dominant factor. In the wire mesh reactor, however, the forced convection provided by the oven, significantly helped dissipating the heat from the system. Consequently, the variation of packing density in the wire-mesh tests significantly affected the heat loss, and thus the coal critical ambient temperature.

The reactivities of coal samples tested in isothermal and wire-mesh reactors with various packing density showed a general trend that the higher the packing density,

the higher the reactivity, which corresponded to the critical ambient temperatures observed.

4.4.5 Low-Temperature Oxidation Kinetics Estimated from Different Experimental Techniques

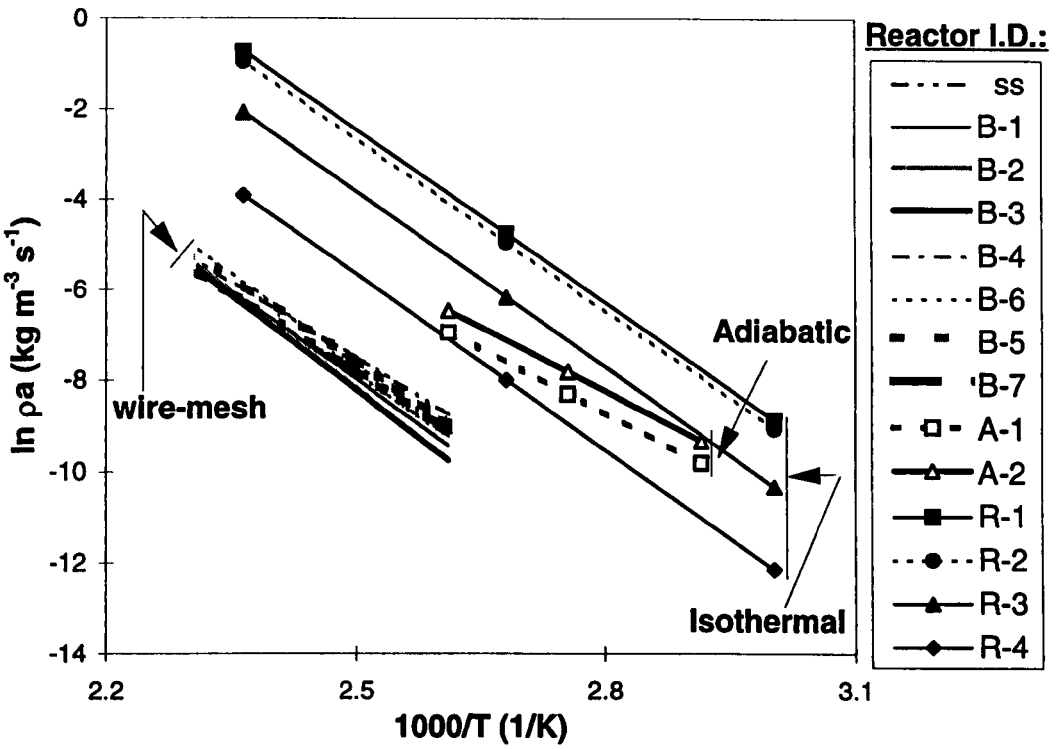

Figure 4.48 The reactivity of coal oxidation in air estimated from isothermal reactor in various reactor sizes (R-1:○, R-2:●, R-3: ▲, and R-4:◆), adiabatic reactor (A-1:□, A-2:■), and wire-mesh reactors in various sizes (B-1 to B-7)

The low-temperature oxidation kinetics of Coal M for each technique were estimated using an energy balance approach. For the isothermal and adiabatic techniques, the oxidation kinetic constants were estimated using an energy balance when the coal temperature equals to the oven temperature, according to Equation (3-2), while for the wire-mesh reactor, they were estimated using both steady-state and unsteady-state energy balance, as discussed previously in Chapter 3. Assuming

that the reaction order equals to one, the kinetic constants were then used to calculate the apparent reaction rate (ρ_a) of Coal M. The apparent reactivities predicted from three techniques in various reactor sizes were then plotted against the reciprocal temperature in Figure 4.48. As shown in Table 4.8, the sample used in the isothermal reactors was a fresh coal, while for the adiabatic and wire-mesh techniques, it was a nitrogen-dried coal. Furthermore, the particle size range used for the isothermal and wire mesh reactors experiments was 0.25 - 1.00 mm, while for the adiabatic reactor, it was 1.00 - 2.36 mm. These differences certainly cause deviation in the coal reactivities predicted from different techniques.

As shown in Figure 4.48, the coal reactivities estimated from the isothermal and adiabatic reactor lie in a reasonably continuous band. Small differences observed were due to the different in sample type (as discussed above) and temperature ranges used in the experiments. It was observed during the experiments that the rate of temperature increase in the adiabatic reactor, when the sample temperature equals to oven temperature, was much slower than those in the isothermal and wire-mesh reactor. This significantly contributed to the lower values of E and A observed in the adiabatic reactor. Furthermore, the extent of reaction also affected the A values obtained, as has also been discussed in the previous section of this thesis. In general, it is observed that a higher E value determined from different techniques corresponded to a higher A values which resulted in a similar reactivity of the coal.

The reactivities predicted from the wire-mesh reactors both steady-state and unsteady-state methods lie within a reasonable range and were lower than those predicted from the isothermal and adiabatic reactors. As summarised by Chen (1996), the value of the pre-exponential factor (A) varied with temperature and extent of reaction. It was observed during the experiments that the coal critical ambient temperature tested in the wire mesh reactor was higher than that tested in either isothermal or adiabatic reactors. Furthermore, in the wire-mesh reactor tests, the coal was oxidised in air from the beginning of the experiment, while in the isothermal and adiabatic reactors, the coal was started to be oxidised once the coal temperature equals to the oven temperature. The pre-oxidation before the thermal

runaway occurred could have caused a loss of the reactivity for coal tested in the wire-mesh reactors.

4.4.6 Critical Layer Thickness Predicted from Different Experimental Techniques

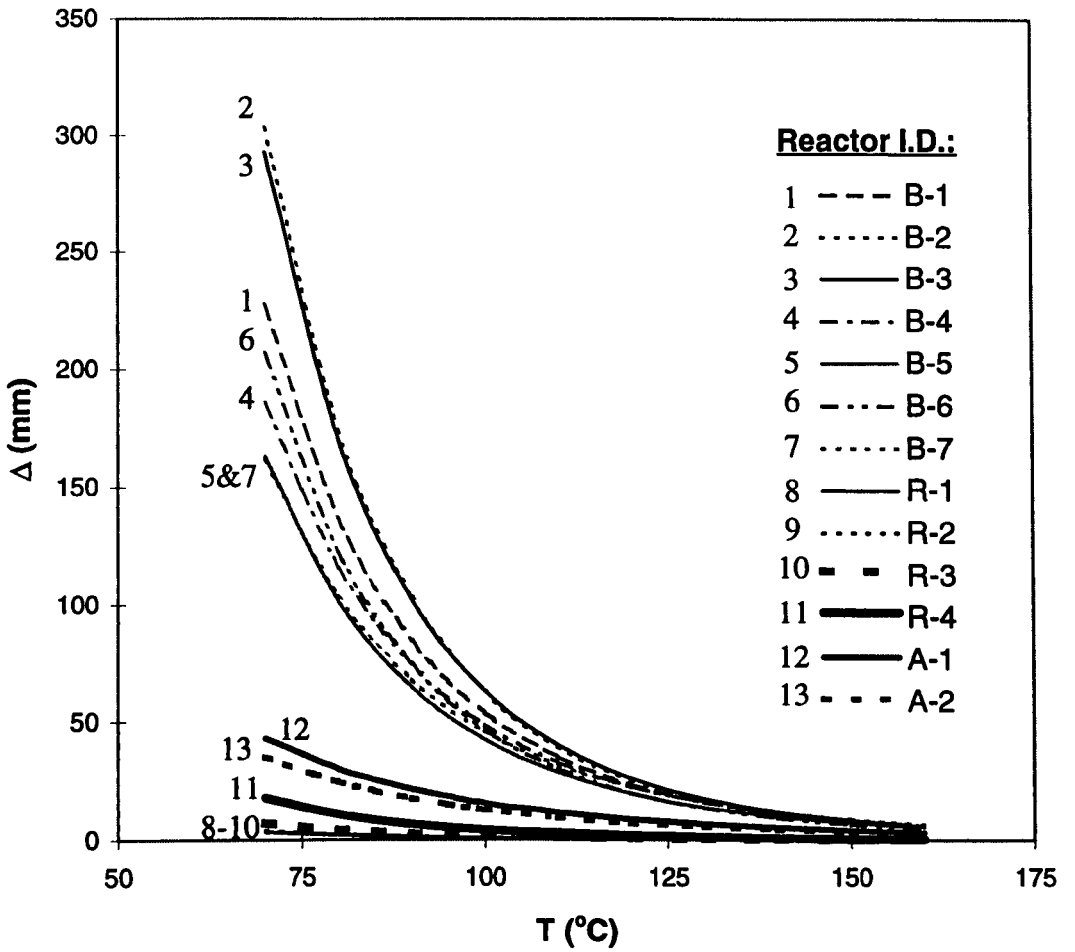

Figure 4.49 A comparison of critical thicknesses of coal deposits (slabs) capable of spontaneous combustion estimated using different experimental techniques and reactor sizes

The kinetic constants, A and E, predicted from different techniques were also used to calculate the critical thickness of a slab, which has been chosen as a basis for comparison. The comparison of critical thicknesses of coal deposits (slabs) capable

of spontaneous combustion estimated using different techniques is presented in Figure 4.49. It is shown that for all techniques used, the critical thickness of the coal deposit decreases with increasing ambient temperature. The critical thicknesses predicted from the isothermal and adiabatic reactors with different reactor sizes compare reasonably well, while those from the wire-mesh reactors are significantly higher particularly at low temperatures, which corresponded to the coal reactivities estimated from different techniques. The maximum variance in the critical thickness predicted from the three different techniques decreases with temperature, and was about 98% at 70 °C and 2% at 170 °C.

4.5 SUMMARY

The experimental results prove that, for a given coal, conditions under which the heat generated in the system can be dissipated to the surrounding easily favours a low risk of spontaneous combustion, while poor heat transfer conditions induce the spontaneous combustion. This study highlights that the coal self-heating behaviour is dependent not only on the coal properties and ambient conditions, but also on the system conditions involved in the experimental techniques used. Precaution must be taken when comparing the results obtained from different techniques so that misleading information can be avoided.

Chapter 5

INHIBITION AND PROMOTION AGENTS OF SPONTANEOUS COMBUSTION OF COAL

5.1 INTRODUCTION

There have been a number of studies carried out to determine the best method of preventing the spontaneous combustion of coal (Chamberlain (1974); Evseev (1985); Smith et al. (1988)). Compaction of coal piles and inerting the atmosphere have been applied (Smith et al. (1988)). Additives, such as carbamide, diammonium phosphate, gel solution from water glass (Evseev (1985)), aqueous solutions of inorganic salts, and salt-clay mixtures have also been examined as potential inhibition agents of spontaneous combustion (Chamberlain (1974)). Smith, et al. (1988) evaluated the effectiveness of ten additives to suppress the self-heating process and revealed that sodium nitrate, sodium chloride, and calcium carbonate inhibited the spontaneous combustion, whereas sodium formate and sodium phosphate stimulated the self-heating process.

The current work is also aimed to examine the effect of inherent inorganic matter and different additives on spontaneous combustion. An isothermal reactor (R-4) was employed to determine the critical ambient temperature, above which a spontaneous ignition (thermal runaway) occurs. The critical ambient temperatures were then used to compare the tendency of various coal samples toward spontaneous combustion. An increase in the critical ambient temperature due to the use of an additive can indicate the effectiveness of the additive to suppress or promote the self-heating

potential of the coal. The effect of the additive bulk loading on the critical ambient temperature was investigated for typical promotion and inhibition additives. The low-temperature oxidation kinetics of these coal samples were also estimated from the temperature measurements, using the same procedure as discussed in Chapter 3.

5.2 THE EFFECT OF INHERENT INORGANIC MATTER

Table 5.1 Summary of critical ambient temperatures, heat of oxidation reaction, and apparent kinetic constants estimated for raw, water-washed, and acid-washed Coal M2

Sample	T_{crit} (°C)	Q (MJ kg^{-1})	E (kJ $mole^{-1}$)	A (kg m^{-3} Pa^{-1} s^{-1})
raw coal	142.5 ± 2.5	22.90	144.5	9.84×10^{10}
water-washed coal	145.0 ± 2.5	23.70	239.7	1.55×10^{22}
acid-washed coal	147.5 ± 2.5	24.20	164.4	2.43×10^{13}

The presence of inorganic matter in coal may catalyse the oxidation reaction of coal. Therefore, removing the inorganic matter may reduce the reactivity of coal. Water-washing removes part of the inherent inorganic matter (ie. water-soluble inorganic matter) in the coal, which are not associated with the organic structure of the coal (Ye (1994)). Acid-washing could remove most of the inorganic matter present in the coal, such as Na^+, K^+, Ca^{2+}, Fe^{2+}, and Fe^{3+}, which may catalyse the spontaneous combustion (Durie (1991)). Therefore, the influence of inherent inorganic matter on the spontaneous combustion can be eliminated by treating the raw coal with an acid. Table 5.1 shows that the critical ambient temperatures of the water-washed sample (145.0 ± 2.5 °C) and the acid-washed sample (147.5 ± 2.5 °C) are higher than that of

the raw coal (142.5 ± 2.5 °C). The increase in critical ambient temperature indicates that removing the inherent inorganic matter from coal helps reduce its self-heating potential.

5.3 BULK LOADING OF ADDITIVES

5.3.1 The Effect of Additives

Table 5.2 Summary of critical ambient temperatures, heat of oxidation reaction, and apparent kinetic constants estimated for various promotion agents-added acid-washed Coal M2 samples

Sample	T_{crit} (°C)	Q (MJ kg^{-1})	E (kJ $mole^{-1}$)	A (kg m^{-3} Pa^{-1} s^{-1})
FeS_2 + coal	110.0 ± 2.5	18.80	79.6	4.91×10^3
KAc + coal	125.0 ± 2.5	21.80	111.9	3.53×10^7
NaAc + coal	137.5 ± 2.5	22.20	109.5	1.79×10^7
$CaCO_3$ + coal	137.5 ± 2.5	21.20	189.6	1.83×10^{17}

Table 5.2 shows that among the eleven additives used, FeS_2, KAc, NaAc, and $CaCO_3$ promote the spontaneous combustion of Coal M2 as their critical ambient temperatures are considerately lower than that of the acid-washed coal. As shown in Table 5.3, NH_4Cl and $NaNO_3$ are effectively neutral, they do not alter the critical ambient temperature of the acid-washed coal. However, $CaCl_2$ and $Mg(Ac)_2$ increase the critical ambient temperature for spontaneous combustion by 5 °C to 155 °C, and Montan powder, KCl, and NaCl push the critical ambient temperature to 157.5 °C, indicating that these additives inhibit the spontaneous combustion. For

additives which show the same critical ambient temperatures of the samples, such as Montan powder, KCl, and NaCl, or $CaCl_2$ and $Mg(Ac)_2$, their abilities to suppress the spontaneous combustion are compared based on the rates of temperature rise at their critical ambient temperatures, as shown in Figure 5.1 and 5.2. In Figure 5.1, it is shown that the development of self-heating of the $CaCl_2$-added coal sample is slower than that of $Mg(Ac)_2$-added-coal, suggesting that $CaCl_2$ could be a slightly better inhibition agent than $Mg(Ac)_2$. On the other hand, the temperature rise of the KCl-added-coal sample is slower than those of Montan Powder and NaCl-added-coal samples, as shown in Figure 5.2. Thus, KCl could be considered to be the best inhibition agent among all additives studied.

Table 5.3 Summary of critical ambient temperatures, heat of oxidation reaction, and apparent kinetic constants estimated for various inhibition agents- added acid-washed Coal M2 samples

Sample	T_{crit} (°C)	Q (MJ kg^{-1})	E (kJ $mole^{-1}$)	A (kg m^{-3} Pa^{-1} s^{-1})
NH_4Cl + coal	147.5 ± 2.5	22.60	160.2	4.21×10^{12}
$NaNO_3$ + coal	147.5 ± 2.5	22.30	203.5	1.42×10^{18}
$CaCl_2$ + coal	152.5 ± 2.5	20.30	145.6	6.53×10^{10}
$Mg(Ac)_2$ + coal	152.5 ± 2.5	22.60	103.2	5.07×10^{5}
Montan powder + coal	157.5 ± 2.5	20.40	102.9	3.52×10^{5}
KCl + coal	157.5 ± 2.5	21.50	109.1	2.00×10^{6}
NaCl + coal	157.5 ± 2.5	15.70	219.5	7.35×10^{19}

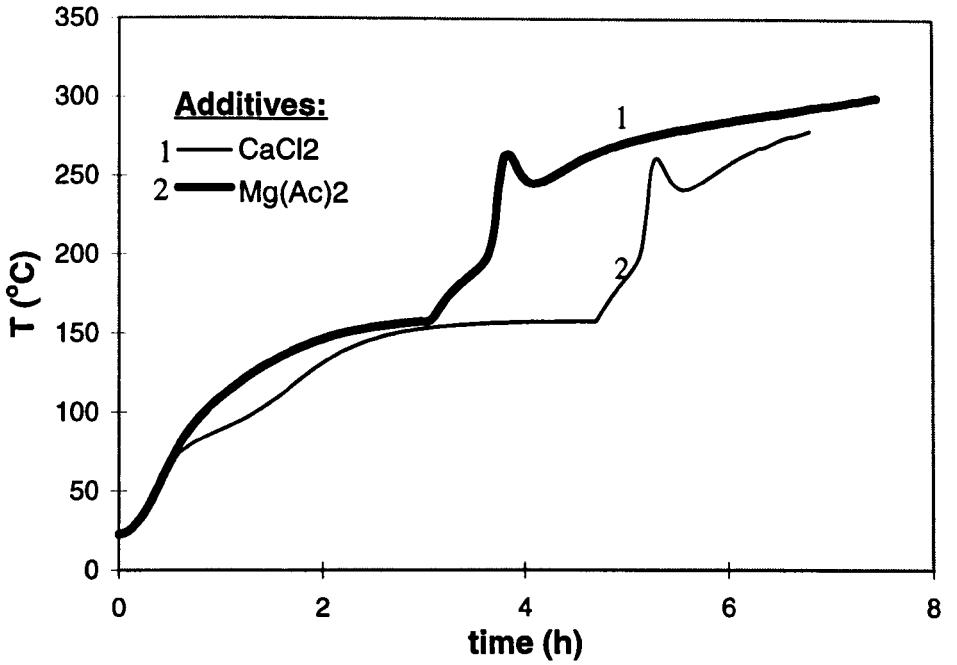

Figure 5.1 Temperature histories of coal samples with the presence of the additives with the same critical temperature of 152.5 ± 2.5 °C

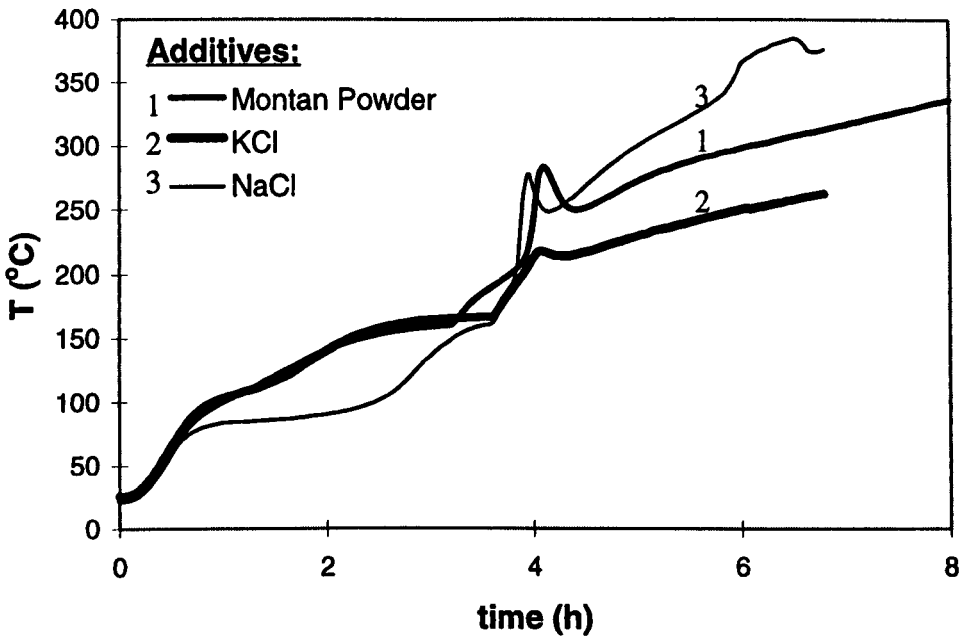

Figure 5.2 Temperature histories of coal samples with the presence of the additives with the same critical temperature of 157.5 ± 2.5 °C

It has been acknowledged (Banerjee (1985)) that FeS_2 in coal catalyses the oxidation reaction. In addition, in a moist air, FeS_2 itself also experiences an exothermic oxidation reaction which helps accelerate the coal self-heating (Banerjee (1985); Durie (1991)). Sodium and potassium also catalyse the spontaneous combustion especially when they are in organic salts (Banerjee (1985); Durie (1991)). These theories are clearly supported by the results for FeS_2, KAc, and NaAc obtained in the present study.

The addition of $CaCO_3$ to the acid-washed coal decreases the critical ambient temperature of the acid-washed coal by 10 °C to 137.5 °C, which could be due to the catalytic effect of the calcium on the spontaneous combustion. $NaNO_3$ does not show any effect on the critical ambient temperature, suggesting that sodium in an inorganic salt would have little catalytic effect compared with its organic salts (eg. NaAc). However, these results do not agree with the previous findings (Smith et al. (1988)) that $NaNO_3$ and $CaCO_3$ inhibited spontaneous combustion. Similar to $NaNO_3$, NH_4Cl also does not significantly affect the spontaneous combustion behaviour of the coal. This may be due to the liberation of the ammonia as a result of NH_4Cl decomposition at 100 °C (Smith et al. (1988)), which would eliminate any catalytic activity that NH_4^+ may have. Furthermore, ammonia vapour could have also hindered oxygen diffusion in the coal structure.

$CaCl_2$ and Montan powder ($CaCl_2$ + 3% SDS) are found to inhibit spontaneous combustion. Previous investigators (Smith et al. (1988)) showed, using a thermogram, that some endothermic reactions occurred between $CaCl_2$ and pyritic compounds in coal at 100 - 150 °C. The sulphur content in the Morwell coal is 0.26 %(db) (Durie (1991)). If this sulphur reacts with $CaCl_2$ to form $CaSO_4$, then the catalytic effect of FeS_2 could be lost. As a result, the critical ambient temperature for initiating the spontaneous combustion increases. In addition, physical changes due to the application of additives could also affect the spontaneous combustion (Smith et al. (1988)), particularly when the additives do not have any catalytic effect on the oxidation reaction. These physical changes include blockage of pore structure of coal, loss of active sites, and additional resistance for oxygen diffusion.

Similar arguments may also be used to explain the inhibitive effect of KCl and NaCl on spontaneous combustion of Morwell coal. In general, alkali and alkali earth metals in organic salts tend to promote the spontaneous combustion while inorganic salts would inhibit spontaneous combustion. However, $Mg(Ac)_2$ seems to be an exception, which inhibits the spontaneous combustion. It has been suggested in the literature that Mg can enhance or catalyse oxidation of carbon (Jackson (1987)), probably at high temperatures. However, one could speculate that Mg^{2+} may have no catalytic effect or be a negative catalyst for low-temperature (< 200°C) oxidation reaction of coal.

It has also been suggested (Smith et al. (1988)) that the ionic radii of anions and cations (Waddington (1959)) of the additives may also be a factor determining the ability of an additive to penetrate into the coal structure. Figures 5.3 and 5.4 present the critical ambient temperatures against the radii of anions and cations, respectively. It is clear that this hypothesis is not evident in the present study, as there are apparently no correlations between critical ambient temperature and radii of anions or cations.

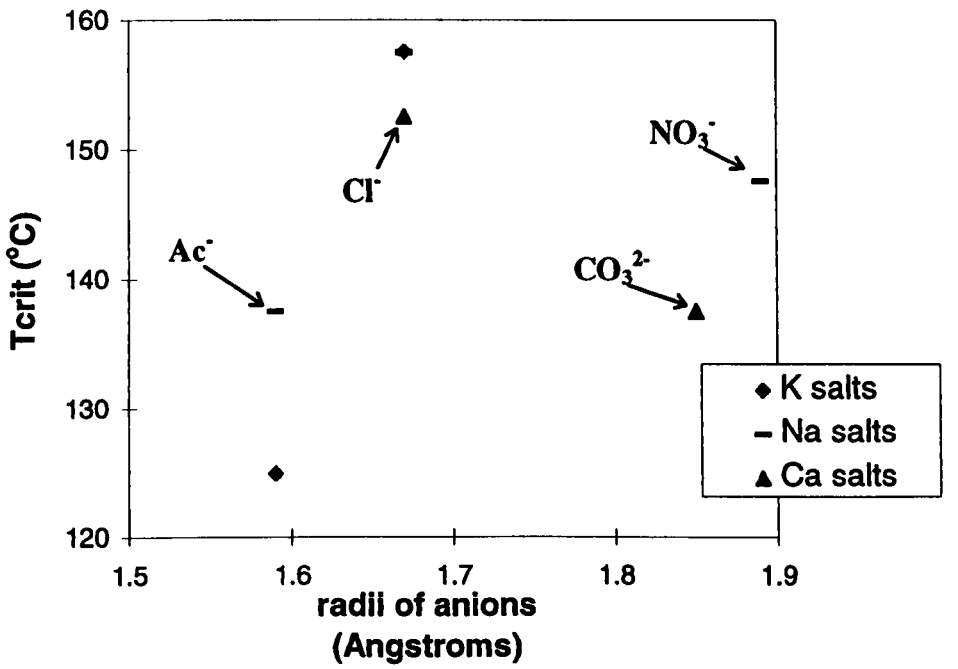

Figure 5.3 Critical ambient temperature versus radii of anions in several additives

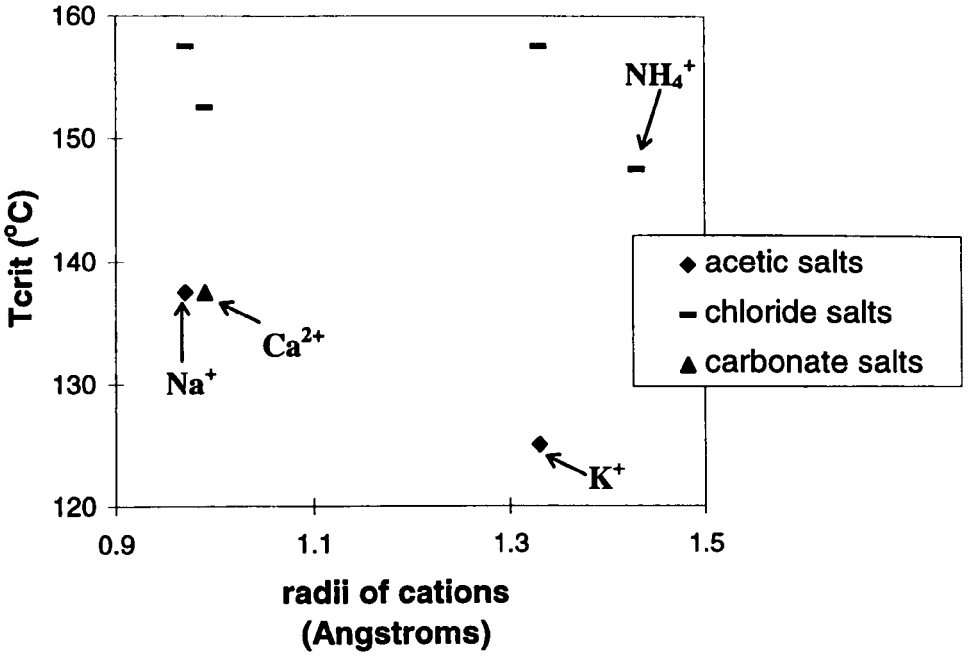

Figure 5.4 Critical ambient temperature versus radii of cations in several additives

5.3.2 The Effect of Additive Loading

In order to investigate the effect of additive loading on promotion and inhibition of spontaneous combustion, samples with 1, 5, and 10 %wt. of NaAc and KCl were prepared and tested. Table 5.4 presents the critical ambient temperatures of these samples. In general, the critical ambient temperature decreases with increasing NaAc loading but increases with KCl loading, indicating that promotion and inhibition effects of these additives on spontaneous combustion depend on their loading levels. Although 1% and 5% NaAc loadings in the samples offered a similar critical ambient temperature, within the accuracy (± 2.5 °C) of the experiments, a closer examination of the temperature profiles during the self-heating revealed that for 5% NaAc loading a higher rate of temperature rise was experienced. Similarly, in the presence of 1% KCl the sample showed the same critical ambient temperature as the acid-washed coal but its rate of temperature rise was lower than that of the acid-washed coal due to the inhibition effect of KCl. The temperature histories of 1,

5, and 10% of NaAc and KCl-added-coal are shown in Figures 5.5 to 5.10, respectively.

Table 5.4 Summary of the critical ambient temperatures and kinetic constants estimated for samples with various additive loadings

Sample	Tcrit (°C)	Q (MJ kg^{-1})	E (kJ mol^{-1})	A (kg m^{-3} Pa^{-1} s^{-1})
Acid-washed coal	137.5 ± 2.5	24.20	103.6	1.62×10^{6}
1% NaAc-added-coal	132.5 ± 2.5	23.11	180.1	8.92×10^{15}
5% NaAc-added-coal	132.5 ± 2.5	22.20	208.0	4.34×10^{19}
10% NaAc-added-coal	122.5 ± 2.5	21.01	256.5	5.78×10^{26}
1% KCl-added-coal	137.5 ± 2.5	22.40	164.0	9.03×10^{13}
5% KCl-added-coal	142.5 ± 2.5	21.50	179.5	5.64×10^{15}
10% KCl-added-coal	147.5 ± 2.5	20.40	179.1	2.45×10^{15}

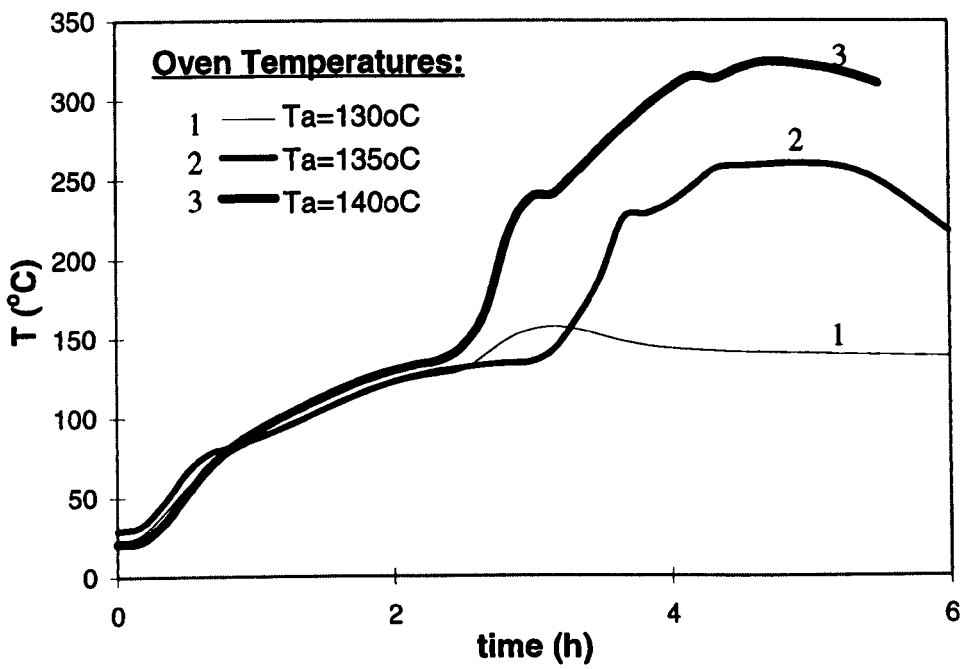

Figure 5.5 Temperature histories of 1% NaAc-added-Coal M3 in an isothermal reactor (R-4) at several oven temperatures

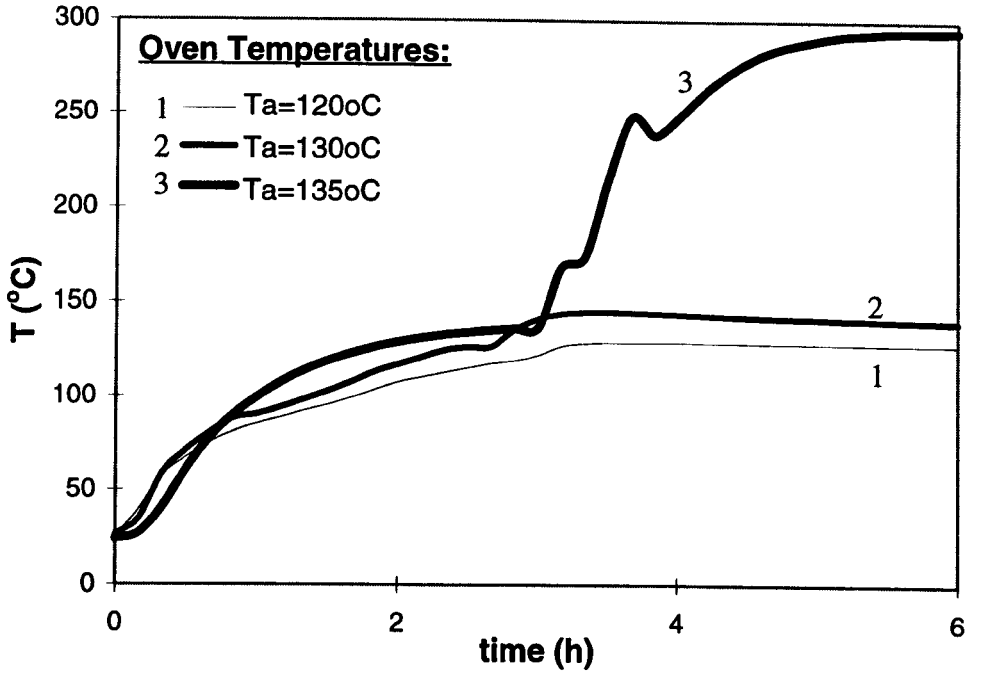

Figure 5.6 Temperature histories of 5% NaAc-added-Coal M3 in an isothermal reactor (R-4) at several oven temperatures

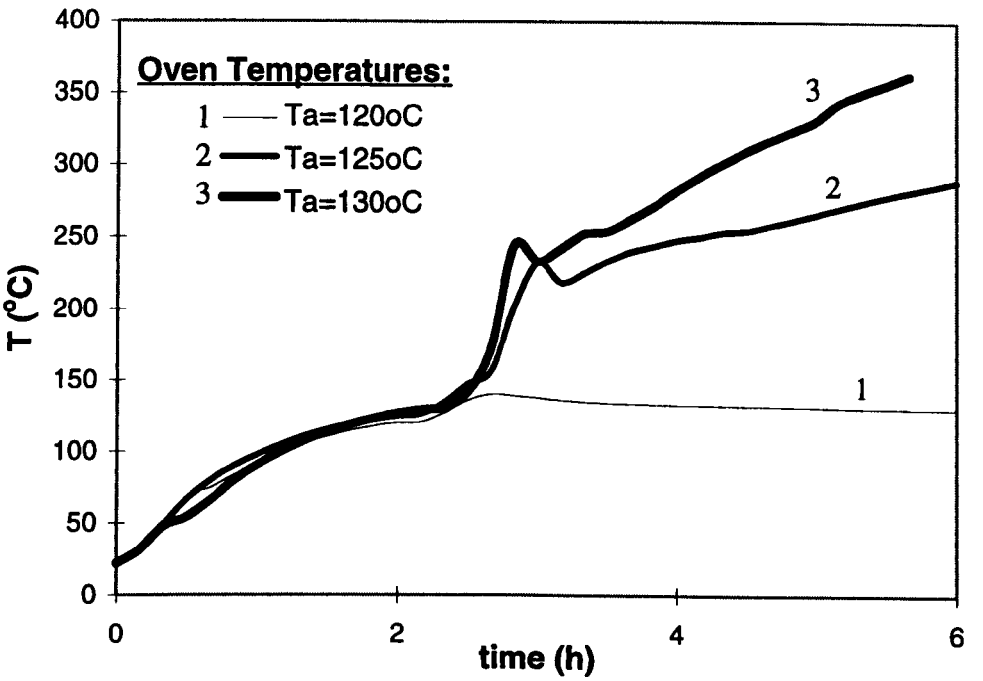

Figure 5.7 Temperature histories of 10% NaAc-added-Coal M3 in an isothermal reactor (R-4) at several oven temperatures

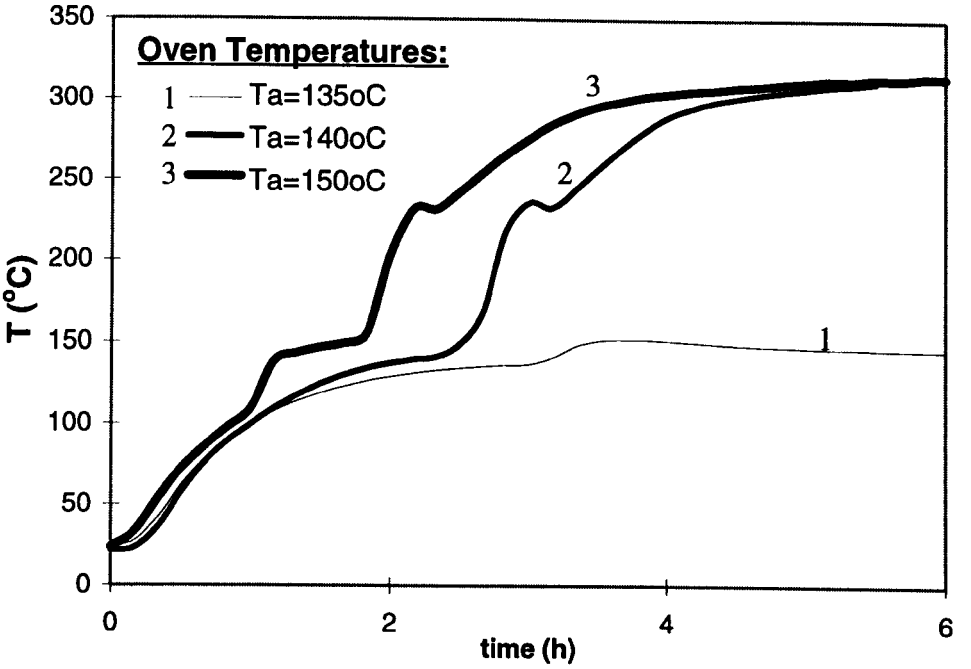

Figure 5.8 Temperature histories of 1% KCl-added-Coal M3 in an isothermal reactor (R-4) at several oven temperatures

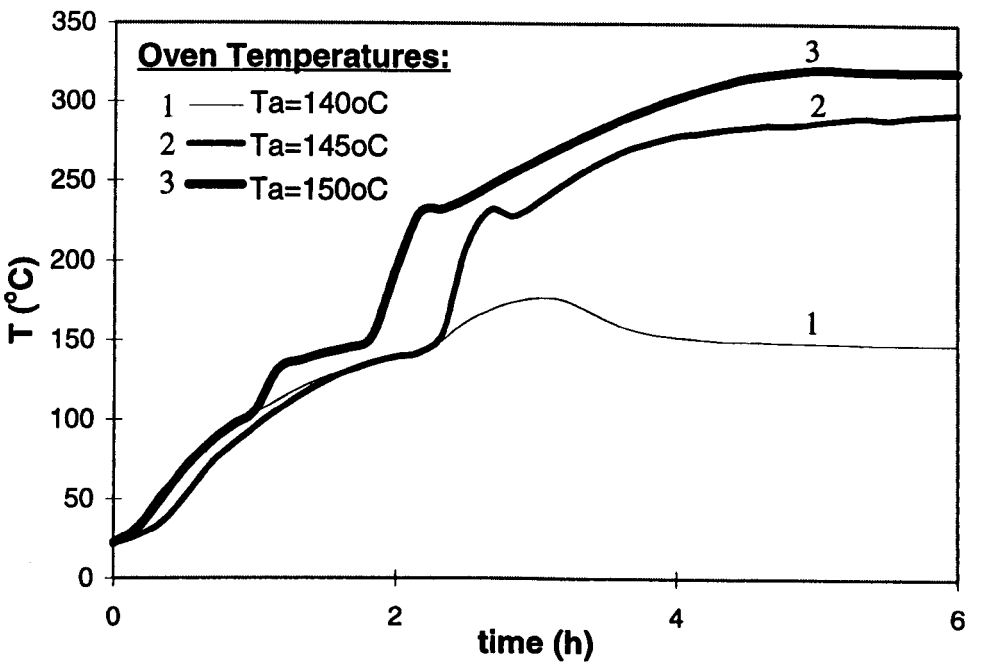

Figure 5.9 Temperature histories of 5% KCl-added-Coal M3 in an isothermal reactor (R-4) at several oven temperatures

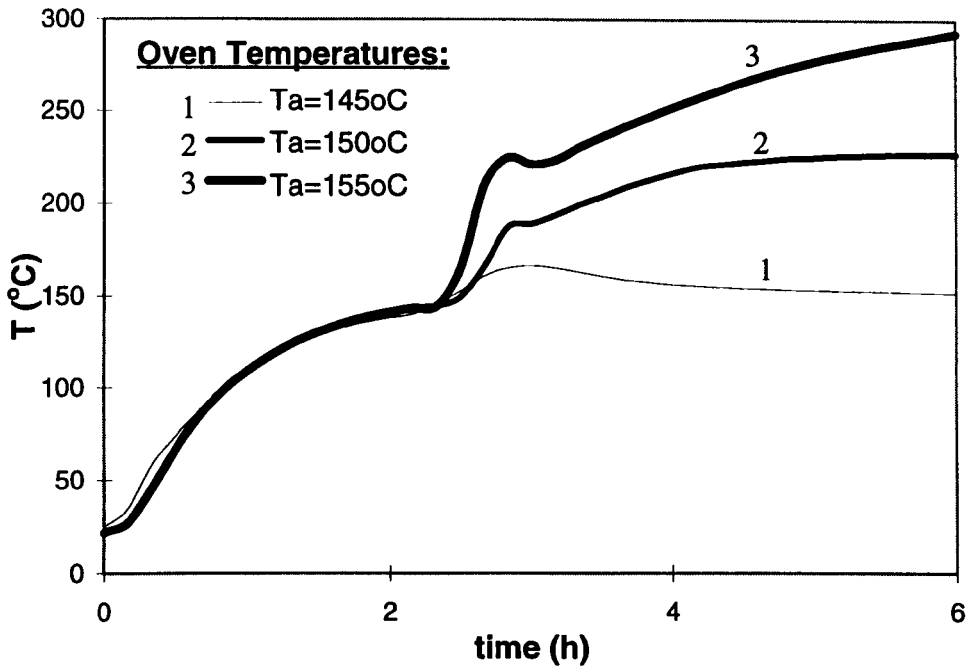

Figure 5.10 Temperature histories of 10% KCl-added-Coal M3 in an isothermal reactor (R-4) at several oven temperatures

5.3.3 Estimation of Low-Temperature Oxidation Kinetics

In order to compare reactivities of the samples and correlate the reactivities with their self-heating behaviour observed in the experiments, low-temperature oxidation kinetics were estimated by an energy balance approach described in Equation (3-2).

From the plot of ln $(dT/dt)_o$ versus $1000/T_o$, A and E can be determined. Figures 5.11 to 5.30 show typical ln $(dT/dt)_o$ ~ $1000/T_o$ plots for raw coal, water-washed coal, acid-washed coal, and various additive-added coal samples. The range of T_o over which the kinetic experiments were carried out is 110-160°C.

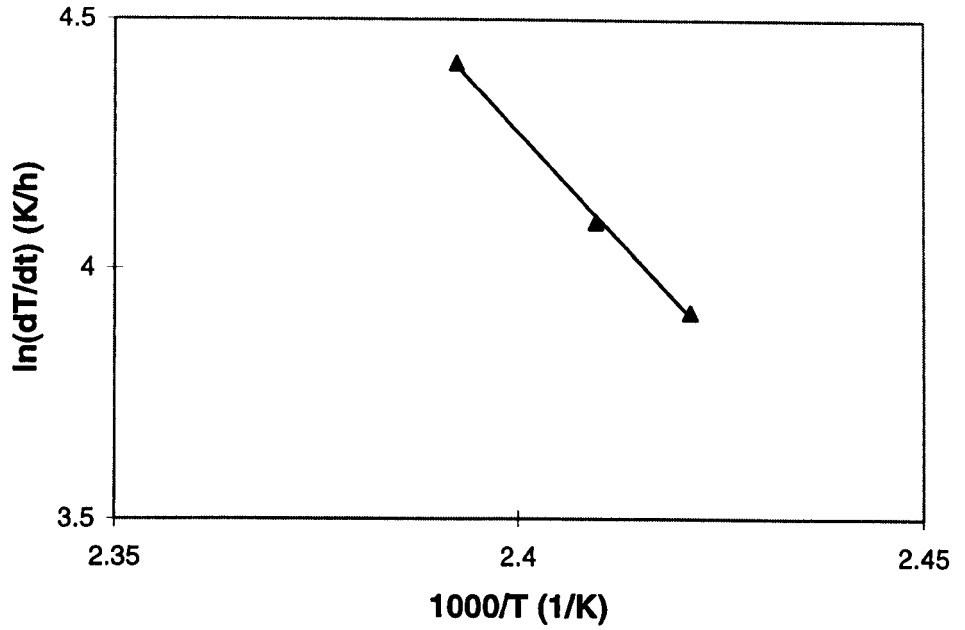

Figure 5.11 A linear plot of $\ln\left[\frac{dT}{dt}\right]_o$ versus $\frac{1000}{T_o}$ for nitrogen-dried Coal M2 in an isothermal reactor (R-4)

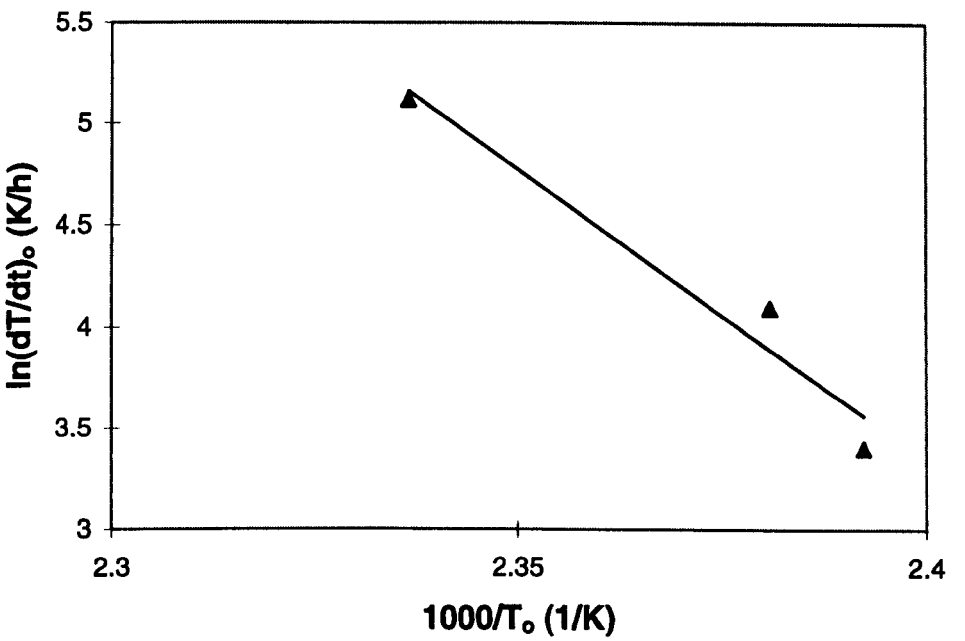

Figure 5.12 A linear plot of $\ln\left[\frac{dT}{dt}\right]_o$ versus $\frac{1000}{T_o}$ for water-washed Coal M2 in an isothermal reactor (R-4)

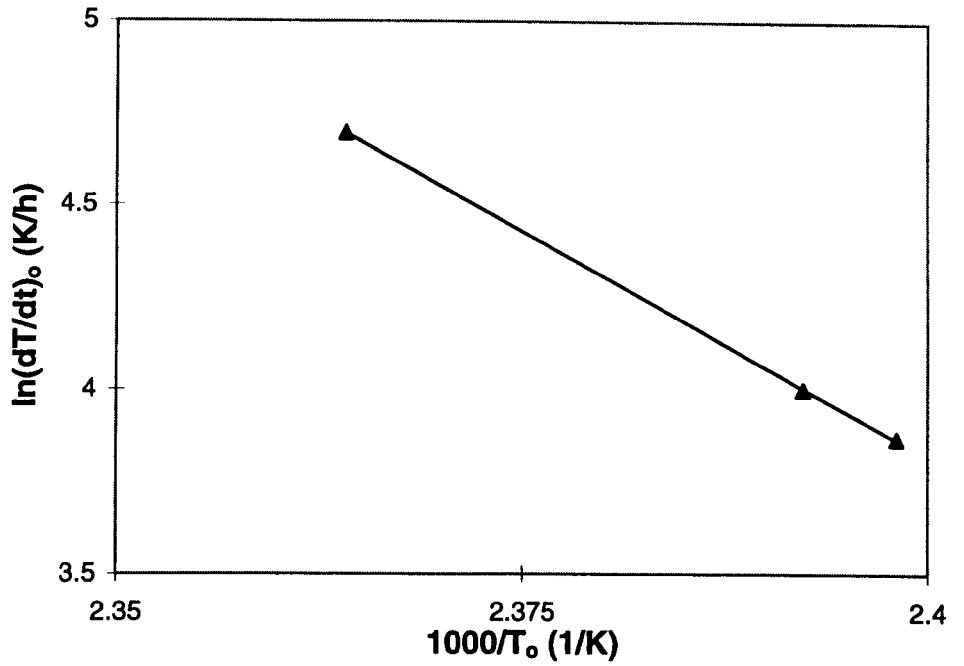

Figure 5.13 A linear plot of $\ln\left[\frac{dT}{dt}\right]_o$ versus $\frac{1000}{T_o}$ for acid-washed Coal M2 in an isothermal reactor (R-4)

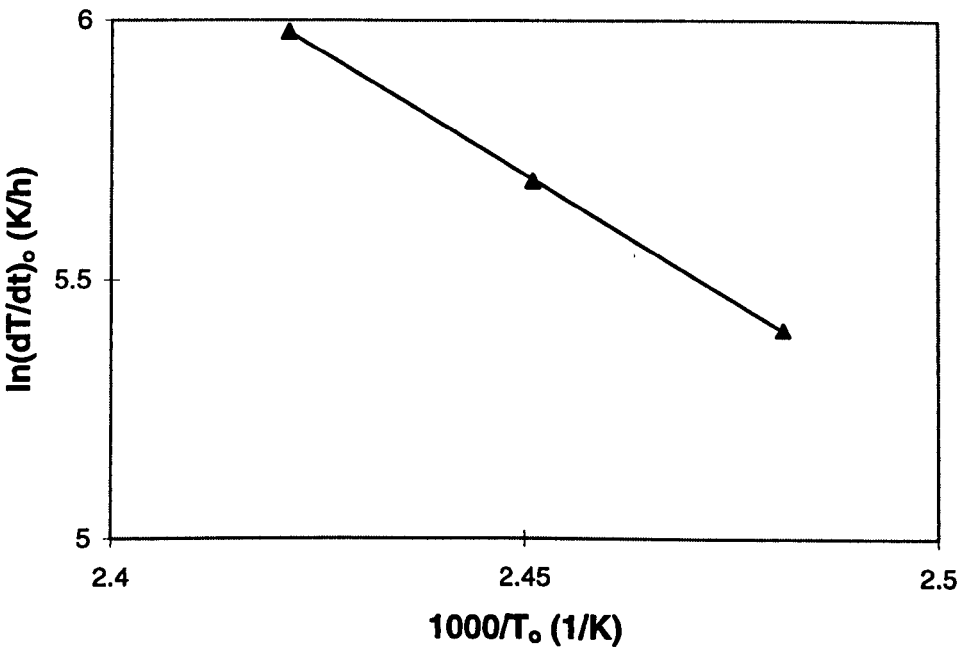

Figure 5.14 A linear plot of $\ln\left[\frac{dT}{dt}\right]_o$ versus $\frac{1000}{T_o}$ for FeS_2-added-Coal M2 in an isothermal reactor (R-4)

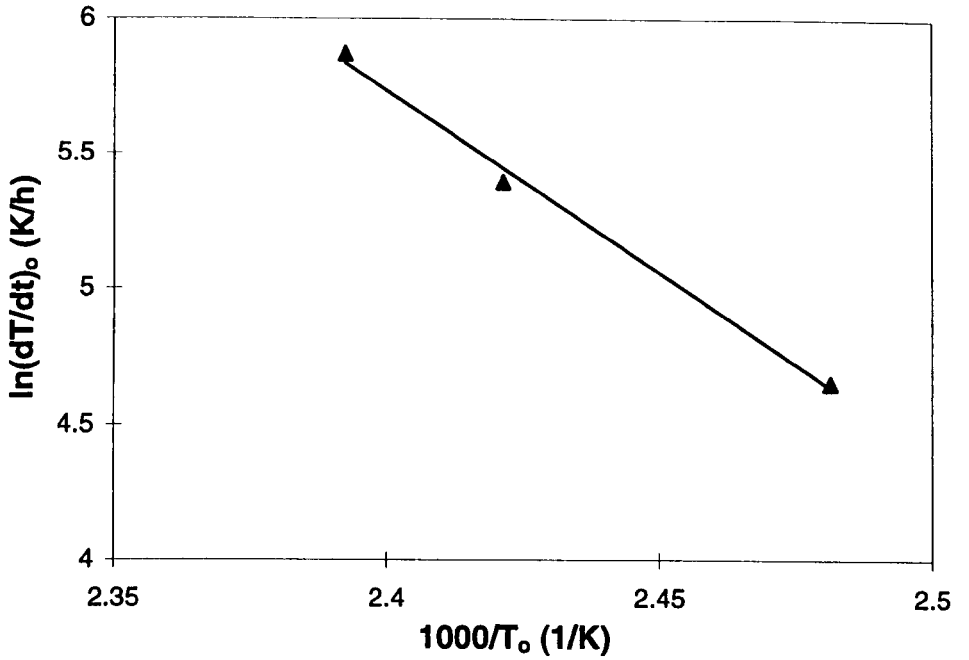

Figure 5.15 A linear plot of $\ln\left[\frac{dT}{dt}\right]_o$ versus $\frac{1000}{T_o}$ for KAc-added-Coal M2 in an isothermal reactor (R-4)

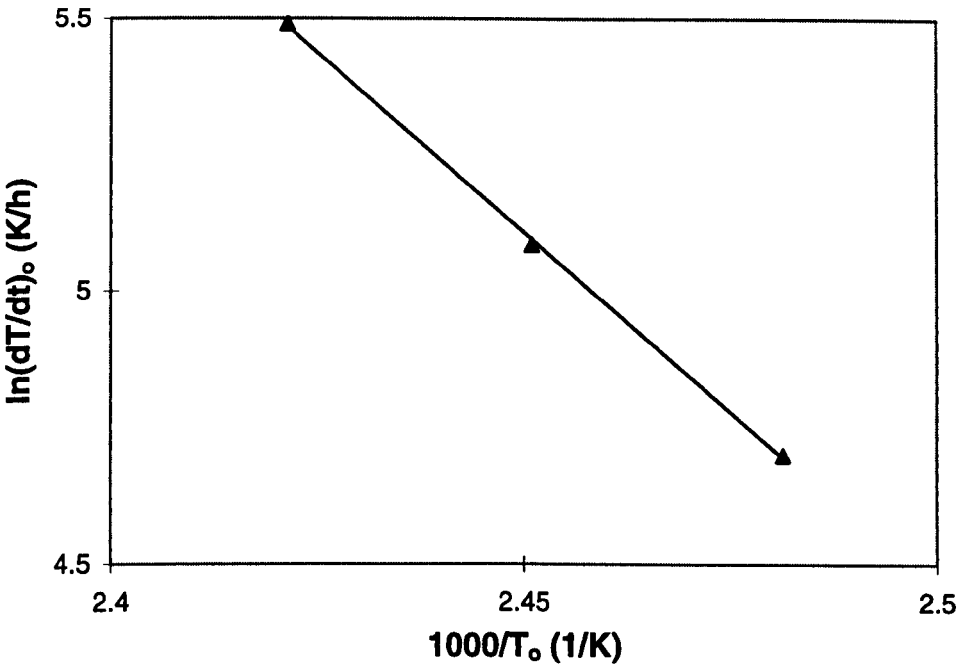

Figure 5.16 A linear plot of $\ln\left[\frac{dT}{dt}\right]_o$ versus $\frac{1000}{T_o}$ for NaAc-added-Coal M2 in an isothermal reactor (R-4)

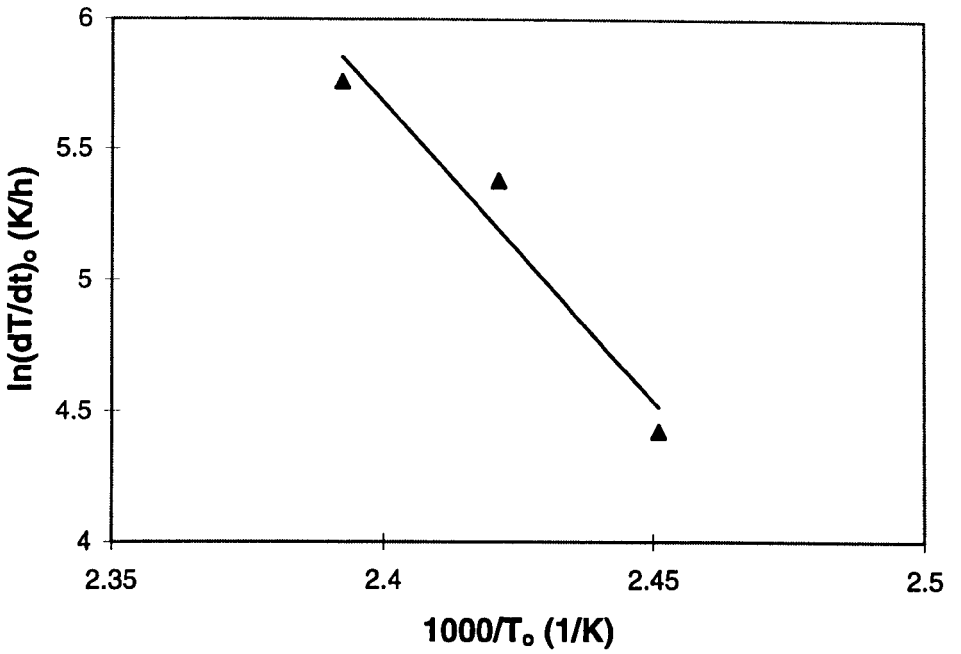

Figure 5.17 A linear plot of $\ln\left[\frac{dT}{dt}\right]_o$ versus $\frac{1000}{T_o}$ for $CaCO_3$-added-Coal M2 in an isothermal reactor (R-4)

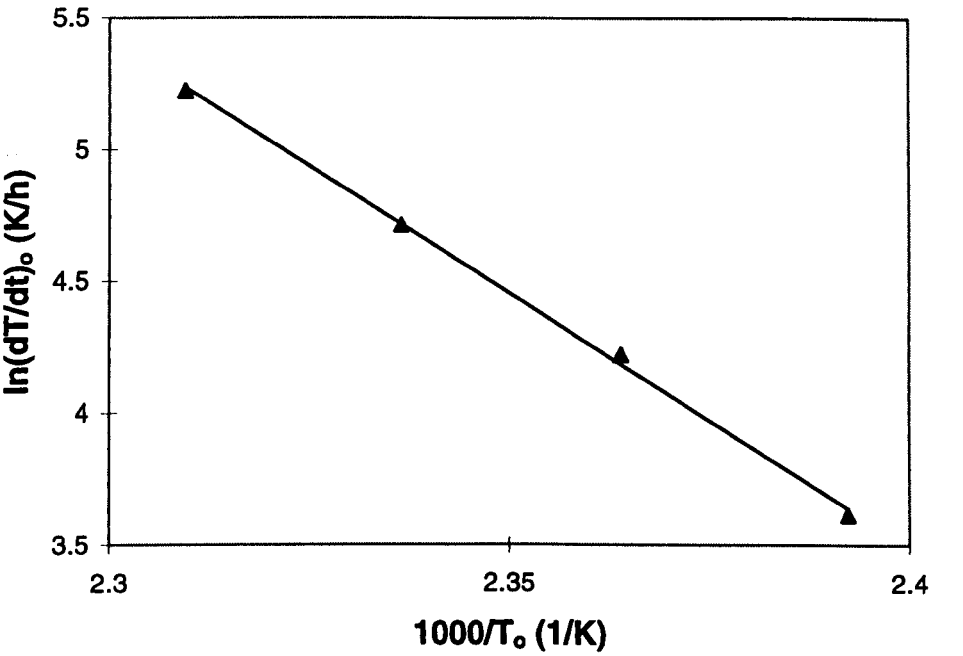

Figure 5.18 A linear plot of $\ln\left[\frac{dT}{dt}\right]_o$ versus $\frac{1000}{T_o}$ for NH_4Cl-added-Coal M2 in an isothermal reactor (R-4)

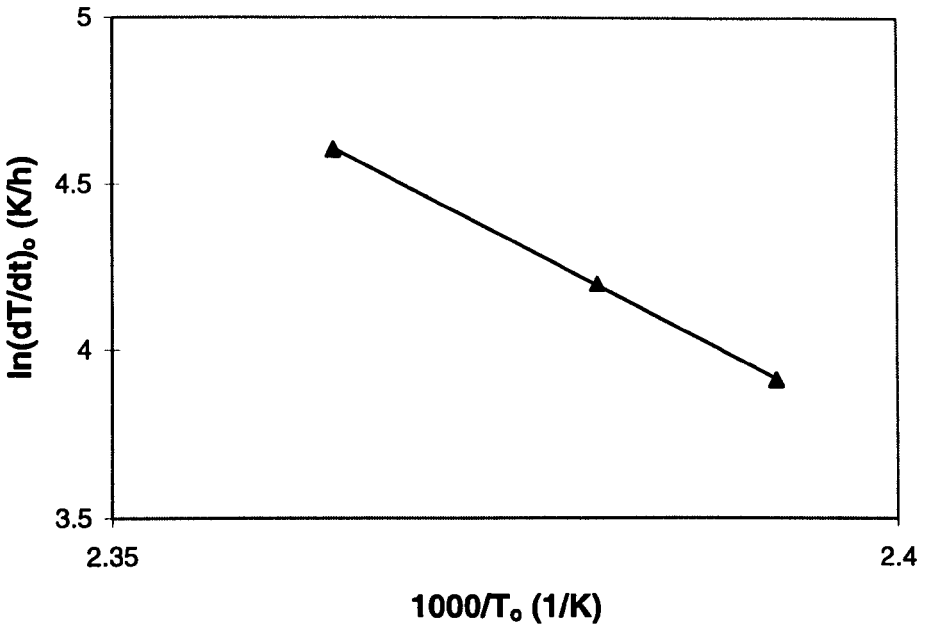

Figure 5.19 A linear plot of $\ln\left[\frac{dT}{dt}\right]_o$ versus $\frac{1000}{T_o}$ for $NaNO_3$-added-Coal M2 in an isothermal reactor (R-4)

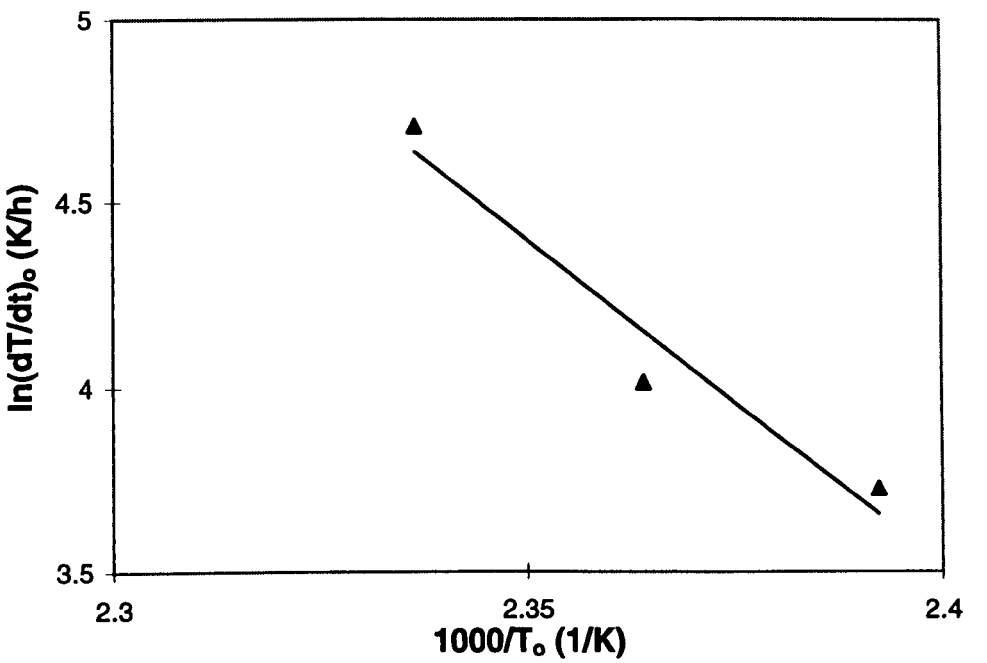

Figure 5.20 A linear plot of $\ln\left[\frac{dT}{dt}\right]_o$ versus $\frac{1000}{T_o}$ for $CaCl_2$-added-Coal M2 in an isothermal reactor (R-4)

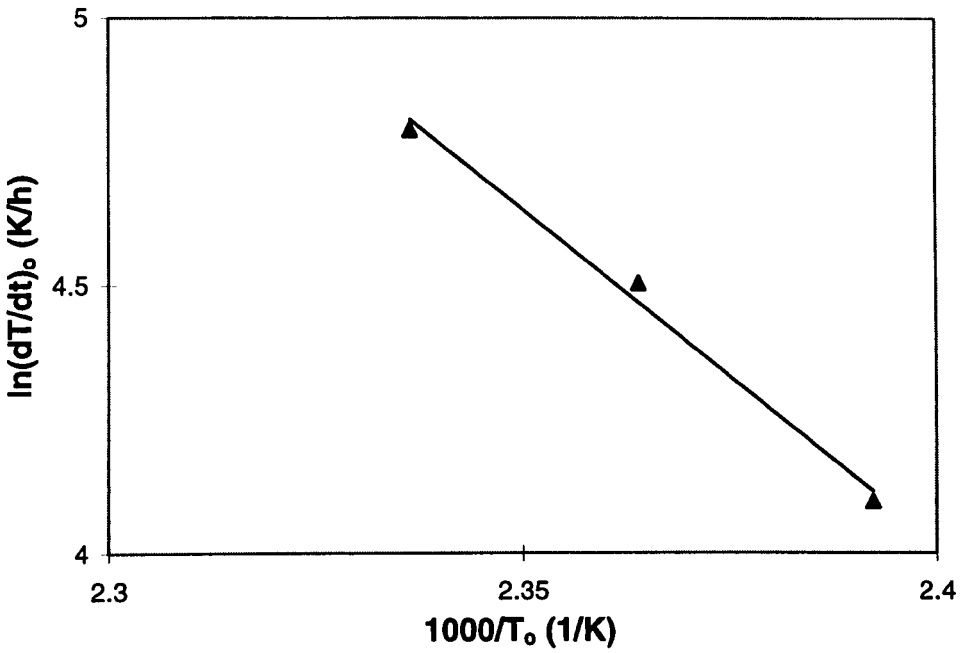

Figure 5.21 A linear plot of $\ln\left[\frac{dT}{dt}\right]_o$ versus $\frac{1000}{T_o}$ for $Mg(Ac)_2$-added-Coal M2 in an isothermal reactor (R-4)

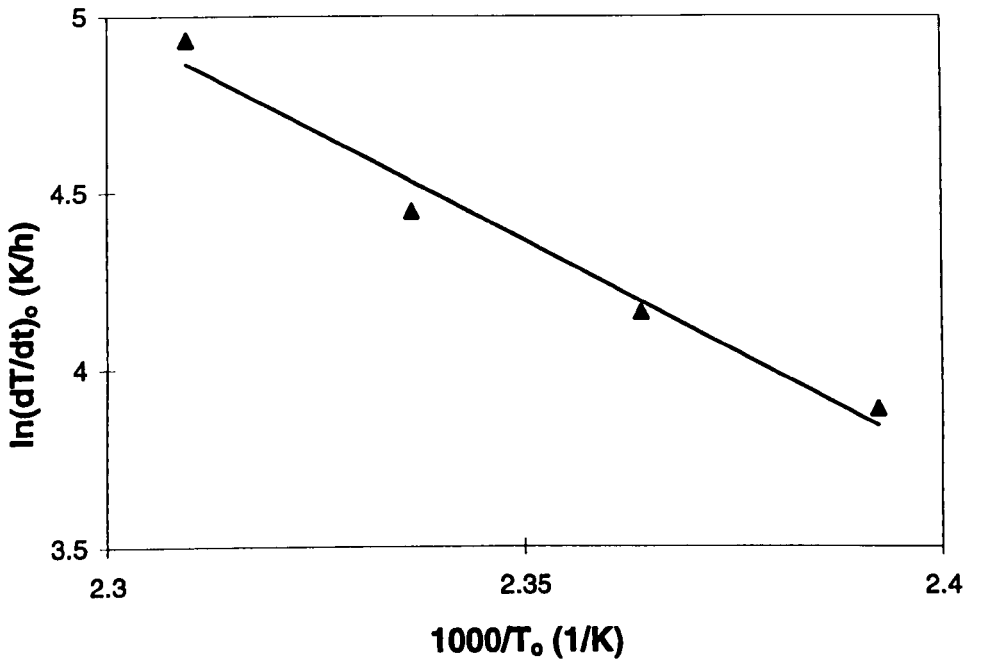

Figure 5.22 A linear plot of $\ln\left[\frac{dT}{dt}\right]_o$ versus $\frac{1000}{T_o}$ for Montan Powder-added-Coal M2 in an isothermal reactor (R-4)

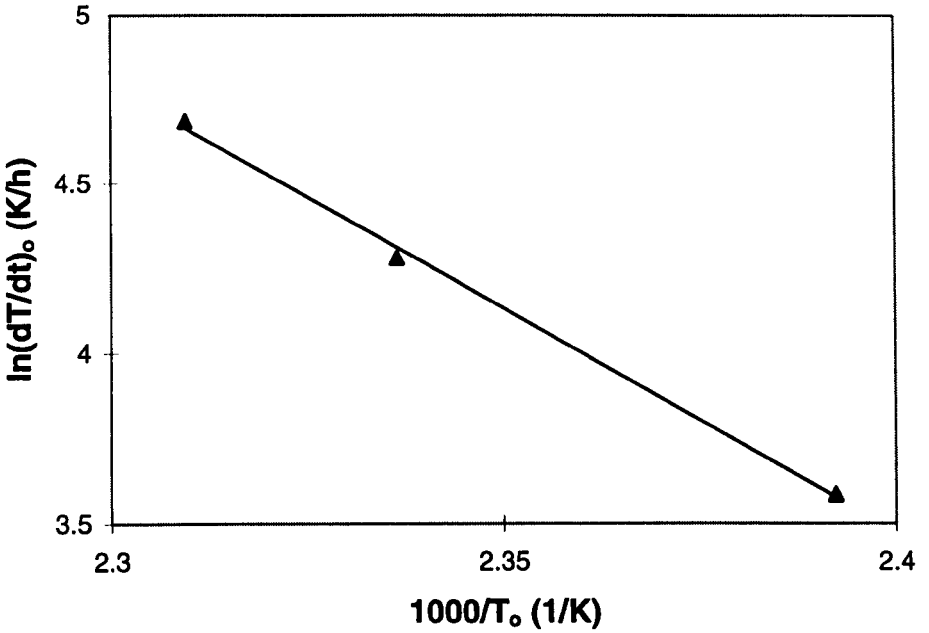

Figure 5.23 A linear plot of $\ln\left[\frac{dT}{dt}\right]_o$ versus $\frac{1000}{T_o}$ for KCl-added-Coal M2 in an isothermal reactor (R-4)

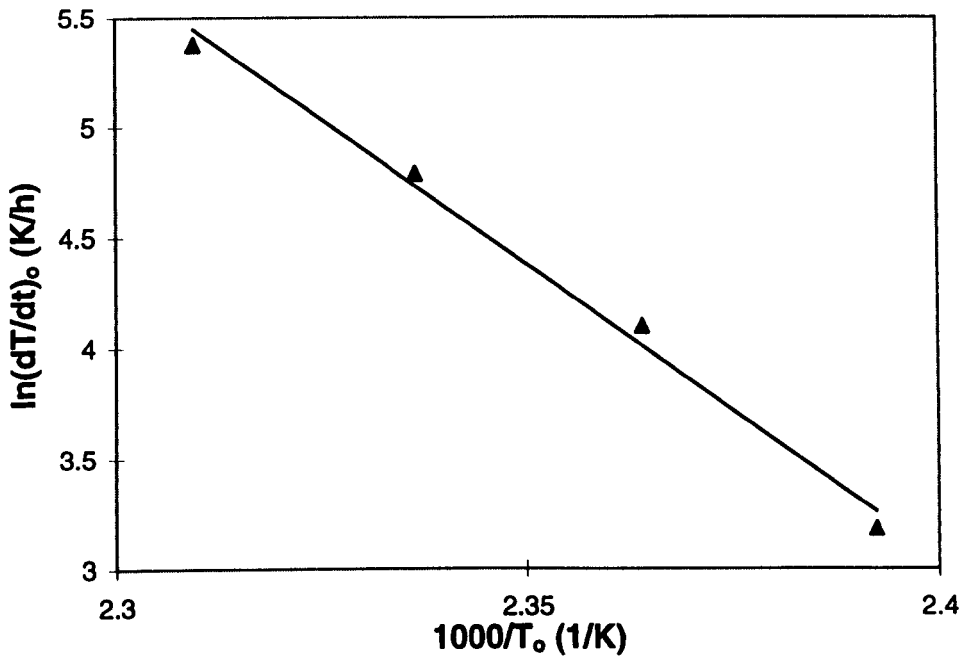

Figure 5.24 A linear plot of $\ln\left[\frac{dT}{dt}\right]_o$ versus $\frac{1000}{T_o}$ for NaCl-added-Coal M2 in an isothermal reactor (R-4)

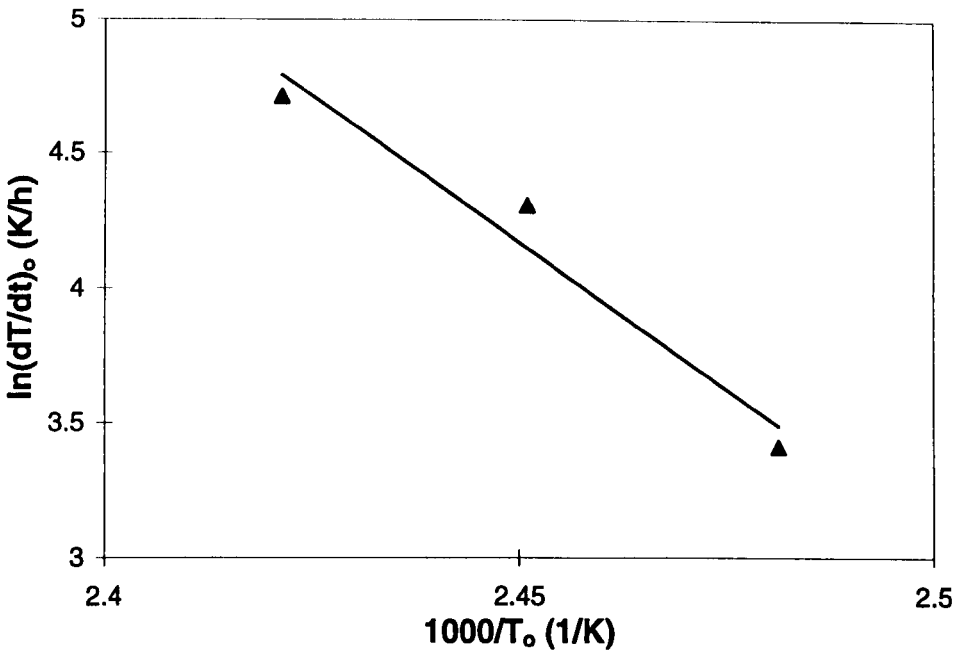

Figure 5.25 A linear plot of $\ln\left[\frac{dT}{dt}\right]_o$ versus $\frac{1000}{T_o}$ for 1% NaAc-added-Coal M3 in an isothermal reactor (R-4)

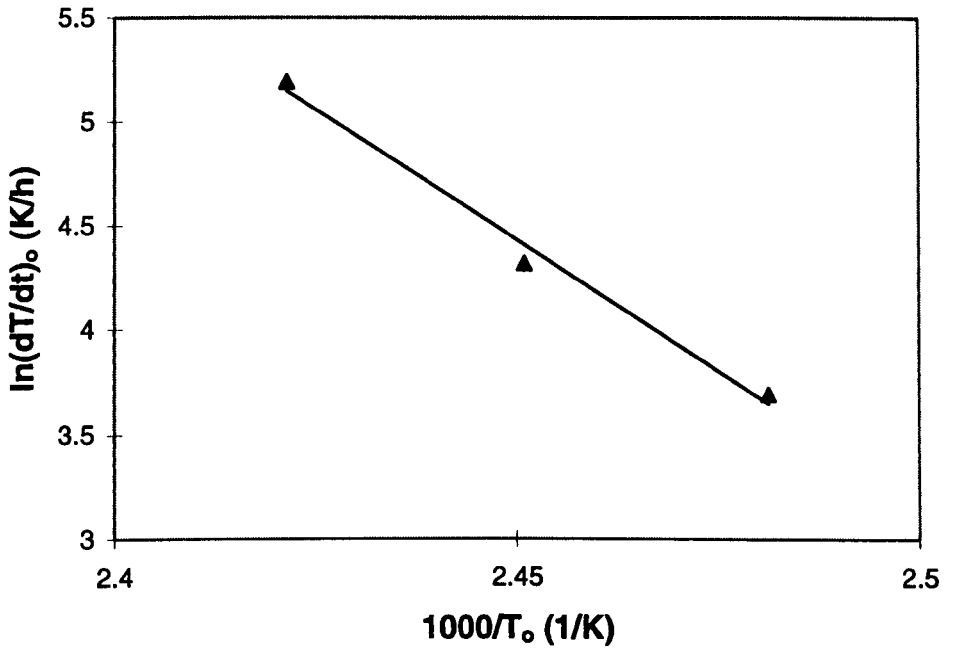

Figure 5.26 A linear plot of $\ln\left[\frac{dT}{dt}\right]_o$ versus $\frac{1000}{T_o}$ for 5% NaAc-added-Coal M3 in an isothermal reactor (R-4)

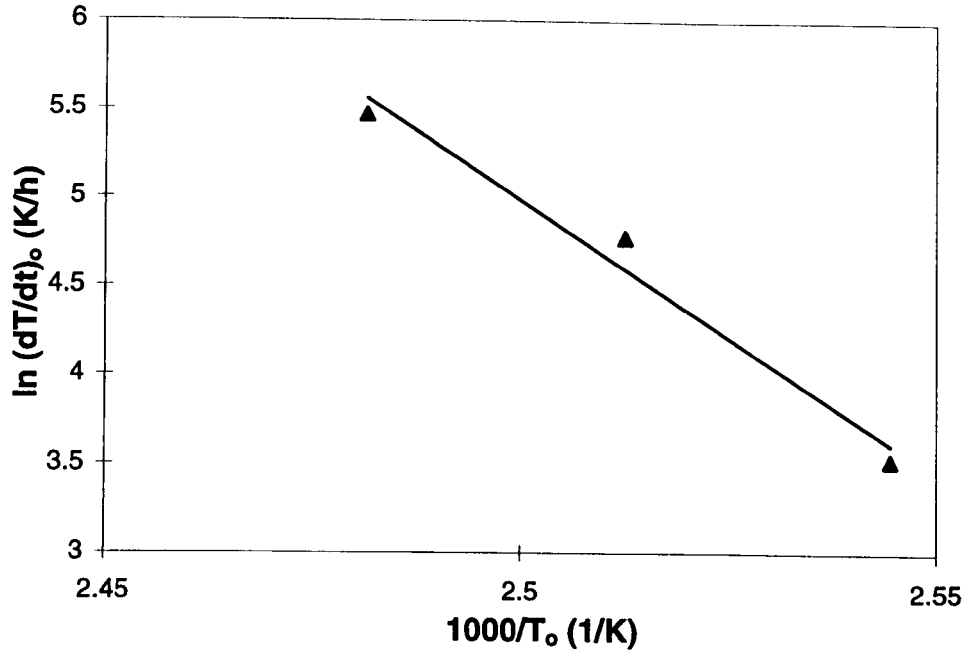

Figure 5.27 A linear plot of $\ln\left[\frac{dT}{dt}\right]_o$ versus $\frac{1000}{T_o}$ for 10% NaAc-added-Coal M3 in an isothermal reactor (R-4)

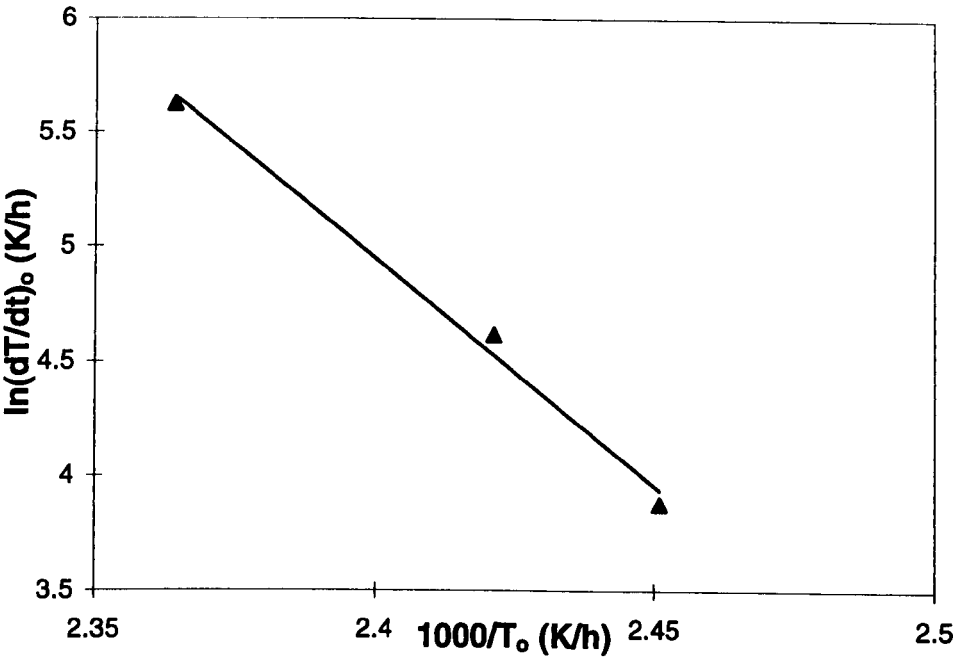

Figure 5.28 A linear plot of $\ln\left[\frac{dT}{dt}\right]_o$ versus $\frac{1000}{T_o}$ for 1% KCl-added-Coal M3 in an isothermal reactor (R-4)

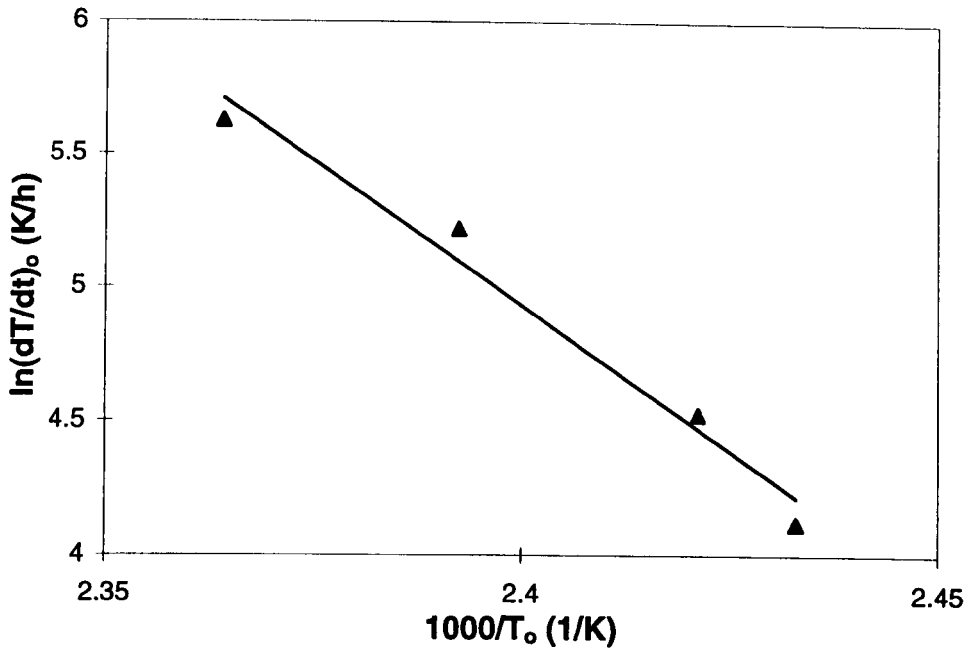

Figure 5.29 A linear plot of $\ln\left[\frac{dT}{dt}\right]_o$ versus $\frac{1000}{T_o}$ for 5% KCl-added-Coal M3 in an isothermal reactor (R-4)

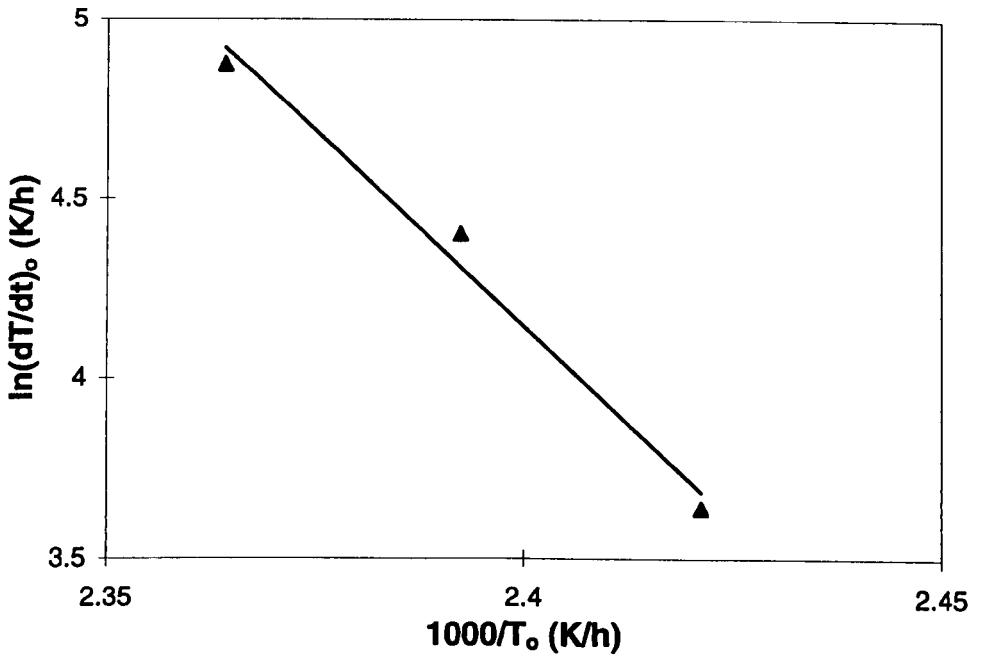

Figure 5.30 A linear plot of $\ln\left[\frac{dT}{dt}\right]_o$ versus $\frac{1000}{T_o}$ for 10% KCl-added-Coal M3 in an isothermal reactor (R-4)

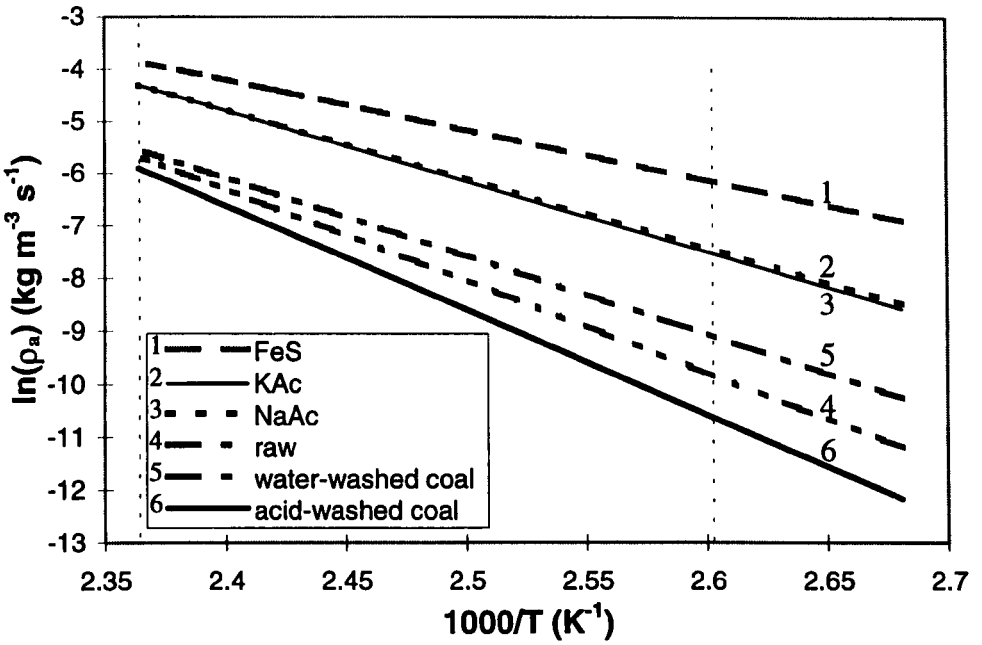

Figure 5.31 Comparison of reaction rates for various samples in temperature range of 110-150°C, assuming an oxygen partial pressure of 21 kPa

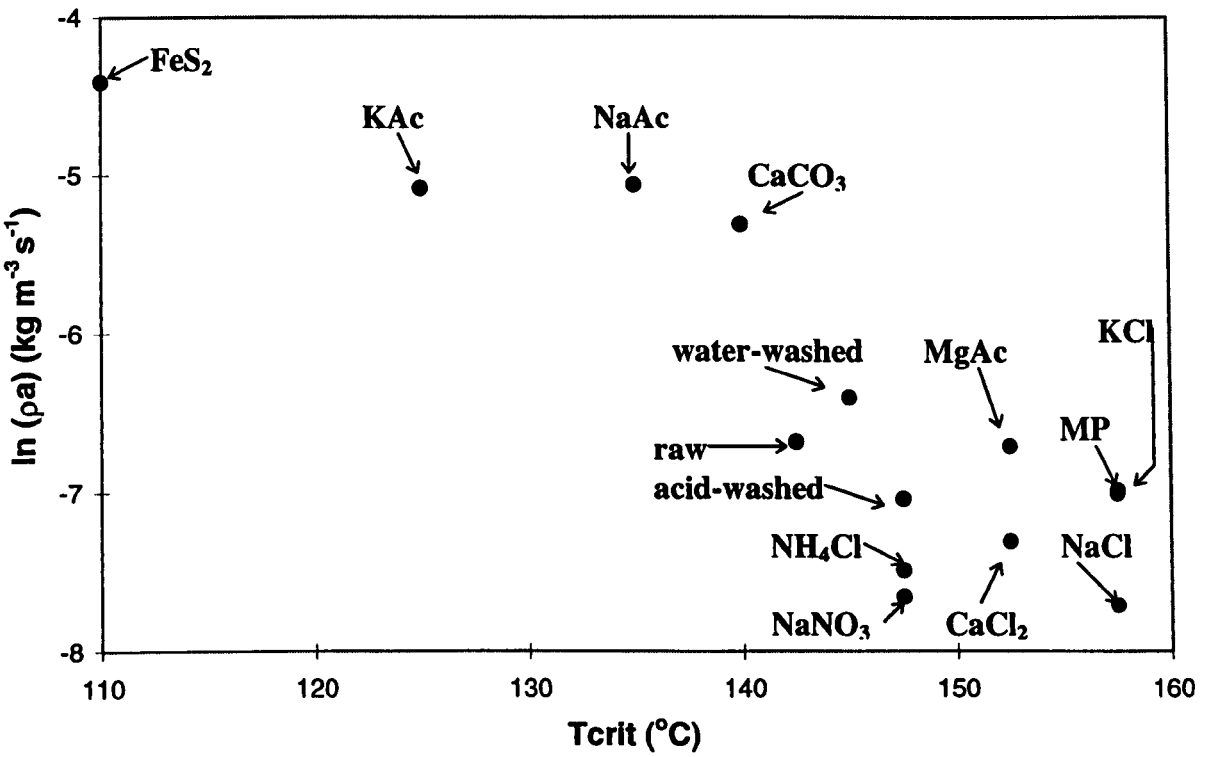

Figure 5.32 Low-temperature oxidation rates versus the critical temperature for various samples in air at 140°C

Figure 5.31 compares the Arrhenius plots of several samples in the presence of promotion agents, raw coal, water-washed, and acid-washed coal. The presence of FeS_2 in the coal results in the highest reactivity which corresponds to the lowest critical ambient temperature observed. The reactivity of the samples with the presence of KAc and NaAc are lower than that of the sample with FeS_2, but higher than those of raw coal, water-washed, and acid-washed coal samples. However, the reactivity of the water-washed coal is higher than that of the raw coal, which is not in agreement with their critical ambient temperature data. To further clarify this, the reaction rates estimated using the kinetics calculated are plotted against the critical ambient temperatures for all samples studied in Figure 5.32. In general, Figure 5.32 shows an overall trend that the lower the critical ambient temperature of a sample, the higher its oxidation reactivity. However, the data are more scattered for those samples with the inhibition agents in them. The reactivities of samples with the inhibition agents do not show a clear trend with their critical ambient temperatures. It is suspected that inaccuracy in the sample density and specific heat capacity of the samples used in Equation (3-2) may have contributed to the inconsistency in reactivity-critical ambient temperature correlation.

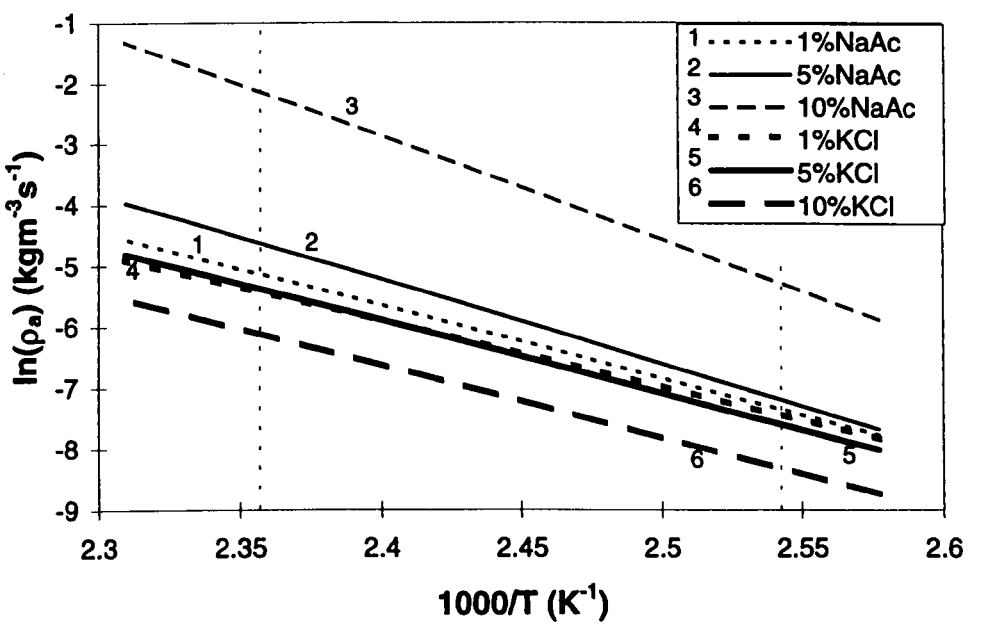

Figure 5.33 The effect of concentration on additive bulk loading on the estimated oxidation rates for NaAc and KCl added coal samples

Figure 5.33 compares the Arrhenius plots of several samples with the presence of NaAc and KCl at various loadings. It shows that 10 %wt. of NaAc in the coal sample has the highest reactivity compared to those with lower NaAc loadings (1 and 5%), which corresponds to the critical ambient temperatures observed. Figure 5.33 also shows that although, within the experimental accuracy, both 1 and 5% NaAc-added-coal samples have the same critical ambient temperature, 5% NaAc-added-coal sample is more reactive towards the oxidation reaction. The reactivities of the samples with KCl in them show the opposite trend; the higher KCl loading, the lower its reactivity.

5.4 SUMMARY

Experiments using an isothermal reactor have been conducted to study the spontaneous combustion of Coal M2 and the influences of inorganic matter. The critical ambient temperatures, above which a thermal runaway occurs, have been determined for the raw coal, water-washed and acid-washed coal, and samples with eleven different additives. Among the additives studied, FeS_2, KAc, NaAc, and $CaCO_3$ are found to promote the spontaneous combustion while Montan powder, KCl, NaCl, $CaCl_2$, and $Mg(Ac)_2$ inhibit the spontaneous combustion. $NaNO_3$ and NH_4Cl, show a very little effect. The low-temperature oxidation kinetics of the samples are also estimated. While the reactivities show a general trend that the lower the critical ambient temperature, the higher the reactivity of the sample, further investigation is required in order to improve the accuracy of the kinetic estimation. The promotion and inhibition effects of NaAc and KCl, respectively, on spontaneous combustion are enhanced with an increase in their loading.

Chapter 6

INVESTIGATIONS INTO THE ROLES OF ADDITIVES IN SPONTANEOUS COMBUSTION OF COAL

6.1 INTRODUCTION

The effects of additives and additive loadings on coal spontaneous combustion have been studied using isothermal reactors, as described in Chapter 5. To further study the inhibition and promotion agents of spontaneous combustion and the effect of cations and anions on the capability of additives to either inhibit or promote the coal spontaneous combustion, a laboratory study using a wire-mesh reactor (B-1) was also carried out.

Acid-washed coal and acid-washed coal doped with fourteen additives were prepared. Each of the samples was then tested in the wire-mesh reactor to obtain its critical ambient temperature. The relative effectiveness of the additives was determined by comparing their critical ambient temperatures with those of the acid-washed coal. An increase in the critical ambient temperature due to the use of an additive can indicate the effectiveness of the additive to suppress or promote the self-heating potential of the coal. The effect of the additive loading on the critical ambient temperature was also investigated for an inhibition agent (calcium acetate) and a promotion agent (sodium acetate). To examine whether the effectiveness of the additive is caused by a chemical or physical reaction between the additive and coal, ion exchange procedure was also applied. Typical promotion (sodium acetate, potassium acetate, and copper acetate) and inhibition (calcium acetate, magnesium

acetate, sodium chloride, and calcium chloride) additives in several solution concentrations were used for this purpose. The low-temperature oxidation kinetics of these coal samples were estimated using the unsteady-state method, as discussed in Chapter 3, and compared with the self-heating potential of these samples. This chapter details the results of the study.

6.2 SAMPLES PREPARATION

6.2.1 Acid-Washing

In the earlier studies, as discussed in Chapter 5, 6M HCl was used in the acid-washing procedure. However, from results of the isothermal experiments, it was suspected that the 6M HCl may be too concentrated which could significantly change the coal structure, and thus affected the coal self-heating behaviour. Accordingly, a very diluted acid was employed. The procedure is described as follows. Coal sample was mixed with 0.2M H_2SO_4 at the ratio of 1 to 20 in a glass beaker. The slurry was then evacuated using a water aspirator to remove air trapped in the coal pores for about an hour. The slurry was stirred for overnight at the ambient temperature, and was then filtered using a Buchner funnel. The coal sample was finally washed with double deionised water until the pH of the filtrate became constant.

6.2.2 Bulk-Loading of Additives

To further investigate the effect of individual inorganic components on spontaneous combustion, fourteen additives, as shown in Figure 6.1, were respectively added into the acid-washed coal. The bulk-loading procedure employed is explained as follows. An additive was mixed with water to form a solution and then added to the acid-washed coal, and stirred. The concentration of the additive in the coal samples was

5% wt. The sample was then dried in a nitrogen oven at 105 °C for overnight, which allowed the water to be evaporated. The sample was finally sieved. The 0.25 ~ 1.00 mm fraction was retained and stored for use in the experiments. To investigate the effect of additive loading, samples with 1 and 10 %wt. of $Ca(Ac)_2$ and NaAc were also prepared and tested.

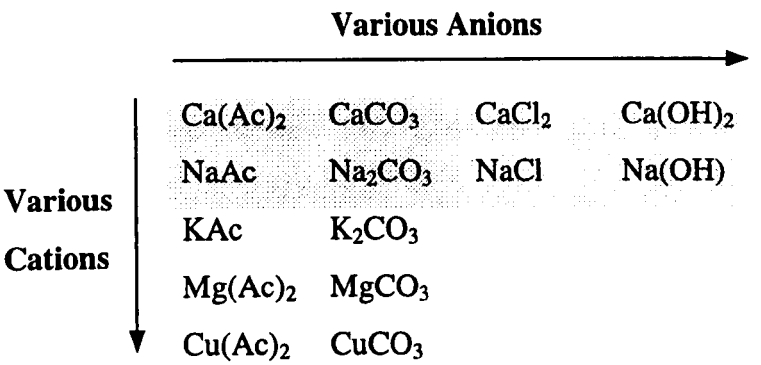

Figure 6.1. The additives used in the wire-mesh experiments

6.2.3 Ion-Exchange

To further examine whether the capability of the additives to inhibit or promote the coal spontaneous combustion is of physical or chemical nature, ion exchange procedure was employed in addition to the bulk-loading procedure. The ion exchange procedure used was described in Chapter 3. Typical promotion ($Cu(Ac)_2$, NaAc, and KAc) and inhibition ($Ca(Ac)_2$, $Mg(Ac)_2$, $CaCl_2$, and NaCl) additives, were used for this purpose. The solution concentrations used for each sample was 0.5M, except for $Cu(Ac)_2$ which was 0.25M. To investigate the effect of solution concentrations on the capability of the additives to affect spontaneous combustion, samples exchanged with 0.1 and 1.0M of $Ca(Ac)_2$ and NaAc were also prepared.

6.3 THE EFFECT OF INHERENT INORGANIC MATTER

From the wire-mesh experiments, it is found that the critical ambient temperatures of the acid-washed Coal M3 (154.5 ± 0.5 °C) was higher than that of the raw coal (152.5 ± 0.5 °C). The increase in critical ambient temperature indicated that removing the inherent inorganic matter from coal helped reduce its self-heating potential. The results were in a good agreement with those obtained from the isothermal tests.

6.4 BULK-LOADING OF ADDITIVES

6.4.1 The Effect of Additives

Table 6.1 Summary of critical ambient temperatures and apparent kinetic constants estimated for acid-washed coal and various acetate salts-added-acid-washed Coal M3 samples

Sample	T_{crit} (°C)	E (kJ mole^{-1})	A (s^{-1})
5% $Cu(Ac)_2$-added- coal	143.5 ± 0.5	95.3	1.40×10^6
5% KAc-added-coal	151.5 ± 0.5	103.2	7.33×10^6
5% NaAc-added-coal	152.5 ± 0.5	110.2	7.68×10^7
acid-washed coal	154.5 ± 0.5	115.4	2.50×10^8
5% $Ca(Ac)_2$-added-coal	156.5 ± 0.5	82.9	2.36×10^4
5% $Mg(Ac)_2$-added-coal	164.5 ± 0.5	68.9	3.03×10^2

Table 6.1 shows that among the acetate salts used, $Cu(Ac)_2$, KAc, and NaAc promoted the spontaneous combustion of Coal M3 as their critical ambient temperatures were considerately lower than that of the acid-washed coal. On the other hand, $Ca(Ac)_2$ and $Mg(Ac)_2$ increased the critical ambient temperature for spontaneous combustion, indicating that these additives inhibited the spontaneous combustion.

Table 6.2 Summary of critical ambient temperatures and apparent kinetic constants estimated for acid-washed coal and various carbonate salts-added-acid-washed Coal M3 samples

Sample	T_{crit} (°C)	E (kJ mole^{-1})	A (s^{-1})
5% $CuCO_3$-added-coal	139.5 ± 0.5	109.9	1.46×10^8
5% Na_2CO_3-added- coal	147.5 ± 0.5	111.5	1.39×10^8
5% K_2CO_3-added-coal	150.5 ± 0.5	106.1	2.15×10^7
5% $CaCO_3$-added-coal	152.5 ± 0.5	113.0	1.68×10^8
acid-washed coal	154.5 ± 0.5	115.4	2.50×10^8
5% $MgCO_3$-added-coal	160.5 ± 0.5	93.2	3.53×10^5

Table 6.2 shows a summary of critical ambient temperatures of samples with various carbonate salts. It is shown that Cu^{2+}, K^+, Na^+, and Ca^{2+} in their carbonate salts promoted the spontaneous combustion of Coal M3 as their critical ambient temperatures were considerately lower than that of the acid-washed. On the other hand, Mg^{2+} in its carbonate salt inhibited the spontaneous combustion.

Table 6.3 summarises the critical ambient temperatures of calcium and sodium ions in their chloride and hydroxide forms. It is observed that both sodium and calcium

in chloride salts inhibited spontaneous combustion, while in the hydroxide forms, they behaved differently. The critical ambient temperature of 5% $Ca(OH)_2$-added-coal (152.5 ± 0.5 °C) was lower than that of acid-washed coal, indicating its promotion effect on spontaneous combustion. On the other hand, the critical ambient temperature 5% NaOH-added-coal (166.5 ± 0.5 °C) was higher than that of acid-washed coal (154.5 ± 0.5 °C), indicating its inhibition effect on spontaneous combustion.

Table 6.3 Summary of critical ambient temperatures and apparent kinetic constants estimated for acid-washed coal and calcium and sodium in chloride and hydroxide forms-added-acid-washed Coal M3 samples

Sample	T_{crit} (°C)	E (kJ $mole^{-1}$)	A (s^{-1})
5% $Ca(OH)_2$-added-coal	152.5 ± 0.5	109.6	6.60×10^7
acid-washed coal	154.5 ± 0.5	115.4	2.50×10^8
5% NaOH-added-coal	166.5 ± 0.5	60.6	3.10×10^1
5% $CaCl_2$-added-coal	160.5 ± 0.5	104.9	8.65×10^6
5% NaCl-added-coal	159.5 ± 0.5	103.6	8.00×10^6

As described in Chapter 5, Sodium and potassium in their organic salts catalysed the spontaneous combustion (Banerjee (1985); Durie (1991)). This theory was again supported by the results for KAc and NaAc obtained in this study. The addition of $Cu(Ac)_2$ to the acid-washed coal decreased the critical ambient temperature of the acid-washed coal by 11 °C to 143.5 °C, indicating its strong catalytic effect on spontaneous combustion. Similar to the earlier result, $Mg(Ac)_2$ was found to inhibit the spontaneous combustion, which strengthened the argument that Mg^{2+} is a negative catalyst for a low-temperature (< 200°C) oxidation reaction of coal.

The addition of Na_2CO_3 and K_2CO_3 to the acid-washed coal decreased the critical ambient temperature of the acid-washed coal by 7 and 4 °C, respectively, indicating their catalytic effects on spontaneous combustion. These results implied that sodium and potassium in their inorganic salts were also good catalysts for a low-temperature oxidation reaction. $CaCO_3$ also showed a slight catalytic effect on spontaneous combustion, as its critical ambient temperature (152.5 °C) was 2 °C lower than that of acid-washed coal. This was, again, in a good agreement with the results obtained from the isothermal tests. Furthermore, similar to its behaviour when presented in acetic salt, $MgCO_3$ showed a negative catalytic effect on spontaneous combustion.

The same as the earlier results obtained from the isothermal tests, $CaCl_2$ and NaCl inhibited the spontaneous combustion. The endothermic reactions occurred between $CaCl_2$ and pyritic compounds in coal at 100 - 150 °C (Smith et al. (1988)) and the physical changes due to the application of additives played the roles in the inhibition effects observed. The presence of NaOH in the acid-washed coal was also found to inhibit the spontaneous combustion, indicating that sodium in its hydroxide form could be a negative catalyst for spontaneous combustion. On the other hand, $Ca(OH)_2$ showed a slight catalytic effect on spontaneous combustion.

The experimental results showed that there was not a clear trend, indicating whether cations or anions played more important roles in the effect of additives on spontaneous combustion.

6.4.2 The Effect of Additive Loading

In order to investigate the effect of additive loading on promotion or inhibition of spontaneous combustion, samples with 1, 5, and 10 %wt. of NaAc and $Ca(Ac)_2$ were prepared and tested. Table 6.4 presents the critical ambient temperatures of these samples. It was observed that the critical ambient temperature decreased with increasing NaAc loading, indicating that promotion effect of this additive on spontaneous combustion depended on its loading level. On the other hand, the

critical ambient temperatures of coal samples with $Ca(Ac)_2$ remained unchanged with varying loading, indicating that inhibition effect of this additive on spontaneous combustion did not depend on its loading level.

Table 6.4 Summary of the critical ambient temperatures and kinetic constants estimated for samples with various additive loadings

Sample	Tcrit (°C)	E (kJ mol^{-1})	A (s^{-1})
1% NaAc-added-coal	154.5 ± 2.5	100.3	3.71×10^6
5% NaAc-added-coal	152.5 ± 2.5	110.2	7.68×10^7
10% NaAc-added-coal	150.5 ± 2.5	118.4	1.07×10^9
1% $Ca(Ac)_2$-added-coal	156.5 ± 2.5	87.4	8.02×10^4
5% $Ca(Ac)_2$-added-coal	156.5 ± 2.5	82.9	2.36×10^4
10% $Ca(Ac)_2$-added-coal	156.5 ± 2.5	80.5	9.71×10^3

6.4.3 Estimation of Low-Temperature Oxidation Kinetics

The low-temperature oxidation kinetics were again estimated using the unsteady-state energy balance, i.e. Equation (3-10).

From the plot of ln $(dT/dt)_{T=Tp}$ versus $1/T_p$, the kinetic constants, A and E, can be determined. Figures 6.2 to 6.20 show linear plots of ln $(dT/dt)_{T=Tp}$ versus $1000/T_p$ for acid-washed Coal M3 and samples with various additives. The range of T_p over which the kinetic experiments were carried out was 135-170°C.

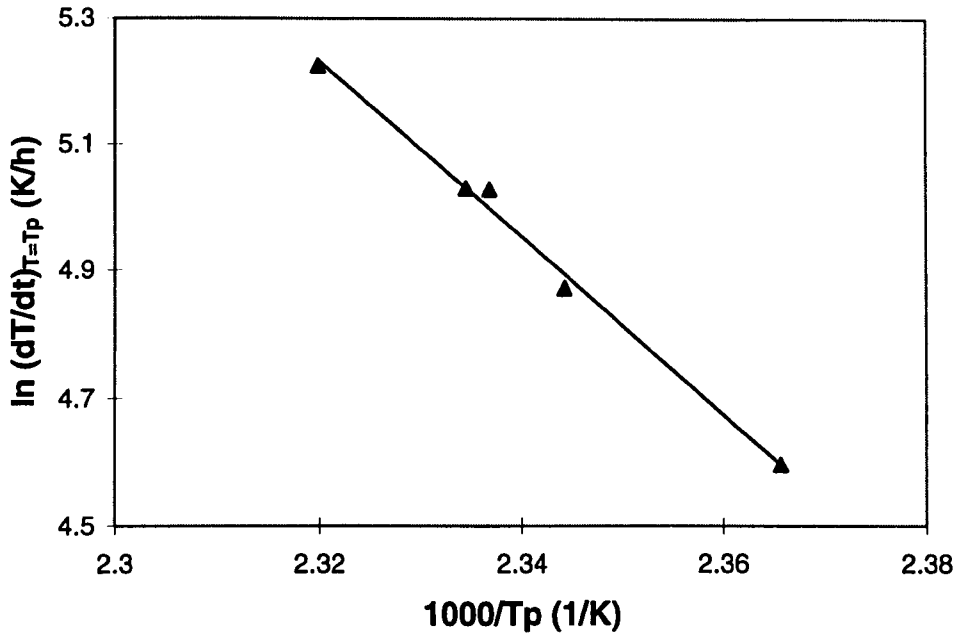

Figure 6.2 A linear plot of $\ln\left[\frac{dT}{dt}\right]_{T=T_p}$ versus $\frac{1000}{T_p}$ for acid-washed Coal M3 in a wire-mesh reactor (B-1)

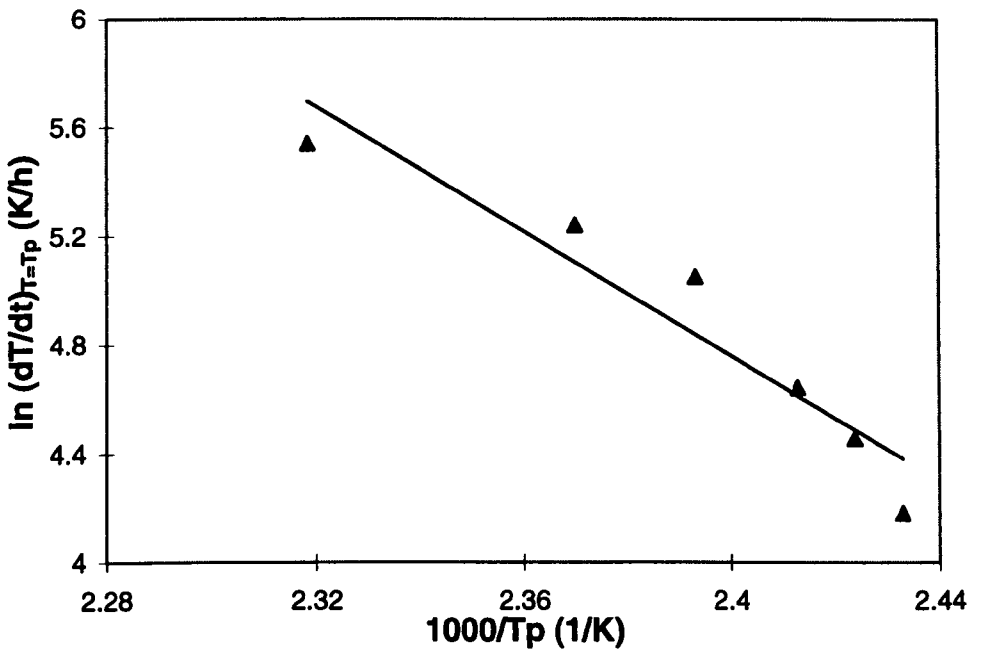

Figure 6.3 A linear plot of $\ln\left[\frac{dT}{dt}\right]_{T=T_p}$ versus $\frac{1000}{T_p}$ for 5% $Cu(Ac)_2$-added-Coal M3 in a wire-mesh reactor (B-1)

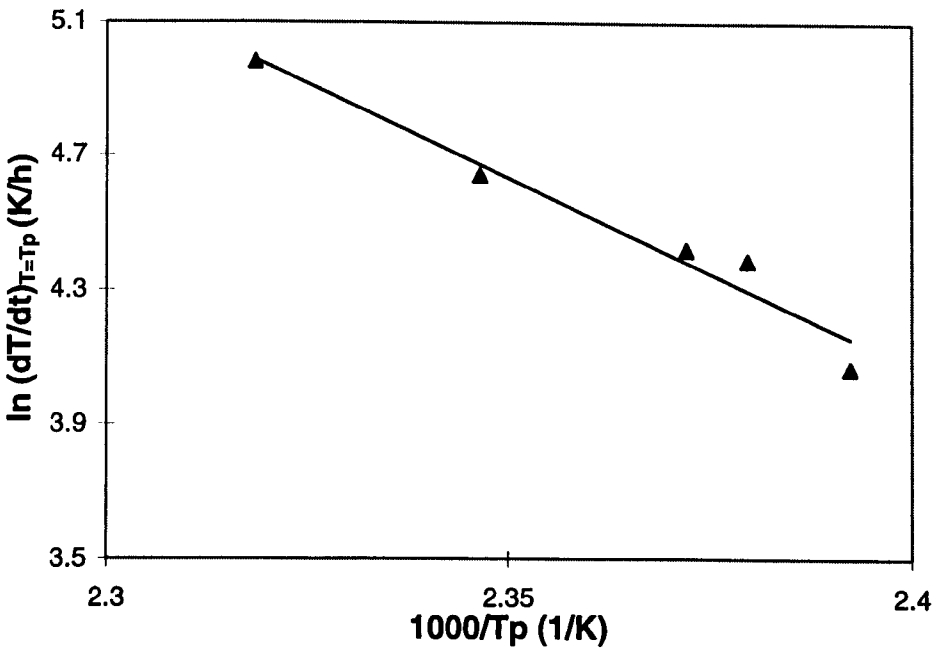

Figure 6.4 A linear plot of $\ln\left[\frac{dT}{dt}\right]_{T=T_p}$ versus $\frac{1000}{T_p}$ for 5% KAc-added-Coal M3 in a wire-mesh reactor (B-1)

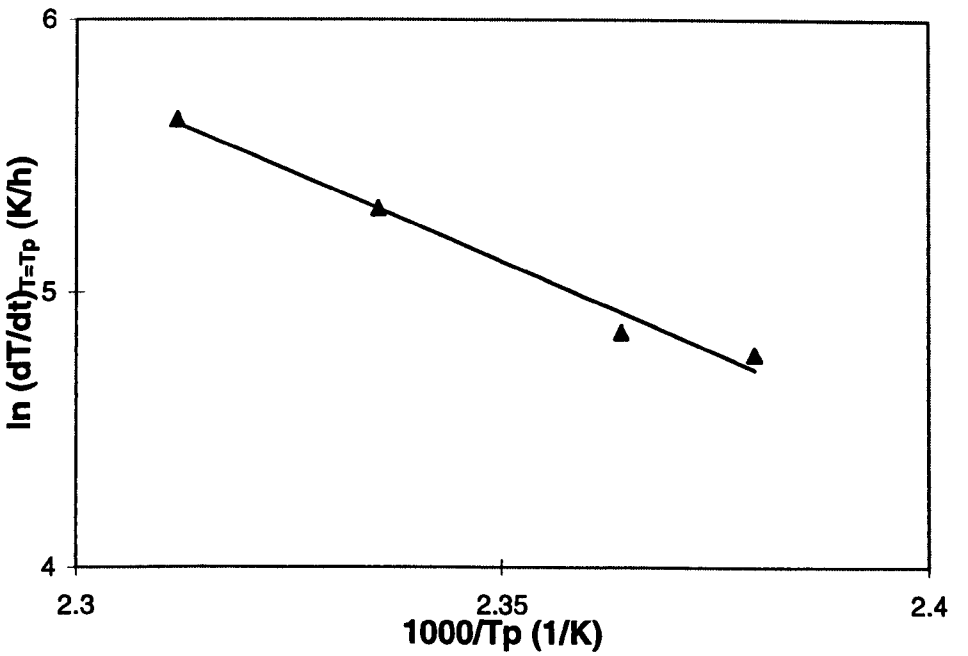

Figure 6.5 A linear plot of $\ln\left[\frac{dT}{dt}\right]_{T=T_p}$ versus $\frac{1000}{T_p}$ for 5% NaAc-added-Coal M3 in a wire-mesh reactor (B-1)

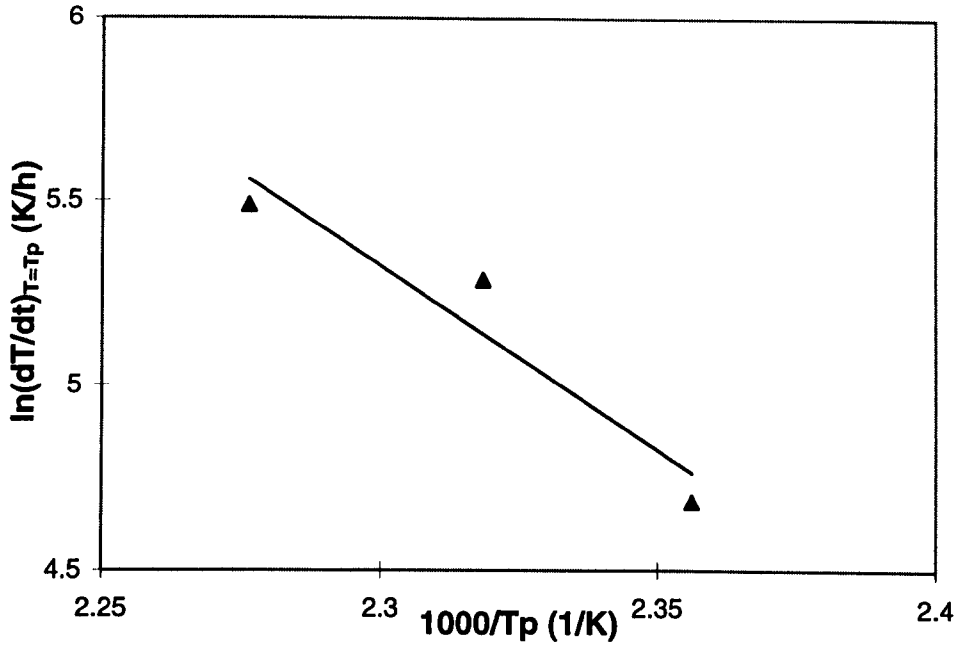

Figure 6.6 A linear plot of $\ln\left[\frac{dT}{dt}\right]_{T=T_p}$ versus $\frac{1000}{T_p}$ for 5% $Ca(Ac)_2$-added-Coal M3 in a wire-mesh reactor (B-1)

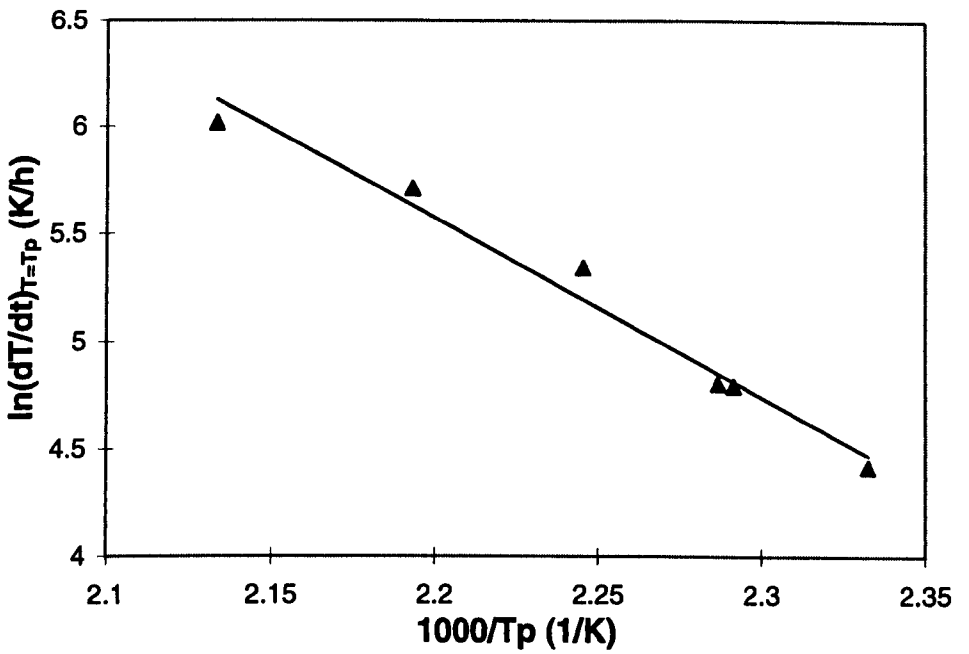

Figure 6.7 A linear plot of $\ln\left[\frac{dT}{dt}\right]_{T=T_p}$ versus $\frac{1000}{T_p}$ for 5% $Mg(Ac)_2$-added-Coal M3 in a wire-mesh reactor (B-1)

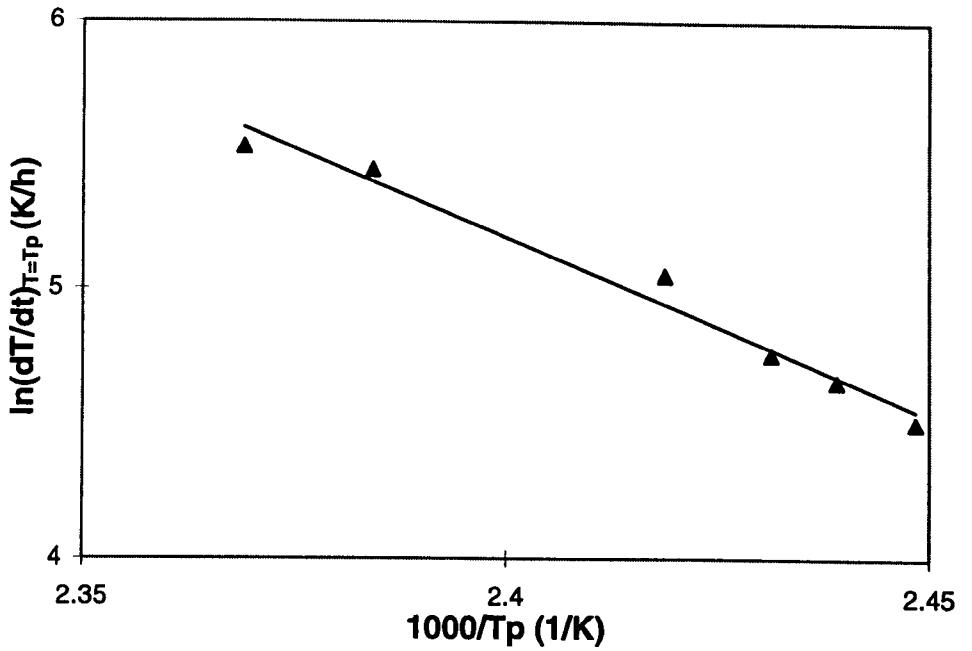

Figure 6.8 A linear plot of $\ln\left[\frac{dT}{dt}\right]_{T=T_p}$ versus $\frac{1000}{T_p}$ for 5% $CuCO_3$-added-Coal M3 in a wire-mesh reactor (B-1)

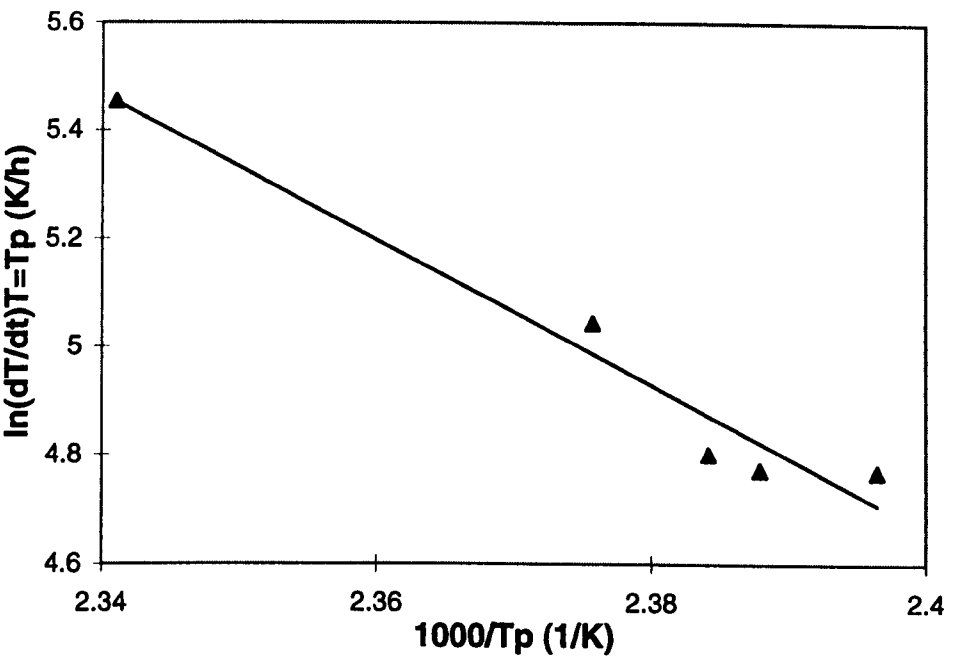

Figure 6.9 A linear plot of $\ln\left[\frac{dT}{dt}\right]_{T=T_p}$ versus $\frac{1000}{T_p}$ for 5% Na_2CO_3-added-Coal M3 in a wire-mesh reactor (B-1)

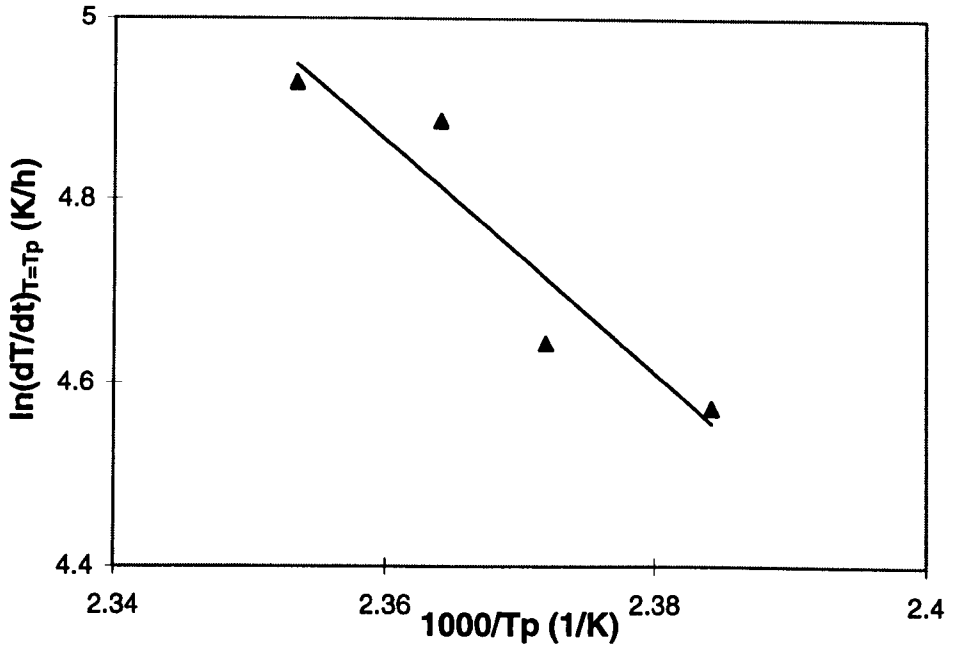

Figure 6.10 A linear plot of $\ln\left[\frac{dT}{dt}\right]_{T=T_p}$ versus $\frac{1000}{T_p}$ for 5% K_2CO_3-added-Coal M3 in a wire-mesh reactor (B-1)

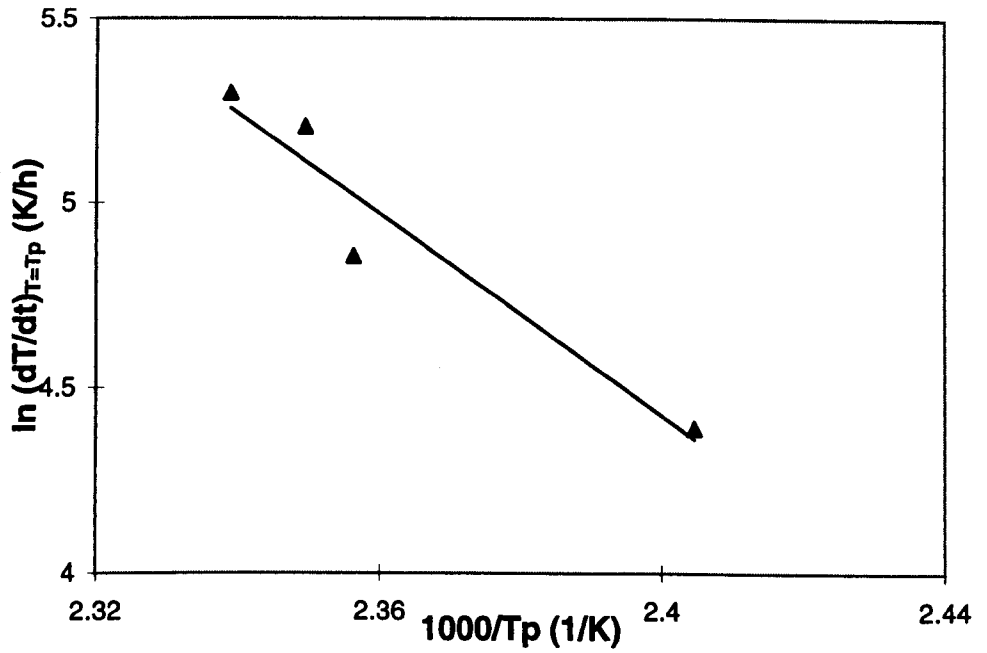

Figure 6.11 A linear plot of $\ln\left[\frac{dT}{dt}\right]_{T=T_p}$ versus $\frac{1000}{T_p}$ for 5% $CaCO_3$-added-Coal M3 in a wire-mesh reactor (B-1)

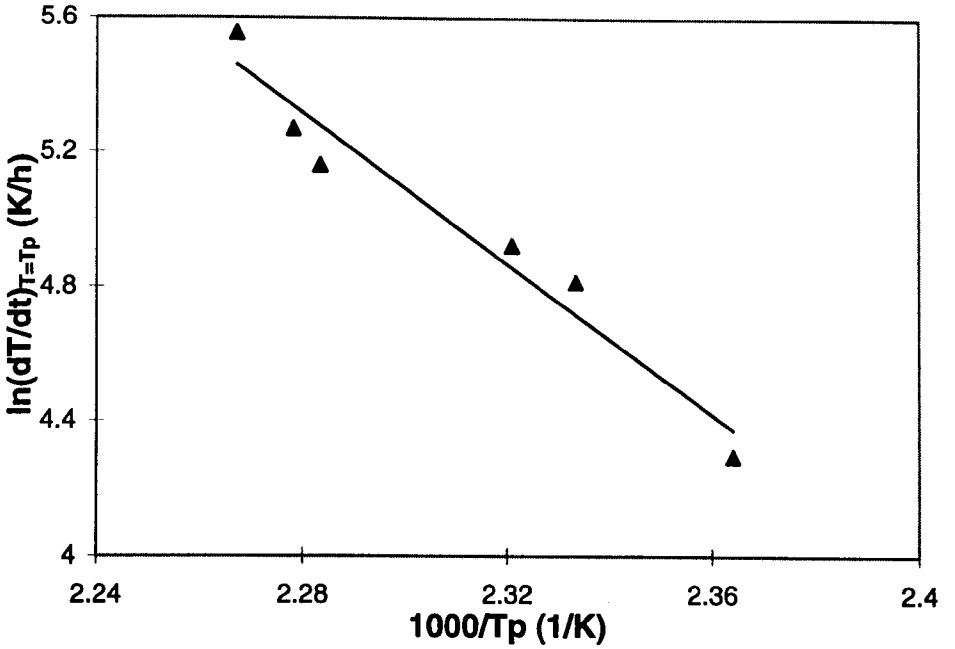

Figure 6.12 A linear plot of $\ln\left[\frac{dT}{dt}\right]_{T=T_p}$ versus $\frac{1000}{T_p}$ for 5% $MgCO_3$-added-Coal M3 in a wire-mesh reactor (B-1)

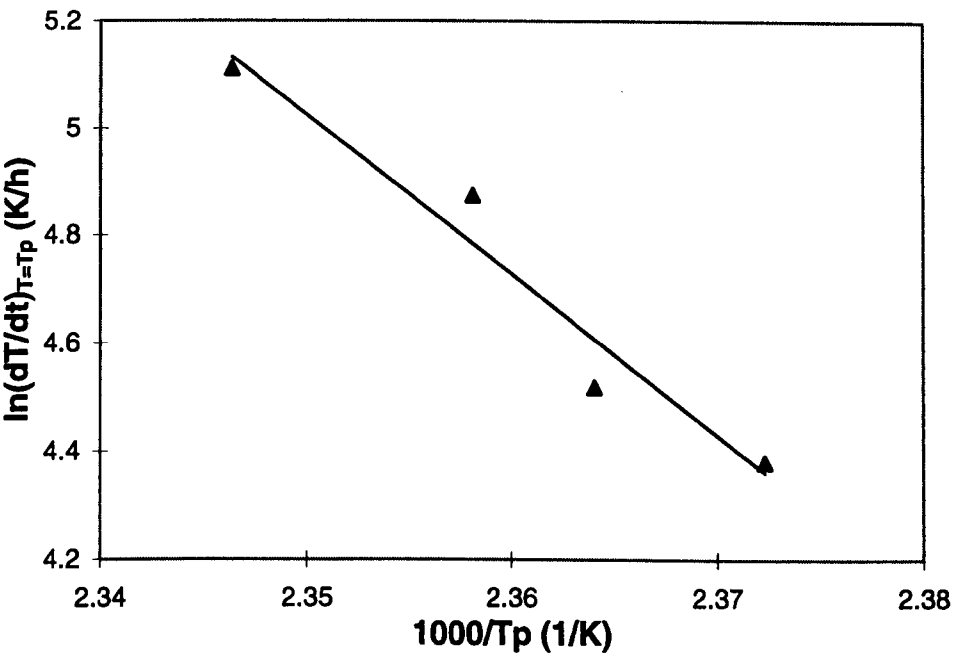

Figure 6.13 A linear plot of $\ln\left[\frac{dT}{dt}\right]_{T=T_p}$ versus $\frac{1000}{T_p}$ for 5% $Ca(OH)_2$-added-Coal M3 in a wire-mesh reactor (B-1)

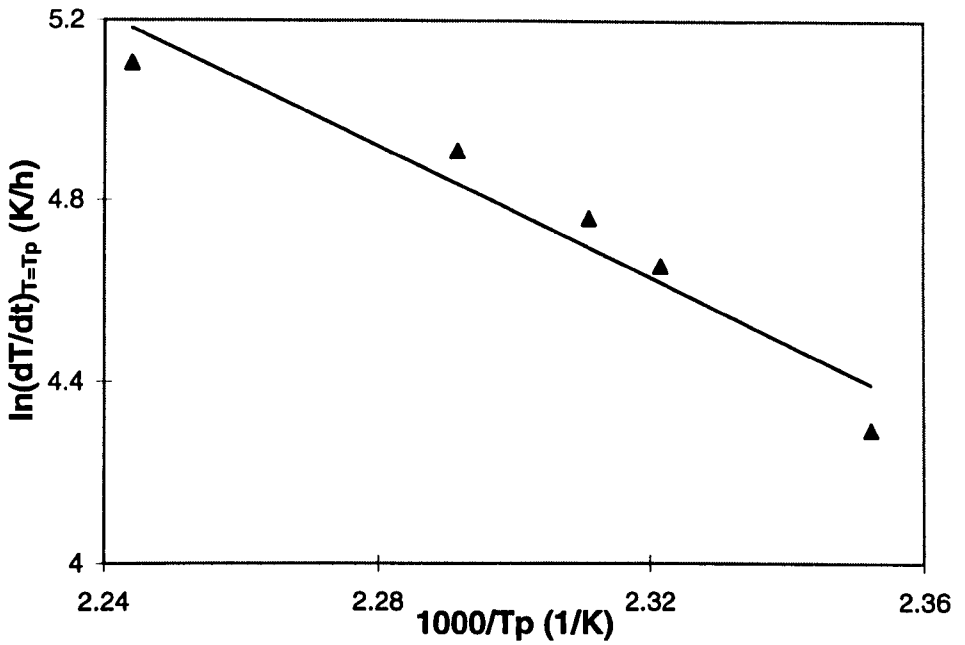

Figure 6.14 A linear plot of $\ln\left[\frac{dT}{dt}\right]_{T=T_p}$ versus $\frac{1000}{T_p}$ for 5% NaOH-added-Coal M3 in a wire-mesh reactor (B-1)

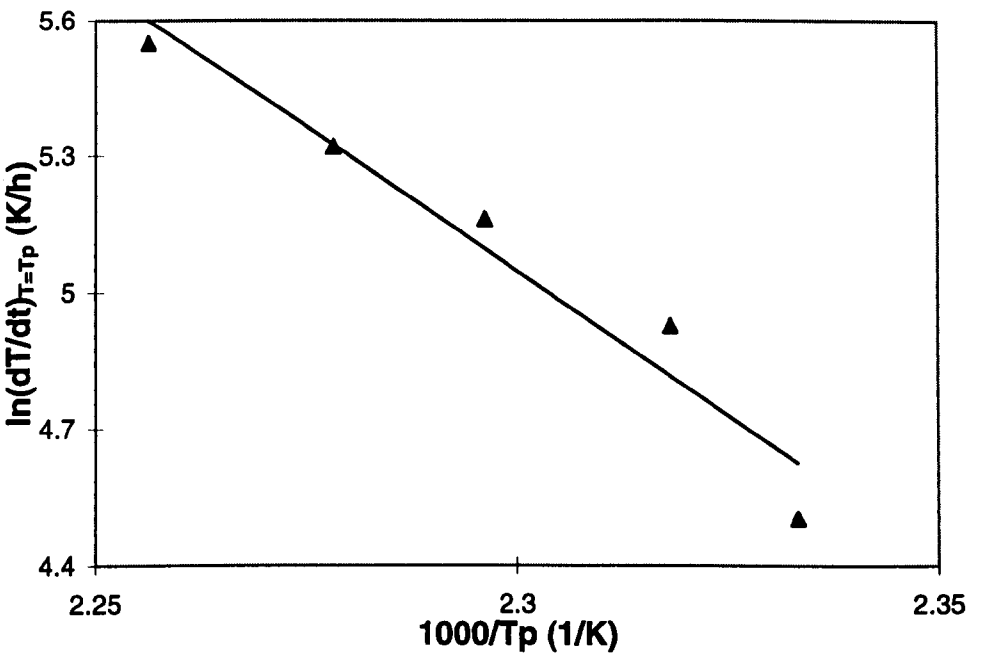

Figure 6.15 A linear plot of $\ln\left[\frac{dT}{dt}\right]_{T=T_p}$ versus $\frac{1000}{T_p}$ for 5% $CaCl_2$-added-Coal M3 in a wire-mesh reactor (B-1)

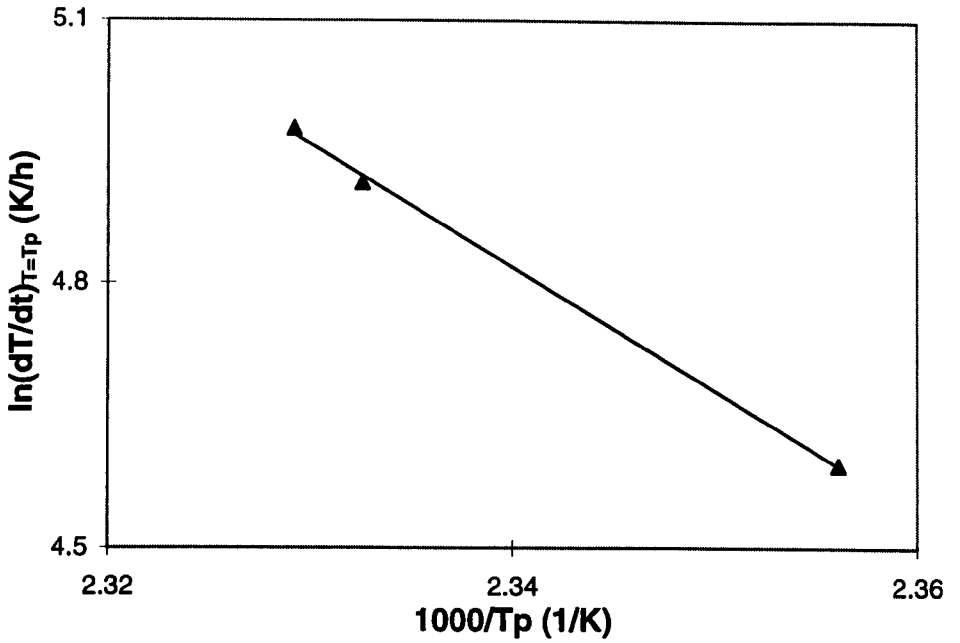

Figure 6.16 A linear plot of $\ln\left[\frac{dT}{dt}\right]_{T=T_p}$ versus $\frac{1000}{T_p}$ for 5% NaCl-added-Coal M3 in a wire-mesh reactor (B-1)

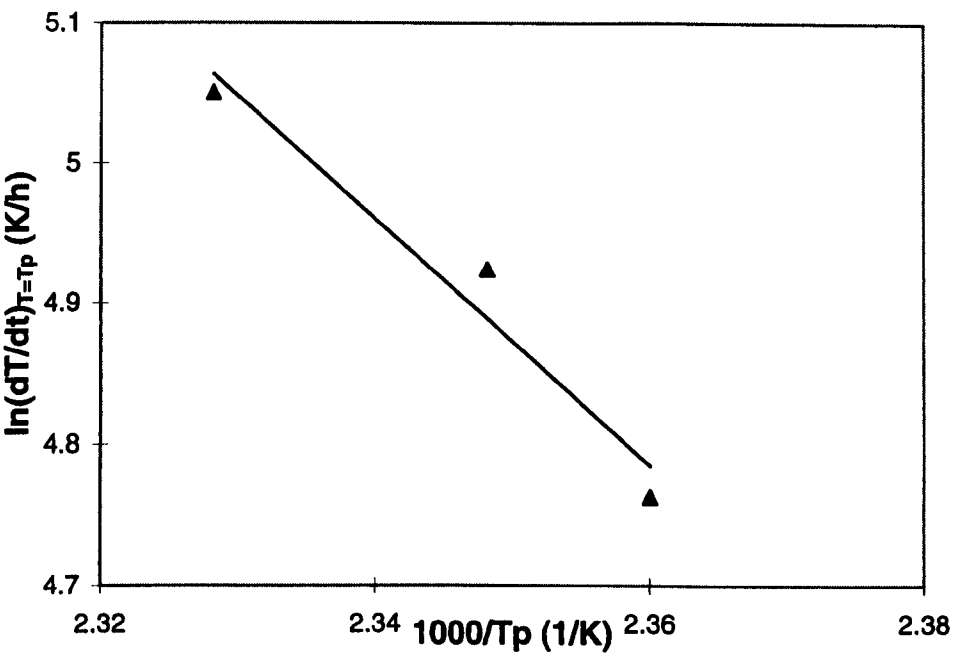

Figure 6.17 A linear plot of $\ln\left[\frac{dT}{dt}\right]_{T=T_p}$ versus $\frac{1000}{T_p}$ for 1% NaAc-added-Coal M3 in a wire-mesh reactor (B-1)

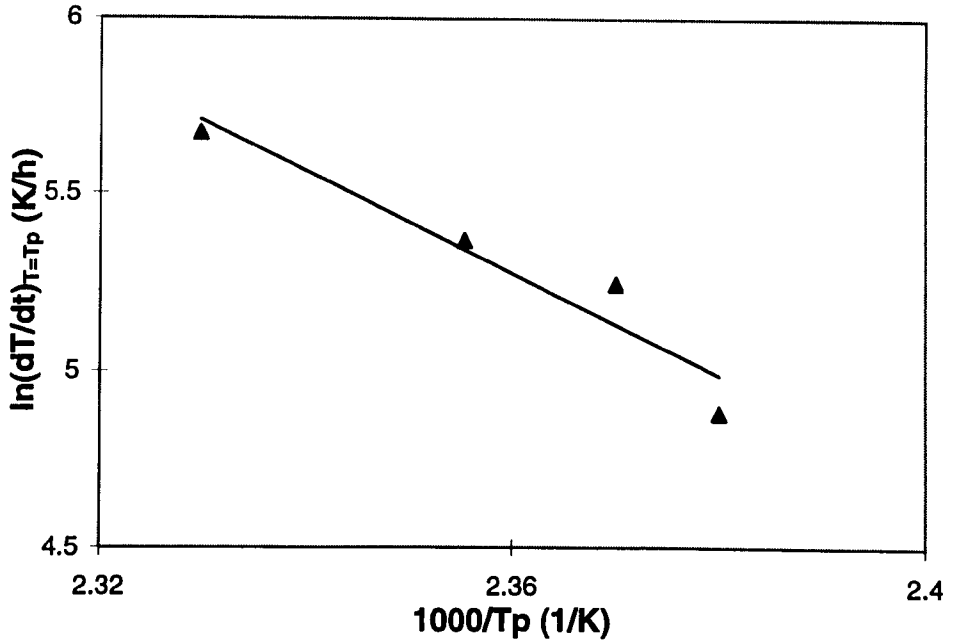

Figure 6.18 A linear plot of $\ln\left[\frac{dT}{dt}\right]_{T=T_p}$ versus $\frac{1000}{T_p}$ for 10% NaAc-added-Coal M3 in a wire-mesh reactor (B-1)

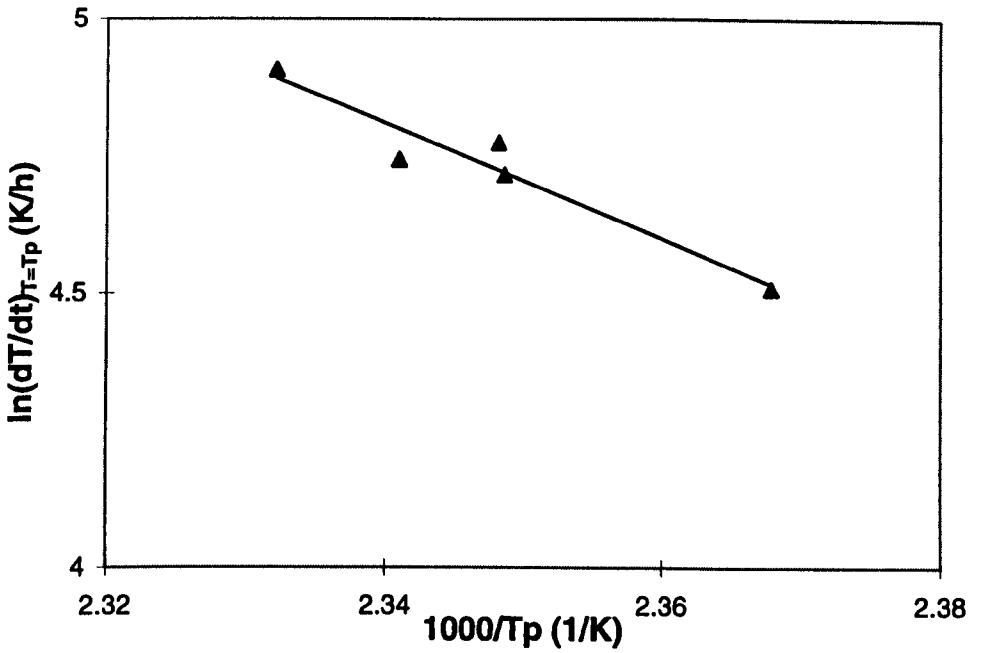

Figure 6.19 A linear plot of $\ln\left[\frac{dT}{dt}\right]_{T=T_p}$ versus $\frac{1000}{T_p}$ for 1% $Ca(Ac)_2$-added-Coal M3 in a wire-mesh reactor (B-1)

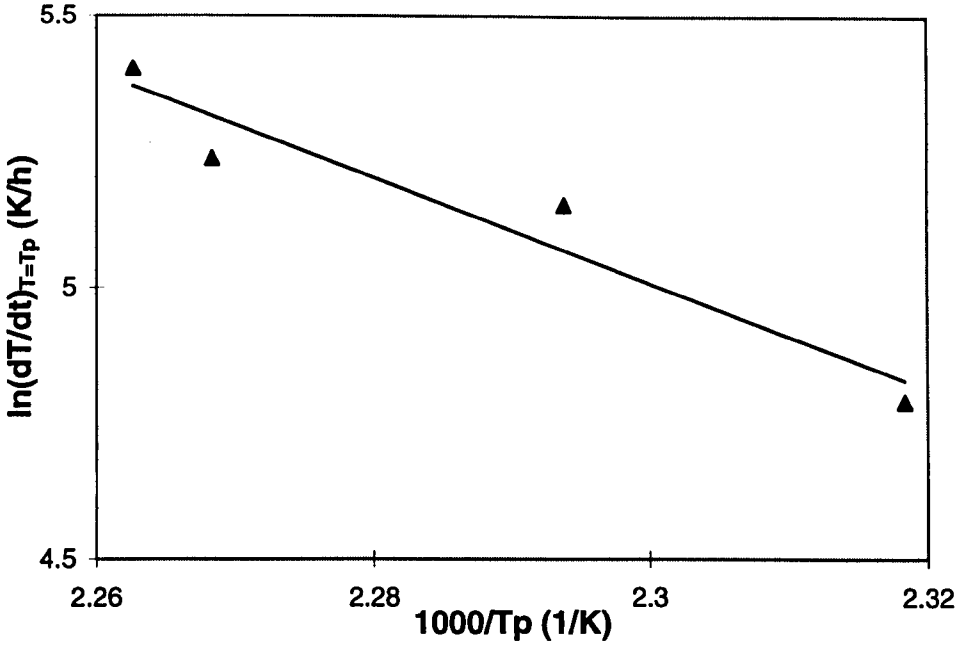

Figure 6.20 A linear plot of $\ln\left[\frac{dT}{dt}\right]_{T=T_p}$ versus $\frac{1000}{T_p}$ for 10% $Ca(Ac)_2$-added-Coal M3 in a wire-mesh reactor (B-1)

The kinetic constants, A and E, for various samples were also summarised in Tables 6.1 to 6.4. The A and E obtained were then used to estimate the reaction rates of the coal samples.

Figure 6.21 compares the Arrhenius plots of reaction rate of acid-washed coal and samples with various promotion agents. It is shown that the presence of $CuCO_3$ in the coal resulted in the highest reactivity, which corresponded to the lowest critical ambient temperature observed. The reactivities of the samples with the presence of $Cu(Ac)_2$ and Na_2CO_3 were lower than that of the sample with $CuCO_3$, but higher than that of the acid-washed coal sample, which again were in a good agreement with the critical ambient temperatures observed. The reactivities of samples with the presence of NaAc, $CaCO_3$, and $Ca(OH)_2$ were similar. However, they were slightly higher than that with K_2CO_3, which was not in agreement with their critical ambient temperature data. Furthermore, the reactivity of sample with KAc was slightly lower than that of acid-washed coal. The small discrepancies observed in reactivity-critical ambient temperature correlation, could be due to inaccuracy in the density and

specific heat capacity of the samples used in Equation (3-10). The values of the density and specific heat capacity of the samples could have changed during various sample preparation procedures. However, they have been assumed to be constant in the kinetic estimations.

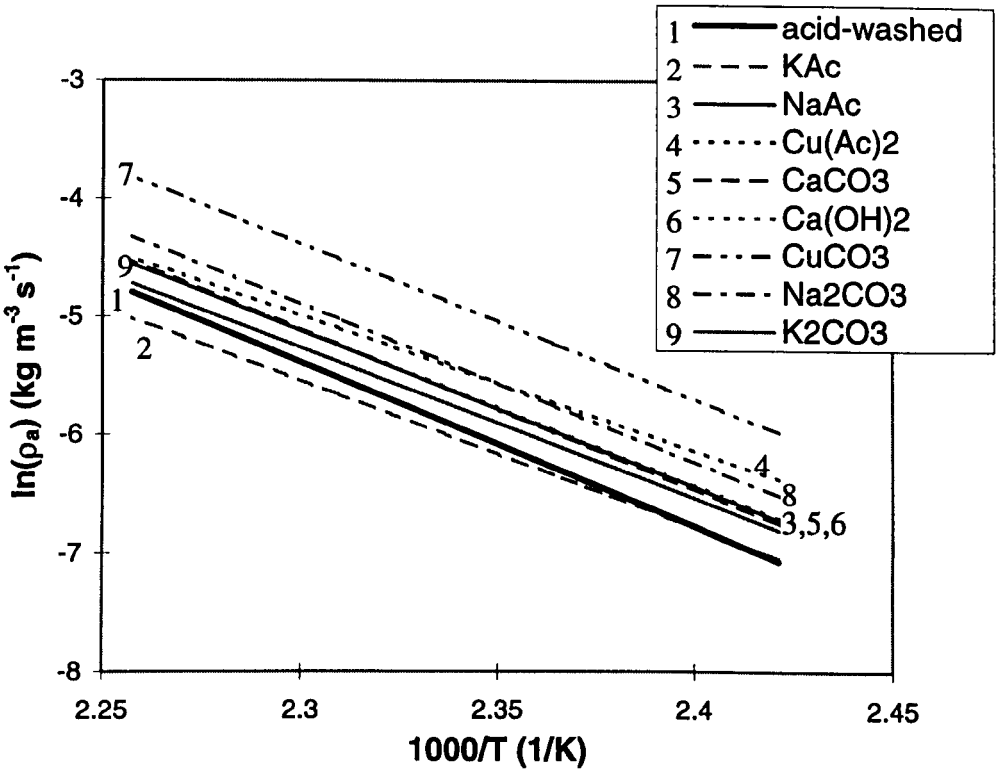

Figure 6.21 Comparison of reaction rates for various samples with promotion agents in temperature range of 140-170°C

Figure 6.22 compares the Arrhenius plots of reaction rate of acid-washed coal and various samples with inhibition agents. It is shown that within the temperature range of 155 to 170 °C, the presence of NaOH and $Mg(Ac)_2$ in the coals resulted in similar reactivities and were lower than others. This corresponded to the lowest critical ambient temperatures observed for these samples. The reactivities of the samples with $CaCl_2$ and $MgCO_3$ were similar and higher than those with NaOH and $Mg(Ac)_2$, but lower than those with NaCl and $Ca(Ac)_2$. These were again in a good agreement with the critical ambient temperatures observed in the experiments. The overall trend of the experimental results showed that the higher the critical ambient temperature of a sample, the lower its oxidation reactivity.

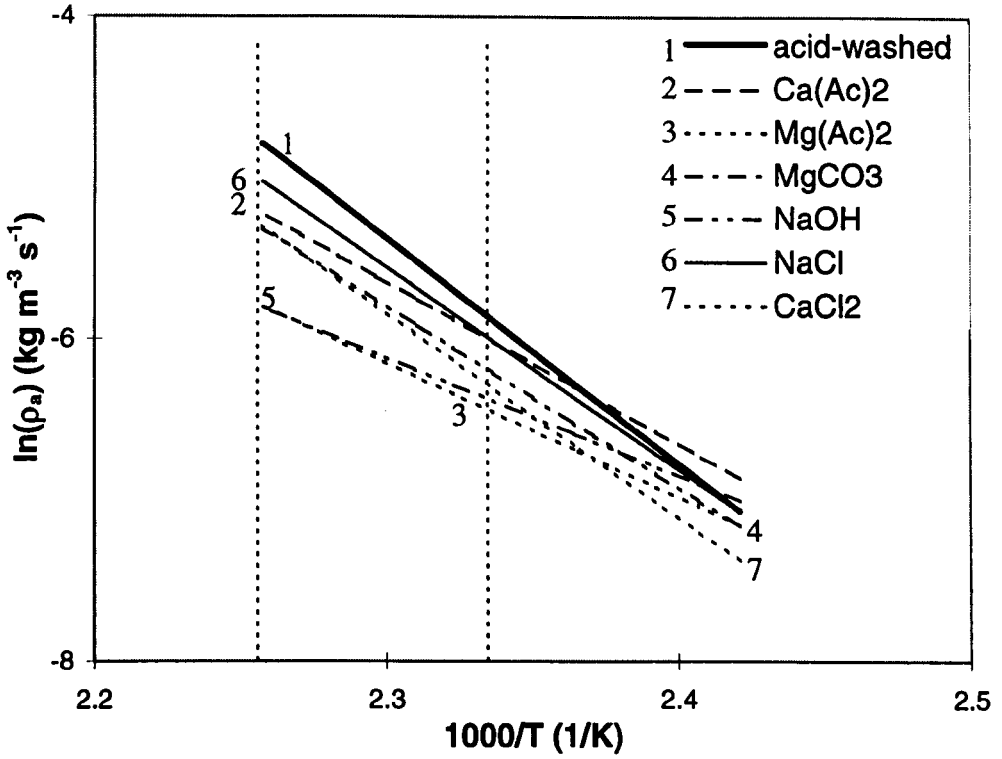

Figure 6.22 Comparison of reaction rates for various samples with inhibition agents in temperature range of 140-170°C

Figure 6.23 compares the Arrhenius plots of reaction rate of several samples with the presence of $Ca(Ac)_2$ and NaAc at various loadings. It is shown that 10 %wt. of NaAc in the coal sample resulted the highest reaction rate compared to those with lower NaAc loadings (1 and 5 %wt.), which corresponded to the critical ambient temperatures observed. Figure 6.23 also shows that although, within the experimental accuracy, samples with 1, 5 and 10 %wt. of $Ca(Ac)_2$ had the same critical ambient temperature, 10% $Ca(Ac)_2$-added-coal sample had the lowest reactivity towards the oxidation reaction. The experimental results indicated that the reactivities of NaAc-added-coal samples increased with an increase in the additive loading, while that of $Ca(Ac)_2$-added-coal samples showed an opposite trend.

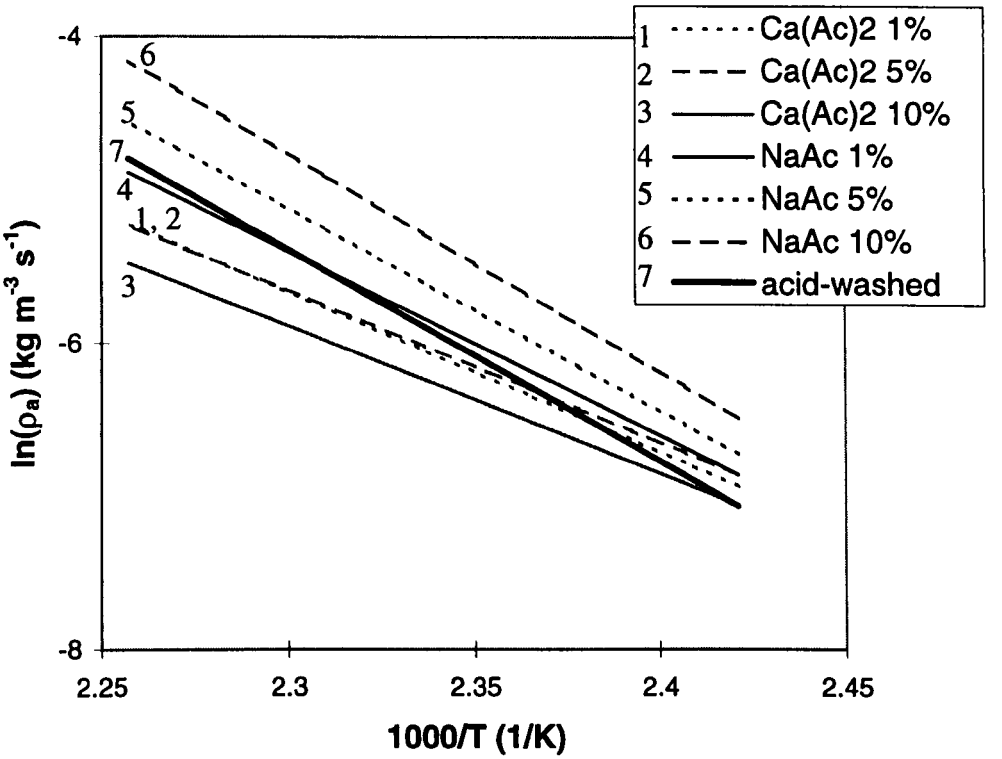

Figure 6.23 The effect of concentration on additive bulk loading on the estimated oxidation rates for $Ca(Ac)_2$ and NaAc-added-coal samples

6.5 ION-EXCHANGE

Whether the capability of the additives to either inhibit or promote the coal spontaneous combustion is physical or chemical in nature was also examined in this study by employing the ion exchange procedure in addition to the bulk-loading procedure. The bulk loading of additives mixed the additives and coal samples both physically and chemically, while the ion exchange mixed them only chemically. The self-heating behaviour of the ion-exchanged samples were compared with those of the bulk-loading samples. Typical promotion (NaAc, KAc, and $Cu(Ac)_2$) and inhibition ($CaCl_2$, $Ca(Ac)_2$, $Mg(Ac)_2$, and NaCl) agents of spontaneous combustion, were used for this purpose. The solution concentration used for each additive was 0.5M, except for $Cu(Ac)_2$ which was 0.25M. To examine the effect of additive solution concentrations for ion-exchanged on the capability of the additives to affect

spontaneous combustion, samples with 0.1M and 1.0M of NaAc and $Ca(Ac)_2$ solutions were also prepared and tested.

6.5.1 Ion-Exchange

Table 6.5 The amount of cations absorbed in various ion-exchanged coal samples

Solution	Cation % w/w (db)
0.25M Cu(Ac)2	4.83
0.5M KAc	2.08
0.1M NaAc	0.78
0.5M NaAc	1.22
1.0M NaAc	1.50
0.1M $Ca(Ac)_2$	1.12
0.5M $Ca(Ac)_2$	1.52
1.0M $Ca(Ac)_2$	1.71
0.5M NaCl	0.13
0.5M $CaCl_2$	0.21
0.5M $Mg(Ac)_2$	0.86

The amounts of cations absorbed in the ion-exchanged samples were measured by Atomic Absorption Spectrophotometry and summarised in Table 6.5. It is shown that the amount of cations in the acetic salts which can be absorbed into the coal were larger than those in chloride salts. Previous work done by Ye (1994) suggested that impregnating coal with the chloride salt solution only caused physical absorption of cation on the coal surface and offered little cation exchange with H^+ from carboxylic functional groups in the coal, while in the solutions of acetate salts, cations were exchanged into functional groups in the coal. Furthermore, it was also observed that for both NaAc and $Ca(Ac)_2$, the loading increased with increasing solution concentration.

6.5.2 The Effect of Additives

Table 6.6 Summary of the critical ambient temperatures and kinetic constants estimated for various ion-exchange samples

Samples	Tcrit (°C)	E (kJ mol^{-1})	A (s^{-1})
0.25M $Cu(Ac)_2$-ion-exchanged-coal	127.5 ± 0.5	116.9	2.61×10^9
0.5M KAc-ion-exchanged-coal	145.5 ± 0.5	125.1	1.19×10^{10}
0.5M NaAc-ion-exchanged-coal	152.5 ± 0.5	114.6	2.76×10^8
Acid-washed coal	154.5 ± 0.5	115.4	2.50×10^8
0.5M $Ca(Ac)_2$-ion-exchanged-coal	154.5 ± 0.5	115.4	2.58×10^8
0.5M NaCl-ion-exchanged-coal	159.5 ± 0.5	119.1	6.59×10^8
0.5M $CaCl_2$-ion-exchanged-coal	161.5 ± 0.5	124.0	2.44×10^9
0.5M $Mg(Ac)_2$-ion-exchanged-coal	161.5 ± 0.5	141.2	2.14×10^{11}

The ion-exchanged coal samples were also tested in the wire-mesh reactor (B-1). Table 6.6 summarises the critical ambient temperatures of various ion-exchanged samples. It is observed that the presence of $Cu(Ac)_2$, KAc, and NaAc in the ion-exchanged samples decreased the critical ambient temperature of acid washed coal by 27, 9, and 2 °C to 127.5, 145.5, and 152.5 °C, respectively, indicating their abilities to promote spontaneous combustion. $Ca(Ac)_2$ in ion-exchanged sample, however, did not have any significant effect on coal spontaneous combustion as its critical ambient temperature (154.5 ± 0.5) was the same as that of acid-washed coal. On the other hand, the critical ambient temperature of ion-exchanged samples with the presence of NaCl, $CaCl_2$, and $Mg(Ac)_2$ were higher than that of acid washed coal, indicating their inhibition effects on spontaneous combustion.

The effects of additives on coal spontaneous combustion observed from experiments using both ion-exchanged and bulk-loading samples were found to be consistent. Detailed comparison of these results is presented in the last section of this chapter.

6.5.3 The Effect of Cation Loading

Table 6.7 Summary of the critical ambient temperatures and kinetic constants estimated for various ion-exchanged samples

Sample	Tcrit (°C)	E (kJ mol^{-1})	A (s^{-1})
1.0M NaAc-ion-exchanged-coal	149.5 ± 0.5	102.8	1.28×10^7
0.5M NaAc-ion-exchanged-coal	152.5 ± 0.5	114.6	2.76×10^8
0.1M NaAc-ion-exchanged-coal	154.5 ± 0.5	111.7	1.16×10^8
Acid-washed coal	154.5 ± 0.5	115.4	2.50×10^8
0.1M $Ca(Ac)_2$-ion-exchanged-coal	154.5 ± 0.5	114.6	2.08×10^8
0.5M $Ca(Ac)_2$-ion-exchanged-coal	154.5 ± 0.5	115.4	2.58×10^8
1.0M $Ca(Ac)_2$-ion-exchanged-coal	154.5 ± 0.5	116.0	3.10×10^8

In order to investigate the effect of additive solution concentrations on the capability of additives to affect spontaneous combustion, samples with 0.1, 0.5, and 1.0 M of NaAc and $Ca(Ac)_2$ were prepared and tested. As stated previously, it is observed that for both NaAc and $Ca(Ac)_2$, the cation loading increased with increasing solution concentration. Table 6.7 presents the critical ambient temperatures of these samples, together with that of acid washed Coal M3 and those of samples with 0.5M NaAc and 0.5M $Ca(Ac)_2$. It is noticed that the critical ambient temperature of coal samples with NaAc decreased with increasing cation loading, indicating that

promotion effect of this additive on spontaneous combustion depended on its cation loading. On the other hand, the critical ambient temperature of coal samples with $Ca(Ac)_2$ (154.5 ± 0.5 °C) remained unchanged with varying cation loadings, and showed the same value as that of the acid-washed coal. This indicated that, regardless of its cation loading, the presence of $Ca(Ac)_2$ in the ion-exchanged samples could not significantly affect the coal spontaneous combustion.

6.5.4 Estimation of Low-Temperature Oxidation Kinetics

The low-temperature oxidation kinetics were again estimated. Figures 6.24 to 6.34 show linear plots of $\ln (dT/dt)_{T=Tp}$ versus $1000/T_p$ for ion-exchanged samples with various additives. The range of T_p over which the kinetic experiments were carried out was 125-165 °C.

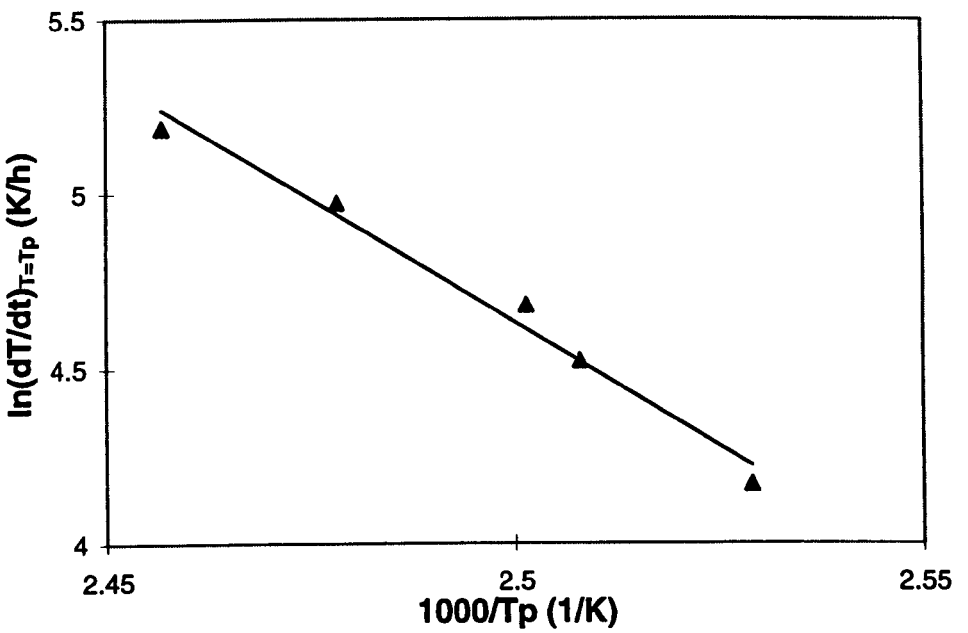

Figure 6.24 A linear plot of $\ln\left[\frac{dT}{dt}\right]_{T=T_p}$ versus $\frac{1000}{T_p}$ for 0.25M $Cu(Ac)_2$-ion-exchanged coal in a wire-mesh reactor (B-1)

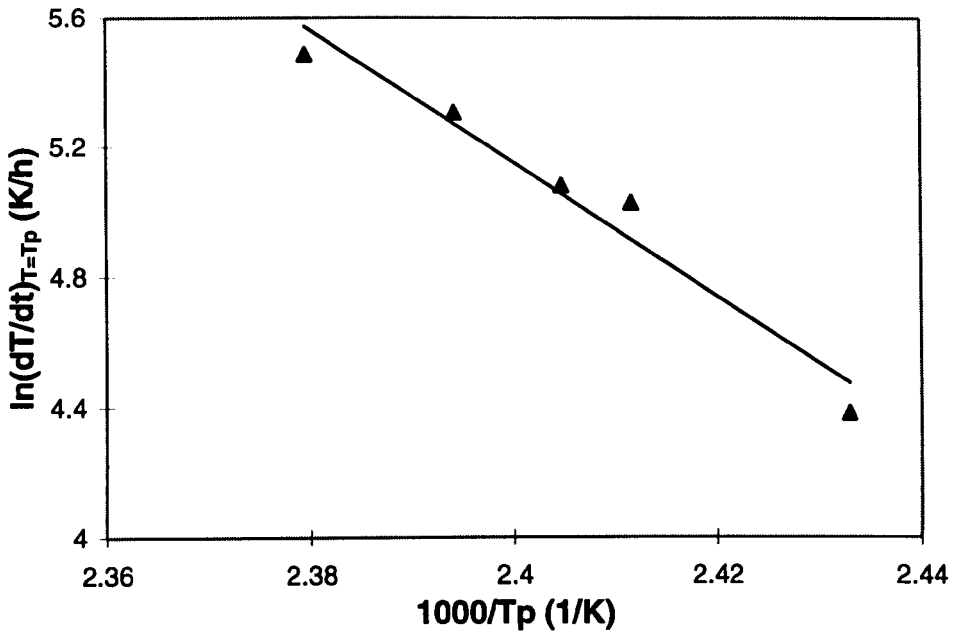

Figure 6.25 A linear plot of $\ln\left[\frac{dT}{dt}\right]_{T=T_p}$ versus $\frac{1000}{T_p}$ for 0.5M KAc-ion-exchanged sample in a wire-mesh reactor (B-1)

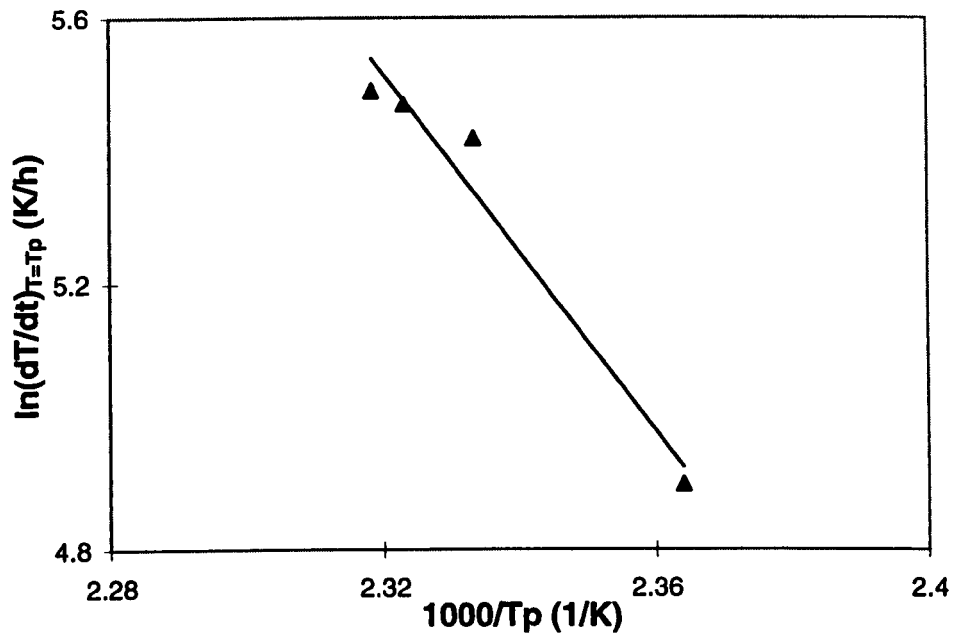

Figure 6.26 A linear plot of $\ln\left[\frac{dT}{dt}\right]_{T=T_p}$ versus $\frac{1000}{T_p}$ for 0.1M NaAc-ion-exchanged sample in a wire-mesh reactor (B-1)

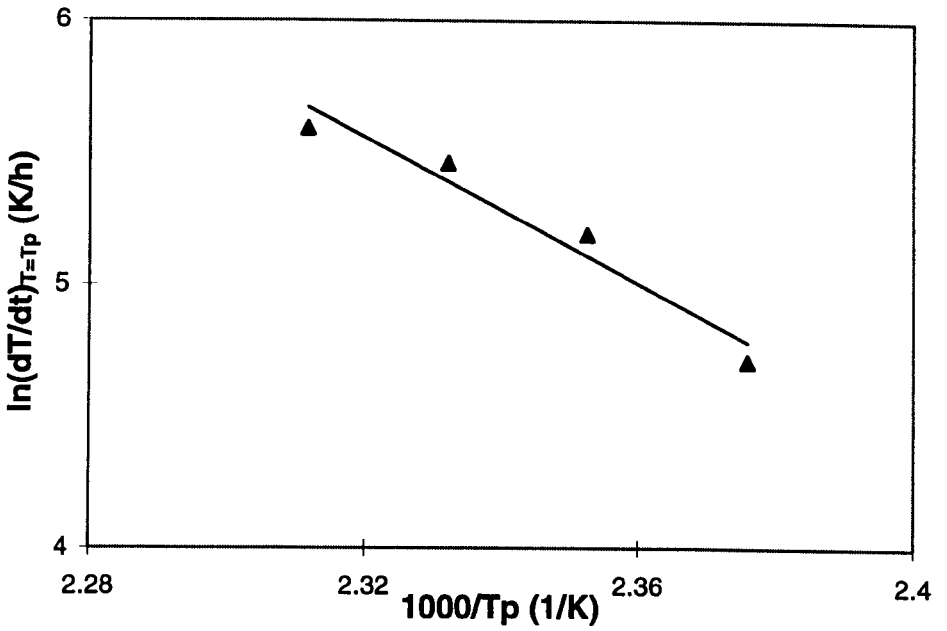

Figure 6.27 A linear plot of $\ln\left[\frac{dT}{dt}\right]_{T=T_p}$ versus $\frac{1000}{T_p}$ for 0.5M NaAc-ion-exchanged sample in a wire-mesh reactor (B-1)

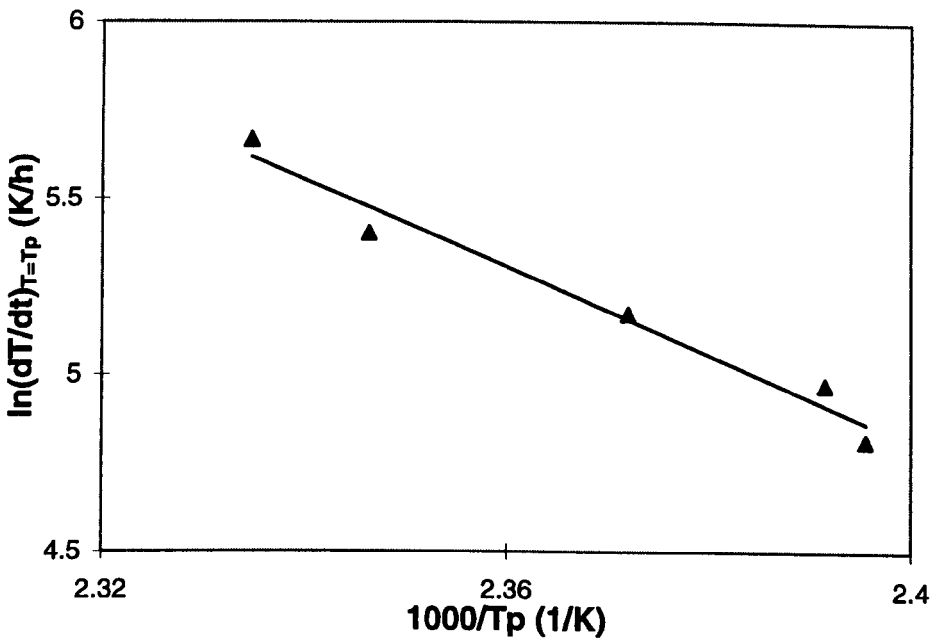

Figure 6.28 A linear plot of $\ln\left[\frac{dT}{dt}\right]_{T=T_p}$ versus $\frac{1000}{T_p}$ for 1.0M NaAc-ion-exchanged sample in a wire-mesh reactor (B-1)

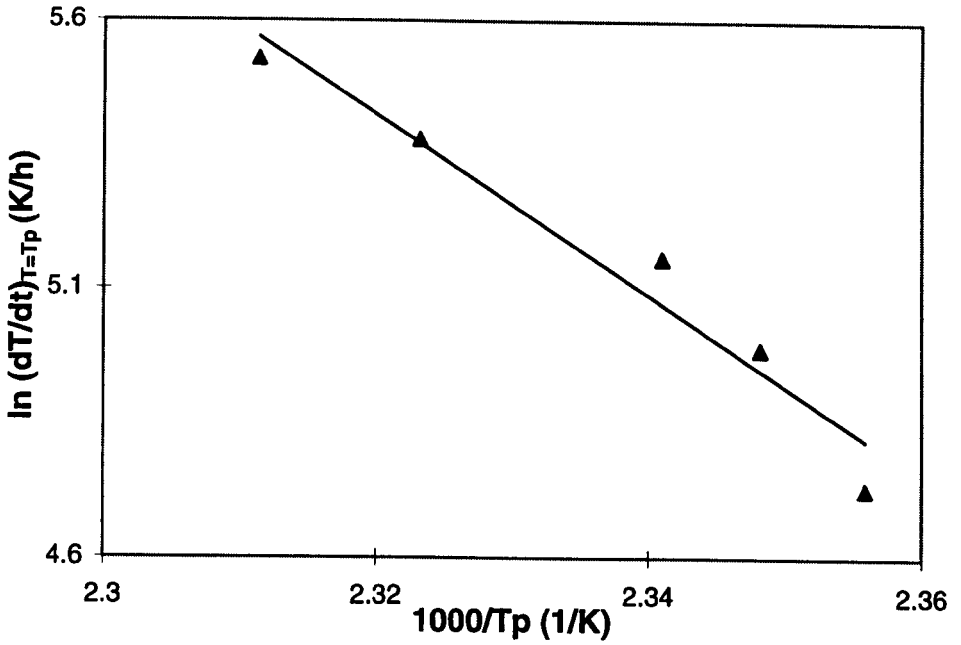

Figure 6.29 A linear plot of $\ln\left[\frac{dT}{dt}\right]_{T=T_p}$ versus $\frac{1000}{T_p}$ for 0.1M $Ca(Ac)_2$-ion-exchanged sample in a wire-mesh reactor (B-1)

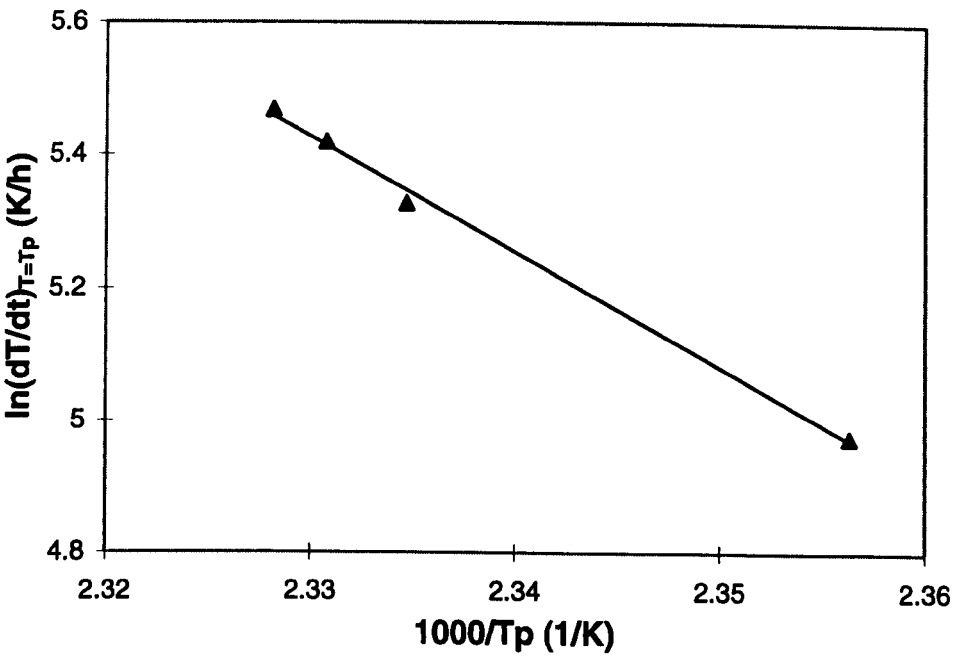

Figure 6.30 A linear plot of $\ln\left[\frac{dT}{dt}\right]_{T=T_p}$ versus $\frac{1000}{T_p}$ for 0.5M $Ca(Ac)_2$-ion-exchanged sample in a wire-mesh reactor (B-1)

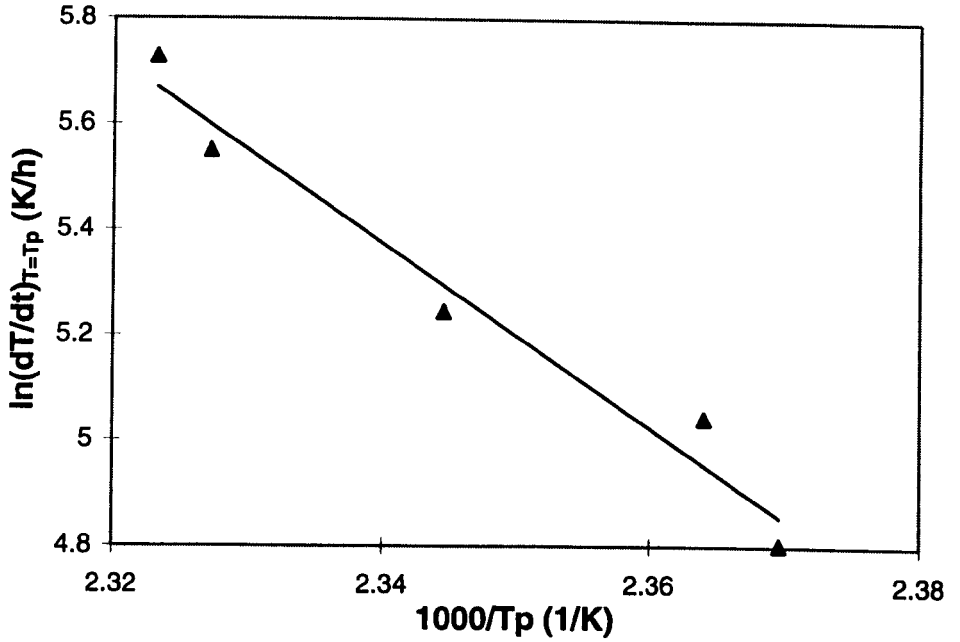

Figure 6.31 A linear plot of $\ln\left[\frac{dT}{dt}\right]_{T=T_p}$ versus $\frac{1000}{T_p}$ for 1.0M $Ca(Ac)_2$-ion-exchanged sample in a wire-mesh reactor (B-1)

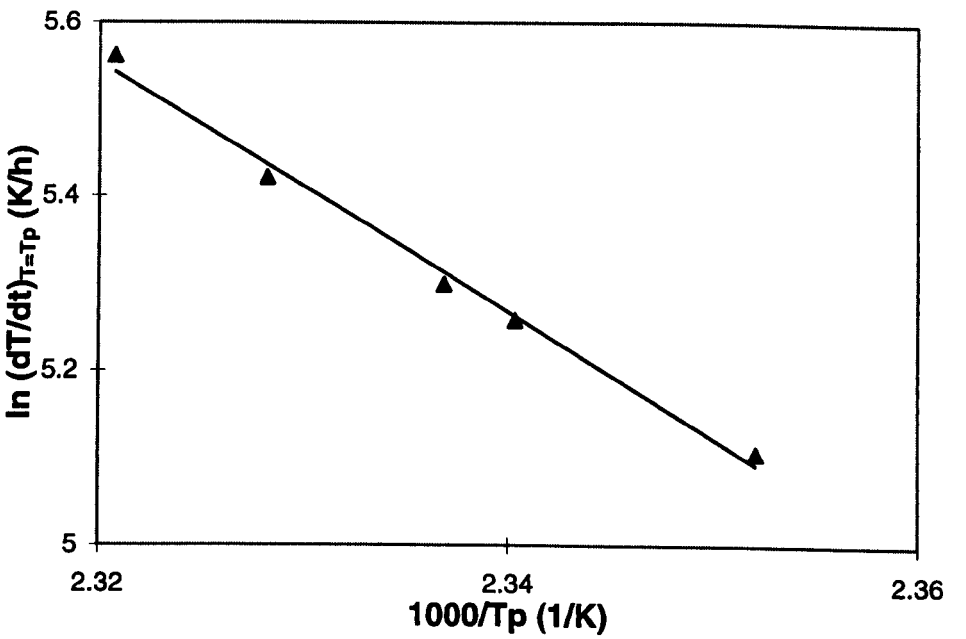

Figure 6.32 A linear plot of $\ln\left[\frac{dT}{dt}\right]_{T=T_p}$ versus $\frac{1000}{T_p}$ for 0.5M NaCl-ion-exchanged sample in a wire-mesh reactor (B-1)

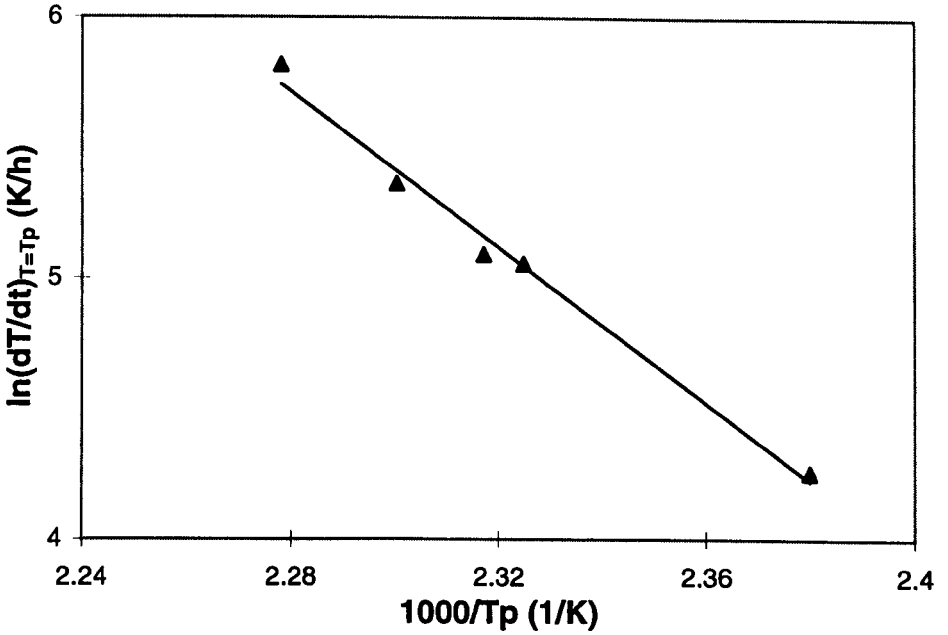

Figure 6.33 A linear plot of $\ln\left[\frac{dT}{dt}\right]_{T=T_p}$ versus $\frac{1000}{T_p}$ for 0.5M $CaCl_2$-ion-exchanged sample in a wire-mesh reactor (B-1)

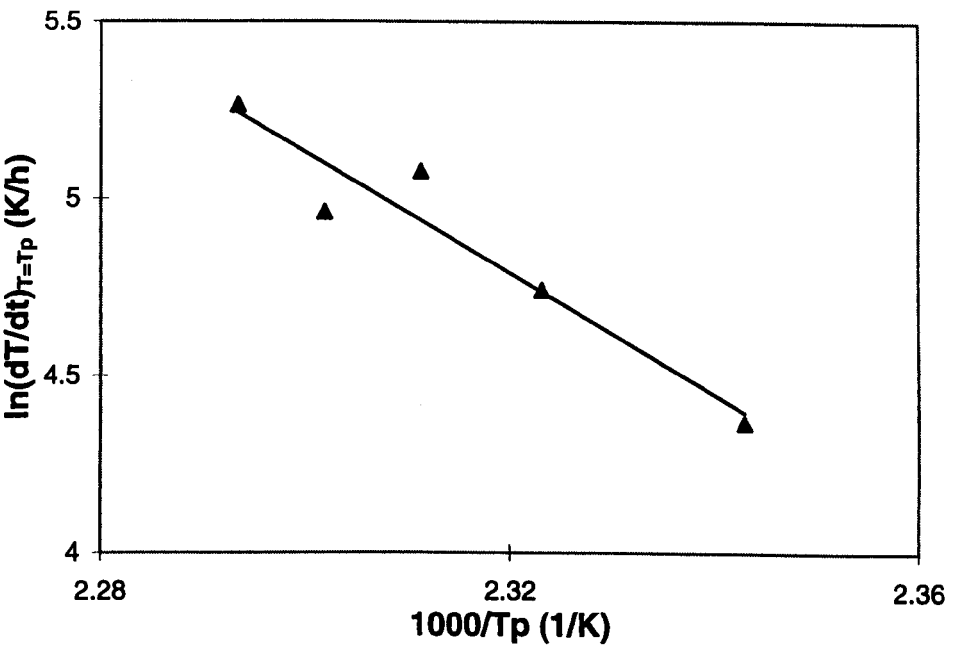

Figure 6.34 A linear plot of $\ln\left[\frac{dT}{dt}\right]_{T=T_p}$ versus $\frac{1000}{T_p}$ for 0.5M $Mg(Ac)_2$-ion-exchanged sample in a wire-mesh reactor (B-1)

The kinetic constants, A and E, for various ion-exchanged samples were also summarised in Tables 6.6 and 6.7. The A and E obtained were then used to estimate the reaction rate of the coal samples.

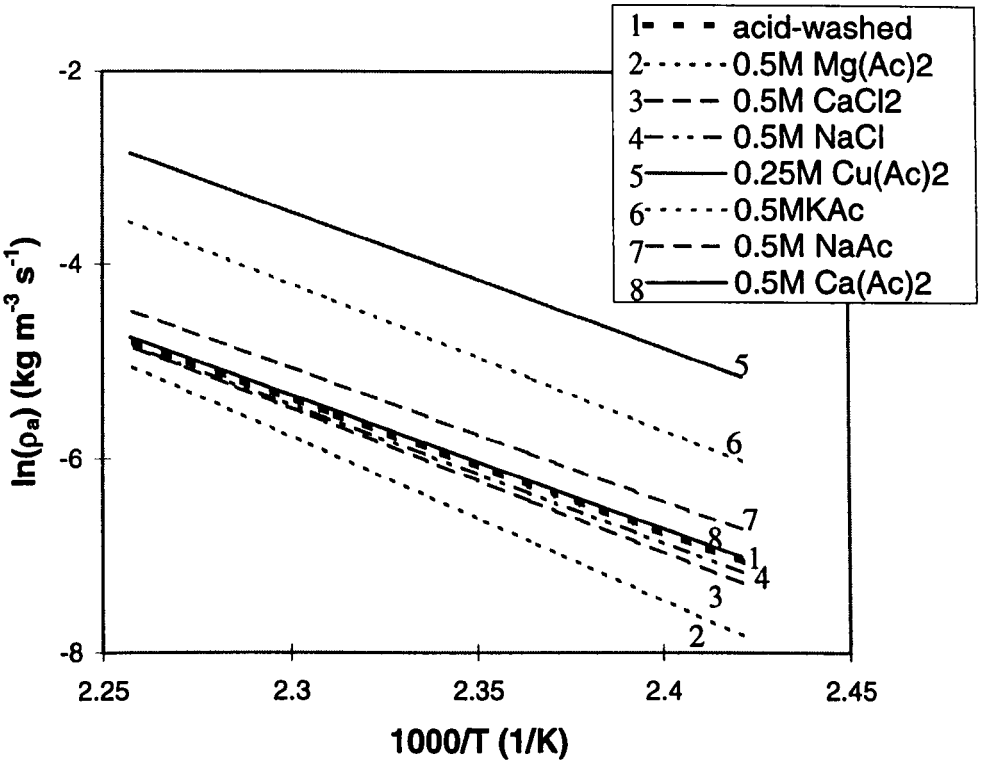

Figure 6.35 Comparison of reaction rates for various ion-exchanged samples in temperature range of 140-170°C

Figure 6.35 compares the Arrhenius plots of reaction rate of various ion-exchanged samples. It is shown that the presence of $Cu(Ac)_2$ in the ion-exchanged coal sample resulted in the highest reaction rate which corresponded to the lowest critical ambient temperature observed. Within temperature range of 140 to 170 °C, the reaction rate of the ion-exchanged samples with the presence of KAc and NaAc were lower than that of the sample with $Cu(Ac)_2$, but higher than that of acid-washed coal sample, which were in a good agreement with the critical ambient temperatures observed. The reaction rates of samples with the presence $Ca(Ac)_2$ was found to be similar to that of acid-washed coal, and was higher than that of 0.5M NaCl-ion-exchanged-coal. Furthermore, although the critical ambient temperatures of 0.5M $CaCl_2$ and $Mg(Ac)_2$-ion-exchanged samples were the same (161.5 ± 0.5

°C), the reactivity of the sample with $Mg(Ac)_2$ was lower than that with $CaCl_2$. This indicated that among the additives chosen for the ion-exchange tests, $Mg(Ac)_2$ was the best inhibition agent for spontaneous combustion.

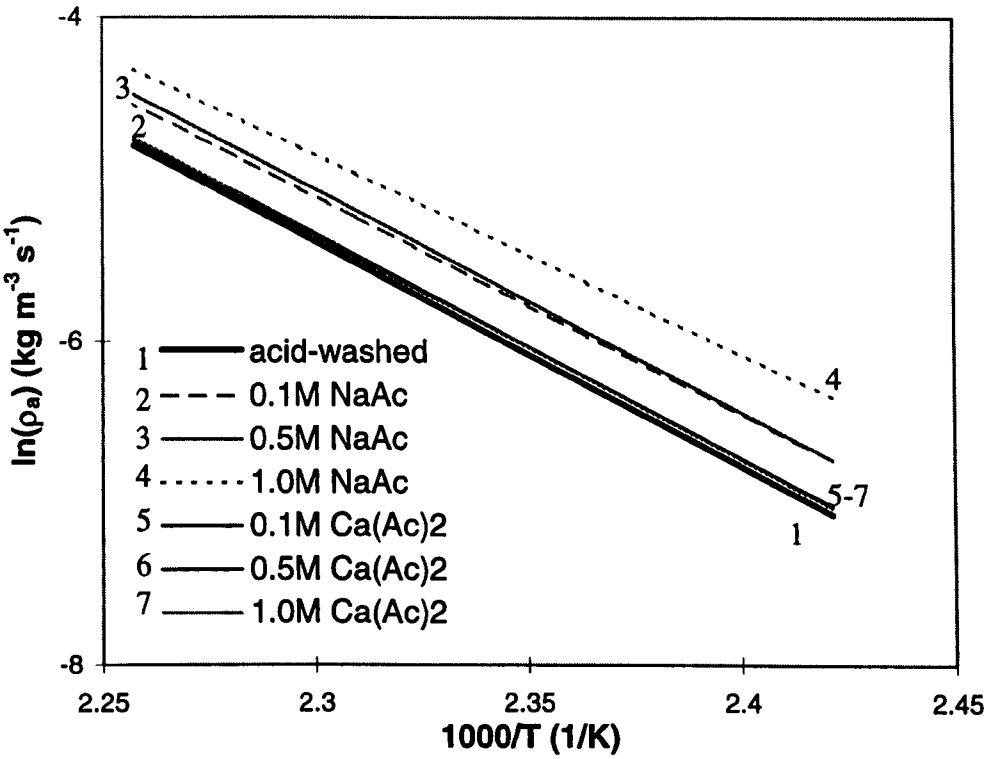

Figure 6.36 The effect of additive solution concentrations on the estimated oxidation rates for NaAc and $Ca(Ac)_2$-ion-exchanged-coal samples in temperature range of 140-170°C

Figure 6.36 compares the reaction rates of $Ca(Ac)_2$ and NaAc-ion-exchanged samples at various solution concentrations. It is shown that 1.0M NaAc applied into the coal sample resulted the highest reactivity compared to those with lower NaAc solution concentrations (0.1 and 0.5M), which corresponded to the critical ambient temperatures observed. Figure 6.36 also shows that the reactivities of the samples with 0.1, 0.5 and 1.0M $Ca(Ac)_2$ were similar to that of acid-washed coal, which were also in a good agreement with the critical ambient temperatures observed. The experimental results using ion-exchanged samples indicated that the reactivities of NaAc-ion-exchanged-coal samples increased with an increase in the additive

solution concentrations, while that of $Ca(Ac)_2$-ion-exchanged-coal samples remained unchanged with varying additive solution concentrations.

6.6 COMPARISON OF RESULTS OBTAINED FROM ION-EXCHANGED AND BULK-LOADING SAMPLES

Table 6.8 Summary of the amount of cations in the ion-exchanged and bulk-loading samples and their respective critical ambient temperatures

ION-EXCHANGE			BULK-LOADING		
Solution	**Cation (%, db)**	**T_{crit} (°C)**	**Additive**	**Cation (%, db)**	**T_{crit} (°C)**
0.25M $Cu(Ac)_2$	4.83	127.5 ± 0.5	5% $Cu(Ac)_2$	1.75	143.5 ± 0.5
0.5M KAc	2.08	145.5 ± 0.5	5% KAc	2.18	151.5 ± 0.5
0.1M NaAc	0.78	154.5 ± 0.5	1% NaAc	0.26	154.5 ± 0.5
0.5M NaAc	1.22	152.5 ± 0.5	5% NaAc	1.12	152.5 ± 0.5
1.0M NaAc	1.50	149.5 ± 0.5	10% NaAc	2.68	150.5 ± 0.5
0.1M $Ca(Ac)_2$	1.12	154.5 ± 0.5	1% $Ca(Ac)_2$	0.30	156.5 ± 0.5
0.5M $Ca(Ac)_2$	1.52	154.5 ± 0.5	5% $Ca(Ac)_2$	1.00	156.5 ± 0.5
1.0M $Ca(Ac)_2$	1.71	154.5 ± 0.5	10% $Ca(Ac)_2$	2.15	156.5 ± 0.5
0.5M NaCl	0.13	159.5 ± 0.5	5% NaCl	1.84	159.5 ± 0.5
0.5M $CaCl_2$	0.21	161.5 ± 0.5	5% $CaCl_2$	1.48	160.5 ± 0.5
0.5M $Mg(Ac)_2$	0.86	161.5 ± 0.5	5% $Mg(Ac)_2$	0.56	164.5 ± 0.5

The experimental results using both bulk-loading and ion-exchanged samples tested in the wire-mesh reactor (B-1), have been described in the previous sections of this

thesis. It was observed that, regardless the additive application procedure used, the additive in the coal showed consistent effects on spontaneous combustion. Variation was observed in the critical ambient temperature obtained from samples with additives applied in different procedures. Table 6.8 summarises the amounts of cations absorbed in various samples and their respective critical ambient temperatures observed in the experiments.

It is shown in Table 6.8 that the amount of cations absorbed in 0.25M $Cu(Ac)_2$-ion-exchanged-coal sample (4.83%) was higher than that in 5% $Cu(Ac)_2$-added-coal sample (1.75%). This resulted a lower critical ambient temperature of the ion-exchanged sample (127.5 ± 0.5 °C) compared to that of bulk-loading sample (143.5 ± 0.5 °C), which indicated that the effectiveness of $Cu(Ac)_2$ to promote the spontaneous combustion was significantly determined by the amount of Cu^{2+} absorbed in the coal. To further investigate the effect of application procedure on the capability of the additive to affect spontaneous combustion, surface area and porosity of both the ion-exchanged and bulk-loading samples were measured by HRL Limited, Australia, as summarised in Table 6.9. It is found that the CO_2 surface area and micropore volume of the ion exchanged sample were larger than those of the bulk loading sample. This provides clear evidence that $Cu(Ac)_2$ added into the coal with the ion-exchange procedure resulted more significant promotion effects on spontaneous combustion compared to that with the bulk-loading procedure.

Table 6.9 Comparison of surface area and micropore volume of samples ion-exchanged and bulk-loaded with $Cu(Ac)_2$

Samples	Tcrit (°C)	CO_2 Surface Area (m^2/g)	Micropore Volume (cm^3/g)
0.25M $Cu(Ac)_2$-ion-exchanged coal	127.5 ± 0.5	280	0.075
5% $Cu(Ac)_2$-added-coal	143.5 ± 0.5	220	0.059

The surface structures and cation loadings of samples, bulk-loaded and ion-exchanged with $Cu(Ac)_2$, were also examined using a Philip XL 20 Scanning Electron Microscope (SEM) with an Energy Dispersive X-ray detector (SEM-EDX). Samples were mounted in an epoxy resin, which was then grounded, polished, and coated with carbon. Figure 6.37 shows the secondary electron images of the surfaces of 5% $Cu(Ac)_2$-added-coal (a-e) and 0.25M $Cu(Ac)_2$-ion-exchanged-coal (f-j) in various magnifications. As shown in Figure 6.37 (e) (bulk-loading) and (j) (ion-exchanged), with a greater magnification (2654×), it can be seen that the pore volume of 0.25M $Cu(Ac)_2$-ion-exchanged-coal is larger than that of 5% $Cu(Ac)_2$-added-coal. This is in a good agreement with the surface area and micropore volume measurements done by HRL Limited, Australia.

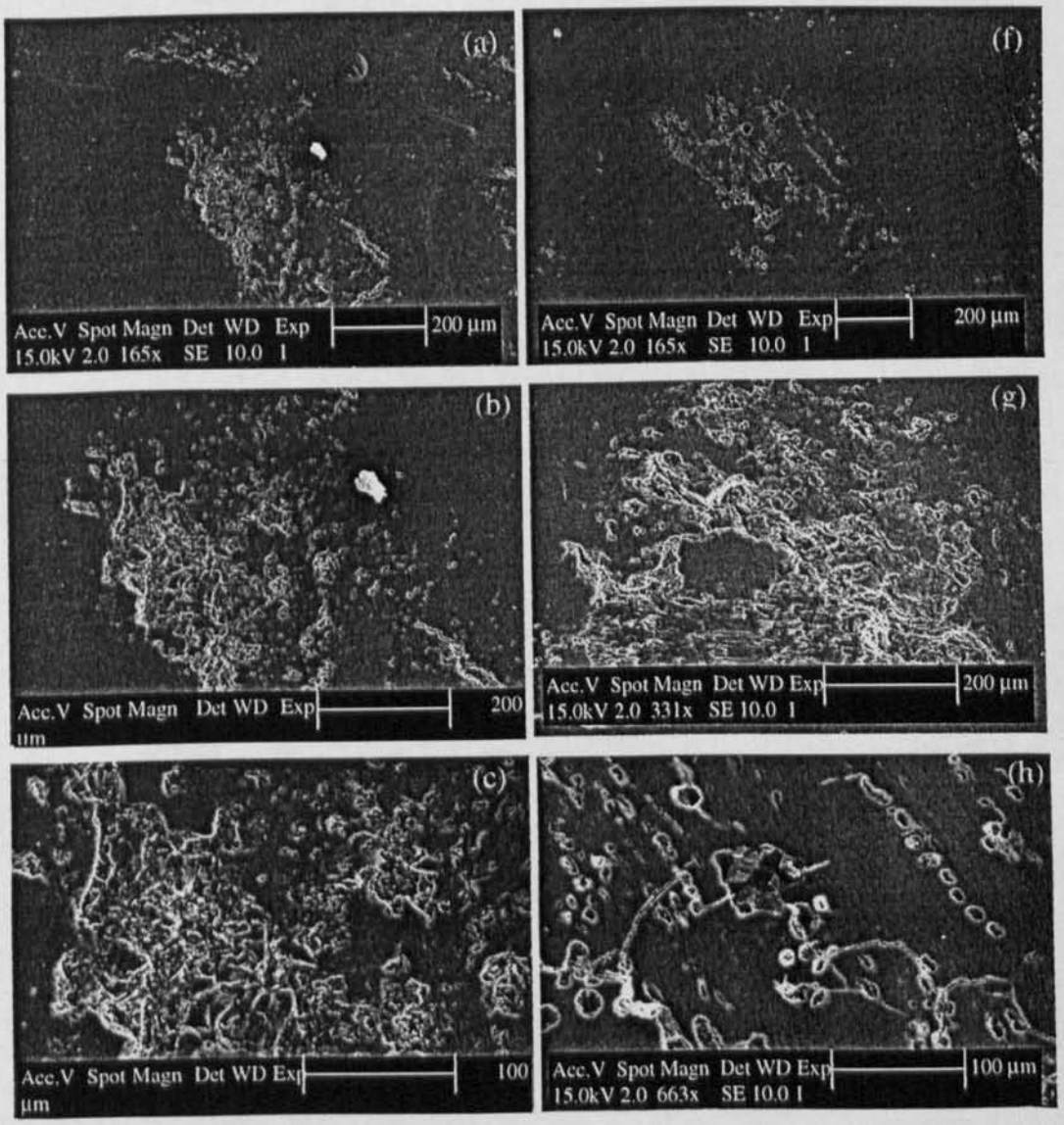

Figure 6.37 (Continued on the next page)

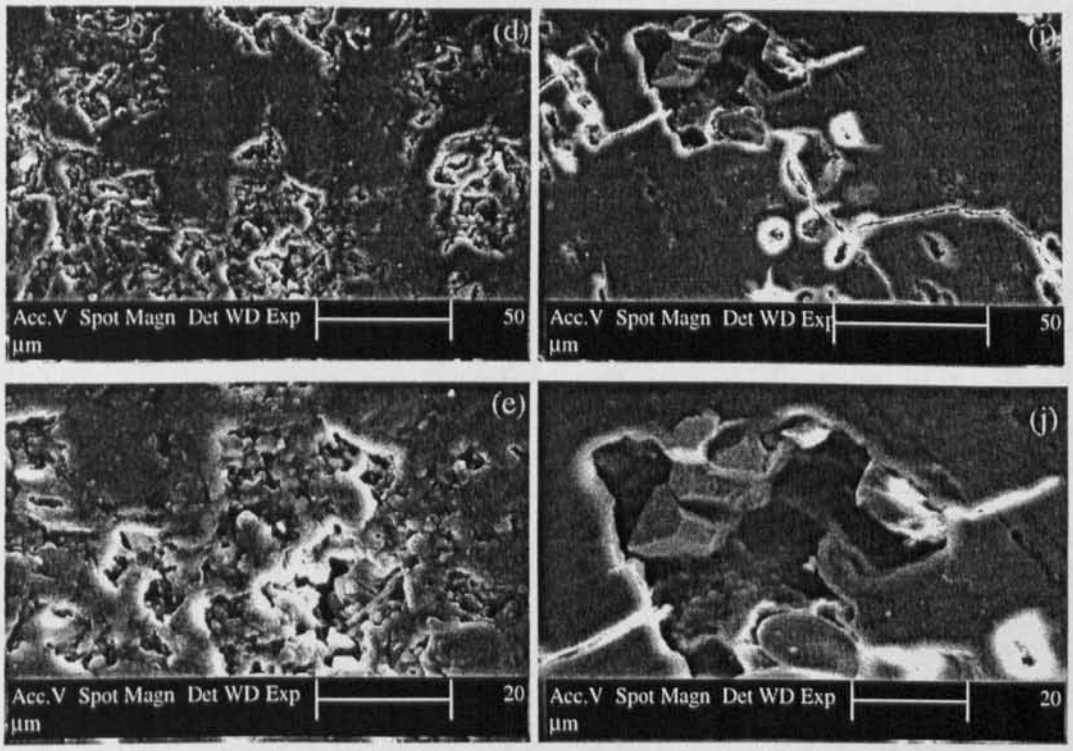

Figure 6.37 Secondary electron images of the surface of 5% $Cu(Ac)_2$-added-coal (a-e) and 0.25M $Cu(Ac)_2$-ion-exchanged-coal (f-j) particle in various magnifications

An EDAX quantitative X-ray detection package (eDXAUTOp) was also employed to conduct multiple spots analysis for various constituents in the coal particle. It was observed that the average percentage of Cu, taken from 20 spots, in the ion-exchanged particle was 7.38 ± 1.80 %wt., which was higher than that in the bulk-loading particle (3.91± 1.28 %wt.). The results are in a good agreement with the result obtained from the Atomic Absorption Spectrophotometry measurement presented previously (Table 6.8).

Back-scattered electron (BSE) images of both 5% $Cu(Ac)_2$-added-coal and 0.25M $Cu(Ac)_2$-ion-exchanged-coal samples were also taken to examine how copper is distributed in the coal particle. Samples analysed in this manner were prepared by mounting the particles on aluminium stubs and then coated with a gold-palladium mixture. Figure 6.38 shows the BSE images of both bulk-loading (a-f) and ion-exchange (g-l) samples in various magnifications. Carbon topography can be

observed from the variation in light and dark shades of grey in the coal particles. As atoms of higher atomic weight, such as Cu, emit higher X-rays intensities, the copper particles are observed as the white inclusions distribute amongst carbon in the particle. Figure 6.38 shows that Cu in the ion-exchanged sample was more intimately and uniformly distributed in the coal matrix. Furthermore, supporting the EDAX quantitative analysis, it was also found that the amount of Cu inclusion in the ion-exchanged coal particle was higher than that in the bulk-loading coal particle.

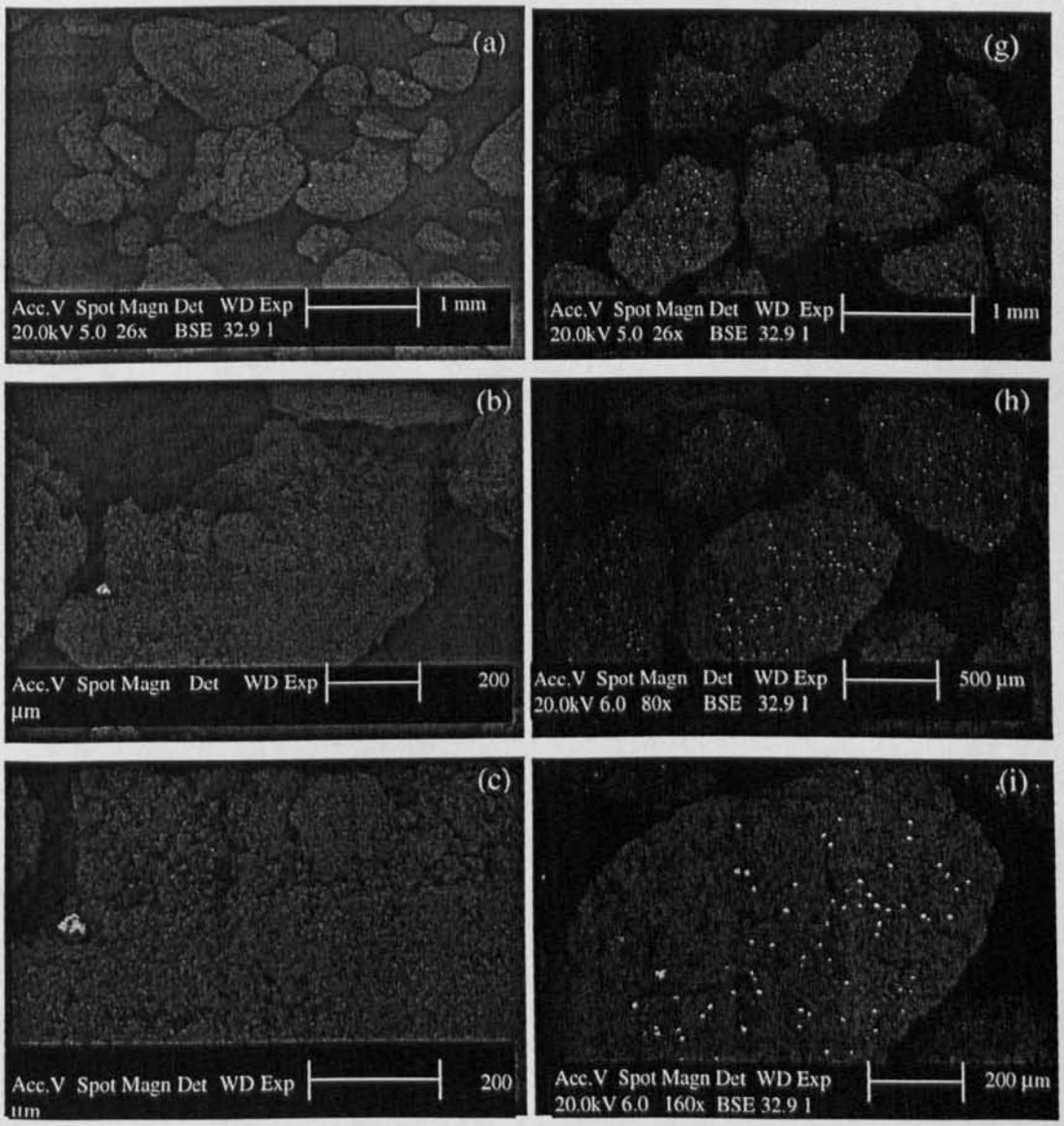

Figure 6.38 (Continued on the next page)

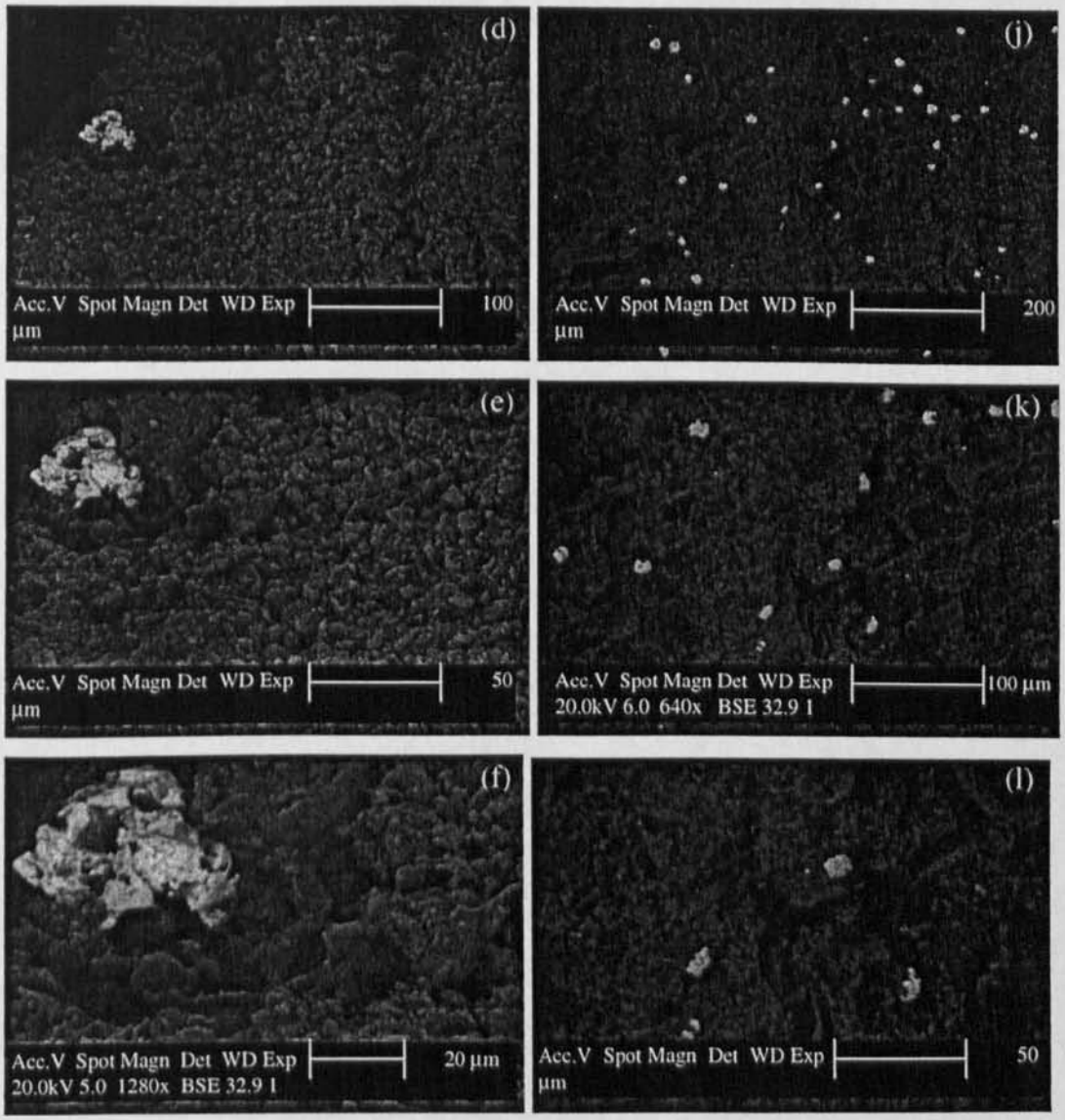

Figure 6.38 Back-scattered electron images of 5% $Cu(Ac)_2$-added-coal (a-f) and 0.25M $Cu(Ac)_2$-ion-exchanged-coal (g-l) particles in various magnifications

Table 6.8 also shows that the amount of K^+ absorbed in the 0.5M KAc-ion-exchanged sample (2.08%) was slightly less than that in 5% KAc-added-coal sample (2.18%). However, the critical ambient temperature of the ion-exchanged sample (145.5 ± 0.5 °C) was lower than that of the bulk-loading sample (151.5 ± 0.5 °C) . It is suspected that the excessive additives in the bulk-loading sample, may have blocked the pore structure of coal, and caused loss of active sites and additional resistance for oxygen diffusion, and thus lower the propensity of the coal with bulk

additive loading towards spontaneous combustion. Furthermore, as observed in samples with $Cu(Ac)_2$, the ion-exchanged sample tend to have a larger surface area for the oxidation reaction.

Moreover, It is also shown that the amount of Na^+ in NaAc absorbed in both ion-exchanged and bulk loading samples, increased with increasing solution concentration and additive loading, respectively. The amount of Na^+ absorbed in 0.1M NaAc-ion-exchanged sample (0.78%) shown a higher value than that in 1% NaAc-added-coal sample (0.26%). However, the critical ambient temperatures of 0.1M NaAc-ion-exchanged coal and 1% NaAc-added-coal sample (154.5 ± 0.5 °C) were the same, which were also the same as that of acid-washed coal. This indicated that, within the range of 0.26-0.78 %wt, Na^+ could not significantly affect the spontaneous combustion. The amount of Na^+ absorbed in 0.5M NaAc-ion-exchanged sample (1.22%) was similar to that in 5% NaAc-added-coal sample (1.12%), which resulted in the same critical ambient temperature (152.5 ± 0.5 °C). On the other hand, Na^+ absorbed in 1.0M NaAc-ion-exchanged sample (1.50%) was lower than that in 10% NaAc-added-coal sample (2.68%). However the critical ambient temperature of the ion-exchanged sample (149.5 ± 0.5 °C) was 1 °C lower than that of 10% NaAc-added-coal sample (150.5 ± 0.5 °C). It is suspected that the excess NaAc in the bulk loading sample may have presented an additional resistance for oxygen penetration into the coal and caused loss of active sites. The experimental errors may also hold the responsibility for the slight deviation observed.

The amount of Ca^{2+} in $Ca(Ac)_2$ absorbed in both ion-exchanged and bulk loading samples were also found to increase with increasing solution concentration and additive loading, respectively. It can also be seen in Table 6.8 that varying the additive solution concentrations or additive loadings could not significantly change the ambient temperatures of ion-exchanged samples (154 ± 0.5 °C) or bulk-loading samples (156 ± 0.5 °C). Furthermore, regardless the amount of Ca^{2+} absorbed in the ion-exchanged coal, the critical ambient temperatures of the samples were the same as that of acid-washed coal, which were 2 °C lower than those of bulk-loading

samples. This indicated that the inhibition effects of $Ca(Ac)_2$ observed in the bulk-loading samples were mainly due to physical in nature.

The amount of Na^+ in NaCl absorbed in the ion-exchanged sample (0.13%) was reasonably smaller than that in the bulk-loading sample (1.84%). However, the critical ambient temperatures of both samples were the same (159 ± 0.5 °C). Similarly, although the amount of Ca^{2+} in $CaCl_2$ absorbed in the ion-exchanged coal (0.21%) was smaller than that in the bulk-loading sample (1.48%), the critical ambient temperatures of both samples were similar, i.e. 161 ± 0.5 °C for the ion-exchanged sample and 160 ± 0.5 °C for the bulk-loading sample. It is suspected that the coal structure of the samples could have changed during the treatment, and thus affecting the self-heating behaviour of the coal. The experimental errors could also hold the responsibilities for the slight deviation observed.

In contrast, although the amount of Mg^{2+} absorbed in the 0.5M $Mg(Ac)_2$ ion-exchanged sample (0.86%) was higher than that in the 5% $Mg(Ac)_2$-added-coal sample (0.56%), the critical ambient temperature of the ion-exchanged sample (161.5 ± 0.5 °C) was 3 °C lower than that of the bulk loading sample (164.5 ± 0.5 °C). It is deemed that the excessive amount of $Mg(Ac)_2$ in the bulk loading sample could have caused physical changes in the coal structure, which could include blockage of pore structure of coal, loss of active sites, and additional resistance for oxygen diffusion, and thus helped reduce the propensity of the coal towards spontaneous combustion. Furthermore, the changes in coal structures during treatments could also affect the self-heating behaviour of the coals.

The reaction rates of samples, ion-exchanged and bulk-loaded with various promotion and inhibition agents, were compared in Figures 6.39 and 6.40, respectively. Figure 6.39 shows that at temperatures from 140 to 170 °C, the presence of the promotion agents, $Cu(Ac)_2$ and KAc, in the ion-exchanged sample resulted higher reaction rates than those in the bulk-loading samples. On the other hand, samples ion-exchanged and bulk loaded with NaAc showed similar reaction rates.

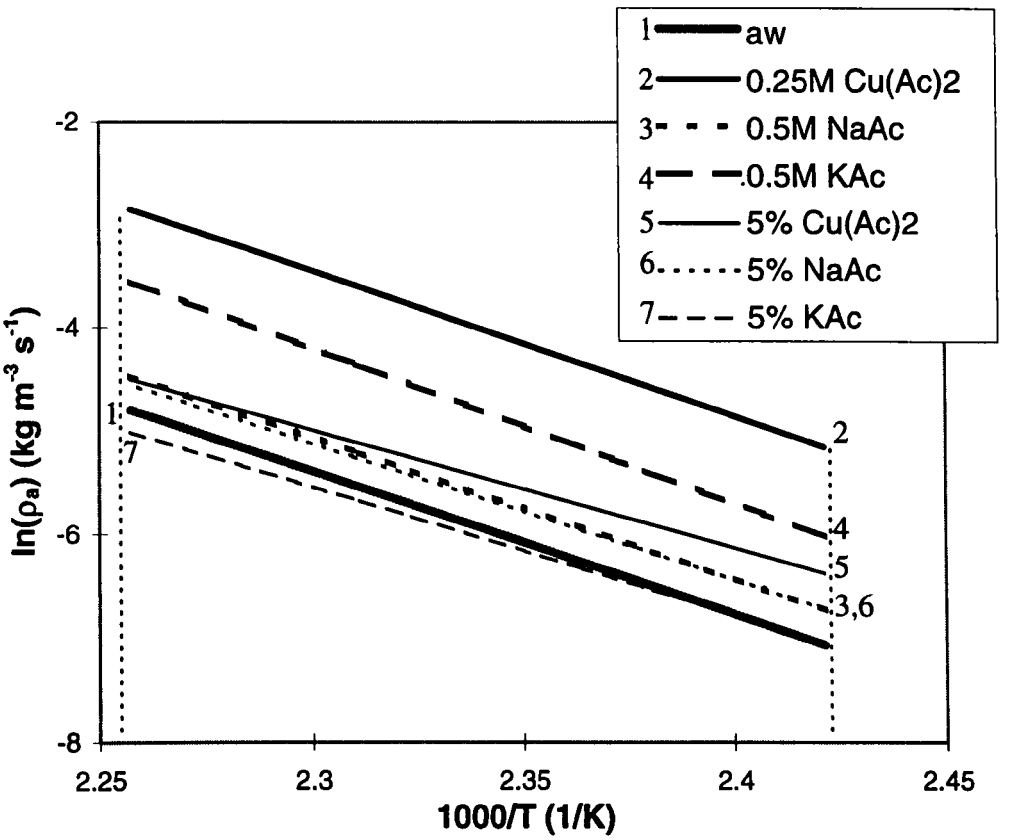

Figure 6.39 Comparison of the estimated oxidation rates for ion-exchanged (lines 2-4) and bulk-loading (lines 5-7) samples with various promotion agents in temperature range of 140 to 170 °C

Figure 6.40 compares the reaction rates of samples ion-exchanged and bulk-loaded with various inhibition agents. It is shown that at temperatures of 140-170 °C, 5% $CaCl_2$-added-coal had lower reaction rate than that of 0.5M $CaCl_2$-ion-exchanged coal. Furthermore, within temperature range of 140 to 148 °C, both $Ca(Ac)_2$ and NaCl in their bulk-loading samples also resulted lower reaction rates than those in their ion-exchanged samples. However in the temperature range of 148 to 170 °C an opposite trend was observed. Likewise, in the temperature range of 140 to 154 °C, 5% $Mg(Ac)_2$-bulk-loading coal had lower reaction rate than that of 0.5M $Mg(Ac)_2$-ion-exchanged, while between 154 to 170 °C, an opposite trend was observed.

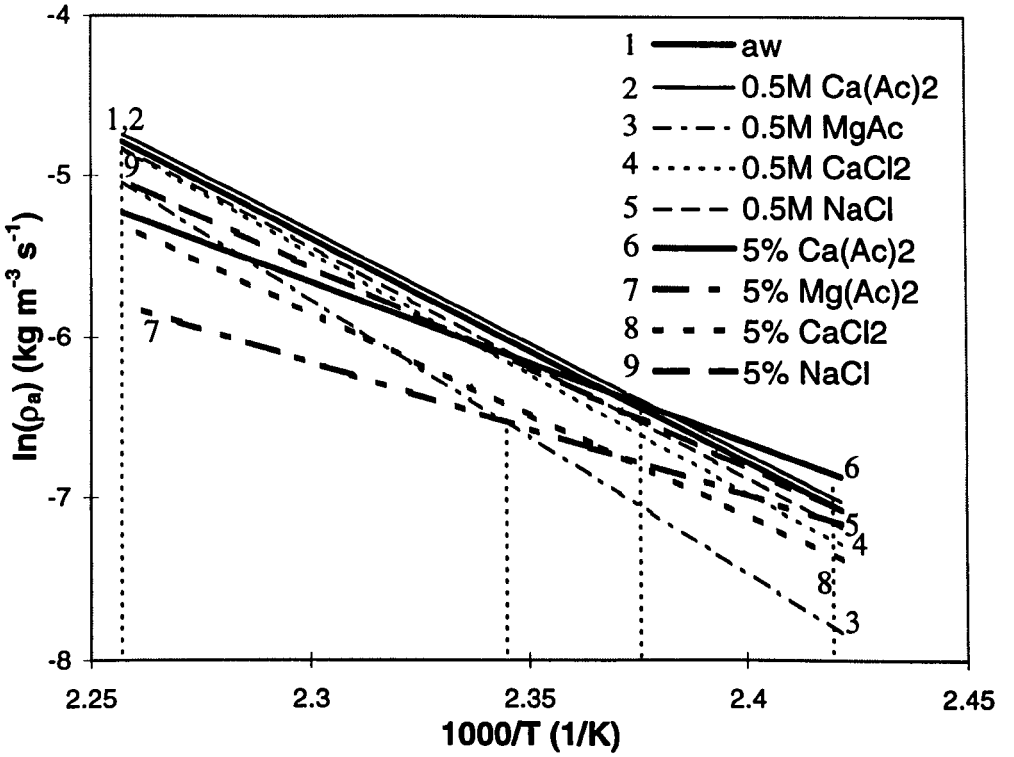

Figure 6.40 Comparison of the estimated oxidation rates for ion-exchanged (lines 2-5) and bulk-loading (lines 6-9) samples with various inhibition agents at temperature range of 140 to 170 °C

The experimental results showed that $Cu(Ac)_2$ and KAc in the ion-exchanged samples showed stronger inhibition or promotion effects on spontaneous combustion than their respective bulk-loading samples, indicating that their effects on spontaneous combustion were mainly chemical in nature. On the other hand, the inhibition effect of $Ca(Ac)_2$ was mainly physical in nature, while NaAc, $Mg(Ac)_2$, $CaCl_2$, and NaCl did not show a clear evidence if their effects were chemical or physical. Therefore, whether the capability of an additive to affect the spontaneous combustion is chemical or physical, is determined by the type of the additive used.

6.7 SUMMARY

The inhibition and promotion agents of coal spontaneous combustion together with the effect of anions and cations on the capability of additives to either inhibit or

promote the spontaneous combustion were further studied using the wire-mesh reactor technique. It is revealed that the presence of Na^+, K^+, and Cu^{2+} in their acetic and carbonate salts, promoted spontaneous combustion, while sodium chloride and hydroxide inhibited spontaneous combustion. Magnesium acetate and carbonate inhibited spontaneous combustion. Ca^{2+} in different salts behaved differently. In its chloride and acetic salts, Ca^{2+} inhibited spontaneous combustion, while in the carbonate and hydroxide forms, it promoted spontaneous combustion. From the results, it can be concluded that the capability of the additives to affect spontaneous combustion depended on both cations and anions in the additives. Low-temperature oxidation kinetics were also estimated by an unsteady-state energy balance approach. The reactivities showed a general trend that the lower the critical ambient temperature, the higher the reactivity of the sample. The effectiveness of sodium acetate to promote spontaneous combustion was enhanced with an increase in both its additive loading and solution concentration, while that of calcium acetate remained unchanged with varying loading or solution concentration. Furthermore. whether the capability of an additive to affect the spontaneous combustion was chemical or physical, was strongly determined by the type of the additive used. SEM analysis was also conducted for samples bulk-loaded and ion-exchanged with $Cu(Ac)_2$. The secondary electron images of both samples showed that the pore volume of ion-exchanged sample is larger than that of bulk-loading sample. Furthermore, the back-scattered electron images of both samples showed that the amount of copper inclusion in the ion-exchanged coal particle was higher and more uniformly distributed in the coal matrix than that in the bulk-loading coal particle, which is in a good agreement with the EDAX quantitative measurement.

Chapter 7

SPONTANEOUS COMBUSTION OF COAL: AN EVALUATION OF THE CURRENT STUDIES

7.1 INTRODUCTION

This chapter presents an integration of the current work and offers an interpretation based on the low-temperature oxidation reaction mechanisms and thermal runaway observations. It attempts to evaluate the current studies based on the gaps identified in the literatures and the objectives set up in the beginning of the studies. The energy balances used for kinetics determination in different techniques are also validated. Practical relevance and significance of the current results are also described in this chapter.

7.2 INTEGRATED MECHANISMS OBSERVED

When a coal in a stockpile contacts with the ambient air, low-temperature oxidation reaction occurs. At the ambient temperature, the oxidation reaction is very slow. However, if the heat is allowed to accumulate inside the stockpile, the oxidation reaction is enhanced, and can cause a spontaneous combustion. Thus, there are clearly two competing processes which determine the possibility of a spontaneous combustion to occur in a stockpile:

(i) heat generation from the oxidation reaction (strongly depends on temperature and oxygen availability), and

(ii) heat dissipation to the surroundings.

Based on the two competing processes, there are two conditions under which a coal stockpile is safe. The first occurs when the heat can be easily dissipated. This usually occurs in the region near the surface of a stockpile. In this region, although the oxygen available for the oxidation reaction is abundant, the greater heat dissipation prevents an increase in oxidation reaction rate, thus the temperature rise in the stockpile (reaction-rate-limited). Therefore, the occurrence of spontaneous combustion is not favoured in this region.

The second condition occurs when the oxygen for the oxidation reaction is limited. This usually occurs in the deep inside of a stockpile. Inside the stockpile where the heat generated from the oxidation reaction may be allowed to accumulate, the coal temperature may increase significantly. At high temperatures, however, the rate of oxidation reaction may be so high that the rate of heat generation is limited by the availability of oxygen in the pile. If the available oxygen in the stockpile is very low, the increase of the rate of heat generation, and thus the increase of coal temperature, are restricted (oxygen-limited). Accordingly, the occurrence of spontaneous combustion is less likely in this region.

Between these two extreme conditions, i.e. reaction-rate-limited and oxygen-limited, there is an intermediate regime in the stockpile where the oxidation reaction is not limited by the reaction rate nor the availability of the oxygen. In this regime, the highest coal temperature and reaction rate may be reached, and therefore favours a high risk of spontaneous combustion.

The Damkohler number, Da, can be used to identify the reaction limited region as follows (Fogler (1981)).

$$Da = \frac{\text{rate of reaction}}{\text{rate of convection}} = k C_{A0}^{n-1} \tau \qquad (7\text{-}1)$$

In the reaction-rate-limited region, the rate of reaction is much slower than the rate of convection, and thus Da goes towards zero. On the other hand, in the oxygen-limited region, the rate of convection is low and the rate of reaction is also low due to oxygen limitation in the system, and therefore Da approaches unity. In the intermediate regime in the stockpile where the oxidation reaction is not limited by the reaction rate nor the availability of the oxygen, the Da number is larger than one. Figure 7.1 qualitatively illustrates the profile of Da from the surface (x = 0) to the bottom part of the stockpile (x = L). Near the surface (x = 0), where the heat can be dissipated easily to the surroundings, Da approaches zero. The Da increases continuously with the depth of the stockpile until it reaches maximum in a certain depth, and then starts to decrease towards unity.

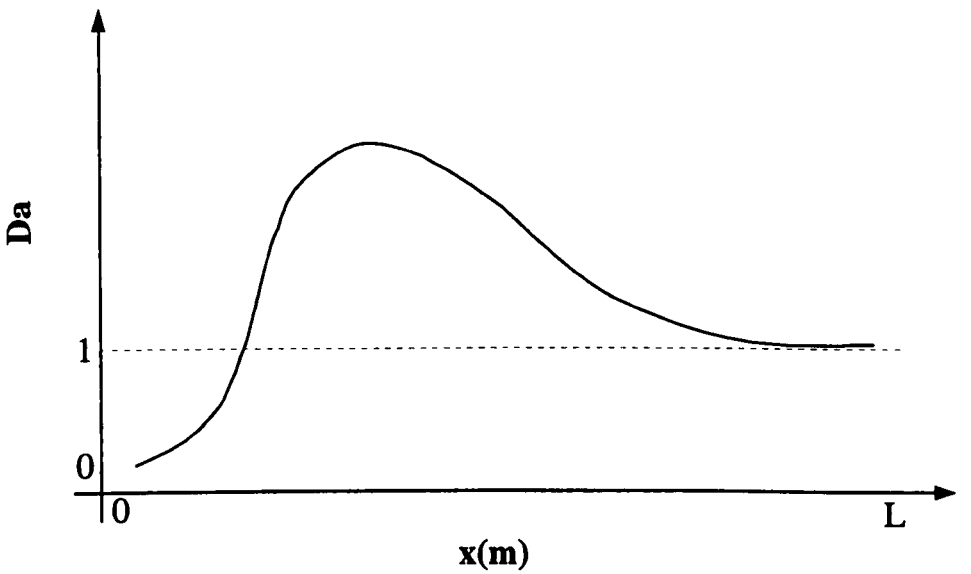

Figure 7.1 Profile of Damkohler number (Da) in the coal stockpile (from the surface (x = 0) to the bottom part of the stockpile (x = L))

From the above, it can be seen that identifying whether the stockpile is reaction-rate-limited or oxygen-limited is very important to determine an appropriate treatment for reducing the risk of spontaneous combustion. For example, crushing the coal particles to smaller sizes and compacting the coal stockpile reduce the risk of spontaneous combustion in an oxygen-limited stockpile, but make the reaction-rate-limited stockpile unsafe (Glasser and Bradshaw (1990)). These are supported

by the results observed in the experiments, as described in Chapter 4. In the isothermal reactor, for example, oxygen is supplied into the reactor and therefore there is no limitation on the amount of oxygen. The heat, however, can be transferred to the surrounding easily from the reactor surface and by the flowing gas, therefore the reaction-rate is limited. From the experimental results of the effect of particle size on spontaneous combustion using the isothermal reactor, it is observed that the smaller the particle size, the lower the critical ambient temperature. Furthermore, experiments on the effect of packing density show that the higher the packing density, the lower the critical ambient temperature. Accordingly, the results are in a good agreement with the theory described earlier. Similar trend can also be observed from the wire-mesh experimental results.

As the spontaneous combustion is not favourable when the oxygen is limited, covering a stockpile with a reactive materials may be considered to be a possible way to reduce the spontaneous combustion risk of a coal stockpile. However, one has to be cautious because as time progresses, the reactive material may lost its ability to absorb the oxygen, and acts as a barrier for the heat transfer (Glasser and Bradshaw (1990)). When this situation occurs, it is necessary to replace or cover the stockpile with a fresh material, so that the oxygen will not be able to penetrate inside the stockpile. Therefore, it is important to continuously monitor the oxygen penetration inside the stockpile to determine whether a new layer of a reactive material is required. The limiting region of the stockpile also significantly determined whether covering a stockpile is an appropriate way to reduce the risk of spontaneous combustion (Glasser and Bradshaw (1990)). For the oxygen-limited stockpile, the treatment further lowers the opportunity of the oxygen to penetrate into the stockpile, however it also lowers the heat dissipation to the surroundings. Therefore, the usefulness of the treatment depends on which process is more dominant. For the reaction-rate-limited stockpile, on the other hand, covering a stockpile hinders the heat dissipation to the surroundings, and thus increase the risk of spontaneous combustion of the stockpile.

7.3 VALIDITY OF ENERGY BALANCE APPROACH FOR ESTIMATION OF KINETICS

The energy balances used for different techniques for kinetic estimation involved various simplifications. Therefore, evaluation of the kinetic constants and reaction rates estimated are required. This section describes this in detailed.

7.3.1 Isothermal and Adiabatic Reactors

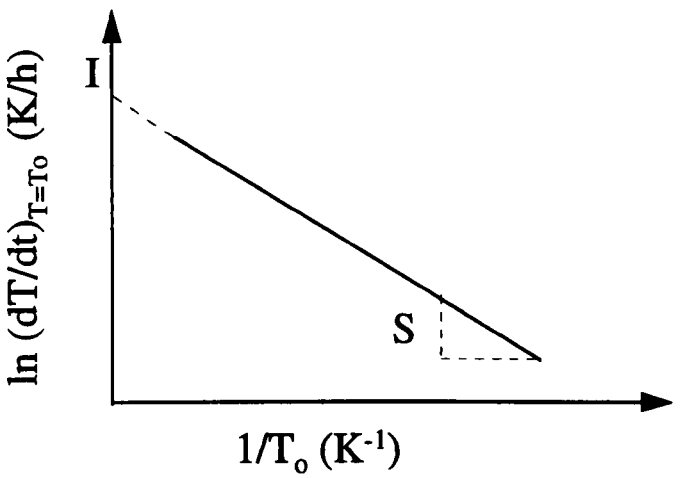

Figure 7.2 A typical linear plot of $\ln\left[\frac{dT}{dt}\right]_o$ versus $\frac{1}{T_o}$ for coal tested in isothermal and adiabatic reactors

As described in Equation (3-2), the values of apparent pre-exponential factor and activation energy, A and E, of samples tested in isothermal and adiabatic reactors were obtained from the intercept (I) and slope (S) of the linear plot of $\ln\left[\frac{dT}{dt}\right]_o$ versus $\frac{1}{T_o}$, respectively, as illustrated in Figure 7.2. Equations used to calculate A,

E, and reaction rates (ρ_a) of samples tested in either isothermal and adiabatic reactor are described in Equations (7-2) to (7-4), respectively.

$$A = \frac{e^{I} \rho_s Cp_s}{Q P_{O_2}} \tag{7-2}$$

$$E = S \times R \tag{7-3}$$

$$\rho_a = A e^{-E/RT} P_{O_2} \tag{7-4}$$

As shown in Equations (7-2) and (7-3), the A value is proportional to ρ_s, Cp_s, and inversely proportional to Q and P_{O_2}, while the E value depends only on the temperature history of the coal. The reaction rate appears to be proportional to A and P_{O_2}, and thus it is proportional to ρ_s, Cp_s, and inversely proportional to Q.

The heating values, Q, of various samples were determined experimentally, while the values of ρ_s and Cp_s were assumed to be constant for all samples. Although, it has been reported that the specific heat capacity of solid does not significantly vary within a narrow temperature range (100 - 400 °C) (Perry (1984)), it could vary according to the coal type, sample treatment, reactant depletion, and etc. Similarly, the value ρ_s may also vary according to the coal type, particle size, packing density, sample treatment, reactant depletion, and etc. Furthermore, the measurements of the physical properties themself may already contain a certain error. Therefore, sensitivity of kinetic estimation is tested by varying the values of Cp_s, ρ_s, and Q. If ± 20% variation in the value of Cp_s or ρ_s is applied, the pre-exponential factor, A, and reaction rate, ρ_a, are also varied by ± 20%, as they are proportional to Cp_s and ρ_s. For heating value, the gross heating value of the raw Coal M was measured experimentally and used for the kinetic calculation. However, in the low-temperature oxidation reaction, only carbon may be reacted with oxygen. Therefore, the uncertainty in the kinetic estimation is also calculated by employing the heats of combustion of carbon to form carbon monoxide ($Q_{C\rightarrow CO}$ = 9210 kJ/kg (Perry (1984)) and to form carbon dioxide ($Q_{C\rightarrow CO2}$ = 32792.7 kJ/kg (Perry (1984)). With $Q_{C\rightarrow CO}$, the error of A, which equals to that of ρ_a, is found to be 148.8%, while with $Q_{C\rightarrow CO2}$, it is

equal to 30.1%. It can be seen that the errors calculated with variation in the Q value are significantly high. Accordingly, one should take precaution when determining the Q value used for the kinetic estimation. Variation in the reaction rate of Coal M3 tested in the isothermal reactor (R-1) with different heating values, is illustrated in Figure 7.3.

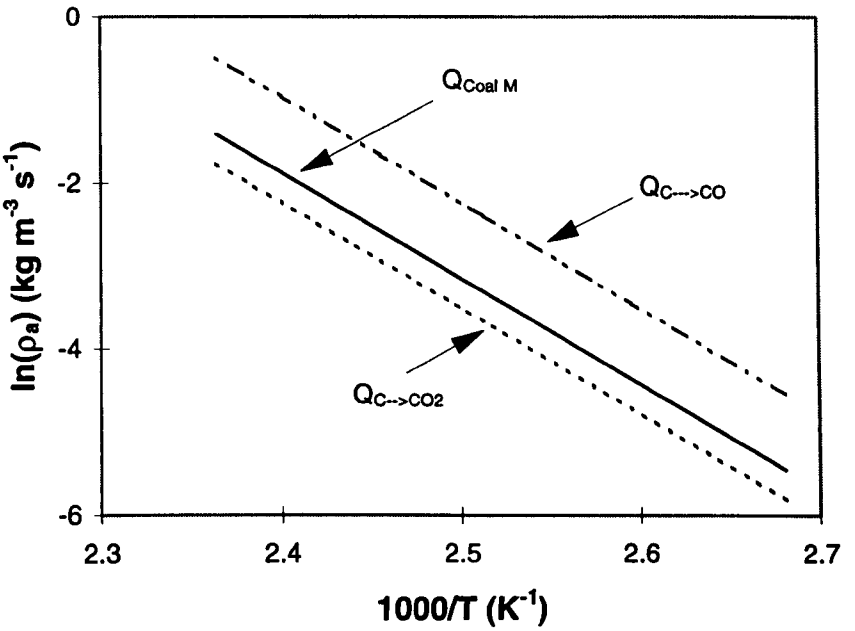

Figure 7.3 The reaction rate of coal oxidation in air estimated from isothermal reactor (R-1) with different heating values, at temperature range of 100-150 °C

Furthermore, it is very unlikely that the maximum uncertainty for Q, Cp_s, and ρ_s, will be obtained in any given measurement. There is a possibility that overestimates of Q and Cp_s will be accompanied by an underestimate of ρ_s, or an overestimate of Q will be accompanied by underestimates of Cp_s and ρ_s, or etc. Since the direct addition of errors may be overly simplified and overestimates the true uncertainty, addition in quadrature error analysis is employed (Milton and Arnold (1995)). The addition in quadrature error analysis is commonly used if there are several measurements which are subject to independent random errors (Milton and Arnold (1995)). Equations (7-5) and (7-6) show the additional quadrature of pre-exponential factor, A, and reaction rate (ρ_s), respectively.

$$\delta(A) = \sqrt{\left(\frac{\delta(A)}{\delta(Cp_s)}\,\delta(Cp_s)\right)^2 + \left(\frac{\delta(A)}{\delta(\rho_s)}\,\delta(\rho_s)\right)^2 + \left(\frac{\delta(A)}{\delta(Q)}\,\delta(Q)\right)^2}$$

$$= \sqrt{\left(\frac{e^I \rho_s}{Q P_{O_2}}\,\delta(Cp_s)\right)^2 + \left(\frac{e^I Cp_s}{Q P_{O_2}}\,\delta(\rho_s)\right)^2 - \left(\frac{e^I \rho_s Cp_s}{Q^2 P_{O_2}}\,\delta(Q)\right)^2}$$

$$\delta(A) = \frac{e^I}{Q P_{O_2}} \sqrt{[\rho_s\,\delta(Cp_s)]^2 + [Cp_s\delta(\rho_s)]^2 - \left[\frac{\rho_s Cp_s}{Q}\,\delta(Q)\right]^2} \qquad (7\text{-}5)$$

and

$$\delta(\rho_a) = \sqrt{\left(\frac{(\rho_a)}{\delta(A)}\,\delta(A)\right)^2} = P_{O_2}\, e^{-E/RT}\,\delta(A) \qquad (7\text{-}6)$$

To test the uncertainty in the kinetics estimation, data obtained from Coal M3 tested in the isothermal reactor (R-1) is used. If the values of Cp_s and ρ_s are varied by 20% and $Q_{C\rightarrow CO}$ is used, the uncertainty of A, which is equal to that of ρ_a, is ± 28.3%. Similar error is detected when the combined 20% variation in Cp_s and ρ_s, and $Q_{C\rightarrow CO2}$ are used.

From the evaluation of the energy balance used in the kinetic estimations in the isothermal and adiabatic reactor techniques, it is evident that the uncertainties in the pre-exponential factor and reaction rate are sensitive to the variations in the coal physical properties. It can be seen that with 20% variation in the values Cp_s and ρ_s, the uncertainty of ρ_a is the same (± 28.3%), either by using $Q_{C\rightarrow CO}$ or $Q_{C\rightarrow CO2}$. However, as shown in Figure 7.3., if only variation in Q is considered, the reaction rate predicted by using $Q_{C\rightarrow CO}$ is higher than others. Eventhough it is unlikely that CO will be the sole combustion product at low-temperature, the use of $Q_{C\rightarrow CO}$ prevents underestimation in the reaction rate prediction. Furthermore, measurements of physical properties of each sample are necessary to provide more reliable kinetics estimation.

7.3.2 Wire-Mesh Reactor

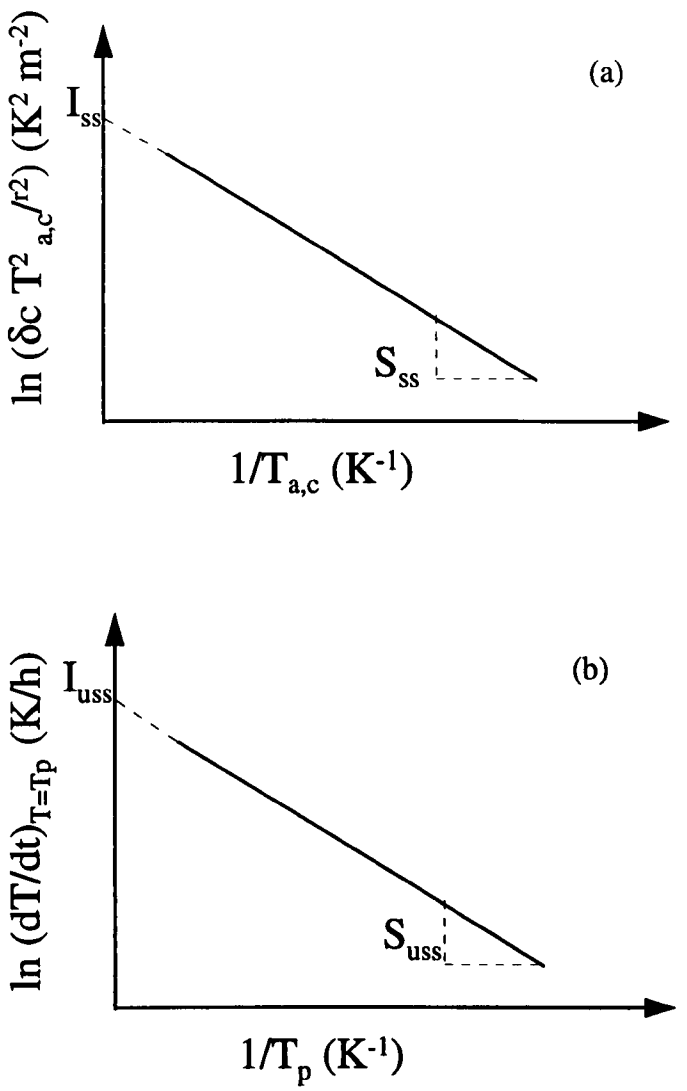

Figure 7.4 Typical linear plots to determine the kinetic constants for coal tested in wire mesh reactors with (a) steady-state; and (b) unsteady-state methods

As also discussed in Chapter 3, Equation (3-8) is used to estimate the kinetic constants for the steady-state method, while Equation (3-10) is used for the unsteady-state method. For the steady state method, it is shown that the values of apparent pre-exponential factor and activation energy, A_{ss} and E_{ss}, are obtained from the intercept (I_{ss}) and slope (S_{ss}) of linear plot of $\ln(\delta_c\, T_{a,c}^2/r^2)$ and $1/T_{a,c}$, respectively, as shown in Figure 7.4(a). For the unsteady-state method, the values of A_{uss} and E_{uss}

were determined from intercept (I_{uss}) and slope (S_{uss}) of the linear plot between $\ln(\delta T/\delta t)_{T=Tp}$ and $1/T_p$, respectively, as shown in Figure 7.4(b). Equations used to calculate A, E, and ρ_a for both methods are shown in Equations (7-7) to (7-12), respectively.

$$A_{ss} = \frac{e^{I_{ss}} k_t R}{\rho_s E Q} \quad (7\text{-}7)$$

$$E_{ss} = S_{ss} \times R \quad (7\text{-}8)$$

$$(\rho_a)_{ss} = A_{ss} e^{-E_{ss}/RT} \rho_s \quad (7\text{-}9)$$

$$A_{uss} = \frac{e^{I_{uss}} Cp_s}{Q} \quad (7\text{-}10)$$

$$E_{uss} = S_{uss} \times R \quad (7\text{-}11)$$

$$(\rho_a)_{uss} = A_{uss} e^{-E_{uss}/RT} \rho_s \quad (7\text{-}12)$$

For both steady-state and unsteady-state methods, it is noted that the E values only depend on the temperature history of the coal (slope). The values of A, on the other hand, depend on various physical properties of the coal. A_{ss} is proportional to k_t, and inversely proportional to ρ_s, and Q, while A_{uss} is proportional to Cp_s and inversely proportional to Q. For both methods, the reaction rate is proportional to A and ρ_s.

Similar to Cp_s, it has also been reported (Badzioch (1964)) that the thermal conductivity (k_t) of coal remains approximately constant between 100 to 400 °C, however it may vary with coal type, coal treatment, experimental condition, reactant depletion, and etc. Furthermore, as stated earlier, the physical property measurements themself carry a certain error. Accordingly, the uncertainty in the kinetic estimation is again determined by varying the values of Cp_s, ρ_s, Q, and k_t.

For the steady-state method, if ± 20% variation in the k_t or ρ_s value is applied, A_{ss} and $(\rho_a)_{ss}$ values will also be varied by ± 20%. Furthermore, if $Q_{C\rightarrow CO}$ is used, the error of A_{ss}, which equals to that of ρ_a, is found to be 59.8 %, while with $Q_{C\rightarrow CO2}$, it is equal to 43.1%.

Equation (7-13) shows the additional quadrature of A_{ss} when variations of the values of ρ_s, k_t, and Q are combined, while Equation (7-14) shows the additional quadrature of the reaction rate $(\rho_a)_{ss}$.

$$\delta(A_{ss}) = \sqrt{\left(\frac{\delta(A)_{ss}}{\delta(k_t)}\,\delta(k_t)\right)^2 + \left(\frac{\delta(A)_{ss}}{\delta(\rho_s)}\,\delta(\rho_s)\right)^2 + \left(\frac{\delta(A)_{ss}}{\delta(Q)}\,\delta(Q)\right)^2}$$

$$= \frac{e^{I_{ss}}\,R}{\rho_s EQ}\sqrt{\left[\delta(k_t)\right]^2 - \left[\frac{k_t}{\rho_s}\delta(\rho_s)\right]^2 - \left[\frac{k_t}{Q}\,\delta(Q)\right]^2} \qquad (7\text{-}13)$$

and

$$\delta(\rho_a)_{ss} = \sqrt{\left(\frac{\delta(\rho_a)_{ss}}{\delta(A)_{ss}}\,\delta(A)_{ss}\right)^2 + \left(\frac{\delta(\rho_a)_{ss}}{\delta(\rho_s)}\,\delta(\rho_s)\right)^2}$$

$$= e^{-E/RT}\sqrt{\left[\rho_s\,\delta(A)_{ss}\right]^2 + \left[A_{ss}\,\delta(\rho_s)\right]^2} \qquad (7\text{-}14)$$

With variation of 20% in the k_t and ρ_s values, and by using $Q_{C\rightarrow CO}$, the uncertainty in A_{ss} is 66.2%, while that in $(\rho_a)_{ss}$ is 20 %. On the other hand, with the same variations in the values of k_t and ρ_s, but using $Q_{C\rightarrow CO2}$, the uncertainty in A_{ss} is 51.6%, while that in $(\rho_a)_{ss}$ is 20%. Variation in the reaction rate of Coal M3 tested in the wire-mesh reactors with 20% variation in k_t and ρ_s, and with $Q_{C\rightarrow CO2}$, is illustrated in Figure 7.5.

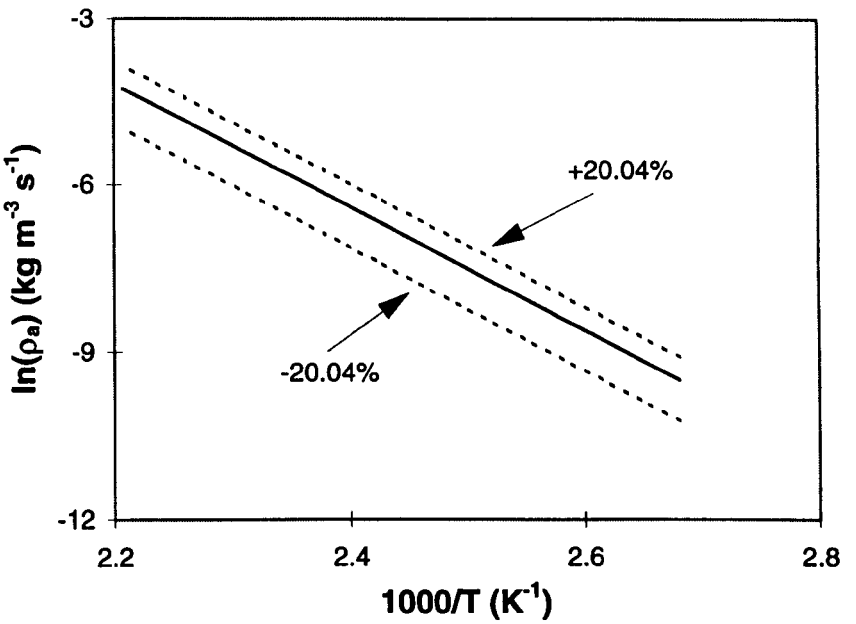

Figure 7.5 The reaction rate of coal oxidation in air estimated from wire-mesh reactor (B-1) steady-state method with 20% variation in the values of ρ_s, k_1, and $Q_{C\rightarrow CO2}$, at temperature range of 140-170 °C

For the unsteady-state method, if ± 20% variation of Cp_s is applied, A_{uss} and $(\rho_a)_{uss}$ values, which are proportional to Cp_s, will also be varied by ± 20%. Furthermore, if the heat combustion of carbon to form carbon monoxide ($Q_{C\rightarrow CO}$ = 9210 kJ/kg) is used, the error of A_{ss} which equals to that of $(\rho_a)_{ss}$, is found to be 81.9 %, while with $Q_{C\rightarrow CO2}$, it is equal to 59.1%.

Equation (7-15) shows the additional quadrature of A_{uss} when variations in the values of Cp_s and Q are combined, while Equation (7-16) presents the additional quadrature of the reaction rate $(\rho_a)_{uss}$.

$$\delta(A_{uss}) = \sqrt{\left(\frac{\delta(A)_{uss}}{\delta(Cp_s)}\,\delta(Cp_s)\right)^2 - \left(\frac{\delta(A)_{uss}}{\delta(Q)}\,\delta(Q)\right)^2}$$

$$= \frac{e^1}{Q}\sqrt{[\delta(Cp_s)]^2 - [Cp_s\,\delta(Q)]^2} \qquad (7\text{-}15)$$

and

$$\delta(\rho_a)_{uss} = \sqrt{\left(\frac{\delta(\rho_a)_{uss}}{\delta(A_{uss})}\,\delta(A_{uss})\right)^2 + \left(\frac{\delta(\rho_a)_{uss}}{\delta(\rho_s)}\,\delta(\rho_s)\right)^2}$$

$$= e^{-E/RT}\sqrt{\left[\rho_s\,\delta(A_{uss})\right]^2 + \left[A_{uss}\,\delta(\rho_s)\right]^2} \qquad (7\text{-}16)$$

Data obtained from Coal M3 tested in the wire-mesh reactor (B-1) is used in this example. If the value of Cp_s and ρ_s are varied by 20% and $Q_{C\rightarrow CO}$ is used, the uncertainties in A_{uss} and $(\rho_a)_{uss}$ will be 86.4% and 88.7%, respectively, while with $Q_{C\rightarrow CO2}$, the uncertainties in A_{uss} and $(\rho_a)_{uss}$ will be 65.1% and 68.1%, respectively.

From the evaluation of the energy balance used in the kinetic estimations for the wire-mesh reactors with both steady-state and unsteady-state methods, it is evident that the uncertainties in the kinetic constant and reaction rate estimated from both methods are sensitive to the variations of the coal physical properties, particularly Q. Similar to the trends observed in the isothermal and adiabatic reactors, the uncertainty of the reaction rate calculated using $Q_{C\rightarrow CO}$, predicted from either steady-state or unsteady method, is higher than that with $Q_{C\rightarrow CO2}$. Accordingly, if the kinetic estimations are to be used in the mathematical model, the use of $Q_{C\rightarrow CO}$ prevents underestimation in the reaction rate prediction. Furthermore, measurements of physical properties of each sample are necessary to provide more accurate kinetics estimation, particularly if the kinetic estimated is to be used for a comparison basis.

7.4 JUSTIFICATION OF TIME-TO-IGNITION DETERMINATION

The time-to-ignition is employed to determine the time when the thermal runaway occurred. As discussed in Chapter 4, to identify the time-to-ignition, the first-order time derivative of temperature (dT/dt) and the second-order time derivative of temperature (d^2T/dt^2) are computed and plotted against time. Figure 7.6 presents typical plots of the coal temperature, the first-order time derivative of temperature

(dT/dt) and the second-order time derivative of temperature (d^2T/dt^2) against time for coal tested in different techniques. It can be clearly seen that the thermal runaway starts to occur when the temperature acceleration (d^2T/dt^2) reached maxima.

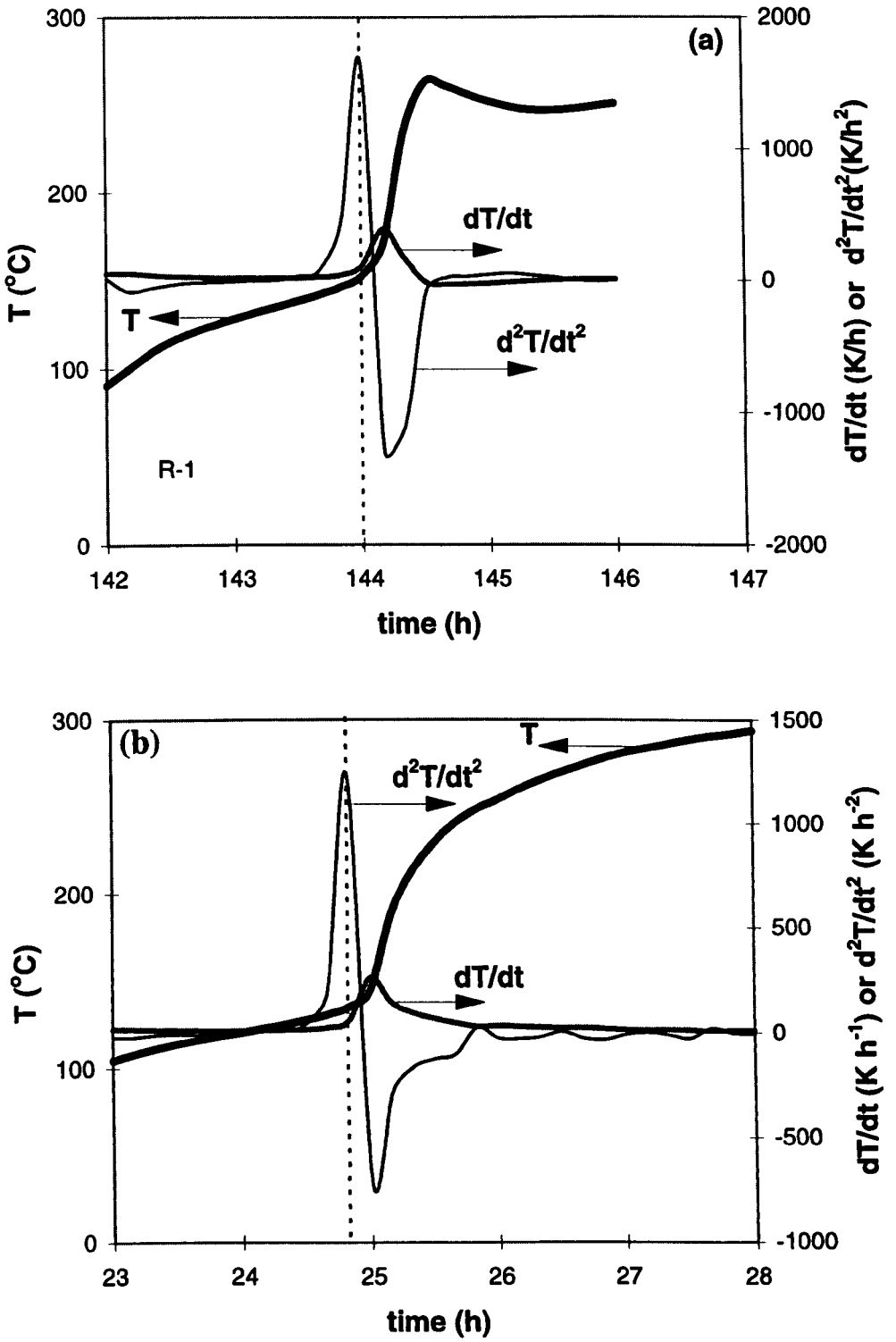

Figure7.6 (Continued on the next page)

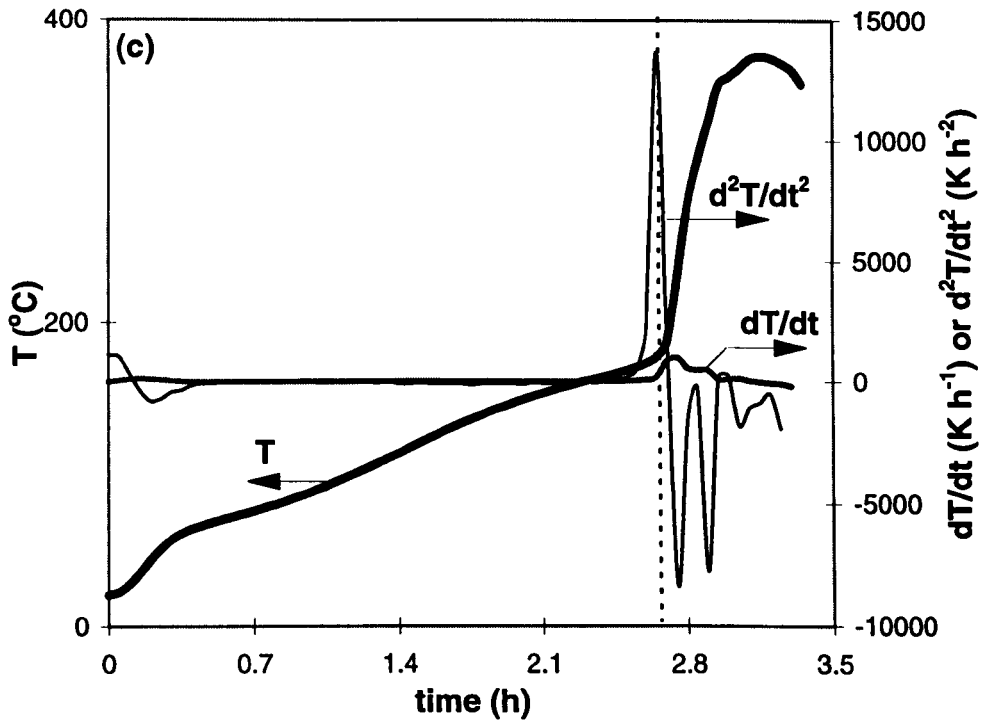

Figure 7.6 Determination of time-to-ignition for (a) Coal M3 tested in an isothermal reactor (R-1) at 85 °C; (b) Coal M2 tested in an adiabatic reactor (A-1) at 100 °C, and (c) Coal M3 tested in a wire-mesh reactor (B-2) at 138 °C

The energy balance of low-temperature oxidation kinetics of a porous reactive solid can be simplified as:

$$\rho_s \, Cp_s \frac{\partial T}{\partial t} = k_t \nabla^2 T + Q \, A \exp\left(-\frac{E}{RT}\right) P_{O_2} \qquad (7\text{-}17)$$

where many terms, such as reactant consumption, oxygen diffusion, natural convection, forced convection, conduction in the pore structure, mass and heat transfer of water vapour, and etc., are neglected. However, to obtain a reliable prediction of the time-to-ignition from a mathematical model, one requires to employ a complete mathematical model which involves all parameters and factors contributing to the spontaneous combustion, and therefore this will be an extremely arduous task. With experimental work, however, a reliable prediction of the time-to-

ignition can be obtained by identifying the time when second-order time derivative of temperature (d^2T/dt^2) is maxima.

7.5 PRACTICAL IMPLICATION OF THE CURRENT STUDIES

The current investigation of the self-heating behaviour of a material using different techniques is initially motivated by the concerns of various conflicting, confusing and inconsistent results presented in the literatures. In the current work, the influence of system conditions involved in the different techniques is identified. This certainly helps provide an improved understanding of the spontaneous combustion phenomenon.

Determination of low-temperature kinetics using different experimental techniques is accomplished in the present project. The energy balance analysis technique is applied with consideration of different system conditions, and therefore more reliable low-temperature oxidation kinetics and coal reactivity can be deduced for further development of mathematical modelling of spontaneous combustion. As described previously in Chapter 4, although the wire-mesh experiments required less time than those of isothermal or adiabatic experiments, the reaction rates predicted from the wire-mesh experiment are lower than those from isothermal or adiabatic reactors. Therefore, if the kinetic constants and reaction rate are to be used for mathematical model development, results from adiabatic or isothermal reactors are recommended to be used to avoid underestimation in the kinetic predictions. On the other hand, if the reaction rates predicted are to be used to compare the risk of various materials or a material under various conditions, the unsteady-state wire-mesh reactor technique will be the quickest and cheapest technique to use.

The critical ambient temperature is one of the indicative measurements, which can be determined in the small-scale laboratory experiments, to examine the risk of a

coal in a certain condition towards spontaneous combustion. By comparing the critical ambient temperatures of various coals or a coal under various conditions, one could qualitatively compare the risk of the coals towards the spontaneous combustion.

Furthermore, the roles of ambient conditions and coal properties, which are well acknowledged to have significant effects on coal spontaneous combustion, are identified in the current work. Air flow rate which simulates the effect of wind on the self-heating in a coal stockpile is examined using both isothermal and adiabatic reactors. In the isothermal tests, it is observed that there is an optimum range of air flow rates at which the spontaneous combustion becomes the most easily possible. On the other hand, within the adiabatic experiments, the air flow rate does not affect the critical ambient temperature but the time-to-ignition. Due to the time limitation, only a narrow range of air flow rate are employed in this study. Furthermore, it is also observed that a humid environment enhances the self-heating. Again, only two extreme conditions are used for this purpose. The use of wider ranges of air flow rates and air humidities could provide a better understanding on how the ambient conditions affect the coal self-heating behaviour. The effect of coal particle size on the self-heating is also examined. It is found that the smaller the particle size, the lower the critical ambient temperature. The coal drying is found to influence the amount of coal moisture content and the coal structure, and thus the self-heating behaviour of coal.

Although, it is acknowledged that the results obtained from the small-scale laboratory study cannot be directly applied into the real stockpile, the experimental results provide an improved understanding on how various factors affect the coal spontaneous combustion, which can then be used to eliminate many assumptions used to simplify the model. Therefore, although mathematical model is not attempted in the project, the information and knowledge obtained from the current study will be of great support for further development of a more reliable and comprehensive model for spontaneous combustion.

Furthermore, it is also acknowledged that preventing or reducing the risk of coal spontaneous combustion using additives is not practicable in reality. However, current experimental studies provide an improved understanding on how individual inorganic matter and additives affect the coal self-heating behaviour. Moreover, by comparing the chemical composition of the coals, one may compare the propensity of the coals towards spontaneous combustion. For instance, coal contains a high percentage of pyrite has a higher risk towards spontaneous combustion, and etc.

Chapter 8

CONCLUSIONS AND RECOMMENDATIONS

8.1 CONCLUSIONS

1. Three most commonly used experimental techniques are chosen in this study to examine the self-heating behaviour of a Victorian brown coal, which is well known to have a high susceptibility towards spontaneous combustion. The study is the first to use different experimental techniques to study the spontaneous combustion behaviour of the same material. The techniques employed include:

i) isothermal reactor,

ii) adiabatic reactor, and

iii) wire-mesh reactor, with

a) steady-state method, and

b) unsteady-state method.

In each technique, the critical ambient temperature of the coal is determined and used to indicate the tendency of coal towards spontaneous combustion. The higher the critical ambient temperature of the coal, the lower the propensity of coal towards spontaneous combustion.

2. Ambient conditions, including ambient temperature, air humidity, and air flow rate, are found to significantly affect the coal spontaneous combustion. An optimum range of air flow rates at which the spontaneous combustion becomes the most easily possible, is observed in isothermal experiments. On the other hand, within the

adiabatic experimental range, the air flow rate does not affect the critical ambient temperature but the time-to-ignition. The higher the air flow rate, the shorter the time-to-ignition. A high ambient temperature and a humid environment enhance the self-heating.

3. Coal particle size also significantly affects the spontaneous combustion. The smaller the particle size, the lower the critical ambient temperature, and thus the higher the propensity of coal towards spontaneous combustion. The method of coal drying influences the amount of coal moisture content and coal structure, and therefore significantly affects the low-temperature oxidation reaction.

4. Coal packing density influences the spontaneous combustion. The higher the packing density, the lower the critical ambient temperature.

5. Experimental results from different techniques show that the critical ambient temperature of a given coal differs significantly according to the techniques used. It is observed that the critical ambient temperatures of coal samples tested in the wire-mesh reactors are higher than those tested in the isothermal and adiabatic reactors. On the other hand, the samples tested in the adiabatic reactors result in the lowest critical ambient temperatures and reach the highest maximum coal temperature, indicating that for a given coal, an adiabatic condition favours a higher risk of spontaneous combustion.

Furthermore, the critical ambient temperatures of coals tested in both isothermal and wire-mesh reactors are also found to vary with the coal mass and specific external surface area of the reactors, while those of adiabatic reactors do not. For both isothermal and wire-mesh reactors, the critical ambient temperature increases linearly with reactor specific external surface area. The results indicate the important roles of external heat transfer coefficient in different techniques.

6. The coal reactivity towards low-temperature oxidation plays a key role in the self-heating process of the coal. The study is the first to examine how different

techniques contribute to the difference in the observed kinetics. It is revealed that the coal reactivities estimated from the isothermal and adiabatic reactors lie in a reasonably continuous band and are higher than those predicted from the wire-mesh reactors.

7. Regardless the techniques used, the critical thickness of the coal deposit decreases with increasing ambient temperature. The critical thicknesses predicted from the isothermal and adiabatic reactors with different reactor sizes compare reasonably well, while those from the wire-mesh reactors are significantly higher particularly at low temperatures.

Furthermore, the study proves that the critical thickness predicted from the steady state method compares well with those from the unsteady-state method, particularly at higher temperatures. This paves a way for future testing using the transient method for more cost-effective assessment of spontaneous combustion of different materials.

8. The time-to-ignition of the coal tested in different techniques is defined as the time required for the coal to experience thermal runaway, and is determined when the temperature acceleration (d^2T/dt^2) reaches maxima. The time-to-ignition is found to vary with ambient conditions, coal particle size, coal drying method, coal packing density, and reactor size. In general, it is observed that, regardless the experimental techniques used, the higher the ambient temperature, the shorter the time-to-ignition.

9. From the experimental results using different techniques, it is concluded that the coal self-heating behaviour is dependent not only on ambient conditions and coal properties, but also on the system conditions involved in the experimental techniques used. Therefore, precautions must be taken when comparing the results obtained from different techniques so that misleading information can be avoided.

10. The controlling regimes of the coal stockpile needs to be identified in order to determine effective ways to reduce the risk of coal spontaneous combustion.

11. The uncertainty calculations for the kinetic estimations using different techniques show that the A and ρ_a calculated for isothermal reactors, adiabatic reactors, and wire-mesh reactors with unsteady-state method, are not significantly affected by variations of the coal physical properties values. On the other hand, the A and ρ_a calculated for the wire-mesh reactor steady-state method significantly vary with ρ_s and k_t of the coal.

12. Experimental studies using isothermal and wire-mesh reactor techniques have been carried out to examine the effect of inherent inorganic matter and additives on coal spontaneous combustion. The critical ambient temperature of each sample is determined and used to compare the propensity of the coal samples towards spontaneous combustion.

13. The critical ambient temperature is increased by washing the raw coal with water and with acid. Water-washing removes the water-soluble inorganic matter and acid-washing removes most of the inorganic matter from the raw coal. The critical ambient temperatures of the acid-washed sample and water-washed coal are higher than that of the raw coal, which indicates that the inherent inorganic matter in the coal catalyses the low-temperature oxidation reaction of coal.

14. Among the additives studied using both the isothermal and wire-mesh reactor techniques, FeS_2, KAc, NaAc, $Cu(Ac)_2$, $CuCO_3$, Na_2CO_3, K_2CO_3, $CaCO_3$, and $Ca(OH)_2$ are found to promote the spontaneous combustion while Montan powder, KCl, NaCl, $CaCl_2$, $Ca(Ac)_2$, $Mg(Ac)_2$, $MgCO_3$, and NaOH inhibit the spontaneous combustion. $NaNO_3$ and NH_4Cl, show a very little effect.

15. The capabilities of the additives to affect spontaneous combustion depend on both cations and anions in the additives.

16. The promotion and inhibition effects of NaAc and KCl, respectively, on spontaneous combustion are enhanced with an increase in their loadings. On the other hand, the inhibition effect of $Ca(Ac)_2$ remains unchanged with varying loading.

17. Whether the capability of an additive to affect the spontaneous combustion is chemical or physical, is determined by the type of the additive used.

18. The secondary electron images of samples bulk-loaded and ion-exchanged with $Cu(Ac)_2$ showed that the pore volume of ion-exchanged sample is larger than that of bulk-loading sample. Furthermore, the back-scattered electron images of both samples showed that the amount of copper inclusion in the ion-exchanged coal particle was higher and more uniformly distributed in the coal matrix than that in the bulk-loading coal particle, which is in a good agreement with the EDAX quantitative measurement. The results show that the ion-exchanged procedure results a larger surface area for the oxidation reaction and provides a better additives distribution in the coal matrix, which have greater effects on coal spontaneous combustion than the bulk-loading of additives.

19. The low-temperature oxidation kinetics estimated for various samples tested in both isothermal and wire-mesh reactors show a general trend that the lower the critical ambient temperature, the higher the reactivity of the sample.

8.2 RECOMMENDATIONS FOR FUTURE WORK

1. The use of a larger experimental scale will provide a better understanding of the influence of the transport processes occurring in a stockpile.

2. Following the gas composition of the reaction products in future experiments will provide opportunities for better estimation of the kinetics and identification of reaction mechanisms under conditions prevailing spontaneous combustion.

3. The use of wider ranges of air flow rates and ambient humidities may provide a better understanding on how the ambient conditions affect the coal critical ambient temperature.

4. The critical particle size of the Coal M has not yet been determined. Smaller fractions of particle sizes are required for this purpose.

5. The effect of coal drying method on spontaneous combustion has been proved to be significant. However, evidence is still required to show how the coal drying methods change the coal structure. This may be done by measuring the surface area and porosity of each sample.

6. The physical property measurements of each sample, e.g. heat capacity, density, thermal conductivity constant, and heating value, are necessary to improve the kinetic estimations of the samples, particularly for the wire-mesh steady-state method.

7. The methods of acid-washing could significantly affect the coal structure, and thus the self-heating behaviour of the coal. Therefore, applying various acid-washing methods using various acid solutions in different concentrations may provide a better understanding on how the acid-washing method influences the self-heating behaviour of the coal.

8. The surface area and porosity measurements of each sample may provide an improved understanding on how the additives and additive application procedures affect the spontaneous combustion.

9. A comprehensive mathematical model which does not oversimplify the complex conditions involved in a coal spontaneous combustion process, could be an effective tool to describe the spontaneous combustion phenomenon and predict the risk of a coal stockpile to spontaneously combust.

10. A complete mathematical model which involves all parameters and factors contributing to the spontaneous combustion, could provide a reliable prediction of the time-to-ignition.

NOMENCLATURES

A	Arrhenius pre-exponential factor	$[s^{-1}]$
a	Elovich empirical constant (generally depend on the temperature)	
A_c, A_w	constants determined by experiment	[-]
C_A	bulk concentration of gas reactant (oxygen)	$[mol\ m^{-3}]$
C_i	initial concentration of the coal	$[mol\ m^{-3}]$
C_r	concentration of the coal after time t	$[mol\ m^{-3}]$
C_p	specific heat capacity	$[J\ kg^{-1}\ K^{-1}]$
Da	Damhkohler number	[-]
D_c	diffusion coefficient for oxygen	$[m^2\ s^{-1}]$
D_w	diffusion coefficient for water vapour	$[m^2\ s^{-1}]$
E	apparent activation energy	$[J\ mol^{-1}]$
E_w	apparent activation energy of change of phase by water vapour	$[J\ mol^{-1}]$
G	molar flow rate per unit area	$[kmol\ m^{-2}\ s^{-1}]$
g	gravitation constant	$[m\ s^{-2}]$
G_h	source term of heat	$[J\ m^{-3}\ s^{-1}]$
h	convection heat transfer coefficient	$[W\ m^{-2}\ K^{-1}]$
h_c	heat transfer coefficient	$[W\ m^{-2}\ K^{-1}]$
H_w	heat of water sorption	$[J\ kg^{-1}]$
k	reaction rate constant	$[s^{-1}]$
k_t	thermal conductivity	$[W\ m^{-1}\ K^{-1}]$
L	length of the bed	[m]
n	reaction order	[-]
q	amount of oxygen taken up per unit mass of carbonaceous material (coal or char)	$[mgO_2/gchar(daf)]$
q_o	rate of heat generation at an oven temperature, T_o	$[J\ m^{-3}\ s^{-1}]$
Q	heat of oxidation reaction	$[J\ kg^{-1}]$
P	pressure	[Pa]
R	universal gas constant	$[J\ mol^{-1}\ K^{-1}]$

r	sample size (half-width of the slab)	[m]
R_o	rate of oxidation	[mol m^{-3} s^{-1}]
R_w	rate of interaction of water vapour	[mol m^{-3} s^{-1}]
S	interfacial area between coal and gas in the reactor	[m^2]
S_r	heat transfer area of the reactor	[m^2]
t	time	[s]
T	absolute temperature	[K]
$\overline{T}$	spatial average temperature of the coal stockpile	[K]
Ta	ambient temperature	[K]
u_w	wind velocity	[m s^{-1}]
U_g	gas velocity	[m s^{-1}]
W	concentration of water vapour in the gas	[mol m^{-3}]
W_c	equilibrium concentration of water vapour	[mol m^{-3}]
x	distance from the slab symmetry	[m]
y	coal conversion	[-]

GREEK SYMBOLS

α	Elovich empirical constant (generally depends on the temperature)	[-]
δ	Frank-Kamenetskii parameter	[-]
Δ	critical thickness of coal deposit	[m]
ε_b	bed porosity	[-]
κ	permeability of coal matrix	[-]
θ	angle of inclination from horizontal	[deg]
τ	dimensionless time	[-]
μ	viscosity of air	[kg m^{-1} s^{-1}]
ρ	density	[kg m^{-3}]
ρ_a	apparent reaction rate of the coal	[kg $m^{-3}s^{-1}$]

SUBSCRIPTS

0	initial
a	ambient
c, crit	critic
g	gas
i	ignition
max	maximum
M	coal M
o	oven
O_2	oxygen
p	crossing point
s	solid

REFERENCES

Akgun, F., and Arisoy, A. (1994). "Effect of Particle Size on the Spontaneous Heating of a Coal Stockpile." *Combustion and Flame*, 33(6), 1321-146.

Allan, R. R., and Parry, V. F. (1954). *Report of Investigation No. 5034*, US Bureau of Mines.

Badzioch, S., Gregory, D.R., Field, M.A. (1964). "Investigation of The Temperature Variation of the Thermal Conductivity and Thermal Diffusivity of Coal." *Fuel*, 43, 267-280.

Banerjee, S. C. (1985). *Spontaneous Combustion of Coal and Mine Fires*, A.A. Balkema, Rotterdam.

Berkowitz, N. (1979). *An Introduction to Coal Technology*, Academic Press, New York.

Bhat, S., and Agarwal, P. K. (1996). "The Effect of Moisture Condensation on the Spontaneous Combustibility of Coal." *Fuel*, 75(13), 1523-1532.

Bhattacharya, K. K. (1971). "The Role of Sorption Water of Water Vapour in the Spontaneous Heating of Coal." *Fuel*, 50, 367-380.

Bhattacharya, K. K. (1972). "The Role of Desorption of Moisture from Coal in Its Spontaneous Heating." *Fuel*, 51, 214-220.

Bowes, P. C. (1984). *Self-Heating: Evaluating and Controlling Hazards*, Elseveir Science Publisher, New York.

Brooks, K., Balakotaiah, V., and Luss, D. (1988). "Effect of Natural Convection on Spontaneous Combustion of Coal Stockpiles." *J. AIChe*, 34(3), 353-365.

Brooks, K., and Glasser, D. (1986). "A Simplified Model of Spontaneous Combustion in Coal Stockpiles." *Fuel*, 65, 1035-1041.

Buckmaster, H. A., and Kudynska, J. (1992). "Dynamic In Situ 9 GHz c.w. -e.p.r. Low Temperature Oxidation Study of Selected Alberta Coal: 4. Influence of Moisture on hv Bituminous Coal." *Fuel*, 71, 1147-1151.

Carpenter, D. L., and Giddings, D. G. (1964). "The Initial Stages of the Oxidation of Coal with Molecular Oxygen I-Effect of Time, Temperature and Coal Rank on Rate of Oxygen Consumption." *Fuel*, 43, 247-266.

Carpenter, D. L., and Sergeant, G. D. (1966a). "The Initial Stages of the Oxidation of Coal with Molecular Oxygen III - Effect of Particle Sizes on Rate of Oxygen Consumption." *Fuel*, 45(4), 311-327.

Carpenter, D. L., and Sergeant, G. D. (1966b). "The Initial Stages of the Oxidation of Coal with Molecular Oxygen IV - The Accessibility of The Internal Surface to Oxygen." *Fuel*, 45(6), 429-446.

Carr, R. M., Kumagain, H., Peake, B. M., Robinson, B. H., Clemens, A. H., and Matheson, T. W. (1995). "Formation of Free Radical During Drying and Oxidation of A Lignite and A Bituminous Coal." *Fuel*, 74(3), 389-394.

Carras, J. N. (1997). "Self Heating in Coal, Spoil Piles and Goafs. " *Twenty-Fifth Australian and New Zealand Chemical Engineer's Conference*, Rotorua, New Zealand.

Carras, J. N., Bainbridge, N. W., Saghafi, A., Szemes, F., Roberts, O. C., and Haneman, D. (1994). "The Self-Heating of Spoil Piles from Open Cut Coal Mines.".

Carras, J. N., and Young, B. C. (1994). "Self-Heating of Coal and Related Materials: Methods, Application, and Test Methods." *Prog. Energy. Combust. Sci.*, 20, 1-15.

Chamberlain, E. A. C. (1974). "Spontaneous Combustion of Coal: An Investigation of Inhibitors and Promoters." *Colliery Guardian*(March 1974), 79-82.

Chen, X. D. (1991). "The Spontaneous Heating of Coal: Large Scale Laboratory Assessment and Supporting Theory," PhD thesis, University of Catenbury, New Zealand.

Chen, X. D. (1992). "On The Mathematical Modelling of The Transient Process of Spontaneous Heating in a Moist Coal Stockpile." *Combustion and Flame*, 90, 114-120.

Chen, X. D. (1994). "The Effect of Drying Heat and Moisture Content on the Maximum Temperature Rise during Spontaneous Heating of a Moist Coal Pile." *Coal Preparation*, 14, 223.

Chen, X. D. (1996a). "The Fundamental of Self-Ignition of Water Containing Combustible Materials." *J. AIChE (submitted).*

Chen, X. D. (1996b) "Self-Ignition Hazards-The Phenomena and The Testing Methods." *24th Australian and New Zealand Chemical Engineering Conference*, Sydney, Australia, 109-114.

Chen, X. D. (1996c). "Spontaneous Combustion of Coal in An Adiabatic Device-Modelling of the Effect of Moisture and Oxidative Ageing." , 163-168.

Chen, X. D., and Chong, L. V. (1995). "Some Characteristics of Transient Self-Heating Inside an Exothermically Reactive Porous Solid Slab." *Trans IChemE*, 73(B), 101-107.

Chen, X. D., and Stott, J. B. (1993). "The Effect of Moisture Content on the Oxidation Rate of Coal During Near-Equilibrium Drying and Wetting at 50°C." *Fuel*, 72(6), 787-792.

Chen, X. D., and Stott, J. B. (1997). "Oxidation Rates of Coals as Measured from One-Dimensional Spontaneous Heating." *Combustion and Flame*, 109, 578-586.

Chen, X. D., and Wake, G. C. (1994). "Thermal Ignition Kinetics of A Moist Combustible Porous Solid in Either Dry or Humid Environment Obtained Using Frank-Kamenetskii Theory." *Trans IChemE*, 72(B), 135-141.

Chen, Y., and Mori, S. (1995). "Estimating the Combustibility of Various Coals by TG-DTA." *Energy & Fuels*, 9, 71-74.

Chong, L. V., Chen, X. D., and Mackereth, A. R. (1997). "Effect of Composition on the Thermal Ignition of Dairy Powders." *Twenty-Fifth Australian and New Zealand Chemical Engineer's Conference*, Rotorua, New Zealand.

Chong, L. V., Shaw, I. R., and Chen, X. D. (1995). "Thermal Ignition Kinetics of Wood Sawdust Measured by A Newly Devised Experimental Technique." *Process Safety Progress*, 14(4), 266-270.

Chong, L. V., Shaw, I. R., and Chen, X. D. (1996). "Exothermic reactivities of Skim and Whole Milk Powders as Measured Using a Novel Procedure." *Journal of Food Engineering*, 30, 185-196.

Clemens, A. H., and Matheson, T. W. (1996). "The Role of Moisture in The Self-Heating of Low-Rank Coals." *Fuel*, 75(7), 891-895.

Clemens, A. H., Matheson, T. W., and Rogers, D. E. (1990). "DTA Studies of the Low-Temperature Oxidation of low Rank Coals." *Fuel*, 69, 255-256.

Clemens, A. H., Matheson, T. W., and Rogers, D. E. (1991). "Low-Temperature Oxidation Studies of Dried New Zealand Coals." *Fuel*, 70, 215-221.

Dack, S. W., Hobday, M. D., Smith, T. D., and Pillow, J. R. (1983). "Free Radical Involvement in the Oxidation of Victorian Brown Coal." *Fuel*, 62, 1510-1512.

Deevi, S. C., and Suuberg, E. M. (1987). "Physical Changes Accompanying Drying of Western US Lignites." *Fuel*, 66, 454-460.

Duane, T. C., and Synnott, E. C. (1992). "Ignition Characteristics of Spray-Dried Milk Product Powders in Oven Tests." *Journal of Food Engineering*, 17, 163-175.

Durie, R. A. (1991). *The Science of Victorian Brown Coal: Structure, Properties and Consequences for Utilisation*, Butterworth-Heinemann Ltd., Australia.

Evseev, V. (1985). "New Methods for the Prevention of Spontaneous Fires in Underground Coal Mines." *The 21st International Conference of Safety in Mines Research Institute*, Sydney, 481-483.

Fogler, H. C. (1981). *Elements of Chemical Reaction Engineering*, Prentice-Hall, New Jersey.

Frank-Kamenetskii, D. A. (1969). *Diffusion and Heat Transfer in Chemical Kinetics*, J.P. Appleton, translator, Plenum Press, New York.

Furimsky, E., Palmer, A., Duguay, D. G., McConell, D. G., and Henson, D. E. (1988). "Characterization of Carboneous Solids by Oxygen Chemisorption." *Fuel*, 67, 798-802.

Gatica, J. E., Viljoen, H. J., and Hlavacek, V. (1989). "Interaction Between Chemical Reaction and Natural Convection in Porous Media." *Chemical Engineering Science*, 44(9), 1853-1870.

Glasser, D., and Bradshaw, S. (1990). "Spontaneous Combustion in Beds of Coal." Handbook of Heat and Mass Transfer, 1071-1148.

Gorbaty, M. L. (1978). "Effect of Drying on The Adsorptive Properties of Sub-Bituminous Coal." *Fuel*, 57, 796-797.

Gray, B. F., Griffiths, J. F., and Hasko, S. M. (1984). "Spontaneous Ignition Hazards in Stokpiles of Cellulosic Material : Criteria for Safe Storage." *J. Chem. Tech. Biotechnol*, 34(A), 453-463.

Gray, B. F., Little, S. G., and Wake, G. C. (1992). "The Prediction of a Practical Lower Bound for Ignition Delay Times and a Method of Scaling-Times-To-Ignition in Large Reactant Masses from Laboratory Data-II." *Twenty-Fourth Symposium (International) on Combustion*, The Combustion Institute, Pittsburgh, 1785-1791.

Gray, B. F., Merkin, J. H., and Griffiths, J. F. (1990). "The Prediction of a Practical Lower Bound for Ignition Delay Times and a Method of Scaling-Times-To-Ignition in Large Reactant Masses from Laboratory Data." *Twenty-Third Symposium (International) on Combustion*, The Combustion Institute, Pittsburgh, 1775-1782.

Gray, B. F., and Wake, G. C. (1990). "The Ignition of Hygroscopic Combustible Materials by Water." *Combustion and Flame*, 79, 2-6.

Griffiths, J. F., Kordylewski, W. (1992). "Combustion Hazards Associated With The Hot Stacking of Processed Materials." *Twenty-Fourth Symposium (International) on Combustion*, The Combustion Institute, Pittsburgh, 1777-1784.

Harris, D. J. (1997). "Char Reactivity during Combustion and Gasification." *Continuing Education Course on Fluid Bed Processes for Coal Utilisation*, Adelaide.

Harris, J. A., and Evans, D. G. (1975). "Low-Temperature Oxidation of Brown Coal.2. Elovich Adsorption Kinetics and Porous Materials." *Fuel*, 54, 276-278.

Inggram, G. R., and Rimstidt, J. D. (1984). "Natural Weathering of Coal." *Fuel*, 63, 292-296.

Jackson, P. J. (1987). "Mineral Matter in Pulverised Coal Combustion." *Fundamentals of the Physical-Chemistry of Pulverised Coal Combustion*, J. Lahaye, Prado, G., ed., Martinus Nijhoff Publisher, Dordrecht, 273.

Jenkins, R. G., Nandi, S. P., and Walker, P. L. (1973). "Reactivity of Heat-Treated Coals in Air at 500°C." *Fuel*, 52, 288-293.

Jones, J. C. (1993). *Combustion Science: Principles and Practice*, Millenium Book, NSW, Australia.

Jones, J. C. (1996). "A Single-Point Estimation of the Combustion Rate Expression for a Bituminous Coal." *Journal of Fire Sciences*, 14, 325-330.

Jones, J. C., and Raj, S. C. (1988). "The Self-Heating and Ignition of Vegetation Debris." *Fuel*, 67, 1208-1210.

Jones, J. C., and Wake, G. C. (1990). "Measured Activation Energies of Ignition of Solid Materials." *J. Chem. Tech. Biotechnol*, 48, 209-216.

Juntgen, H., and Nat, R. (1987). "Coal Characterization in relation to Coal Combustion." Fundamentals of the Physical-Chemistry of Pulverised Coal, Martinus Nijhoff Publisher, Dordrecht, 5.

Kaji, R., Hishinuma, Y., and Nakamura, Y. (1985). "Low-Temperature Oxidation of Coals : Effect of Pore Structure and Coal Composition." *Fuel*, 64, 297-302.

Kaji, R., Hishinuma, Y., and Nakamura, Y. (1987). "Low-Temperature Oxidation of Coals - A Calorimetry Study." *Fuel*, 66, 154.

Karsner, G. G., and Perlmutter, D. D. (1981). "Reaction Regimes in Coal Oxidation." *J. AIChE*, 27(6), 920-927.

Karsner, G. G., and Perlmutter, D. D. (1982). "Model for Coal Oxidation Kinetics. 1. Reaction Under Chemical Control." *Fuel*, 61, 29-34.

Khan, M. R., Everitt, C. E., and Alain, P. L. (1990). "Modelling of Oxygen Chemisorption Kinetics on Coal Char." *Combustion and Flame*, 80, 83-93.

Kim, A. G., and Chaiken, R. F. (1993). "Fires in Abandoned Coal Mines and Waste Banks." *Information Circular /1993*, Bureau of Mines, USA.

Krishnawamy, S., Agarwal, P. K., and Gunn, R. D. (1996a). "Low-Temperature Oxidation of Coal. 3. Modelling Spontaneous Combustion in Coal Stockpiles." *Fuel*, 75(3), 353-362.

Krishnawamy, S., Bhat, S., Gunn, R. D., and Agarwal, P. K. (1996b). "Low-Temperature Oxidation of Coal .1. A Single-Particle Reaction-Diffusion Model." *Fuel*, 75(3), 333-343.

Krishnawamy, S., Gunn, R. D., and Agarwal, P. K. (1996c). "Low-Temperature Oxidation of Coal .2. An Experimental and modelling Investigation Using a Fixed-Bed Isothermal Flow Reactor." *Fuel*, 75(3), 344-352.

Levenspiel, O. (1972). *Chemical Reaction Engineering*, Wiley & Sons, New York.

Liotta, R., Brons, G., and Isaacs, J. (1983). "Oxidative Weathering of Illinois No.6 Coal." *Fuel*, 62, 781-791.

McIntosh, A. C., and Tolputt, T. A. (1990). "Critical Heat Losses to Avoid Self-Heating in Coal Piles." *Combust. Sci. and Tech.*, 69, 133-145.

Milton, J. S., and Arnold, J. C. (1995). *Introduction to Probability and Statistics: Principles and Applications for Engineering and the Computing Sciences*, McGraw Hill, New York.

Nordon, P. (1979). "A Model for Self-Heating Reaction of Coal and Char." *Fuel*, 58(6), 456-464.

Nordon, P., Bainbridge, N. W., Szemes, F., and Myers, C. (1985). "A Low Temperature Reaction Calorimeter of The Calvet Type for the Measurement of the Heat of oxidation of Coal." *J. Phys. E: Sci. instrum.*, 18, 338-341.

Nordon, P., Young, B. C., and Bainbridge, N. W. (1979). "The Rate of Oxidation of Char and Coal in Relation to Their Tendency to Self-Heat." *Fuel*, 58, 443-449.

O'Mahony, J. G., and Synnott, E. C. (1988). "Influence of Sample Shape and Size on Self-Ignition of a Fat-Filled Milk Powder." *Journal of Food Engineering*, 7, 271-280.

Ogunsola, O. I., and Mikula, R. J. (1991). "A Study of Spontaneous Combustion Characteristics of Nigerian Coals." *Fuel*, 70, 258-261.

Ogunsola, O. I., and Mikula, R. J. (1992). "Effect of Thermal Upgrading on Spontaneous Combustion Characteristics of Western Canadian Low rank Coals." *Fuel*, 71, 3-8.

Palmer, A. D., Cheng, M., Goulet, J.-C., and Furimsky, E. (1990). "Relation between Particle Size and Properties of Some Bituminous Coal." *Fuel*, 69, 183-188.

Perry, H. P., Green, D. (1984). *Perry's Chemical Engineer's Handbook*, McGraw-Hill, New York.

Petit, J. C. (1991). "A Comprehensive Study of The Water Vapour/Coal System: Application to The Role of Water in The Weathering Coal." *Fuel*, 70, 1053-1058.

Polat, S., and Harris, I. J. (1984). "Low-Temperature Oxidation of Victorian Brown Coal." *Fuel*, 63, 669-672.

Salinger, A. G., Aris, R., and Derby, J. J. (1994). "Modelling the Spontaneous Ignition of Coal Stockpiles." *J. AIChE*, 40(6), 991-1004.

Schmal, D., Duyzer, J. H., and Van Heuven, J. W. (1985). "A Model for the Spontaneous Heating of Coal." *Fuel*, 64, 963-972.

Schmidt, L. D. (1945). *Chemistry of Coal Utilisation*, John Wiley&Sons, New York.

Semenov, N. N. (1928). *J. Phys. Chem*, 48, 571.

Shrivastava, K. L., Tripathi, R. P., and Jangid, M. L. (1992). "Spontaneous Combustion of Coal: a Mossbauer Approach." *Fuel*, 71, 377-380.

Siegel, J. S., and Temchin, J. R. (1991). Energy and Environment in the 21st Century, J. W. Tester, D. O. Wood, and N. A. Ferrari, eds., MIT Press, Cambridge, 623.

Singer, S. (1984). *Pulverised Coal Combustion: Recent Developments*, Noyes Publications, USA.

Smith, A. C., and Lazzara, C. P. (1987). "Spontaneous Combustion Studies of U.S. Coal." *Report of Investigation - U.S. Bureau of Mines, RI 9079.*

Smith, A. C., Miron, Y., and Lazzara, C. P. (1988). "Inhibition of Spontaneous Combustion of Coal." *Report of Investigation - U.S. Bureau of Mines, RI 9196.*

Speight, J. G. (1994). *The Chemistry and Technology of Coal*, Marcel Dekker, Inc., New York.

Stott, J. B., and Chen, X. D. (1992). "Measuring the Tendency of Coal to Fire Spontaneously." *Colliery Guardian*(Jan. 1992), 9-16.

Stott, J. B., Harris, B. J., and Hansen, P. J. (1987). "A 'Full-Scale' Laboratory Test for The Spontaneous Heating of Coal." *Fuel*, 66, 1012-1013.

Sujanti, W., and Zhang, D. K. (1997). "The Effect of Additive Concentrations on Spontaneous combustion of Coal." *1997 Australian Symposium on Combustion and The Fifth Australian Flame Days*, The University of Sydney, Sydney, Australia, 100-104.

Sujanti, W., and Zhang, D. K. (1997). "Inhibition and Promotion Agents of Spontaneous Combustion of Coal." *The 25th Australian and New Zealand Chemical Engineer's Conference and Exhibition*, Rotorua, NZ.

Sujanti, W., and Zhang, D. K. (1998a). "A Laboratory Study of Spontaneous Combustion of Coal: The Influence of Inorganic Matter and reactor Size." *Fuel* (in press).

Sujanti, W., Zhang, D.K., and Chen, X.D. (1998b). "A Low-Temperature Oxidation Study Using Wire-Mesh Reactors with Both Steady-State and Transient Methods" *Combustion and Flame* (in press).

Swan, P. D., Harris, J. A., Siemon, S. R., and Evans, D. G. (1973). "Compound Isolation from Brown Coal by Low-Temperature Evacuation." *Fuel*, 52, 154.

Swann, P. D., and Evans, D. G. (1979). "Low-Temperature Oxidation of Brown Coal.3. Reaction with Molecular Oxygen at Temperature Closed to Ambient." *Fuel*, 58, 276-280.

Szekely, J. (1977). "Reaction Between Porous Solids and Gases." Chemical reactor Theory: A Review, L. Lapidus and Amundson, eds., Prentice-Hall, N.R.Inc., New Jersey, 273.

Van Krevelen, D. W., and Schuyer, J. (1957). *Coal Science*, Elsevier Publishing Company, Amsterdam.

Vance, W. E., Chen, X. D., and Scott, S. C. (1996). "The Rate of Temperature Rise of A Sub-Bituminuous Coal during Spontaneous Combustion in An Adiabatic Device : The Effect of Moisture Content and Drying Methods." *Combustion and Flame*, 106, 261-270.

Waddington, T. C. (1959). "Lattice Energies and Their Significance in Inorganic Chemistry." Advances in Inorganic Chemistry and Radiochemistry, H. J. Emeleus and A. G. Sharpe, eds., Academic Press Inc., New York, 180.

Ye, D.-P. (1994). "Gasification of South Australian Lignite," PhD thesis, The University of Adelaide, Adelaide.

Young, B. C., and Nordon, P. (1978). "Methods for Determining the Rate of Oxygen Sorption by Coals and Chars at Low-Temperatures." *Fuel*, 57, 574-575.

Young, B. D., Williams, D. F., and Bryson, A. W. (1986). "Two-Dimensional Natural Convection and Conduction in A Packed Bed Containing a Hot Spot and Its Relevance to The Transport of Air In A Coal Dump." *Int. J. Heat Mass Transfer*, 29(2), 331-336.

APPENDIX A

PUBLICATIONS LIST

Refereed Journal Publications

Sujanti, W. and Zhang, D.K. (1998) "The Effect of Inherent and Added Inorganic Matter on Low-Temperature Oxidation of Coal." *Chemical Engineering Science* (submitted).

Zhang, D.K. and **Sujanti, W.** (1998) "The Effect of Inorganic Matter on Low Temperature Oxidation and Self-Heating of A Victorian Brown Coal." *Energy & Fuels* (submitted).

Sujanti, W. and Zhang, D.K. (1998) "Investigation Into The Roles of Inherent Inorganic Matter and Additives in Low-Temperature Oxidation of A Victorian Brown Coal." *Combustion Science and Technology* (submitted).

Sujanti, W. and Zhang, D.K. (1998) "A Low-Temperature Oxidation and Spontaneous Combustion Study of A Brown Coal: The Influences of Experimental Techniques." *Chemical Engineering Science* (submitted).

Sujanti, W. and Zhang, D.K. (1998) "A Laboratory Study of Spontaneous Combustion of Coal: The Influence of Inorganic Matter and Reactor Size." *Fuel* (in press).

Sujanti, W., Zhang, D.K. and Chen, X.D. (1998) "A Low-Temperature Oxidation Study Using Wire-Mesh Reactors with Both Steady-State and Transient Methods." *Combustion and Flame* (in press).

Conference Papers

Sujanti, W. and Zhang, D.K. (1998). "An Experimental Study of Spontaneous Combustion of A Victorian Brown Coal." *The 26th Australasian Chemical Engineering Conference (Chemeca'98)*, Port Douglas, Australia.

Sujanti, W. and Zhang, D.K. (1998). "Laboratory Studies of Spontaneous Combustion of Morwell Coal Using Different Techniques." *The 5th CRC for Power Generation fom Low-Rank Coal Annual Conference*, Melbourne, 41-49.

Sujanti, W., and Zhang, D. K. (1997). "The Effect of Additive Concentrations on Spontaneous combustion of Coal." *1997 Australian Symposium on Combustion and The Fifth Australian Flame Days*, The University of Sydney, Sydney, Australia, 100-104.

Sujanti, W. and Zhang, D.K. (1997). "Inhibition and Promotion Agents of Spontaneous Combustion." *The 25th Australasian Chemical Engineering Conference (Chemeca'97)* , Rotorua, New Zealand, ISBN:0-0908-22-0, ISSN:0111-9532 Vol.23 Issue 1(CH).

Sujanti, W. and Zhang, D.K. (1997). "Spontaneous Combustion of Coal." *The 4th CRC for Power Generation fom Low-Rank Coal Annual Conference*, Melbourne.

Posters

Sujanti, W. and Zhang, D.K. (1998). "A Laboratory Study of Spontaneous Combustion of Coal: The Influence of Inorganic Matter and Reactor Size." presented as work-in-progress poster at *27th International Symposium on Combustion*, The Combustion Institute, Pittsburg.

Sujanti, W., Zhang, D.K. and Chen, X.D. (1998). "A Low-Temperature Oxidation Study Using Wire-Mesh Reactors with Both Steady-State and Transient Methods." presented as work-in-progress poster at *27th International Symposium on Combustion*, The Combustion Institute, Pittsburg.

Reports

Sujanti, W. and Zhang, D.K. (1998). "Laboratories Studies of Spontaneous Combustion of A Victorian Brown Coal." End-of-Grant Report, CRC Project 8-4-24., CRC for Power Generation fom Low-Rank Coal.

Sujanti, W. and Zhang, D.K. (1997). "Studies of Spontaneous Combustion of Coal: A Literature Review." CRC for Power Generation fom Low-Rank Coal.